Modelling and Coverage Improvement of DVB-T Networks

A thesis submitted for the degree of
Doctor of Philosophy

By
Kasampalis Stylianos

Supervised By: **Professor John Cosmas,**
Dr Lazaridis Pavlos

Department of Electronic and Computer Engineering
College of Engineering, Design and Physical Sciences
Brunel University London
Uxbridge, UK

March 2018

ABSTRACT

The necessity of accurate point-to-area and point-to-point prediction tools arises from the enormous demand in designing broadcasting systems for digital TV and cellular communications. Up to now, a considerable number of coverage prediction models for radio coverage has been developed. In electromagnetic wave propagation theory, there are three types of propagation models. Empirical models that are based on a large quantity of measurement data are elementary but not very accurate. Semi-deterministic models that are based on measurement data and electromagnetic theory of propagation, which are more precise. Finally, deterministic models based on theoretical physics, like diffraction theory and Fresnel theory, that require a significant amount of geometrical data about the propagation terrain profile but are the most accurate.

The primary outcomes of this research are the comparative study and improvement of several propagation models, using a significant quantity of measurements and simulations and the deduction of useful conclusions to be used by engineers to improve propagation predictions further. In this research, the Longley-Rice (ITM) Irregular Terrain Model model was used, a classic model used for TV coverage prediction, which model is to date the preferred model of the FCC (Federal Communications Commission) in the US for FM-TV coverage calculations. To run the model, the Radio Mobile program (Radio Propagation and Virtual Mapping Freeware) was used based on the Longley-Rice Model ITM, including the 3-arc-second Satellite Radar Terrain Mission (SRTM) maps and the SPLAT! program (an RF Signal Propagation, Loss, And Terrain analysis tool), which also relies on the Longley-Rice ITM model and makes use of SRTM maps. Both programs work in Windows operating system (Windows7 Professional, 64 bits).

Another model used in this research was SPLAT! with ITWOM (Irregular Terrain with Obstructions Model) which combines empirical data from the ITU-R P.1546 model and other ITU recommendations in conjunction with Beer's and Snell's laws. The ITU-R Recommendation P.1546 model and the empirical Hata-Davidson model using HAAT were also utilized in this research.

The Single Knife-Edge (SKE) model was coded in MATLAB and utilized in this research as a simple reference model, where only one main obstacle is considered. Other well-known multiple knife-edge diffraction models employed in this study are the Epstein-Peterson, Deygout, and Giovaneli models. For these deterministic models,

individual MATLAB programs were written. Simulations produced by the models were limited to the main two knife-edges of the propagation path for immediate comparison with the Longley-Rice model which uses the “double knife-edge” approach. All measurement campaigns took place in Northern Greece and Southern (F.Y.R.O.M) Former Yugoslav Republic of Macedonia using a Rohde & Schwarz FSH-3 portable spectrum analyser and precision calibrated antennas.

ACKNOWLEDGMENTS

I am very thankful to my principal supervisor, Professor John Cosmas, who gave me valuable guidance, and helped me and supported me to complete my research.

I am also thankful for my supervisor Pavlos Lazaridis. He helped me in conducting this research and supported me over the last four years regarding technical assistance, proposed ideas and results verifications. He helped me, a lot and encouraged me when I was tired psychologically and I was thinking to abandon. He is a more a friend than a supervisor. I do not forget the hundreds of hours we spent visiting cities and climbing mountains to take our measurements.

Lastly, I owe my most profound gratitude to my wife and children, for their patience, without whom I would not have made it through my Ph.D. studies.

Thank you all.

DEDICATION

Dedicated to my wife Eleni, my sons Apostolos and Nikolaos and my mother Panagiota.

TABLE OF CONTENTS

LIST OF FIGURES

LIST OF TABLES

LIST OF ABBREVIATION

0.6F	0.6 times of the first Fresnel zone
1F	First Fresnel zone
AP	Access Points
ASO	Analog Switch Off
CDMA	Code Division Multiple Access
CEPT	European Conference of Postal and Telecommunications Administrations
COFDM	Coded Orthogonal Frequency Division Multiplexing
DAB	Digital Audio Broadcasting
DKE	Double Knife-Edge
DSO	Digital Switchover
DVB-T	Digital Video Broadcasting-Terrestrial
DVB-T/H	Digital Video Broadcasting-Terrestrial/Handheld
DVB-T2	Digital Video Broadcasting-Second Generation Terrestrial
EIRP	Equivalent Isotropically Radiated Power
ERP	Effective Radiated Power
FCC	Federal Communication Commission of United States
FEC	Forward Error Correction
GI	Guard Interval
GSM	Global System for Mobiles
GTD	Geometrical Theory of Diffraction
HAAT	Height Average Above Terrain
ITM	Irregular Terrain Model
ITU-R	International Telecommunications Union
ITWOM	Irregular Terrain with Obstructions Model
LOS	Line-Of-Sight
LTE-4G	Long Terms Evolution - 4th Generation
MFN	Multi-Frequency Network
MPEG	Moving Picture Experts Group
NMSA	National Managers Spectrum Association
NTIA	National Telecommunications & Information Administration
ITS	Institute for Telecommunications Sciences
OHLOSS	Over-the-Horizon-Loss programs
ORCA	Optimization and Rational Use of Wireless Communications Bands
QAM	Quadrature Amplitude Modulation
QPSK	Quadrature Phase Shift Keying
SEAMCAT	Spectrum Engineering Advanced Monte Carlo Analysis Tool
SFN	Single Frequency Network
SKE	Single Knife-Edge
SPLAT!	Signal Propagation, Loss and Terrain Analysis Tool

SRTM1	Shuttle Radar Topography Mission (1 arc-second)
SRTM3	Shuttle Radar Topography Mission (3 arc-seconds)
TCA	Terrain Clearance Angle
TIA	Telecommunications Industry Association
TVWS	TV White Spaces
UHF	Ultra High Frequency
VHF	Very High Frequency
WSD	White Spaces Devices

AUTHOR'S DECLARATION

The work described in this thesis has not been previously submitted for a degree in this or any other university and unless otherwise referenced it is the author's work.

STATEMENT OF COPYRIGHT

CHAPTER 1

INTRODUCTION

1.1 OVERVIEW

This chapter provides a background theory of path loss calculation, aims, and objectives of this research. In addition, the research methodology is described, and finally, the thesis structure is outlined.

1.2 BACKGROUND

In this research, a significant number of comparisons between simulations, produced by empirical and deterministic path loss models and measurements are presented. Also, results for path loss calculations and conclusions are shown. The models used in this research are listed below.

- The NTIA-ITS, Longley-Rice model, also known as the ITM (Irregular Terrain Model).

In simulations-calculations that take place in this research, the NTIA-ITS Longley Rice model, also known as the ITM (Irregular Terrain Model) coverage prediction model [1] is used and compared with other models [2]. It is a widely accepted model adopted by the Federal Communication Commission (FCC) of United States of America as a standard and is used for frequencies from 20 MHz to 20 GHz, antenna heights from 0.5m to 3000m and distances from 200 m to 500 km. The ITM software was developed by the NTIA (National Telecommunications & Information Administration) [3] for a point-to-point approach, and in combination with the freely available SRTM maps produce accurate results of path loss [4]. In this research, Radio Mobile software [5], SPLAT! with ITM [6] and SPLAT! with ITWOM [7] (a combination of Longley-Rice and ITU-R P.1546 Recommendation) software, were used to run the Longley-Rice model.

- The Hata-Davidson model

The Hata-Davidson model [8] a modification to the Hata model, that was recommended by "The Telecommunications Industry Association (TIA)," in order to cover a broader range of input parameters and distances than Hata's model is also used in our research. The Hata-Davidson model use HAAT [9] (Height Average Above Terrain) in its calculations. A MATLAB program was written for this model.

- The ITU-R P.1546 Recommendation

In this research "Recommendation ITU-R P.1546" [10] proposed by The Radio Communication Sector of ITU also is used. A MATLAB program is used to calculate simulation results.

- The Epstein-Peterson model [12], Deygout's model [13-14] and Giovaneli's model [15] are also used.

MATLAB programs were written to produce simulated results for Epstein-Peterson's, Deygout's and Giovaneli's models.

Epstein-Peterson's, Deygout's and Giovaneli's models are based on Single Knife Edge Diffraction theory. The specific way these models use this approach to calculate path loss for two obstacles, i.e., Double-Knife Edge Diffraction (DKE), or more obstacles distinguish one model from the other.

- Also, models for "Double isolated edges and "rounded obstacles" presented by "Recommendation ITU-R P.526-13" [11] were used.

Let's first try to calculate the effect of a single obstacle placed in the path between receiver and transmitter and considering the obstacle as a wide screen which allows no energy to pass through it, an absorbing screen, a semi-infinite screen. The upper edge of the obstacle is called Knife-Edge. To do this, Huygens's principle will be used to predict diffraction of a plane wave over this Knife-Edge. According to Huygens's principle, every point on a wave front is a source of wavelets, which spread forward at the same speed. On the other hand, diffraction is the bending of a wave around the edge of an obstacle, and it depends on the type of terrain and vegetation. Huygens's principle and diffraction can be seen in Figure 1-1

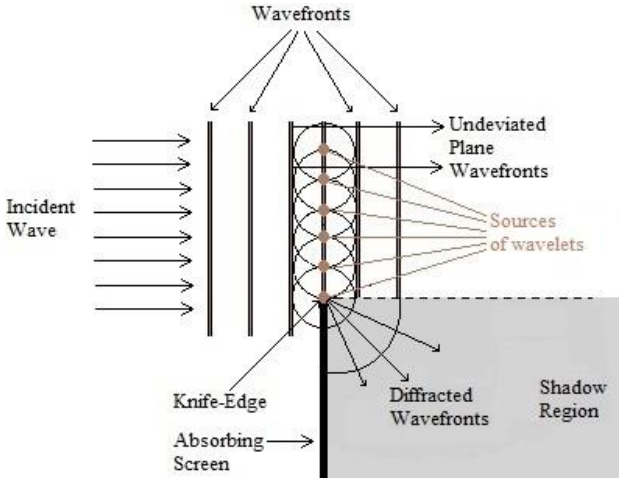

Figure 1-1: Huygens' principle for Knife-Edge diffraction.

The geometry of Knife-Edge diffraction with Huygens' principle is shown in Figure 1-2, [16].

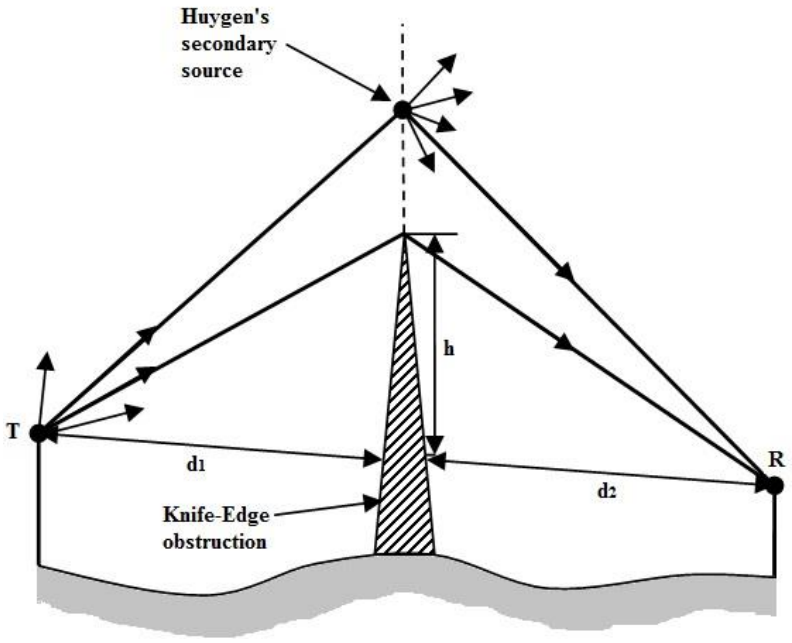

Figure 1-2: Knife-Edge diffraction geometry. Receiver R is in the shadow area. TR is the LOS line. Reproduced from Gibson, 1996.

Now applying Huygens's principle in a mathematical form, the diffracted field strength can be predicted. The contribution of all the secondary sources in the region above the edge is summed taking due account their relative amplitudes and phases. The result expresses the reduction in field strength due to the Knife-Edge diffraction in decibels, it is the propagation loss and can be calculated with the use of Fresnel parameter $\boldsymbol{v}$.

The diffraction gain due to Knife-Edge diffraction is given by

$$G_d\left(dB\right) = 20 \cdot log_{10}\left(\left|\frac{E_d}{E_i}\right|\right) = 20 \cdot log_{10}\left|F\left(v\right)\right| \tag{1.1}$$

where E_d is the diffracted field, E_i is the incident field (usually $E_i = E_o$, where E_o is the field strength of free space) and $F(v)$ is the Fresnel integral

$$F\left(v\right) = \frac{1+j}{2}\int_v^\infty \exp\left(-\frac{j\pi v^2}{2}\right)dv \tag{1.2}$$

An alternative form is

$$\left|F\left(v\right)\right| = \frac{1}{2}\left(\frac{1}{2} + C^2\left(v\right) - C\left(v\right) + S^2\left(v\right) - S\left(v\right)\right) \tag{1.3}$$

where $C(v)$ and $S(v)$ are the Fresnel cosine and sine integrals which can be mathematically evaluated.

The dimensionless Fresnel parameter v is calculated from the formula

$$v = h\left[\frac{2}{\lambda}\left(\frac{1}{d_1}+\frac{1}{d_2}\right)\right]^{\frac{1}{2}} \tag{1.4}$$

or

$$v = \theta\left[\frac{2}{\lambda\left(\frac{1}{d_1}+\frac{1}{d_2}\right)}\right]^{\frac{1}{2}} \tag{1.5}$$

where,

h is the height between the Knife-Edge (top of the obstacle) and the line of sight (LOS – the straight line joining the transmitter with the receiver)

θ is the diffraction angle in radians

d_1 is the distance between the transmitter and the obstruction along the LOS

d_2 is the distance between the receiver and the obstacle along the line of sight

λ is the wavelength.

The following approximations must hold for this theory to be valid:

$$d_1,\ d_2 >> h \text{ and } d_1 d_2 >> \lambda$$

Height h can be positive or negative as shown in Figure 1-3, below.

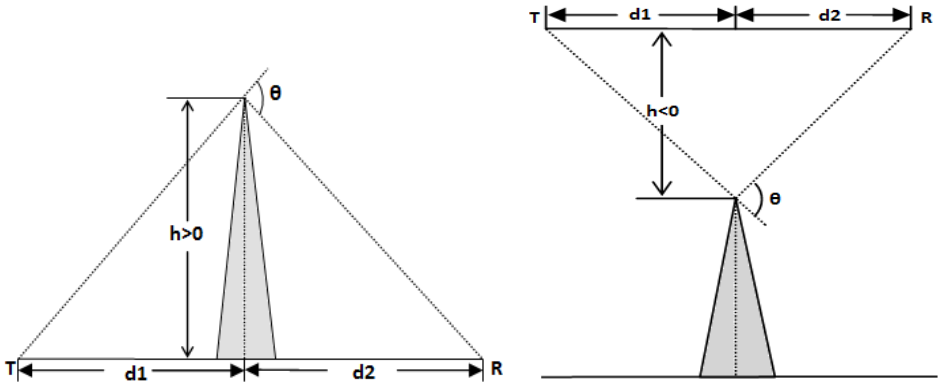

Figure 1-3: Positive height, h>0 and negative height, h<0.

Equation (1.1) can be evaluated using numerical solutions. An approximate solution provided by Lee [17] is given by equation (1.6).

$$
\begin{aligned}
G_d\left(dB\right) &= 0 && \nu \le -1 \\
G_d\left(dB\right) &= 20\log_{10}\left(0.5-0.62\nu\right) && -1 < \nu \le 0 \\
G_d\left(dB\right) &= 20\log_{10}\left(0.5e^{(-0.95\nu)}\right) && 0 < \nu \le 1 \\
G_d\left(dB\right) &= 20\log_{10}\left(0.4-\sqrt{0.1184-\left(0.38-0.1\nu\right)^2}\right) && 1 < \nu \le 2.4 \\
G_d\left(dB\right) &= 20\log_{10}\left(\frac{0.225}{\nu}\right) && \nu > 2.4
\end{aligned}
\tag{1.6}
$$

For ν>-0.7 the following approximation also can be used

$$G_d\left(dB\right) = 6.9 + 20\cdot\log_{10}\left(\sqrt{\left(\nu-0.1\right)^2+1}+\nu-0.1\right) \tag{1.7}$$

The use of Fresnel zones is another useful way to consider Knife-Edge diffraction. Fresnel zones are concentric cylindrical ellipsoids drawn between transmitter and receiver. They are defined by the locus of points where the distance $(a+b)$ equals the distance (d_1+d_2) between transmitter and receiver (LOS line) plus n half-wavelengths. They are illustrated in Figure 1-4.

$$a+b = d_1+d_2+\frac{n\lambda}{2} \tag{1.8}$$

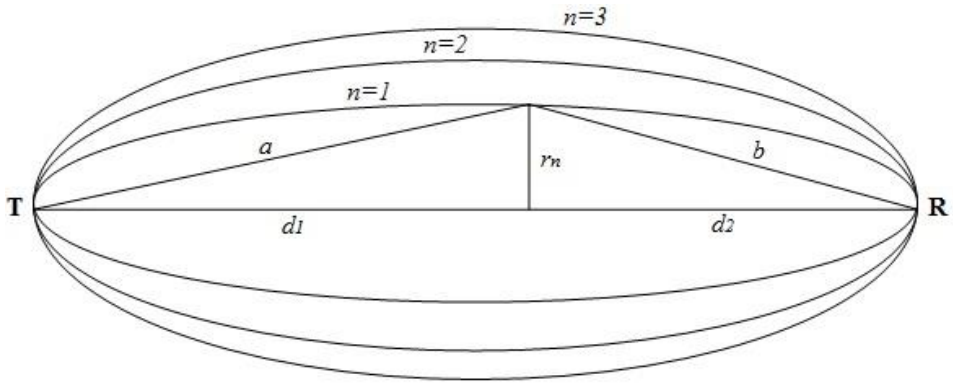

Figure 1-4: Fresnel zones.

The radius of the *n*th Fresnel zone r_n is given by applying the equation (1.8).

If $r_n << d_1$ and $r_n << d_2$, the radius r_n of the n Fresnel zone can be expressed regarding n, λ, d_1 and d_2 by the approximation formula:

$$r_n \approx \sqrt{\frac{n\lambda d_1 d_2}{d_1+d_2}} \tag{1.9}$$

The Fresnel zone clearance is defined as (h/r_n) and can be expressed as a function of dimensionless Fresnel parameter ν.

$$\nu \approx h\sqrt{\frac{2(d_1+d_2)}{\lambda d_1 d_2}} = \frac{h}{r_n}\sqrt{2n} \tag{1.10}$$

If Knife-Edges obstruct Fresnel zones, then the field strength can be calculated at any place, because they can be thought of as containing the main propagation energy in the electromagnetic wave.

The Knife-Edge diffraction gain $G_d(dB)$ as a function of Fresnel diffraction parameter v is shown in Figure 1-5. Observing this figure, we see that the Fresnel parameter v is approximate -0.8 when the obstruction occupies 0.6 times the first Fresnel zone and the obstruction loss is then 0 dB. This clearance is the main criterion to decide whether an obstacle is to be treated as a significant obstacle or not.

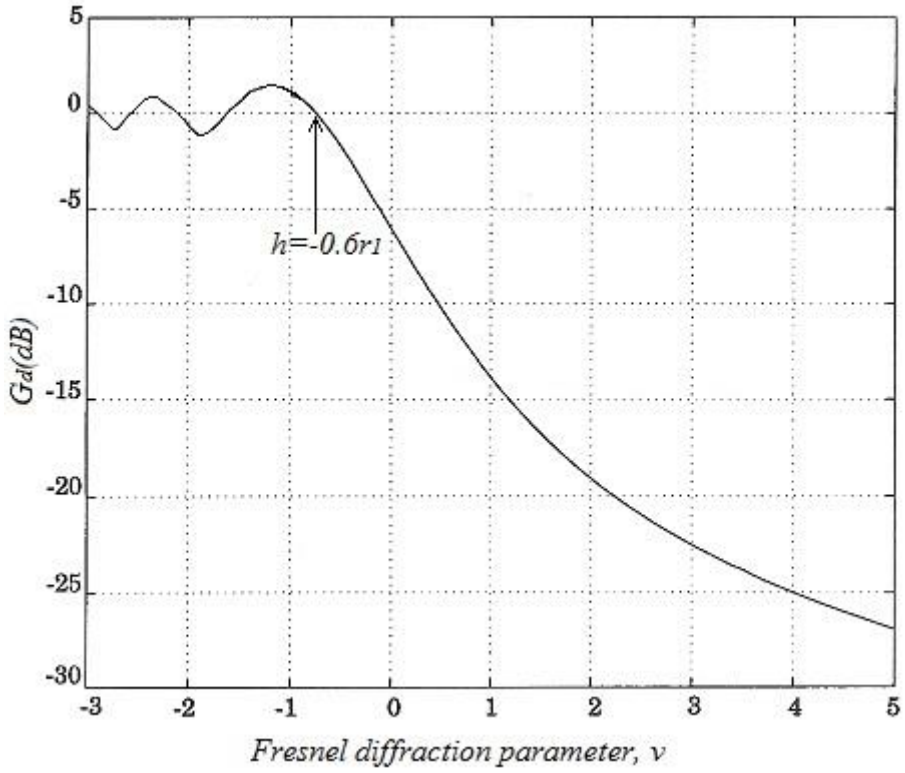

Figure 1-5: Knife-Edge diffraction attenuation.

Thus, the region of 0.6 times of first Fresnel zone (0.6F) is regarded as an unobstructed area and sometimes called “forbidden” region [18], and if this region is clear, then the total path loss will be practically the same as if there were no obstacles.

The unobstructed area of 0.6 times 1st Fresnel zone also called “forbidden” region is shown in the simplified Figure 1-6.

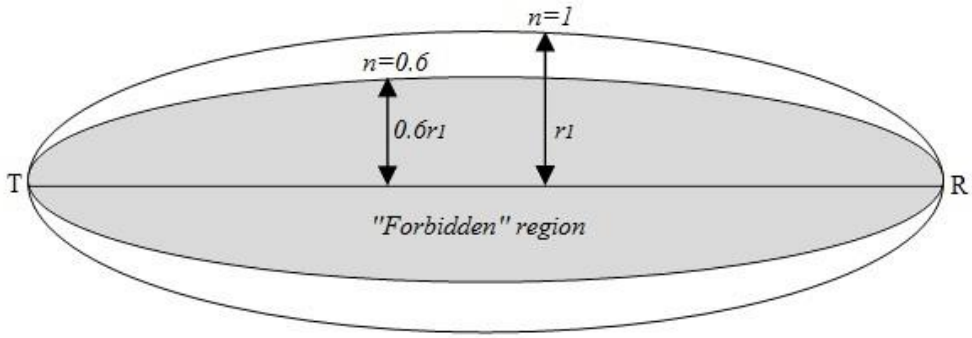

Figure 1-6: 0.6 times first Fresnel zone clearance.

In practice, the elevation profile between transmitter and receiver, the line of sight (LOS), the 1st Fresnel zone and the 0.6 times 1st Fresnel zone, which is the unobstructed region and called “forbidden” zone is shown in Figure 1-7. The “forbidden” zone, where no obstacles are allowed is the shaded region in Figure 1-7.

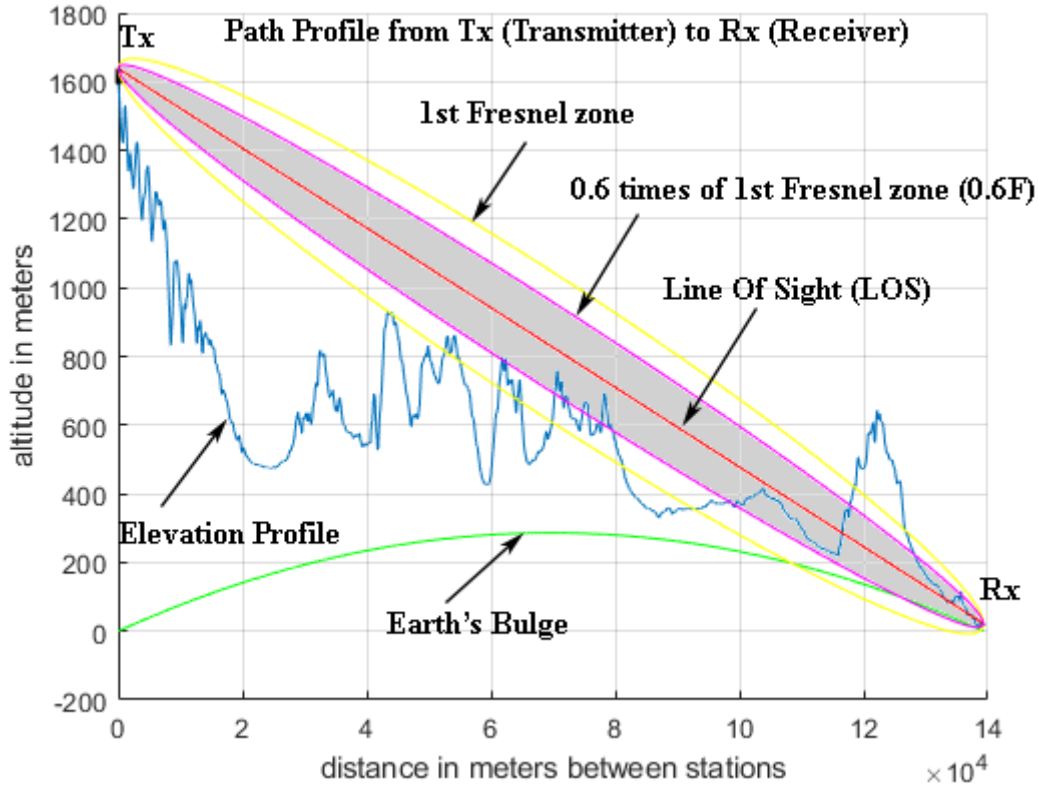

Figure 1-7: "Forbidden zone," 0.6 times of 1st Fresnel zone.

1.3 AIMS AND OBJECTIVES

The purpose of the research in this thesis is to provide accurate coverage prediction maps for DVB-T/DVB-T2 services and validate the simulation results with field measurements taken in field trials. Coverage prediction maps will be used in conjunction with various electromagnetic propagation models. Therefore, many

electromagnetic propagation models will be utilized, and their accuracy will be extensively assessed by precision measurements performed by our measurement equipment.

The measuring equipment consists of a Rohde & Schwarz FSH-3 portable spectrum analyser (100 kHz-3 GHz), low-loss cable by Suhner, two high-precision calibrated biconical antennas by Schwarzbeck (25 MHz – 6 GHz), and the more recently acquired equipment, an Agilent portable spectrum analyser (up to 6 GHz) and a log-periodic precision calibrated Schwarzbeck antenna (0.25-6 GHz). Furthermore, a complete DVB-T HD testbed has been already put in place on the campus of TU Thessaloniki by the laboratory of electrical measurements that can cover the entire city, and transmission experiments are conducted during the past few years. The testbed consists of a Rohde & Schwarz low power UHF DVB-T transmitter, a 11 dBd UHF antenna panel by Aldena placed on a tower of 10 m on top of the electronics building, a power UHF amplifier, an MPEG-4 (H.264) HD Encoder with ASI output, a professional satellite receiver with ASI output.

The resulting conclusions will be described in this thesis helping to improve the particular techniques.

1.4 CONTRIBUTION TO KNOWLEDGE

This thesis contributes to knowledge in the research area doing the following:

- It checks the reliability of the propagation models involved in this research, comparing their simulation results with measurements.
- Proposes methods for their use.
- Suggests methods of improvement of the models, so to produce precise coverage prediction to improve coverage.
- Proves that the so-called old models, have room for improvement and can be applied to Digital TV. These models with the use of the today's powerful PC's, performing a significant number of calculations become very useful producing quite accurate simulation results.
- Demonstrates the need to create accurate simulation results leading so to better coverage with less power consumption from the transmitters, helping in this way the environmental protection.
- Propose new implementations of the Models, (i.e. Automobile radars)

1.5 RESEARCH METHODOLOGY

The research methodology for this thesis is as follows:

- In the initial phase, a detailed and in-depth literature review took place, which included the current and past work done in the area of electromagnetic propagation and path loss calculation.
- Various technical books [19-29] on radio wave propagation were studied for understanding theoretical and technical approaches towards radio wave propagation. A lot of propagation models were studied in depth.
- MATLAB was used for simulation purposes and comparisons.
- Measurements campaigns took place in different areas of Greece and elsewhere for the concentration of a significant number of measurements, necessary for our work.
- Briefly about our research, first, we create an elevation profile between transmitter and receiver using the proper software and maps. Then we draw 0.6 times first Fresnel zone. If this zone is unobstructed we implement free space propagation theory. Otherwise, we apply the proper models for calculating the attenuation of the electromagnetic wave finding the field strength finally at a specific point.
- Publishing in IEEE international conferences was another field where various experts reviewed our work.

1.6 RESEARCH OUTPUT

During this research, our work was published and presented at top-ranked international IEEE conferences. The list of publications is given below:

1. Stylianos Kasampalis, Pavlos I. Lazaridis, Zaharias D. Zaharis, Aristotelis Bizopoulos, Spiridon Zettas and John Cosmas, Senior Member IEEE.
   "Longley-Rice model prediction inaccuracies in the UHF and VHF TV bands in mountainous terrain," IEEE International Symposium on Broadband Multimedia Systems and Broadcasting (BMSB) 2015, Ghent, Belgium, 17-19/06/2015.

2. Stylianos Kasampalis, Brunel University London, UK, stylianos.kasampalis@brunel.ac.uk
Pavlos I. Lazaridis, University of Huddersfield, pavloslazaridis@hotmail.com
Zaharias D. Zaharis, Aristotle University of Thessaloniki, Greece.
Octavian Fratu, Alexandru Martian, Razvan Craciunescu, Alexandru Vulpe, Simona Halunga, University Politehnica of Bucharest, Romania.
ofratu@elcom.pub.ro, martian@radio.pub.ro "Comparative study of Radio Mobile and ICS Telecom propagation prediction models for DVB-T," IEEE International Symposium on Broadband Multimedia Systems and Broadcasting (BMSB) 2015, Ghent, Belgium, 17-19/06/2015.

3. Stylianos Kasampalis [(1)], Pavlos I. Lazaridis [(2)], Zaharias D. Zaharis [(3)], John P. Cosmas [(1)], and Ian A. Glover [(2)].
[(1)] Brunel University, London, UB8 3PH, UK.
[(2)] University of Huddersfield, Queensgate, Huddersfield, HD1 3DH, UK.
[(3)] Aristotle University of Thessaloniki, GR-54124 Thessaloniki, Greece.
"Longley-Rice model precision in case of multiple diffracting obstacles," URSI AT-RASC 2015, Gran Canaria, Canary Islands, 18-22 May 2015.

4. Stylianos Kasampalis, Pavlos I. Lazaridis, Zaharias D. Zaharis, Aristotelis Bizopoulos, Spiridon Zettas, John Cosmas, "Comparison of Longley-Rice, ITU-R P.1546 and Hata-Davidson propagation models for DVB-T coverage prediction coverage prediction," IEEE International Symposium on Broadband Multimedia Systems and Broadcasting (BMSB) 2014, Beijing, China, 06/2014.

5. S. Kasampalis, P. I. Lazaridis, Z. D. Zaharis, J Cosmas, A Bizopoulos, P. Latkoski, L. Gavrilovska, O. Fratu, R. Prasad, "UHF TV band spectrum and field-strength measurements before and after analog switch-off," GWS (GLOBAL WIRELESS SUMMIT) 2014, Aalborg, Denmark, 05/2014.

6. Stylianos Kasampalis, Pavlos I. Lazaridis, Zaharias D. Zaharis, Aristotelis Bizopoulos, Spyridon Zettas, John Cosmas, "Comparison of ITM and ITWOM Propagation Models for DVB-T Coverage Prediction," IEEE International

Symposium on Broadband Multimedia Systems and Broadcasting (BSMB) 2013; London, 06/2013.

7. Stylianos Kasampalis, Pavlos I. Lazaridis, Zaharias D. Zaharis, Aristotelis Bizopoulos, Spiridon Zettas, John Cosmas, "Comparison of Longley-Rice, ITM, and ITWOM propagation models for DTV and FM Broadcasting," GWS (GLOBAL WIRELESS SUMMIT) 2013, The 16th International Symposium on Wireless Personal Multimedia Communications WPMC 2013, Atlantic City, New Jersey, USA, 24-27 June 2013.

8. Stylianos Kasampalis, Pavlos Lazaridis, Aristotelis Bizopoulos, John Cosmas, Zaharias Zaharis, "Evaluation of Prediction Accuracy for the Longley-Rice model in the FM and TV bands," XI International Conference ETAI 2013, Ohrid, 09/2013.

9. Stylianos Kasampalis, Aristotelis Bizopoulos, Pavlos Lazaridis, Evangelia Paparouni, Dimitrios Drogoudis, Ioannis Dalis, Liljana Gavrilovska, "Coverage Prediction and Validation for DVB-T services," ETAI 2011, Ohrid, 09/2011.

10. Stylianos Kasampalis, Pavlos Lazaridis, Aristotelis Bizopoulos, Emilija Lazarevska, Zaharias Zaharis, Anastasia Papastergiou, "A fully portable apparatus for surveillance of electromagnetic broadcast spectrum and measurement of electromagnetic radiation levels," 13th WSEAS International Conference on COMMUNICATIONS, Rodos, Greece, 07/2009.

1.7 REFERENCES

[1] P.L. Rice, A.G. Longley, K.A. Norton, and A.P. Barsis. "Transmission loss predictions for tropospheric communications circuits," Technical Note 101, revised 1/1/1967, U.S. Dept. of Commerce NTIA-ITS.

[2] S. Kasampalis, P. Lazaridis, Z. Zaharis, A. Bizopoulos, S. Zettas, J. Cosmas "Comparison of ITM and ITWOM propagation models for DVB-T coverage prediction," IEEE BMSB 2013 conference, London, June 2013.

[3] NTIA, National Telecommunications & Information Administration. Available online at https://www.ntia.doc.gov/home

[4] NASA, "Shuttle Radar Topography Mission data,". Available online at http://www2.jpl.nasa.gov/srtm/.

[5] Roger Coud Coudé, Web page of Radio Mobile, a site for downloads and How to http://www.cplus.org/rmw/english1.html, freeware by VE2DBE.

[6] SPLAT! A Terrestrial RF Path Analysis Application for Linux/Unix. Available online at http://www.qsl.net/kd2bd/splat.html.

[7] S. E. Shumate, "Longley-Rice and ITU-P.1546 combined: A new international terrain-specific propagation model," in *Proc. 2010 IEEE 72nd Vehicular Technology Conference Fall (VTC 2010-Fall),* Sept. 2010, pp.1-5.

[8] Hata/Davidson, "A Report on Technology Independent Methodology for the Modeling, Simulation and Empirical Verification of Wireless Communications System Performance in Noise and Interference Limited Systems Operating on Frequencies between 30 and 1500MHz," TIA TR8 Working Group, IEEE Vehicular Technology Society Propagation Committee, May 1997.

[9] Federal Communication commission's terrain database calculator. Available at: https://www.fcc.gov/media/radio/haat-calculator.

[10] "Method for point-to-area prediction for terrestrial services in the frequency range 30 MHz to 300MHz," Recommendation ITU-R P.1546-5, 2013. Available at: http://www.itu.int

[11] "Propagation by diffraction," Recommendation ITU-R P.526-13, 11/2013, P Series, Radiowave propagation. Available at: www.itu.int/rec/R-REC-P.526-13-201311-I

[12] J. Epstein and D. W. Peterson, "An experimental study of wave propagation at 850 Mc," Proc. IRE, vol. 41, pp. 595-611, 1953.

[13] J. Deygout, "Multiple Knife-Edge Diffraction of Microwaves," IEEE Trans on Antennas and Propagation. Vol. 14, pp. 480-489, Apr. 1966.

[14] J. Deygout, "Correction Factor for Multiple Knife-Edge Diffraction," IEEE Trans on Antennas and Propagation. Vol. 39, No. 8, pp. 1256-1258, August 1991.

[15] C. L. Giovaneli, "An analysis of simplified solutions for multiple knife-edge diffraction," IEEE Trans on Antennas and Propagation, vol. 32, pp. 297-301, Mar. 1984.

[16] D. J. Gibson, "The Communications Handbook," 1996, USA, CRC Press, Inc.

[17] W. C. Y. Lee, “Mobile Cellular Telecommunications: Analog and Digital Systems,” McGraw-Hill, 1995.

[18] S. R. Saunders, A. Aragon-Zavala, “Antennas and Propagation for Wireless Communication Systems,” Book, ISBN 978-0-470-84879-1, John Wiley & Sons, Ltd, p.52, 2007.

[19] W. Fischer, “Digital Video and Audio Broadcasting Technology,” Book, 3rd Edition, ISBN 978-3-642-11611-7, Springer, 2010.

[20] C. Haslett, “Essentials of Radio Wave Propagation,” Book, Cambridge Wireless Essentials Series, ISBN-13 978-0-521-87563-3, Cambridge University Press, 2008.

[21] R. L. Freeman, “Fundamentals of Telecommunications,” Book, 2nd Edition, ISBN 0-471-71045-8, John Wiley & Sons Publication, 2005.

[22] T. Manning, “Microwave Radio Transmission Design Guide,” Book, 2nd Edition, ISBN-13 978-1-59693-456-6, Artech House, 2009.

[23] J. D. Parsons, “The Mobile Radio Propagation Channel,” Book, 2nd Edition, ISBN 0-471-98857-X, John Wiley & Sons Ltd, 2000.

[24] P. Fontán, M. Espiñeira, “Modeling the Wireless Propagation Channel: A simulation Approach with MATLAB,” Book, ISBN 978-0-470-72785-0, John Wiley & Sons Publication, 2008.

[25] R. L. Freeman, “Radio System Design for Telecommunications,” Book, 3rd Edition, ISBN 978-0-471-75713-9, John Wiley & Sons Inc. Publication, 2007.

[26] K. Chang, “RF and Microwave Wireless Systems,” Book, ISBN 0-471-35199-7, John Wiley & Sons Inc., 2000.

[27] C. J. Bouras, “Trends in Telecommunications Technologies,” Book, ISBN 978-953-307-072-8, InTech, 2010.

[28] A. F. Molisch, “Wireless Communications,” Book, 2nd Edition, ISBN 978-0-470-74186-3, John Wiley & Sons Ltd., 2011.

[29] J. C. Whitaker (Editor-in-Chief), “The Electronics Handbook,” 2nd Edition, ISBN 0-8493-1889-0, Taylor & Francis Group, 2005.

CHAPTER 2

2.1 LITERATURE REVIEW

2.1.1 OVERVIEW

Radio propagation is significant in everyday life because information distributed wirelessly, like television, radio and mobile telephony signals, Wi-Fi signals, and computer data are carried out by electromagnetic waves.

When radio propagation takes place without any problems and covers the area that was designed for, everything is working fine. Otherwise, detailed analysis of the received signal must be done to ensure that information will be received intact. In that case propagation models are used to predict the strength signal in an area.

Radio propagation is a term that refers to radio waves as they travel from one place to another, typically from a transmitter to a receiver over some distance through the atmosphere and are affected by various phenomena such as reflection, refraction, diffraction, absorption, scattering, and polarization. The signal strength becomes weaker, less stable, its shape may be distorted, and even its frequency may change. The most interesting feature, in our research, is the signal strength. When the radio wave is transmitted over a great distance, the strength signal weakens because the power density decreases and so the field strength decreases too. In free space radio waves travel in straight lines. Changes in moisture and temperature in the troposphere and local temperature, air pressure, and moisture can occasionally increase the distance of radio waves propagation by bending their path over the horizon. It can also cause a very significant rise in signal strength levels at great distances for a short period (Ducting). The fact is that taking on-site measurements is inconvenient because it costs in time and money. Therefore, the use of a prediction model becomes a necessity.

The massive increase in designing broadcast systems for digital TV and cellular systems necessitates the development of accurate point-to-area prediction tools. In electromagnetic wave propagation theory there is a significant number of coverage prediction models for DVB-T coverage. The main types of propagation models are three (for other authors are two, empirical and deterministic models). The empirical models that are based on measurement data, they are simple and use statistical data, but they are not very accurate. The semi-deterministic models that are based on empirical data and deterministic aspects. And the more accurate deterministic models that are based on electromagnetic theory require a lot of geometrical information about the site and the

terrain profile and need a very significant computational effort.

2.1.2 PAPERS AND BOOKS STUDIED FOR THIS SURVEY

The ITS (Irregular Terrain Model) [1-2] is a radio propagation model for frequencies between 20 MHz and 20 GHz, it is also known as Longley-Rice model, named for Anita Longley & Phil Rice and it was published in 1968. The model, predicts the path loss of a radio signal considering the distance between transmitter and receiver and the variability of the radio signal in time and space. The ITS model is based on electromagnetic theory and statistical analyses combining terrain features and radio measurements. Even today, the model is officially used for prediction purposes in the United States of America.

Kenneth Bullington [3] proposed a simplified method that replaces two or more knife-edge obstructions by an equivalent single knife-edge. In practice, this approach gives far too optimistic results. Epstein and Peterson [4] proposed a procedure that has no physical support and only estimates the diffraction loss appropriately at each obstacle or knife-edge and then adds the losses. Millington [5] in his paper gave a complete mathematical analysis of the double knife-edge diffraction and explained Epstein-Peterson's method. Also, Deygout [6] proposed another more accurate geometrical construction to consider multiple diffracting knife-edges. Its approach can easily be extended to three or more knife-edge obstacles repeating the procedure of two knife-edges systematically.

Deygout's approximation used a nomograph proposed by Millington at al. to correct the excess of path loss that took place between hills close to each other and with the same individual loss. In his paper [7] published in 1991, he proposed a mathematical expression to replace that nomograph and which is easy to use. He claims that the utilitation of this correction factor gives a mean error, between measurements and evaluations, less than 1 dB. Deygout's method with its correction factor is often used today.

Giovaneli's method [8] is a modification of Deygout's method that could result in a better accuracy in some cases. This method can be easily extended to multiple knife-edges. A rigorously exact diffraction loss for more than two knife-edges can be calculated using Vogler's method [9].

The empirical Hata model [10] on the other hand, uses mathematical equations that involve antenna heights of transmitter and receiver, frequency 150 MHz to 1500 MHz, distance from the base station ranges from 1 km to 20 km in urban, suburban and open

area environments. It is an extension of Okumura's method, and it is based on Okumura's field test results for the city of Tokyo, Japan [11]. The Telecommunications Industry Association (TIA) recommended a modification to the Hata model to cover a broader range of input parameters and distances. The model is known as Hata-Davidson model and provides corrections for links up to 300 km distance and transmitters at an altitude up to 2500 m. It was published as TSB-88A [12].

The BBC R&D White Paper WHP 048 [13] describes the coverage prediction models used for planning DVB-T services in the UK. The UKMP (UK Planning Model) is used in this paper that was derived from an earlier so-called "BBC" model. It was previously used for analog TV planning, and the principles of field strength prediction methods are described by J. H. Causebrook and B. Davis [14]. These methods can also be used to produce a computer software to calculate field strengths at UHF. The described models have a lot of similarities to the "Longley-Rice" model that was used for analog TV planning in the US. The UK Planning Model predicts the received strength signal at a location considering the geographical area between transmitter and receiver. The model creates an elevation profile between the two points, runs the Edge Detection module, computes the diffraction loss and the clutter loss and finally calculates the strength of the received signal. Paper [15] presents, analytically, the main propagation prediction methods developed during the last 60 years, resulting from purely theoretical models, statistical models, deterministic ray-optical models and measurement directed methods. Authors propose seven significant categories for path loss models which are: (1) theoretical/foundational, (2) basic, (3) terrain, (4) supplementary, (5) stochastic fading, (6) many-rays, and (7) active measurement models and fourteen subcategories. Authors also believe that the next generation of prediction models will be data-centric that arising from direct measurements and hybrid prediction techniques. Furthermore, the same authors in [16] implement and analyse 30 propagation models of different popularity that were presented in a time span of 65 years. This publication uses five new metrics to gauge performance, gives an analysis based on collected measurements in various frequency bands (900 MHz, 2.4 GHz, 5.8 GHz) and calculates a Root Mean Square Error (RMSE) of the accuracy of the predictions in the range of 12-15 dB that can be lowered after fine-tuning of the models with measurement results to about 8-9 dB.

In the ITU-R Recommendation P.1546-4 (10/2009) [17] a complete method is proposed for the calculation of field-strengths based on formulas and graphs. The ITU

recommends this method for the coverage prediction of DVB-T services. Furthermore, in this document, a procedure for compatibility between ITU-R P.1546 recommendation and the Okumura-Hata empirical method is described. Moreover, in the ITU-R Report BT.2137 [18] there are comparisons between measurements and propagation prediction methods used in the UK (the UKPM method), Canada (CRC-PREDICT propagation model), Japan (similar to that used in UK), Australia (Longley-Rice model, Anderson 2D model, Recommendation ITU-R P.1546, Recommendation ITU-R P.370+RMD, Free-Space+RMD), and Brazil (similar to that used in UK). There is also, in this report a section on software development, Swiss software, Canadian CRC software, etc. and measurements in the Trondheim area in Norway. It is to be noticed that results are compared to the Longley-Rice, ITU-R P.1546, ITU-R P.370+RMD (Reflection plus Multiple Diffraction loss), Anderson 2D and Free-Space+RMD models. In [19] there is a detailed presentation of how the Irregular Terrain Model (ITM-Longley-Rice) and the ITU-R 1546-4 model are incorporated into the SEAMCAT (Spectrum Engineering Advanced Monte Carlo Analysis Tool) propagation prediction software and their respective calculation parameters. SEAMCAT is an open source free licensing software, and it is based on the Monte-Carlo simulation method. It was developed at the European Communications Office (ECO) within the frame of European Conference of Postal and Telecommunication Administrations (CEPT).

In the EBU technical review [20] a comparison between semi-empirical and entirely deterministic models are presented for DVB-T and DAB coverage and spectrum planning. The combination of a slope diffraction technique in conjunction with suitable path profiles, antenna patterns, and relevant planning margins had, as a result, the creation of an efficient platform for accurate predictions. Comparisons are made between CDS (Cellular Design Services) model and Causebrook model. Parameters for network performance optimization are discussed. The impact of high-resolution terrain data, taken from stereo aerial photography and Laser interferometry, on calculation accuracy is also shown. In [21] there is an extensive comparison of multiple-diffraction models such as Deygout, Causebrook, Giovaneli and Vogler models, for more than 20.000 measured path-profiles. The above deterministic models are selected because they produce high accuracy prediction results and have low computation times. In this study, the Vogler's exact solution is found, as expected, to have the best accuracy the same as the Slope-UTD deterministic method developed by the authors. Causebrook solution gives better results than Deygout and Giovaneli solutions which have lower

accuracy. Furthermore, in [22] a computationally efficient method is proposed for the calculation of the Vogler's multiple integrals for multiple diffractions of cylindrical waves, only in the case of obstacles of constant height and spacing, like in the case of a center of a city environment. In paper [23] some results are presented for the Longley-Rice model using the NASA S.R.T.M (Shuttle Radar Mission Topography) [24] terrain database and the SPLAT! [25] (Signal Propagation, Loss and Terrain analysis tool for Linux) software which use ITM (Longley-Rice) and ITWOM [26] models. The author, S.E. Shumate presents the ITWOM model as a new propagation model that is arising from the combination of the Longley-Rice model, ITU-R P.1546 Recommendation, and other ITU Recommendations, Snell's Law and Beer's Law. In that paper, there is also a comparison between the ITU-R P.1546 and Okumura-Hata models. In the technical report [27] by the Radiocommunications Agency Netherlands, there is a detailed description of a measurement campaign that has been performed along paths between The Netherlands and the United Kingdom, relating to TV interferences and the prediction accuracy of the ITU-R P.1546. A modified version of ITU-R P.1546-4 with added improved Terrain Clearance Angle (TCA) correction gives promising results for very flat terrain and distances up to 100 kilometres. The latter is found to require improvements for mixed paths (land-sea), but also for paths over the very flat terrain. During this study, some flaws in commercial propagation prediction and planning software have been found.

In [28] the validity of the three ITU models, ITU-R P.1546-0, ITU-R P.1546-1, and ITU-R P.1546-2 is analysed in a short-range terrestrial environment for common rural areas in Australia, and it is found that P.1546-2, on average, underestimates field-strength by 10 dB. Vegetation information provided by the Department of Agriculture, Western Australia, and land usage are incorporated in the predictions. A proposed definition for the effective antenna height is given. Models ITU-R P.1546-0 and ITU-R P.1546-1 compared with Okumura-Hata model (urban, suburban) provide a better prediction of path loss. In [29] a case study on the Island of Mauritius is described by the authors. A comparative study of path loss took place with the use of existing propagation models and the selection of the best ones. Models like Free Space Propagation model, Okumura-Hata path loss model, Extended COST-231 Hata model, Lee model and ITU-R P.370 Propagation prediction method are described analytically in this study. Extended COST-231 and Okumura-Hata empirical models show the best results, but in general, for the regions of Mauritius, all models were insufficient. In [30]

a measurement campaign around a 1 kW UHF Channel 48 (677 MHz) DTV station is described. Service coverage was measured using 16 radials plus five more radials at the major lobe. In total, 92 test (measurement) points were used and 3 receiving antenna heights. Antenna heights of 9 meters and 6 meters were used for fixed reception when antenna heights of 1.5 meters were used for portable reception. The path loss exponents are calculated from the measured data for the three antenna heights and compared to the empirical Okumura-Hata and COST 231 models. The whole study took place around Quezon City in the Philippines.

In [31] an extensive and carefully planned field trial was performed during the winter of 2007/2008 in Uxbridge (UK) to validate predictions from theoretical modeling and laboratory simulations. The transmissions were conducted in the 730 MHz (UHF Ch 53) frequency band with a DVB-T/H transmitter, two 100 W amplifiers, and an EIRP of 18.4dBW (70 Watts). In this work, it is proving, that the quality of reception, in fast fading mobile broadcasting applications, is remarkably improved if transmit delay diversity is applied to systems using the DVB-T standard. In [32] some common path loss models are presented, especially in the context of mobile communications. Models such as Okumura-Hata, COST 231-Walfish-Ikegami, the COST 207 GSM model, ITU-R models, the 3GPP Spatial Channel Model, the ITU-Advanced Channel Model and the 802.15.4a UWB Channel Model have presented analytically and in depth.

In [33] a DVB-T measurement campaign is described and documented in detail. This work presents the research efforts of Brunel University, Broadreach systems, and Dibcom SA in the context of the EC funded project PLUTO that explored the use of diversity to improve coverage in difficult propagation conditions. In [34] investigation of mobile reception for DVB-T signals in SFN (Single Frequency Networks) and MFN (Multi Frequency Networks) is performed using the new open standard for multimedia and data broadcasting DVB-T. Many field trials of DVB-T are presented in various cities (Cologne, Berlin, Amsterdam), in view of mobile reception (MOTIVATE project-Mobile Television and Innovative Receivers), and the thresholds of correct reception are identified. In the early publication [35] Recommendation ITU-R BT.1368-3, the main characteristics of a DVB-T system are described from frequency planning, minimum required field-strengths, and protection from interferences. In [36], a comparative study between the results of a measurement campaign conducted in northern Greece, simulations produced by Radio Mobile (ITM) and ICS Telecom software by ATDI and estimations generated from ITU-R P.1546 recommendation, Okumura-Hata-Davidson

models and ITU525/526 recommendation is performed in the context of digital TV planning in Greece according the ITU GE-06 frequency plan. In this work [37] related to the European project COST 273, an investigation of two types of vehicular antennas, roof antennas, and window antennas, took place. Several field trials and measurement campaigns were carried out in the city of Paris, as well as simulations with specialized software in view of improving mobile DVB-T reception antennas, mainly used in cars. Field tests have shown a more effective behaviour for the window antennas.

In CEPT/ERC Recommendation 74-02 E [38] the guidelines and Spectrum Analyser settings for accurately measuring FM, DAB, ATV, and DTV signal field strength. The method of measuring the field strength at specific points refers to the frequency range of 29.7-960 MHz. In the BBC, White Paper [39] a detailed description of TV signal measurements in the VHF/UHF TV Bands and the accurate use of calibrated log-periodic reception antennas is presented. The method that BBC R&D uses to calibrate the field strength measurement equipment it is described in detail, so it can be used for fieldwork.

In [40] a DVB-T test-bed development is presented for experimental transmissions and a measurement plan for evaluating transmit diversity in DVB-T networks, field-trials are described, and some laboratory and field experiments are identified. It is also mentioned that transmit diversity is more practical than receive diversity, because, on the one hand, it is quite difficult to place two receive antennas far enough apart in a small mobile apparatus and on the other side, transmit diversity improves the transmission of signals in Non-Line-Of-Sight (NLOS) cluttered environments.

In [41], comparisons are made between precision field strength measurements taken by a Rohde & Schwarz FSH-3 portable spectrum analyser with simulation results derived from coverage prediction models, like the NTIA-ITS Longley-Rice model, using the 3-arc-second SRTM (Shuttle Radar Topography Mission) data that is available freely, and the recently developed ITWOM (Irregular Terrain with Obstructions Model). In paper [42] comparisons between measurements and estimations produced by ITU-R, Deygout, Epstein-Peterson, Edward-Darkin and Blomquist-Ladell methods are taking place in the hilly terrain of Tirupati of Southern India. The main conclusion is that only Blomquist-Ladell method overestimates the observed path loss. In [43] measurements taken in the complex environment of Vladivostok in Russia for COFDM-based digital television system are compared with estimations produced by the Longley-Rice model. The conclusion is that for line-of-sight paths, Longley-Rice model gives satisfactory results

but for non-line-of-sight paths gives underestimated values. An evaluation [44] between Longley-Rice Model and GTD (Geometrical Theory of Diffraction) models is taking place in that paper. In [45] the authors modifying the universal Okumura-Hata model to compare field strength predictions with measurements taken in a commercial CDMA network in rural Australia.

In [46] a comparative study of path loss for digital television broadcasting at UHF band using existing propagation models such as Free-Space, Lee, Hata and Extended COST-231, took place at the Mauritius tropical island in the Indian Ocean during October 2005. The field strength measurements carried out at three different distances of 5 km, 10 km, and 15 km with the use of two receiving antennas of 4 m and 6 m height. According to the authors, Hata models give better results.

In [47] the National Managers Spectrum Association (NMSA) working group provides a new version of Over-the-Horizon Loss (OHLOSS) programs. This tutorial analyses many factors that affect point to point propagation and describes algorithms and steps for calculating path loss. The most important propagation mechanisms are involved in the OHLOSS computation. In this recommendation, ITU-R P.526-13 [48] several propagation models are presented. The reader will be able to evaluate the result of diffraction on the received field strength. The models that are included can be implemented to different types of obstacles and paths of various geometries. It must be mentioned that some well-known models are not described under their known names, for example, methods described on page 22 are Epstein-Peterson and Deygout methods.

In [49] instructions are given for the correct implementation and use of the Longley-Rice model for evaluating TV interference and service coverage. This bulletin is divided into three parts. In part one, information is provided for assessing TV coverage. In part two, information is provided for assessing interference for analogue (NTSC) and digital (DTV) TV. In part three, information is provided for the correct implementation of the FCC's Longley-Rice computer program.

In [50] comparison between popular models is taking place in parts of West Germany, in the VHF range. Topographical data were received from IABG terrain data bank. This study shows advantages and shortcomings of the involved methods in predicting path loss and field strength. In [51] author demonstrates how the Knife-Edge Diffraction (KED) formula contains similar physics to other more rigorous half screen diffraction solutions, so taking into consideration this, engineers can apply common Geometrical Theory of Diffraction (GTD) formulations for all screen diffraction problems.

In [52] terrain path loss is calculated with a new method based on the combination of image theory and multiple knife-edge diffraction theory. Ground reflections are considered for path loss calculation. The method easily can be extended to multiple knife-edge diffractions. In [53] the computational accuracy and speed of Bullington, Epstein-Peterson, Deygout, and Giovaneli models are compared with the rigorous Vogler's method. All models were implemented in MATLAB and found that all are of similar accuracy except the Bullington model. On the other hand, the computation speed of the Bullington, Epstein-Peterson, Deygout and Giovaneli models is much faster than the Vogler's method (microseconds vs. seconds).

In this paper [54] the results of multiple Knife-Edge models, the 'Slack-String' model are presented. The results are compared with those produced by Deygout, Epstein-Peterson, Giovaneli models and Vogler's method. This 'Slack-String' model produces good predictions for most of the presented cases, without adding much computational complexity to the model's code. In [55] investigation of the ITU recommendation for calculating multiple Knife-Edge diffractions is presented. The original ITU formulas are modified into ITU2 formulas to produce more accurate predictions. In [56] information is provided for the R&S® FSH3 Spectrum Analyser, which was our primary measurement tool.

Finally, in [57-59], the datasheets and calibration data of the Schwarzbeck precision antennas, used for measurements in our research, can be found.

For the creation of the elevation profiles an excellent MATLAB program, named "readhgt.m" coded by Francois Beauducel, was used [60].

2.2 SUMMARY

Considering all these papers and books, it can be seen the great interest that exists for the propagation of the electromagnetic waves. Models Longley-Rice, Hata-Davidson, ITU-R P.1546, Deygout, Epstein-Peterson and Giovaneli, are selected for this survey. A significant number of comparisons between simulation results produced by the propagation models and extensive field measurements took place to evaluate the accuracy of the propagation models. The exact scope of this study is to compare accurate field-strength measurements with simulation results around Greece and in some cases around Former Yugoslav Republic of Macedonia (F.Y.R.O.M) and evaluate the precision of the propagation models in various circumstances. Programs, for propagation models involved in that study, were coded in MATLAB for simulation purposes.

2.3 REFERENCES

[1] P.L. Rice, A.G. Longley, K.A. Norton, and A.P. Barsis. "Transmission loss predictions for tropospheric communications circuits," Technical Note 101, revised 1/1/1967, U.S. Dept. of Commerce NTIA-ITS.

[2] P.L. Rice, A.G. Longley, "Prediction of Tropospheric Radio Transmission Loss Over Irregular Terrain – A computer method 1968," Essa Technical Report ERL 79-IT S67.

[3] K. Bullington, "Radio Propagation at frequencies above 30 megacycles," Proc. IRE, vol.35 pp. 1122-1136, especially Fig. 9, p.1131, Oct. 1947.

[4] J. Epstein and D. W. Peterson, "An experimental study of wave propagation at 850 Mc," Proc. IRE, vol. 41, pp. 595-611, 1953.

[5] G. Millington, "Double Knife-Edge Diffraction in Field-Strength Predictions," The Institution of Electrical Engineers, Monograph No. 507E, Mar. 1962.

[6] J. Deygout, "Multiple Knife-Edge Diffraction of Microwaves," IEEE Trans on Antennas and Propagation. Vol. 14, pp. 480-489, Apr. 1966.

[7] J. Deygout, "Correction Factor for Multiple Knife-Edge Diffraction," IEEE Trans on Antennas and Propagation. Vol. 39, No. 8, pp. 1256-1258, August 1991.

[8] C. L. Giovaneli, "An analysis of simplified solutions for multiple knife-edge diffraction," IEEE Trans on Antennas and Propagation. Vol. 32, pp. 297-301, Mar. 1984.

[9] L.E. Vogler, "An attenuation function for multiple knife-edge diffraction," Radio Sci., vol.17, pp. 1541-1546, Nov.-Dec. 1982.

[10] M. Hata, "Empirical Formula for Propagation Loss in Land Mobile Radio Services," IEEE Transactions on Vehicular Technology, Vol. VT-29, No. 3, August 1980.

[11] N. Faruk, Y.A. Adediran, A.A. Ayeni, "Optimization of Davidson Model based on RF measurement conducted in UHF/VHF bands," ICIT 2013, The 6th International Conference on Information Technology, May 8, 2013.

[12] Hata/Davidson, "A Report on Technology Independent Methodology for the Modeling, Simulation and Empirical Verification of Wireless Communications System Performance in Noise and Interference Limited Systems Operating on Frequencies between 30 and 1500MHz," TIA TR8 Working Group, IEEE Vehicular Technology Society Propagation Committee, May 1997.

[13] BBC R&D White Paper WHP 048, “UK planning model for digital terrestrial television coverage,” P.G. Brown, K. Tsioumparakis, M. Jordan, and A. Chong, Sept. 2002.

[14] J.H. Causebrook and B. Davies, “Tropospheric radio wave propagation over irregular terrain: The computation of Field Strength for UHF Broadcasting,” BBC Research Department Report RD 1971/43, 1971.

[15] Phillips, C., D. Sicker, and D. Grunwald, “A survey of wireless path loss prediction and coverage mapping methods,” IEEE Communications, Surveys, Tutorials, vol. 15, 1, pp. 255-270, 2013.

[16] Phillips, C., D. Sicker, and D. Grunwald, “Bounding the practical error of path loss models,” International Journal of Antennas and Propagation, Vol. 2012, 1–21, 2012, doi:10.1155/2012/754158.

[17] ITU-R Recommendation P.1546-4 (10/2009), “Method for point-to-area predictions for terrestrial services in the frequency range 30 MHz to 3000 MHz,”.

[18] ITU-R Report BT.2137, “Coverage prediction methods and planning software for digital terrestrial television broadcasting (DTTB) networks,” 2008.

[19] Dariusz Więcek and Dariusz Wypior, “New SEAMCAT Propagation Models: Irregular Terrain Model and ITU-R P. 1546-4,” National Institute of Telecommunications, Wroclaw, Poland, Journal of Telecommunications and Information Technology, 3/2011, pp. 131-140.

[20] B. Belloul, S. Saunders, “Accurate coverage prediction and optimization for digital broadcasting,” EBU technical review, April 2004.

[21] C. Tzaras, S. R. Saunders, “Comparison of multiple-diffraction models for digital broadcasting coverage prediction,” IEEE Transactions on Broadcasting, vol. 46, No.3, Sept. 2000.

[22] J.L. Leonardo, L. Ramos, “An Explicit Solution for the Diffraction of Cylindrical Waves by Multiple Knife Edges Based on the Vogler Attenuation Function,” Microwave and Optical Technology Letters, Vol.27, No. 4, November 20, 2000.

[23] S. Kasampalis, P. Lazaridis, Z. Zaharis, A. Bizopoulos, S. Zettas, J. Cosmas “Comparison of ITM and ITWOM propagation models for DVB-T coverage prediction,” IEEE BMSB 2013 conference, London, June 2013.

[24] NASA, “Shuttle Radar Topography Mission data,”. Available on line at http://www2.jpl.nasa.gov/srtm/.

[25] SPLAT! A Terrestrial RF Path Analysis Application for Linux/Unix. Available online at http://www.qsl.net/kd2bd/splat.html.

[26] S. E. Shumate, "Longley-Rice and ITU-P.1546 combined: A new international terrain-specific propagation model," in Proc. 2010 IEEE 72nd Vehicular Technology Conference Fall (VTC 2010-Fall), Sept. 2010, pp.1-5.

[27] "Comparison of UHF measurements with the propagation model of Recommendation ITU-R P.1546," The Radiocommunications Agency Netherlands, 2010.

[28] E. Ostlin, H. Suzuki, H.J. Zepernick, "Evaluation of the Propagation Model, Recommendation ITU-R P.1546 for Mobile Services in Rural Australia," IEEE Transactions on Vehicular Technology, vol. 57, no. 1, Jan. 2008.

[29] V. Armoogum, K.M.S., N. Mohamudally, T. Fogarty, "Propagation Models and their Applications in Digital Television Broadcast Network Design and Implementation," Book "Trends in Telecommunications Technologies," ISBN 978-953-307-072-8, Published: March 1, 2010.

[30] F. S. Caluyo, J.C. Dela Cruz, "Antenna Characterization and Determination of Path Loss Exponents for 677MHz Channel using Fixed and Portable Digital Terrestrial Television," Progress in Electromagnetics Research C, Vol.29, 149-161, 2012.

[31] R. Di Bari, M. Bard, A. Arrinda, P. Ditto, G. Araniti, J. Cosmas, Kok Keonk Loo, R. Nilavalan, "Measurement Campaign on Transmit Delay Diversity for Mobile DVB-T/H Systems," IEEE Transactions on Broadcasting, vol. 56, No.3, June 2010.

[32] "Wireless Communications, 2nd Edition," Book edited by Andreas F. Molisch, ISBN 978-0-470-74186-3, 2011. Appendices 7.6.1-7.6.7.

[33] R. Di Bari, M. Bard, K.M. Nasr, Y. Zhang, J. Cosmas, K.K. Loo, R. Nilavalan, H. Shirazi, K. Krishnapillai, Gerard Pousset, Vincent Recrosio, "Evaluation of Diversity Gains for DVB-T Systems," project PLUTO, Brunel University, February 20, 2015.

[34] The MOTIVATE project (Mobile Television and Innovative Receivers), http://cordis.europa.eu/project/rcn/46611_en.html.

[35] Recommendation ITU-R BT.1368-3. Planning criteria for digital terrestrial television services in the VHF/UHF bands.

[36] O. Fratu, A. Martian, R. Craciunescu, A. Vulpe, S. Halunga, P. Lazaridis, Z. Zaharis, S. Kasampalis, "Comparative Study of radio Mobile and ICS Telecom propagation prediction models for DVB-T," IEEE BMSB 2015 conference, Ghent, Belgium, June 2015.

[37] A. Guena, D. Zapparata, A. Sibille, G. Pousset "Mobile diversity reception of DVB-T signals using roof or window antennas," European Cooperation in the field of scientific and technical research, EURO-COST, COST 273, Athens, Greece, 26-28, Jan 2004.

[38] CEPT/ERC Recommendation 74-02 E (Bucharest 1999). "Method of Measuring the Field Strength at Fixed Points in the Frequency Range 29.7 – 960 MHz," Located at http://www.erodocdb.dk/docs/doc98/official/pdf/Rec7402e.pdf

[39] BBC, R & D White Paper, WHP 001. "The calibration of VHF/UHF field strength measuring equipment," April 2001.

[40] H. Shirazi, R. Di Bari, J. Cosmas, R. Nilavalan, Y. Zhang, J. Loo, M. Bard, "Testbed Development & Measurement Plan for Evaluating Transmit Diversity in DVB Networks," IEEE, Mobile and Wireless Communications Summit, 2007, 16th, IST, Budapest, July 2007.

[41] S. Kasampalis, P. Lazaridis, Z. Zaharis, S. Zettas, J. Cosmas, "Comparison of Longley-Rice, ITM, and ITWOM propagation models for DTV and FM broadcasting," WMPC 2013 conference, Atlantic City, New Jersey, USA, June 24-27, 2013.

[42] T. Rama Rao, S. Vijaya Bhaskara Rao, M.V.S.N. Prasad, S.K. Sarkar, "Single Knife-Edge diffraction propagation studies over a hilly terrain," IEEE Transactions on Broadcasting, Vol. 45, No. 1, March 1999.

[43] S. Shkolniy, "Applicability of the Longley-Rice Model for COFDM-Based Digital Television Broadcasting," Department of Electronic and Communications Facilities, School of Engineering, Far Eastern Federal University, Vladivostok, 690091, Russian Federation.

[44] K. A. Champerlin, R. J. Luebbers, "An Evaluation of Longley-Rice and GTD Propagation Models," IEEE Transactions on Antennas and Propagation, vol. ap-30, No.6, pp. 1093-1098, November 1982.

[45] L. Akhoondzadch-Asl, N. Noori, "Modification and Tuning of the Universal Okumura-Hata Model for Radio Wave Propagation," Proceedings of Asia-Pacific Microwave Conference 2007.

[46] V. Armoogum, K.M.S. Soyjaudah, N. Mohamudally, T. Fogarty, "Comparative study of Path Loss using Existing Models for Digital Television Broadcasting for Summer Season in the North of Mauritius," IEEE, The Third Advanced International Conference on Telecommunications, AICT'07, 2007.

[47] NSMA (National Spectrum Managers Association), Recommendation WG 2.99.052 (Supersedes Rec. 2.89.023), Ohloss Path Loss Computation with Ohloss Tutorial (formerly Rep. WG 2.95.010)

[48] Recommendation ITU-R P.526-13 (11/2013). P Series Radiowave propagation.

[49] Federal Communication Commission US, OET Bulletin No.69, "Longley-Rice Methodology for Evaluating TV Coverage and Interference," February 06, 2004.

[50] R. Grosskopf, "Comparison of Different Methods for the Prediction of the Field Strength in the VHF Range," IEEE Transactions on Antennas and Propagation, Vol. Ap-35, No. 7, July 1987.

[51] G. D. Durkin, "The Practical Behavior of Various Edge-Diffraction Formulas," IEEE Antennas and Propagation Magazine, Vol. 51, No. 3, June 2009.

[52] J. Komijani, A. Mirkamali, J. Nateghi, "Combining Multiple Knife-Edge Diffraction and Ground Reflections for Terrain Path Loss Calculation," Antennas and Propagation (EuCAP), 2010 Proceedings of the Fourth European Conference on, 12-16 April 2010.

[53] D. A. Bibb, J. Dang, Z. Yun, M. F. Iskander, "Computational Accuracy and Speed of Some Knife-Edge Diffraction Models," IEEE Antennas and Propagation Society International Symposium (APSURSI), 6-11 July 2014.

[54] T. L. Rusy, "A Study of the 'Slack-String' Knife-Edge Diffraction Model," Antennas and Propagation, 2009, EuCAP 2009, 3rd European Conference on, 23-27 March 2009.

[55] J. Li, J. -F. Wagen, E. Lachat, "ITU model for multi-knife-edge diffraction," IEE Proceedings – Microwaves, Antennas and Propagation, Vol. 143, No. 6, December 1996.

[56] https://www.rohde-schwarz.com/us/product/fsh3-6-18-productstartpage_63493-358532.html

[57] http://www.schwarzbeck.de/Datenblatt/k9113.pdf

[58] http://www.schwarzbeck.de/Datenblatt/91159135.pdf

[59] http://www.schwarzbeck.de/Datenblatt/k9143.pdf.

[60] François Beauducel, “READHGT: Import/download NASA SRTM data files (.HGT). Created on 25 August 2012 and updated on 27 December 2016. Available online at URL: https://www.mathworks.com/MATLABcentral/fileexchange/36379-readhgt-import-download-nasa-srtm-data-files---hgt-

CHAPTER 3

A SURVEY ON PROPAGATION MODELS

3.1 OVERVIEW

Physical mechanisms of electromagnetic wave propagation are free space propagation, reflection, diffraction, and scattering. These mechanisms determine the propagation of electromagnetic signals. Methods and models have been developed for predicting radio wave propagation. One must remember that the radio channel is time variant. Propagation models are divided into empirical-statistical models and deterministic-geometrical models. Empirical models are better adapted to a quick and approximate calculation of coverage. Empirical models calculate field strength without requiring a detailed knowledge of the terrain. These models use data obtained from extensive measurements in different environments and use simple equations with little dependence on the cartographic data. Deterministic-geometrical models may be computationally-intensive and time-consuming, but they result in a much more accurate calculation of geographical radio coverage. These models require a detailed knowledge of the terrain and take into account the earth's curvature. In some literature, a third category of propagation models can be found, named as semi-empirical models or semi-deterministic models; it is the combination of the two above mentioned types of models.

3.2 THE FREE SPACE PROPAGATION MODEL

This model is used to predict received power at a point when between transmitter and receiver there are no obstacles. The received power by a receiver antenna which has a distance d from the transmitter is given by the Friis free space equation (Friis, 1946).

$$P_r(d) = \frac{P_t G_t G_r \lambda^2}{(4\pi)^2 d^2} \tag{3.1}$$

where, P_t is the transmitted power, P_r is the received power, G_t is the transmitter antenna gain, G_r is the receiver antenna gain, d is the distance between transmitter and receiver and λ is the wavelength in meters. The path loss is given by,

$$P_L(dB) = 10log_{10}\left(\frac{P_r}{P_t}\right) = 10log_{10}\left[\frac{(4\pi)^2 d^2}{G_t G_r \lambda^2}\right] \tag{3.2}$$

Developing the logarithm and replacing λ by the well-known formula $\lambda=c/f$, the equation (3.2) can be expressed regarding distance, *d(km)* and frequency of operation, *f(MHz)*, with the expanding formula (3.3)

$$P_L(dB) = -G_t(dB) - G_r(dB) + 32.44 + 20\log_{10} d(Km) + 20\log_{10} f(MHz) \quad (3.3)$$

3.3 EMPIRICAL-STATISTICAL MODELS

3.3.1 The Okumura Model

One of the most widely used models for signal prediction in urban areas is Okumura's model [1]. It is used for frequencies in the range of 150 MHz to 1920 MHz, distance from the base station ranging from 1 km to 100 km and base station antenna heights ranging from 30 m to 1000 m. Okumura developed a set of curves resulting from many measurements that took place in and around the city of Tokyo.

The formula for the Okumura model is:

$$L_{50}(dB) = L_F + A_{mu}(f,d) - G(h_{te}) - G(h_{re}) - G_{AREA} \quad (3.4)$$

where,

L_{50} is the median (50th percentile) value of propagation path loss.

L_F is the free space propagation loss.

A_{mu} is the median attenuation relative to free space.

$G(h_{te})$ is the base station antenna height gain factor.

$G(h_{re})$ is the mobile antenna height gain factor.

G_{AREA} is the gain due to the type of environment.

Okumura found that $G(h_{te})$ and $G(h_{re})$ gain factors vary.

$G(h_{te})$ varies at a rate of 20dB/decade, and $G(h_{re})$ varies at a rate of 10dB/decade for heights less than 3m.

Variations of the $G(h_{te})$ and $G(h_{re})$ parameters are given below,

$$G(h_{te}) = 20\log_{10}\left(\frac{h_{te}}{200}\right) \qquad 1000\ m > h_{te} > 30\ m \quad (3.5)$$

$$G(h_{re}) = 10\log_{10}\left(\frac{h_{re}}{3}\right) \qquad h_{re} \le 30\ m \quad (3.6)$$

$$G(h_{re}) = 20\log\left(\frac{h_{re}}{3}\right) \qquad 10\ m > h_{re} > 3\ m \quad (3.7)$$

For a broad range of frequencies, plots of $A_{mu}(f, d)$ and G_{AREA} are shown in Figure 3-1 and Figure 3-2.

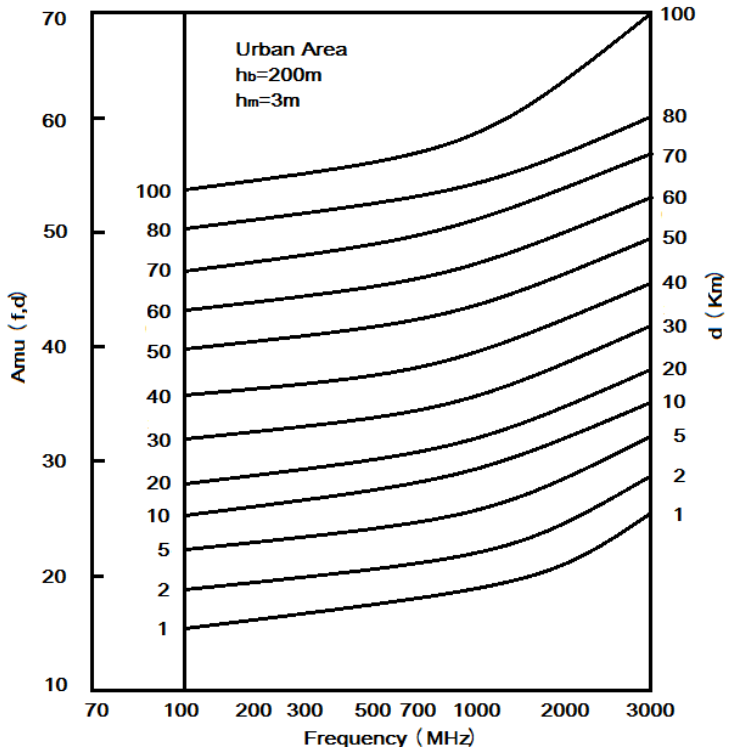

Figure 3-1: Median attenuation relative to free space *($A_{mu}(f, d)$)*, over the quasi-smooth terrain. Reproduced from Okumura et al. [1968].

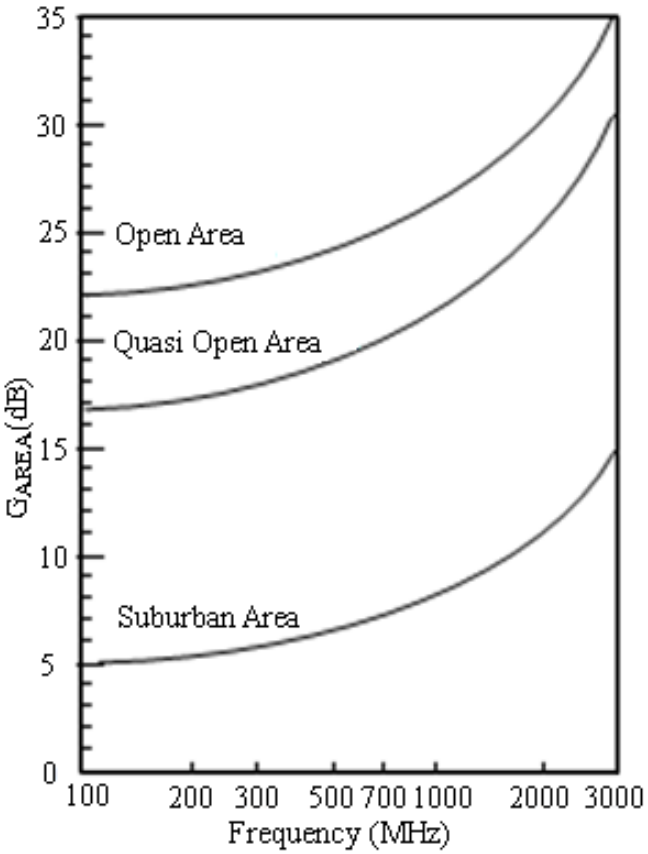

Figure 3-2: *G_{AREA}*, for different types of terrain. Reproduced from Okumura et al.[1968].

3.3.2 The Okumura–Hata Model

This model is one of the most popular models even today and is an entirely empirical model [2]. It is wholly based upon an extensive series of measurements took place in and around Tokyo. To make Okumura's model easier for computer implementation, Hata, produced a series of formulae from Okumura's curve. It uses mathematical equations that involve antenna heights of transmitter and receiver, frequency 150 MHz to 1500 MHz, distance from the base station ranges from 1 km to 20 km in urban, suburban and open area environments. The model is widely used even today.

The standard formula for path loss calculation in urban areas is given by,

$$L_{50}(urban)(dB) = 69.55 + 26.16\log_{10} f_c - 13.82\log_{10} h_{te} - a(h_{re}) + (44.9 - 6.55\log_{10} h_{te})\log_{10} d \quad (3.8)$$

where,

f_c is the frequency in MHz

h_{te} is the effective transmitter antenna height from 30 m to 200 m.

h_{re} is the effective receiver antenna height from 1 m to 10 m.

$a(h_{re})$ is the mobile antenna correction factor, see definition below.

d is the distance between transmitter and receiver in km.

- For medium-sized city, $a(h_{re})$ is given by,

$$a(h_{re}) = (1.1\log_{10} f_c - 0.7)h_{re} - (1.56\log_{10} f_c - 0.8)\ (dB) \quad (3.9)$$

- For large size city, $a(h_{re})$ is provided by,

$$a(h_{re}) = 8.29(\log_{10} 1.54h_{re})^2 - 1.1 \quad (dB) \ \ for\ f_c \le 300\ MHz \quad (3.10)$$

$$a(h_{re}) = 3.2(\log_{10} 11.75h_{re})^2 - 4.97 \quad (dB) \ \ for\ f_c > 300\ MHz \quad (3.11)$$

- For suburban area path loss is provided by,

$$L_{50}(suburban)(dB) = L_{50}(urban)(dB) - 2[\log_{10}(f_c/28)]^2 - 5.4 \quad (3.12)$$

- For open rural areas path loss is given by,

$$L_{50}(open\ rural\ areas)(dB) = L_{50}(urban)(dB) - 4.78(\log_{10} f_c)^2 + 18.33\log_{10} f_c - 40.94 \quad (3.13)$$

3.3.3 The COST 231–Hata Model

The European Cooperative formed the COST 231 [3] working committee for Scientific and Technical Research (EURO-COST). This working committee developed an extended version of the Hata model that covers frequencies from 1500 MHz to 2000 MHz, h_{te} effective transmitter antenna height from 30 m to 200 m, h_{re} effective receiver antenna height from 1 m to 10 m and d distance between transmitter and receiver from 1 km to 20 km.

Path loss calculation is given by,

$$L_{50}(urban)(dB) = 46.33 + 33.9\log_{10} f_c - 13.82\log_{10} h_{te} - a(h_{re}) + (44.9 - 6.55\log_{10} h_{te})\log_{10} d + C_M \quad (3.14)$$

where, $a(h_{re})$ is defined in Okumura-Hata model, and C_M is provided by,

$$C_M = \begin{cases} 0\ dB & \text{for medium sized city and suburban areas} \\ 3\ dB & \text{for metropolitan centres} \end{cases}$$

3.3.4 The Hata-Davidson Model

The Telecommunications Industry Association (TIA) recommended a modification to the Hata model to cover a broader range of input parameters and distances. The model is known as the 'Hata-Davidson' model [4] and provides corrections for links up to 300 km distance and transmitters at an altitude of up to 2500 m and covers a frequency range of 30-150 MHz. The model uses HAAT (antenna Height Above Average Terrain) parameter. Many programs can calculate HAAT, e.g., HAAT can be calculated using NAD83/WGS84, FCC's terrain database, and the GLOBE 1 km database [5]. It should be clarified that the term "HAAT" refers to the HAAT in the direction of the propagation path radial under consideration and not to the overall site HAAT.

The formulas of the Hata-Davidson model are given below, [6] [7],

$$PL_{HD} = PL_{Hata} + A(h_1, d_{km}) - S_1(d_{km}) - S_2(h_1, d_{km}) - S_3(f_{MHz}) - S_4(f_{MHz}, d_{km}) \quad (3.15)$$

where,

$$PL_{Hata} = 69.55 + 26.16\log_{10} f_{MHz} - 13.82\log_{10} h_1 - a(h_2) + (44.9 - 6.55\log_{10} h_1)\log_{10} d_{km} \quad (3.16)$$

and the correction factor for the mobile antenna height, $a(h_2)$ is defined by equation (3.17)

$$a(h_2)\begin{cases}(1.1\log_{10} f_{MHz}-0.7)\cdot h_2-(1.56\log_{10} f_{MHz}-0.8). \\ \text{for medium small city ,quasi}-\text{open, open area} \\ \\ 8.29\left(\log_{10}(1.54\cdot h_2)\right)^2-1.1 \\ \text{for large city and } f_c \le 300\ MHz \\ \\ 3.2\left(\log_{10}(11.75\cdot h_2)\right)^2-4.97 \\ \text{for large city and } f_c > 300\ MHz\end{cases} \quad (3.17)$$

where,

h_1 is the base station antenna height HAAT (20-2500 m).

h_2 is the mobile station antenna height (1-10 m).

d_{km} is the transmission distance in km (1-300 km).

A and S_1 are factors that extend the distance to 300 km

S_2 is a correction factor for the height h_1 of the base station antenna extending the value of h_1 to 2500 m,

S_3 and S_4 are correction factors that extend the frequency to 1500 MHz.

Definitions of the A and S terms are given below in Table 3-1.

Table 3-1. Parameters used in the Hata-Davidson model.

Distance in km (d_{km})	$A(h_1, d_{km})$	$S_1(d_{km})$
$d_{km} < 20$	0	0
$20 < d_{km} < 64.38$	$0.62137(d_{km}-20)\cdot$ $[0.5 + 0.15\log_{10}10(h_1/121.92)]$	0
$64.38 < d_{km} < 300$	$0.62137(d_{km}-20)\cdot$ $[0.5 + 0.15\log_{10}10(h_1/121.92)]$	$0.174(d_{km}-64.38)$

The parameters S_2, S_3, S_4 are defined as

$$S_2(h_1, d_{km}) = 0.00784\,|\log_{10}(9.98/d_{km})|(h_1-300),\ h_1 > 300\ m \quad (3.18)$$

$$S_3(f_{MHz}) = f_{MHz}/250\log_{10}(1500/f_{MHz}) \quad (3.19)$$

$$S_4(f_{MHz} d_{km}) = [0.112\log_{10}(\frac{1500}{f_{MHZ}})](d_{km}-64.38), d_{km} > 64.38\ km \quad (3.20)$$

3.3.5 The Lee Model

The Lee model [8-9] is a simple model. It uses data taken from measurements in several locations, together with the effective base station antenna height which depends on the variations in the terrain.

Path loss formula is given by,

$$L = 10n\log_{10} R - 20\log_{10} h_{b(eff)} - P_o - 10\log_{10} h_m + 29 \quad (dB) \tag{3.21}$$

where,

n and P_o are taken from measurements as shown in Table 3-2, $h_{b(eff)}$ is the effective height of the base station antenna and, h_m is the height of the mobile station antenna. All the measurements were made at 900 MHz, so for other frequencies, correction factors must be applied.

Table 3-2. Parameters n and P_o for the Lee model

Environment		n	P_o
Free space		2	-45
Open area		4.35	-49
Suburban		3.84	-61.7
Urban	Philadelphia	3.68	-70
	Newark	4.31	-64
	Tokyo	3.05	-84
	New York city	4.8	-77

The effective base station height, $h_{b(eff)}$ is defined as the projection of the slope of the terrain where the mobile station is to the base station location. Effective heights h_A, h_B, h_C and h_D are depicted in Figure 3-3.

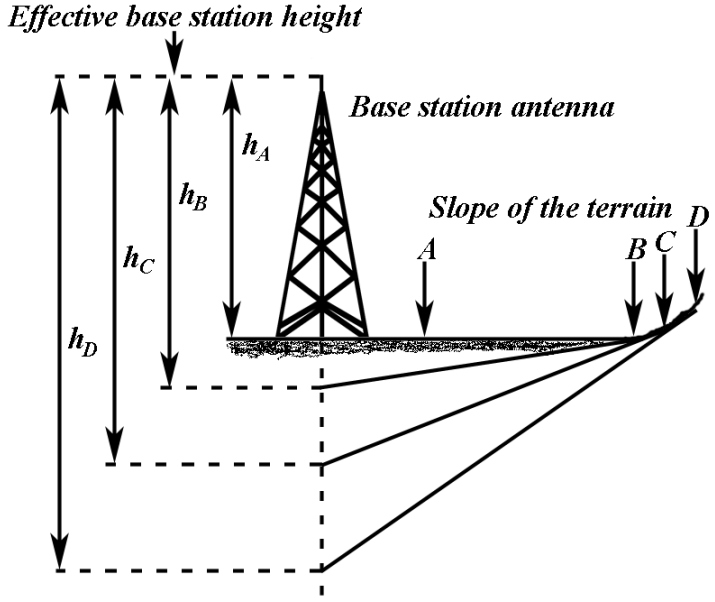

Figure 3-3: Effective base station antenna height for Lee's model.

3.3.6 The ECC-33 Model

Okumura made a series of extensive measurements in and around the city of Tokyo. Typical European suburban areas are entirely different to those found in Tokyo. The ECC (Electronic Communications Committee) proposed the ECC-33 path loss model [10]. In that model, original measurements by Okumura were extrapolated and modified to represent a wireless system carefully.

The path loss model is defined as,

$$P_L(dB) = A_{fs} + A_{bm} - G_t - G_r \tag{3.22}$$

where, A_{fs} is free space attenuation, A_{bm} is basic median path loss, G_t is gain factor for transmitter antenna, G_r is gain factor for receiver antenna and defined as,

$$A_{fs} = 92.4 + log_{10}(d) + log_{10}(f) \tag{3.23}$$

$$A_{bm} = 20.41 + 9.83 log_{10}(d) + 7.894 log_{10}(f) + 9.56 [log_{10}(f)]^2 \tag{3.24}$$

$$G_t = log_{10}(\frac{h_b}{200})[13.98 + 5.8(log_{10}(d))^2] \tag{3.25}$$

for medium-sized cities, G_r is defined as,

$$G_r = [42.57 + 13.7 log(f)][log(h_m) - 0.585] \tag{3.26}$$

f in GHz, h_b height of transmitter antenna in meters, h_m height of transmitter antenna in meters.

3.3.7 ITU-R Models

The Radiocommunication Sector of the ITU (International Telecommunications Union - formerly CCIR), developed a set of international technical standards for Radiowave propagation, known as ITU-R Recommendations. These recommendations describe propagation models that are widely accepted and used for calculation of path loss and field signal strength. The full text of the recommendations may be obtained online from http://www.itu.int/rec/R-REC-P. These recommendations are the results of studies produced by Radiocommunication study groups on Radiowave propagation.

Three recommendations are briefly summarized below.

3.3.8 The ITU-R P.370 Recommendation.

One of the better known and very frequently used classical empirical methods is the one based on ITU-R 370 Recommendation [11]. This approach relies on the use of empirically derived field-strength curves that are of a good statistical accuracy. These

curves are functions of frequency, antenna height, distance and time percentage. Extrapolation and interpolation methods are used to derive data from these empirical curves.

The received power P_r at a distance d is given by,

$$P_r = \frac{|E|^2}{120\pi} A_e \tag{3.27}$$

or

$$P_r(dB) = 20\log E - 10\log(120\pi) + 10\log A_e \tag{3.28}$$

$$P_r(dB) = 2E_{min} - 10\log(120\pi) + A_e \tag{3.29}$$

where,

E is the field strength.

E_{min} is the field strength at the receiving point.

A_e is the effective antenna aperture(dBm^2).

120π is the value of the intrinsic impedance of free space (ohms).

When values of field strength are available in $dB\mu V/m$ from measurements, the path loss in dB can be calculated as follows,

$$P_L(dB) = P_t(dB) - P_r(dB) \tag{3.30}$$

$$P_L(dB) = P_t(dB) - 2E_{min} - A_e(dB) + 10\log(120\pi) \tag{3.31}$$

$$P_L(dB) = P_t(dB) - 2E_{min}\left(\frac{dB\mu V}{m}\right) + 240 - A_e(dB) + 10\log(120\pi) \tag{3.32}$$

where,

$$E_{min} = E_{min}(dB\mu V/m) - 120 \tag{3.33}$$

3.3.9 The ITU-R P.1411 Recommendation.

This model is relevant to macrocell applications (short range propagation), operates in distances from 20 m to 5 km and frequencies from 300 MHz to 100 GHz and applies to LOS (Light of Sight) and non-LOS systems [12]. The model uses a multiple knife-edge diffraction loss and a specific geometry. It is a simplified version of the COST 231 Walfisch-Ikegami model. For urban areas, parameters are defined as below:

h_b is the base station antenna with a range of 4-50 m.

h_m is the mobile station antenna with a range of 1-3 m.

h_o is the height of the mobile station.

f_c frequency ranges from 800 to 2000 MHz, for $h_b \leq h_o$,

f_c frequency ranges from 800 to 5000 MHz, for $h_b > h_o$,

3.3.10 The ITU-R P.1546 Recommendation.

The Radio Communication Sector of ITU has more recently proposed Recommendation ITU-R P.1546 [13], to replace the older ITU-R 370. It is a method for point-to-area-prediction for terrestrial services in the frequency range 30 MHz to 3 GHz. The field strength (dBμV/m) is calculated for 1 kW ERP (Effective Radiated Power).

Sample propagation curves of Recommendation ITU-R P.1546 that are used for the calculation of field strength, with the proper interpolations, are shown in Figure 3-4. The propagation curves are designed for 1 kW effective radiated power (ERP). If the ERP of the transmitter under study is different, then the difference in dB must be added to the values of field strength produced by the propagation curves.

The latest version is ITU-R P.1546-5, released on September 2013.

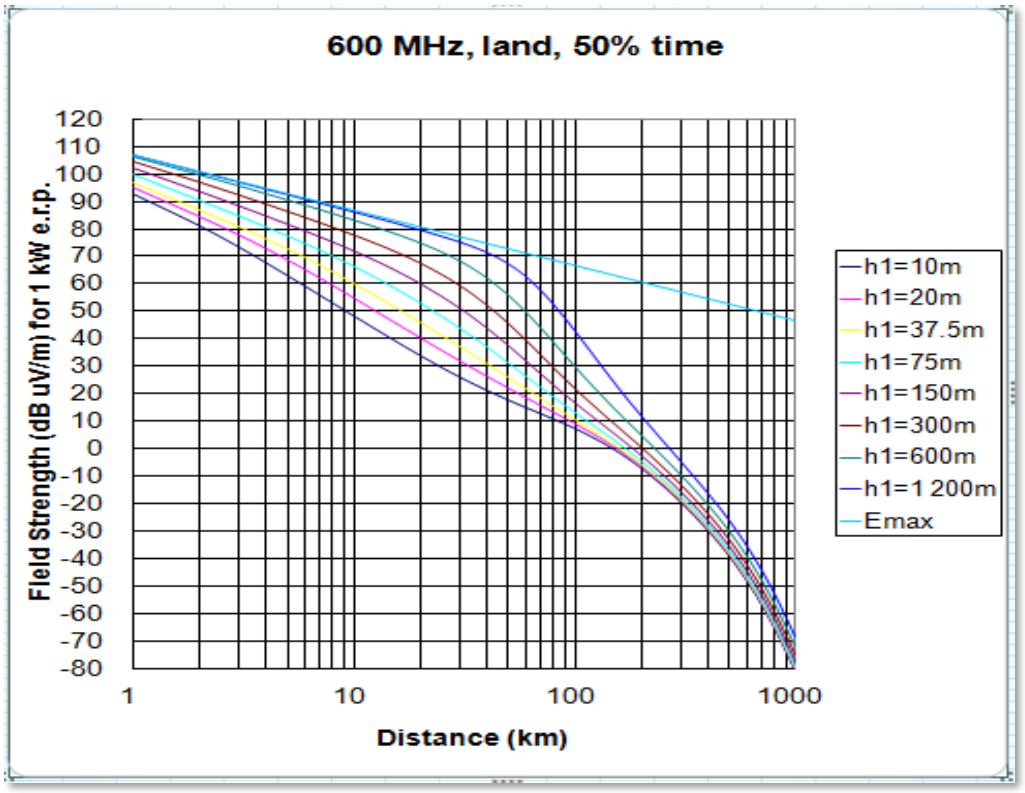

Figure 3-4: Sample propagation curves of Recommendation ITU-R.P.1546.

Paths and elevation profiles can be extracted, e.g., from Google Earth to compute the heights Heff (m) and Hb (m). The time percentage is assumed to be 50%, and the receiver antenna altitude is 10 m.

3.3.11 The Walfisch-Bertoni Model

This model was developed by Walfisch and Bertoni [14]. It can be considered as the limiting case of the flat edge model. It considers the conflict between rooftops and buildings heights for diffraction and scattering and calculates the average signal strength at street level considering that the buildings heights are uniformly distributed, and the separation between buildings is equal. In this model, the path loss is given by,

$$PL(dB) = PL_o + PL_{down} + PL_{rooftops} \tag{3.34}$$

where,

PL_o is the free space path loss between isotropic antennas, at a distance R and is defined as,

$$PL_o = \left(\frac{4\pi R}{\lambda}\right)^2 \tag{3.35}$$

PL_{down} is the rooftop to street diffraction and scattering loss and is defined as

$$PL_{down} = \frac{\lambda}{2\pi^2 (H_B - h_m)} \sqrt{\left(\frac{d}{2}\right)^2 + (H_B - h_m)^2} \tag{3.36}$$

$PL_{rooftops}$ is the multi-screen diffraction due to rows of buildings.

$$PL_{rooftops} = 0.01\left(\frac{h_T - H_B}{0.03R}\right)^{1.8} \left(\frac{d}{\lambda}\right)^{0.9} \tag{3.37}$$

and

λ is the wavelength in meters.

h_T is the transmitter antenna height in meters.

H_B is the building height in meters.

h_m is the mobile antenna height in meters.

d is the space between buildings in meters.

R is the distance between base station transmitter and a mobile station in meters.

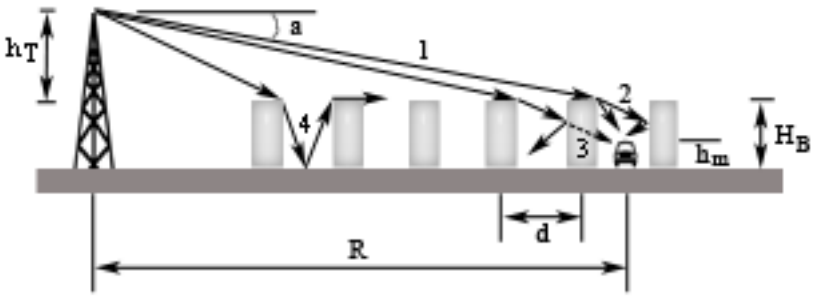

Figure 3-5: Walfisch-Bertoni for UHF propagation geometry for various ray paths in the presence of buildings.

3.4 DETERMINISTIC - GEOMETRICAL MODELS.

3.4.1 Single Knife-Edge Diffraction Model

The classical approach for single knife-edge diffraction and the calculation of path loss over a single sharp obstacle is based on the Fresnel Kirchhoff's theory of optics. The dimensionless parameter *v* is used to express the diffraction loss:

$$v = h\left[\frac{2}{\lambda}\left(\frac{1}{d_1}+\frac{1}{d_2}\right)\right]^{\frac{1}{2}} \tag{3.38}$$

or

$$v = \theta\left[\frac{2}{\lambda\left(\frac{1}{d_1}+\frac{1}{d_2}\right)}\right]^{\frac{1}{2}} \tag{3.39}$$

where,

h is the height between the Knife-Edge (top of the obstacle) and the line of sight (LOS is the straight line joins the transmitter with the receiver), in meters.

θ is the diffraction angle in radians.

d_1 is the distance between the transmitter and the obstruction along the line of sight, in meters.

d_2 is the distance between the receiver and the obstruction along the line of sight, in meters.

λ is the wave length in meters.

The received field strength of a Knife-Edge diffracted wave is given by the well-known complex Fresnel integral:

$$\frac{E}{E_0} = \frac{(1+j)}{2}\int_{\upsilon_0}^{\infty} e^{-j\left(\frac{\pi}{2}\right)v^2}\,dv \tag{3.40}$$

For this theory to be valid, the following approximations must hold:

$$d_1,\ d_2 >> h \text{ and } d_1 d_2 >> \lambda$$

The diffraction attenuation is given by the following equation:

$$G_d(dB) = 20\log|F(v)| \tag{3.41}$$

An approximate solution for the above equation was provided by Lee [15] (see page 5).

3.4.2 The Bullington Method

Bullington [16] proposed a simplified method that replaces the whole profile by a single Knife-Edge. You can see it for two obstacles M1 and M2 in Figure 3-6. In practice, this method gives optimistic results.

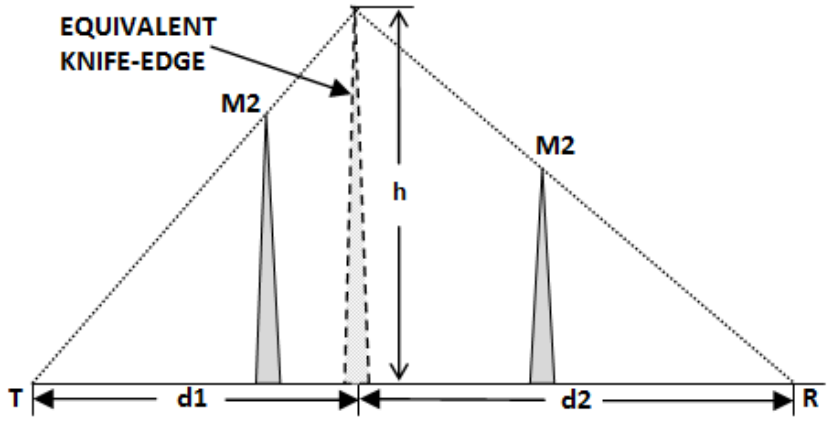

Figure 3-6: Bullington's approach.

3.4.3 Deygout's Approach

Deygout's approach [17-18] for two obstacles is shown in Figure 3-7, M1 is the main obstacle and its associated diffraction loss is calculated as if it were alone, and Fresnel parameter v_1 is calculated as a function of d_1, d_2+d_3, and h_1.

$$v_1 = f(d_1, d_2 + d_3, h_1) \tag{3.42}$$

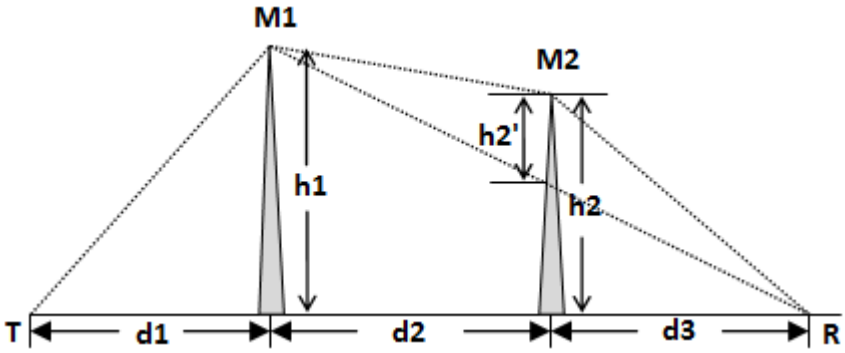

Figure 3-7: Deygout's approach, M1 main hill, M2 on the right.

M2 is the second obstacle, and its diffraction loss is calculated by considering the propagation path between the top of M1 obstacle and the receiver R with an effective height of h_2'. Fresnel parameter v_2 is calculated as a function of d_2, d_3, and h_2'.

$$v_2 = f(d_2, d_3, h_2') \tag{3.43}$$

The case that the secondary hill M2 lies on the left of the main hill M1 is shown in Figure 3-8.

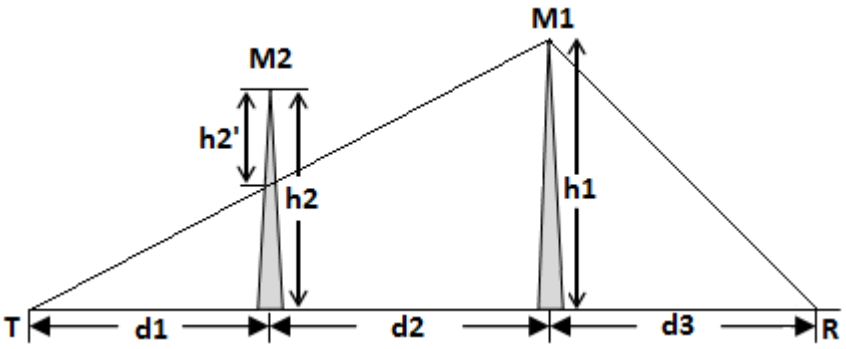

Figure 3-8: Deygout's approach, M1 main hill, and M2 on the left.

M1 again is the main (dominant) obstacle, and its associated diffraction loss is calculated as if it was alone, and Fresnel parameter v_1 is calculated as a function of d_1+d_2, d_3, and h_1.

$$v_1 = f(d_1 + d_2, d_3, h_1) \tag{3.44}$$

M2 is the second obstacle (predominant), lying now on the left of primary obstacle and its diffraction loss is calculated by considering the propagation path between the top of M1 obstacle and the transmitter T with an effective height of h_2'. Fresnel parameter v_2 is calculated as a function of d_1, d_2, and h_2'.

$$v_2 = f(d_1, d_2, h_2') \tag{3.45}$$

Notice that the main obstacle delimits the distances of the second obstacle.

The total path loss then is computed by adding the two individual path losses.

$$G_{dtotal}(dB) = 20\log_{10}|F(v_1)| + 20\log_{10}|F(v_2)| \tag{3.46}$$

In 1991, Deygout [19] published a paper which gives a correction factor (a simple mathematical expression) for his method, which replaces the nomograph proposed by Millington et al. This correction tends to reduce the path loss thus increasing so the calculated field strength.

3.4.4 The Causebrook Correction

In cases where there are many edges, or the pairs of edges are very close together, Deygout's approach tends to overestimate path loss. Causebrook and Davis [20] proposed an approximate correction to this problem. In that correction, only the edges that lie above the relative line of sight paths are considered.

3.4.5 Epstein-Peterson's Method

Epstein and Peterson [21] proposed a method that estimates the diffraction loss at each obstacle or Knife-Edge and then adds the losses. This approach is entirely mathematically explained by Millington [20]. This method is shown in Figure 3-9.

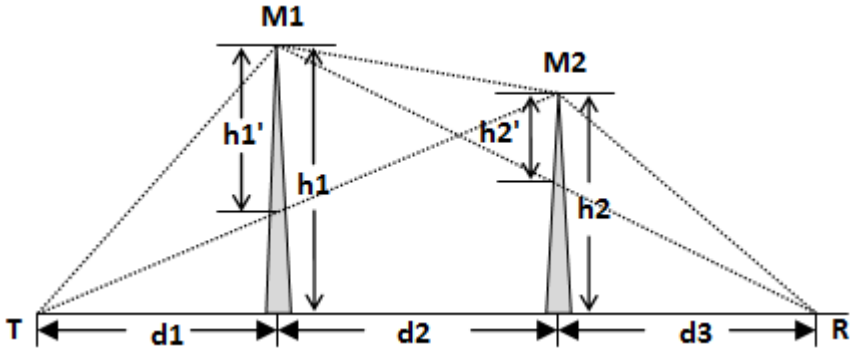

Figure 3-9: Epstein-Peterson's approach. M2 on the right of M1.

First, the diffraction loss is calculated at the Knife-Edge M2 which is caused by the Knife-Edge M1 on the signal from the source at T. The heights considered small compared with the distances d_1, d_2, d_3. Parameter v_1 is computed as a function of d_1, d_2, and effective height h_1'.

$$v_1 = f(d_1, d_2, h_1') \tag{3.47}$$

The Knife-Edge M1 is now treated as a signal source, and the receiving signal at receiver R is calculated considering the diffraction loss caused by Knife-Edge M2. Parameter v is computed as a function of d_2, d_3, and effective height h_2'.

$$v_2 = f(d_2, d_3, h_2') \tag{3.48}$$

The case in which the secondary obstacle M2 lies on the left of the main obstacle M1 is the same as before and is shown in Figure 3-10. The only change is in the used distances for the obstacles M1 and M2.

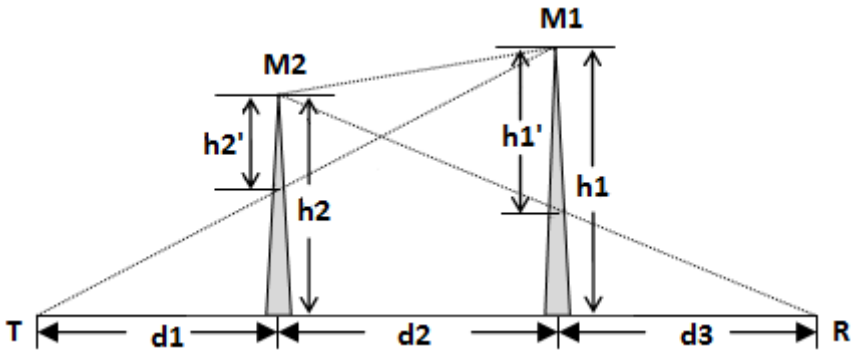

Figure 3-10: Epstein-Peterson's approach. M2 on the left of M1.

Parameter v_1 for obstacle M1 is defined by equation (3.49)

$$v_1 = f(d_2, d_3, h_1') \tag{3.49}$$

And parameter v_2 for obstacle M2 is defined by equation (3.50)

$$v_2 = f(d_1, d_2, h_2') \tag{3.50}$$

Then the total loss is:

$$G_{dtotal}(dB) = 20\log_{10}|F(v_1)| + 20\log_{10}|F(v_2)| \tag{3.51}$$

If losses L_1 and L_2 caused by M1 and M2 obstacles exceed about 15 dB each, a correction term L_c must be added to the total diffraction loss. Term L_c is given by the formula below.

$$L_c = 10\log_{10}\left[\frac{(d_1+d_2)(d_2+d_3)}{d_2(d_1+d_2+d_3)}\right] \tag{3.52}$$

The term is described in Recommendation ITU-R P.526-13 (11/2013).

3.4.6 Giovaneli's Method

Giovaneli [22] proposed another method modifying Deygout's method. This method for two obstacles is shown in Figure 3-11 but easily can extend to multiple edges.

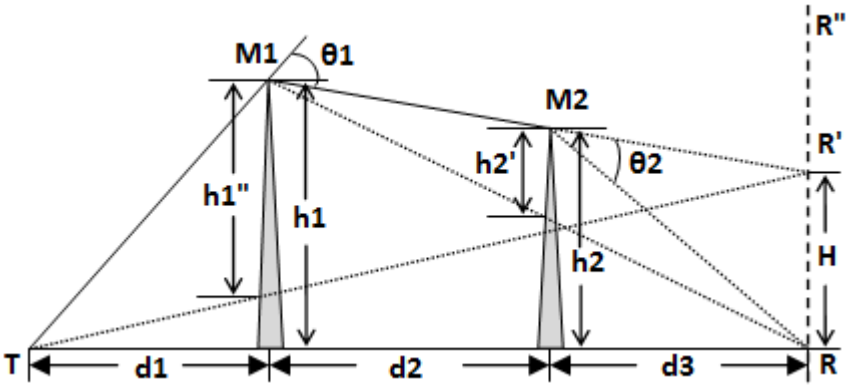

Figure 3-11: Giovaneli's approach, M2 on the right of M1.

Assume that M1 is the main obstacle. An observation plane RR" passing through point R, the receiver, is introduced. The field on surface RR" produced by M1 is derived by projecting M1 onto plane RR", and the effective height h_1'' is given by

$$h_1'' = h_1 - \frac{d_1 H}{d_1 + d_2 + d_3} \tag{3.53}$$

where, parameter H is given by

$$H = h_2 + \frac{(h_2 - h_1)d_3}{d_2} \tag{3.54}$$

Fresnel parameter v_1 now is a function of

$$v_1 = f(d_1, d_2 + d_3, h_1'') \tag{3.55}$$

The effective height h_2'' *of* the secondary obstacle M2 is defined by

$$h_2'' = h_2 - \frac{d_3 h_1}{d_2 + d_3} \tag{3.56}$$

Fresnel parameter v_2 now is a function of

$$v_2 = f(d_2, d_3, h_2') \tag{3.57}$$

and the total loss is given by

$$G_{dtotal}(dB) = 20\log|F(v_1)| + 20\log|F(v_2)| \tag{3.58}$$

The case that the secondary obstacle M2 lies on the left of the main obstacle M1 is shown in Figure 3-12.

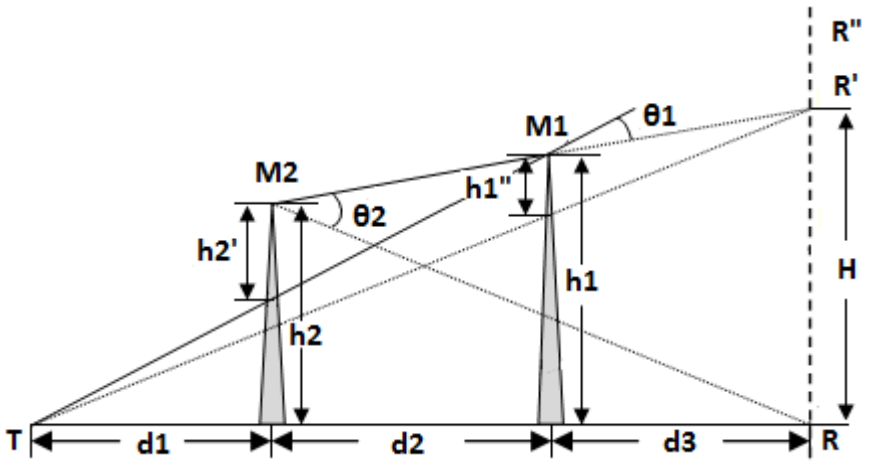

Figure 3-12: Giovaneli's approach. M2 on the left of M1.

Parameters h_1'', H, h_2' are defined as below.

$$h_1'' = h_1 - \frac{(d_1 + d_2)\cdot H}{d_1 + d_2 + d_3},\ H = h_1 + \frac{d_3 \cdot (h_1 - h_2)}{d_2},\ h_2' = h_2 - \frac{d_1 \cdot h_1}{d_1 + d_2} \tag{3.59}$$

Fresnel parameter v_1 now is a function of

$$v_1 = f(d_1 + d_2, d_3, h_1'') \tag{3.60}$$

Fresnel parameter v_2 now is a function of

$$v_2 = f(d_1, d_2, h_2') \tag{3.61}$$

This method can be easily extended to multiple knife-edges. In cases where the secondary obstacle lies on the left of the main one Giovaneli's method usually, fails. Generally, in our study, Giovaneli's model didn't give reasonable results in many cases. A rigorously exact diffraction loss for more than two knife-edges can be calculated using Vogler's method [23].

3.4.7 The ITU-R. P. 526 Model - Propagation by Diffraction

Many of the analytical diffraction calculation methods mentioned above are incorporated into recommendation ITU-R. P. 526 [24]. This recommendation presents several models to enable the reader to evaluate the effect of diffraction on the received field strength. The models apply to different obstacle types and various path geometries. This recommendation is to be used for the calculation of field strengths over diffraction paths, which may include a spherical earth surface or irregular terrain with different kinds of obstacles. This model is a good one for modelling the environment for a DVB-T transmission if it is used with a diffraction model like for example the Deygout method, [13] [14]. The ITU-R. P. 526 - Deygout model considers three worst-cases intrusions into the Fresnel zone.

3.4.8 The Longley Rice Model

The NTIA-ITS Longley Rice model, also known as the ITM (Irregular Terrain Model) coverage prediction model [25] is a widely accepted model, it was adopted by the FCC as a standard, and is used for frequencies from 20 MHz to 20 GHz, antenna heights from 0.5 to 3000 m and distances from 200 m to 500 km. It is based on electromagnetic theory and statistical analyses considering both terrain features and radio measurements. The model predicts the attenuation of a radio signal as a function of distance and the signal variability in space and time. This model is frequently implemented using the NTIA point-to-point approach, in conjunction with the freely available SRTM maps and is of a good accuracy [26]. The algorithm of this model is described analytically by Hufford [27] in the two modes, point to point prediction mode and area prediction mode and by Hufford, Longley, and Kissick [28] in the area prediction mode. A detailed analysis of the Longley-Rice equations is given in [29]. The reference attenuation A_{ref} is a continuous function of distance as that shown in Figure 3-13 below. This reference attenuation, A_{ref} is calculated using different propagation methods for the three distance ranges, called the line-of-sight, diffraction, and scatter regions. In the line of sight region

attenuation is computed with the use of two-ray optics formulas, in the region of diffraction a weighted average, A_d, is used and estimates diffraction attenuation over a double Knife-Edge and irregular terrain and in the scatter region a scatter attenuation, A_s, is used considering the scatter computations described by Rice et al.

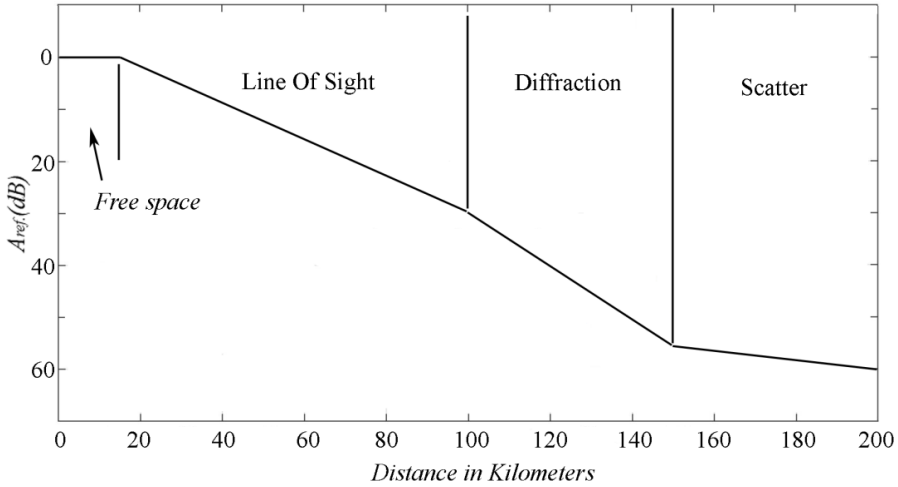

Figure 3-13: Typical plot of reference attenuation A_{ref} versus distance.

The main parameters of the model are frequency; effective radiated power; antenna height; polarization; surface refractivity; permittivity; conductivity; climate zone; earth effective curvature; surface transfer impedance of the ground; situation variability and time variability. These parameters must be correctly estimated to have a more accurate prediction.

This model predicts the reference attenuation A_{ref} as a function of distance d. The variables used to this model are shown in Table 3-3.

Table 3-3. Variables used in the Longley-Rice model.

$\boldsymbol{d}$	Distance between transmitter and receiver
$\boldsymbol{h_{g1}, h_{g2}}$	Transmitter and receiver antenna heights
$\boldsymbol{K}$	Wave number, $k=2\pi/\lambda=f/f_0$, $f_0=47.70$ MHz, λ wavelength in m, f in MHz
$\boldsymbol{\Delta h}$	Terrain Irregularity Parameter
$\boldsymbol{N_s}$	Mean Surface Refractivity in N-units
$\boldsymbol{\gamma_e}$	Earth's Effective curvature in units of reciprocal length
$\boldsymbol{Z_g}$	Surface Transfer Impedance of the ground

Parameters, equations and the procedure are described briefly in the text.

Surface Refractivity is given by,

$$N_S = N_0 e^{-0.1057 z_s} \tag{3.62}$$

where, N_0 is the surface refractivity at sea level, and z_s is the elevation of the surface above mean sea level in km. The earth's effective radius is given by the empirical formula,

$$\gamma_e = \gamma_a \left[1 - 0.04665 e\left(0.005577 N_s\right)\right]^{-1}, \quad \gamma_\alpha = 6370\text{Km}. \tag{3.63}$$

The Terrain Irregularity parameter Δh depends upon terrain profiles and is given in Table 3-4.

Table 3-4. Terrain Irregularity parameter for different terrain profiles

Type of Terrain	**Δh in meters (m)**
Water or very smooth terrain	0-1
Smooth terrain	10-20
Slightly rolling terrain	40-60
Hilly terrain	80-150
Rugged mountains	200-500

The surface transfer impedance is defined as

$$Z_g = \begin{Bmatrix} \sqrt{\varepsilon_r^{'} - 1} & \textit{Horizontal polarization} \\ \sqrt{\varepsilon_r^{'} - \frac{1}{\varepsilon_r^{'}}} & \textit{Vertical polarizaton} \end{Bmatrix} \tag{3.64}$$

where, $\varepsilon_r^{'}$ is the complex relative permittivity defined by,

$$\varepsilon_r^{'} = \varepsilon_r + i Z_o \sigma / \kappa \tag{3.65}$$

ε_r is the relative permittivity, σ is the conductivity of the ground in Siemens per meter, and Z_o=376.62 Ohms.

The reference attenuation A_{ref} is given by the piecewise formula

$$A_{ref} = \begin{Bmatrix} max\left(0, A_{el} + K_1 d + K_2 ln\left(d / d_{Ls}\right)\right) & d \le d_{Ls} \\ A_{ed} + m_d d & d_{Ls} \le d \le d_x \\ A_{es} + m_s d & d_s \le d \end{Bmatrix} \tag{3.66}$$

where,

A_{el} is the attenuation factor due to the line of sight.

A_{ed} is the attenuation factor due to diffraction.

A_{es} is the attenuation factor due to scattering.

The values of the other coefficients are given below.

Initial Calculations for Longley-Rice Model.

Angular distance θ is given in radians by the formula,

$$\theta = \theta_{et} + \theta_{er} + d / \gamma_e \tag{3.67}$$

where, θ_{ej} is the angle between the elevated or depressed horizon rays and the horizon at each antenna j, t for transmitter antenna and r for receiver antenna. The formula for θ_{ej} is

$$\theta_{ej} = \left[0.65 \cdot \Delta h \left(d_{Lsj} / d_{Lj} - 1 \right) - 2h_{ej} \right] / d_{Lsj} \tag{3.68}$$

The distance between transmitter and receiver and the horizontal obstacle is,

$$d_{Lj} = d_{Lsj} e \left[-0.07 \sqrt{\Delta h / max\left(h_{ej}, H3 \right)} \right] \tag{3.69}$$

where,

$H3$=5 m,

$d_{Lsj} = \sqrt{2h_{ej} / \gamma_e}$, j is used for transmitter or receiver either.

$d_{Ls} = d_{Lst} + d_{Lsr}$

$d_L = d_{Lt} + d_{Lr}$

$\theta_e = max\left(\theta_{et} + \theta_{er}, -d_L \gamma_e \right)$, effective angular distance

Diffraction Attenuation

The total diffraction attenuation is given by the formula

$$A_{diff}(d) = (1 - w) A_k + w A_r + A_{fo} \tag{3.70}$$

where,

A_k is the double knife edge attenuation (Epstein-Peterson model is used)

A_r is the rounded earth attenuation

A_{fo} is the clutter factor due to absorption and scattering by water vapor, oxygen, precipitation, and terrain clutter.

The weighting factor w is given by

$$w = \frac{1}{1 + 0.1\sqrt{Q}} \tag{3.71}$$

with

$$Q = \left[1 + 0.045 \left(\frac{\Delta h}{\lambda} \right)^{\frac{1}{2}} \left(\frac{\gamma_a \theta + d_L}{d} \right)^{\frac{1}{2}} \right]^{-1} \tag{3.72}$$

Double Knife Attenuation A_k is given by,

$$A_k = F(v_t) + F(v_r) \tag{3.73}$$

where, $F(v)$ is the Fresnel Integral given by

$$F(v) = 20 \cdot log_{10} \left| \frac{1}{\sqrt{2i}} \int_v^{\infty} e^{i\pi u^2/2} du \right| \tag{3.74}$$

and

$$v_j = \frac{\theta}{2} \cdot \left(\frac{k d_{Lj} (d - d_L)}{\pi d - d_L + d_{Lj}} \right) \tag{3.75}$$

j equals t ($j=t$) for transmitter and j equals r ($j=r$) for receiver

Rounded Earth Attenuation A_r is given by

$$A_r = G(x_0) - F(x_t, K_t) - F(x_r, K_r) - C_1(K_0) \tag{3.76}$$

The three radii method that Vogler's formulation use is used here to find a solution for the above formula. So,

$\gamma_0 = \theta / (d - d_L)$ and $\gamma_j = 2h_{ej} / d_{Lj}^2$, $j=t$ for transmitter and $j=r$ for the receiver

$\alpha_j = (k / \gamma_j)^{1/3}$, $j=t$ for transmitter and $j=r$ for receiver

$K_j = \frac{1}{i\alpha_j Z_g}$, $j=t$ for transmitter and $j=r$ for receiver

$x_o = AB(K_o)\alpha_o \theta + x_t + x_r$ where

$x_j = AB(K_j)\alpha_j \gamma_j d_{Lj}$, $j=t$ for transmitter and $j=r$ for receiver

A is a dimensionless constant with a value of 151.03.

Vogler's formulation solution inserts a special function $W(z)$, for the spherical earth problem.

$$W_i(z) = A_i(z) + iB_i(z) \tag{3.77}$$

the solution is

$$W_t(t_o) = 2^{1/3} K W_t'(t_o) \tag{3.78}$$

The value for B is

$$B = 2^{-1/3} Im\{t_o\} \tag{3.79}$$

and

$$G(x) = 20log_{10}\left(x^{-1/2} e^{x/A}\right) \tag{3.80}$$

$$F(x,K) = 20log_{10}\left|\left(\pi / \left(2^{1/3} AB\right)\right)^{1/2} W_i\left(t_o - \left(x / \left(2^{1/3} AB\right)\right)^2\right)\right| \tag{3.81}$$

$$C_1(K) = 20log_{10}\left|\frac{1}{2}\left(\pi / \left(2^{1/3} AB\right)\right)^{1/2} \left(2^{2/3} K^2 t_o - 1\right) W_i^{'}\left(t_o\right)^2\right| \tag{3.82}$$

Calculation of distances d_3 and d_4 is done using the formulae

$$X_{ae} = \left(k\gamma_e^2\right)^{-1/3} \tag{3.83}$$

$$d_3 = max\left(d_{Ls}, d_L + 1.3787 X_{ae}\right) \tag{3.84}$$

$$d_4 = d_3 + 2.7574 X_{ae} \tag{3.85}$$

$$A_3 = A_{diff}\left(d_3\right) \tag{3.86}$$

and

$$m_d = \left(A_4 - A_3\right) / \left(d_4 - d_3\right) \tag{3.87}$$

Finally, the total diffraction attenuation is given by the formula

$$A_{ed} = A_3 - m_d d_3 \tag{3.88}$$

Line of sight Attenuation

The line of sight attenuation can be calculated using the formula,

$$A_{el} = A_2 - K_1 d_2 \tag{3.89}$$

All the required calculations for solving the above formula are listed below,

$$d_2 = d_{Ls} \quad and \quad A_2 = A_{ed} + m_2 d_2 \tag{3.90}$$

If $A_{ed} \geq 0$, then

$$d_0 = min\left(\frac{1}{2} d_L, 1.908 k h_{et} h_{er}\right) \ and \ d_1 = \frac{3}{4} d_0 + \frac{1}{4} d_L \tag{3.91}$$

and

$$A_0 = A_{los}\left(d_0\right) \quad and \quad A_1 = A_{los}\left(d_1\right) \tag{3.92}$$

$$K_2^{'} = max\left[0, \frac{\left(d_2 - d_1\right)\left(A_1 - A_0\right) - \left(d_1 - d_0\right)\left(A_2 - A_0\right)}{\left(d_2 - d_0\right) ln\left(d_1 / d_0\right) - \left(d_1 - d_0\right) ln\left(d_2 / d_0\right)}\right] \tag{3.93}$$

$$K_1' = \left(A_2 - A_0 - K_2' \ln_e\left(d_2 / d_0\right)\right) / \left(d_2 - d_0\right) \tag{3.94}$$

If $K_1' \geq 0$, then $K_1 = K_1'$ and $K_2 = K_2'$

If $K_1' < 0$, then $K_2'' = \left(A_2 - A_0\right) / \ln_e\left(d_2 / d_0\right)$

and if $K_2'' \geq 0$, then $K_1 = 0$ and $K_2 = K_2''$.

Otherwise, $K_1 = m_d$, $K_2 = 0$.

If $A_{ed} < 0$

$$d_0 = 1.908 k h_{et} h_{er} \tag{3.95}$$

$$d_1 = \max\left(-A_{ed} / m_d, d_L / 4\right) \tag{3.96}$$

If $d_0 \geq d_1$ or $K_2' = 0$, $K_1'' = \left(A_2 - A_1\right) / \left(d_2 - d_1\right)$.

If $K_1'' > 0$, $K_1' = K_1''$ and $K_2 = 0$

Else $K_1 = m_d$, $K_2 = 0$.

So, the attenuation caused due to line of sight is given by

$$A_{los}\left(d\right) = \left(1 - w\right) A_d + w A_t \tag{3.97}$$

The extended diffraction attenuation A_d is given by

$$A_d = A_{ed} + m_d d \tag{3.98}$$

and the two-ray attenuation A_t is given by

$$A_t = -20 \cdot \log_{10}\left|1 + R_e e^{i\delta}\right| \tag{3.99}$$

For the two-ray attenuation,

$$\sin\psi = \frac{h_{et} + h_{er}}{\sqrt{d^2 + \left(h_{et} + h_{er}\right)^2}} \tag{3.100}$$

and if $\left|R_e'\right| \geq \max\left(1/2, \sqrt{\sin\psi}\right)$, then

$$R_e' = \frac{\sin\psi - Z_g}{\sin\psi + Z_g} \exp\left[-k\sigma_h\left(s\right)\sin\psi\right] \tag{3.101}$$

else

$$R_e = \begin{Bmatrix} R_e' \\ \left(R_e' / \left|R_e'\right|\right)\sqrt{\sin\psi} \end{Bmatrix} \tag{3.102}$$

Parameter δ is defined as

$$\delta = \begin{Bmatrix} \delta^{'}, & if\ \delta \le \pi/2 \\ \pi - (\pi/2)^2 / \delta^{'} \end{Bmatrix}$$

where, $\delta^{'} = 2kh_{et}h_{er} / d$

Scattering Attenuation

Distances d_5 and d_6 are defined as

$$d_5 = d_L + D_d \tag{3.103}$$

$$d_6 = d_5 + D_d \tag{3.104}$$

where, D_d=200 km.

Parameters A_5 and A_6 are defined as

$$A_5 = A_{scat}(d_5) \tag{3.105}$$

$$A_6 = A_{scat}(d_6) \tag{3.106}$$

A_{scat} is the component attenuation due to scattering over distance d.

Parameters A_5 and A_6 are undefined sometimes when $d_x = +\infty$ and, A_{es} and m_s is also undefined.

$$m_s = (A_6 - A_5)/D_s \tag{3.107}$$

$$d_x = max\left[d_{Ls}, d_L + X_{ae}log_{10}(kH_s), (A_5 - A_{ed} - m_s d_5)/(m_d - m_s)\right] \tag{3.108}$$

$$A_{es} = A_{ed} + (m_d - m_s)d_x \tag{3.109}$$

where, H_s=47.7 m

The angular distance θ is given by

$\theta = \theta_e + \gamma_e d$, $\theta^{'} = \theta_{et} + \theta_{er} + \gamma_e d$

$r_j = 2k\theta^{'}h_{ej}$, j=t for transmitter and j=r for receiver

If r_r <0.2 and r_t <0.2 attenuation is undefined or infinite over the scattering area.

Else,

$$A_{scat}(d) = 10log_{10}(kH\theta^4) + F(\theta d, N_s) + H_0 \tag{3.110}$$

where, H_0 is the frequency gain function.

So, the total attenuation is calculated, taking into consideration all the above factors.

3.4.9 The Ikegami Model

The Ikegami model [30] tries to produce a deterministic prediction of field strengths at specified points. The model uses a detailed map of building shapes, heights, and positions. The model traces the ray paths between the transmitter and receiver considering only single reflections from walls. Using a single edge approximation, diffraction is calculated at the building nearest the mobile. Wall reflection loss is assumed to be fixed at a constant value. The reflected ray and the diffracted one are summed, resulting in the following approximate model:

$$L_E = 10\log_{10} f_c + 10\log_{10}(\sin\varphi) + 20\log_{10}(h_o - h_m) - 10\log_{10} w - 10\log_{10}(1+\frac{3}{L_r^2}) - 5.8 \quad (3.111)$$

where,

φ is the angle between the street and the direct line from base to mobile station.

h_o is the height of the base station antenna.

h_m is the height of the mobile station antenna.

w is the space between buildings.

Lr is the reflection loss.

The model assumes that the mobile is in the center of the street.

Schematic presentation of the model is shown in Figure 3-14.

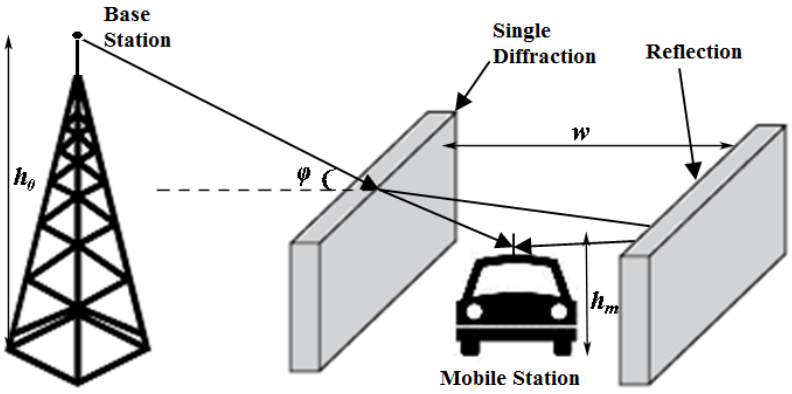

Figure 3-14: The Ikegami model.

3.4.10 The Flat Edge Model

In a mobile phone network, when a macro cell system is operated in a built-up area, the main propagation mode is multiple diffractions over the building rooftops and around the sides of individual buildings. Because buildings are not of the same height, size and spacing the calculation of path loss is complicated enough. In the Flat Edge Model, [31] [32] the whole problem is simplified by assuming that all the buildings have equal height, size, and spacing. The geometry of the model is shown in Figure 3-15.

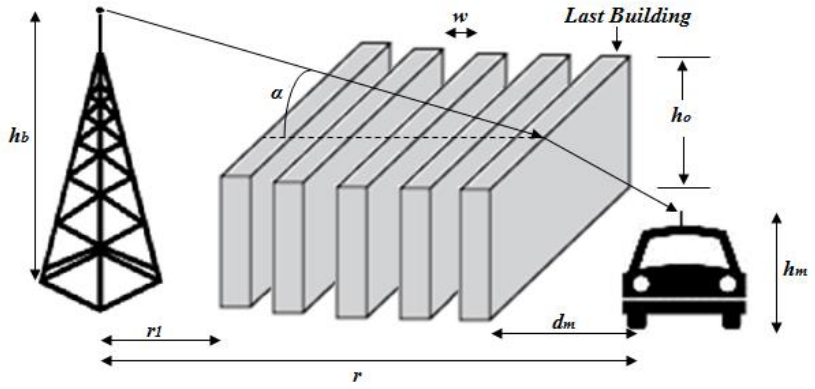

Figure 3-15: The Flat Edge Model.

where,

r_1 is the distance from the base station to the first building.

r is the distance between the base station and mobile station.

a is the elevation angle of the base station antenna from the top of the final building, in radians.

h_b is the height of the base station antenna.

d_m is the distance between mobile station and the last building.

h_m is the height of the mobile station.

h_o is the height of the buildings.

w is the space between buildings.

In this model, the excess path loss is given by equation (3.112)

$$L_{ex} = L_{n-1}(t)L_{ke} \tag{3.112}$$

where,

L_{ke}: calculates single edge diffraction over the final building.

L_{n-1}: calculates multiple edge diffraction over the (n-1) remaining buildings. When the base station is relatively distant from the first building i.e. $r_1 >> nw$ the L_{n-1} is a function of parameter t, where t is given by equation (3.113)

$$t = -\alpha\sqrt{\frac{\pi w}{\lambda}} \tag{3.113}$$

The diffraction parameter $L_n(t)$ is given by equation (3.114)

$$L_n(t) = \frac{1}{n}\sum_{m-0}^{n-1} L_m(t)F_s(-jt\sqrt{n-m}) \;\; for\; n \geq 1 \;\; L_0(t) = 1 \tag{3.114}$$

The Fresnel complex function $F_s(jx)$ is given by equation (3.115)

$$F_s(jx)=\frac{e^{-jx^2}}{\sqrt{2j}}\left\{\left[S\left(x\sqrt{\frac{2}{\pi}}\right)+\frac{1}{2}\right]+j\left[C(x\sqrt{\frac{2}{\pi}})+\frac{1}{2}\right]\right\} \quad (3.115)$$

where,

S and *C* are the standard Fresnel sine and cosine integrals.

$$C(u)+jS(u)=\int_{x=o}^{u} e^{j\pi x^2/2}dx=\int_{x=0}^{u}\cos\frac{1}{2}\pi x^2dx+j\int_{x=0}^{u}\sin\frac{1}{2}\pi x^2dx \quad (3.116)$$

An approximate formula for $L_n(t)$ is given below,

$$L_n(t)=-20\log_{10}A_n(t)=-(c_1+c_2\log_{10}n)\log_{10}(-t)-(c_3+c_4\log_{10}n)(dB) \quad (3.117)$$

where, $c_1=3.29$, $c_2=9.90$, $c_3=0.77$, $c_4=30.26$. Using this formula approximation accuracy is better than ±1.5 dB for

$1\le n\le 100$ and $-1\le t<0$.

Flat edge model uses prediction curves for elevated base antennas.

The total path loss for this model is completed considering the reflections from the buildings across the street using the Ikegami model.

So, the total path loss is given by,

$$L_T=L_n(t)+L_F+L_E \quad (3.118)$$

where,

$L_n(t)$ can be found from (3.114)

L_F is free space path loss

and L_E is the Ikegami formula

$$\begin{aligned}L_E=&10\log_{10}f_c+10\log_{10}(\sin\varphi)+20\log_{10}(h_o-h_m)\\&-10\log_{10}w-10\log_{10}(1+\frac{3}{L_r^2})-5.8\end{aligned} \quad (3.119)$$

3.5 SUMMARY

It is well known that there are many other propagation models but their description here is beyond the scope of this survey. Reference [33] presents, analytically, the primary propagation prediction methods developed during the last 60 years, resulting from purely theoretical models, statistical models, deterministic ray-optical models and measurement directed methods. Some models are designed for mobile telephony and, they are not ideal for broadcasting. Other models are developed for broadcasting, and they are not suitable for mobile telephony, and some models can be used for mobile telephony and broadcasting too. In this survey were used models for broadcasting.

3.6 REFERENCES

[1] Y. Okumura, E. Ohmori, T. Kawano and K. Fukuda, "Field strength and its variability in VHF and UHF land mobile radio service," Review of the Electrical Communications Laboratories, 16, 825–73, 1968.

[2] M. Hata, "Empirical Formula for Propagation Loss in Land Mobile Radio Services", IEEE Transactions on Vehicular Technology, Vol. VT-29, No. 3, p.317-25, August 1980.

[3] COST 231 Final report, Digital Mobile Radio: COST 231 View on the Evolution Towards 3rd Generation Systems, Commission of the European Communities and COST Telecommunications, Brussels, 1999.

[4] Hata/Davidson "A Report on Technology Independent Methodology for the Modeling, Simulation and Empirical Verification of Wireless Communications System Performance in Noise and Interference Limited Systems Operating on Frequencies between 30 and 1500MHz", TIA TR8 Working Group, IEEE Vehicular Technology Society Propagation Committee, May 1997.

[5] Federal Communication Commission's terrain database calculator, https://www.fcc.gov/media/radio/haat-calculator

[6] N. Faruk, Y.A. Adediran, A.A. Ayeni, "Optimization of Davidson Model based on RF measurement conducted in UHF/VHF bands," ICIT 2013, The 6th International Conference on Information Technology, May 8, 2013.

[7] S. Kasampalis, P. Lazaridis, Z. Zaharis, A. Bizopoulos, S. Zettas, J. Cosmas, "Comparison of Longley-Rice, ITU-R.P. 1546, and Hata-Davidson propagation models for DVB-T coverage prediction", IEEE BMSB 2014 conference, Beijing, China, June 2014.

[8] Lee Model W. C. Y. Lee, Mobile Communications Engineering, McGraw-Hill, New York, 1982, ISBN 0-070-37039-7.

[9] W. C. Y. Lee, Mobile Design Fundamentals, John Wiley, New York, 1993, ISBN 0-471-57446-5.

[10] V. Erceg, K.V.S. Hair, M.S. Smith, D.S. Baum, K.P. Sheikh, C. Tappenden, J.M. Costa, C. Bushue, A. Sarajedini, R. Schwartz, D Branlund, T Kaitz, D. Trinkwon, "Channel models for fixed wireless applications," IEEE 802.16 Broadband Wireless Access Working Group, 2001.

[11] "VHF and UHF propagation curves for the frequency range from 30 MHz to 1000 MHz Broadcasting services," Recommendation ITU-R P.370-7, 10/95. URL: http://www.itu.int

[12] International Telecommunication Union, ITU-R Recommendation P.1411-3, "Propagation data and prediction methods for the planning of short-range outdoor radiocommunication systems and radio local area networks in the frequency range 300 MHz to 100 GHz", Geneva, 2005a.

[13] "Method for point-to area prediction for terrestrial services in the frequency range 30 MHz to 300MHz," Recommendation ITU-R P.1546-5, 2013. URL: http://www.itu.int

[14] Walfisch, J., and Bertoni, H. L., "A theoretical model of UHF propagation in urban environments," IEEE transactions on antennas and propagation, Vol. AP-36, pp. 1788-1796, October 1988.

[15] W. C. Y. Lee, "Mobile Cellular Telecommunications: Analog and Digital Systems," McGraw-Hill, 1995.

[16] K. Bullington, "Radio Propagation at frequencies above 30 megacycles," Proc. IRE, vol.35 pp. 1122-1136, October 1947, especially Figure 9, p.1131.

[17] J. Deygout, "Multiple Knife-Edge Diffraction of Microwaves," IEEE Trans on Antennas and Propagation. vol. 14, pp. 480-489, Apr. 1966.

[18] J. Deygout, "Correction Factor for Multiple Knife-Edge Diffraction," IEEE Transactions on Antennas and Propagation. vol. 39, pp. 1256-1258, No.8, August 1991.

[19] J. H. Causebrook and B. Davies, Tropospheric radio wave propagation over irregular terrain: the computation of field strength for UHF broadcasting, BBC Research Report 43, 1971.

[20] J. Epstein and D. W. Peterson, "An experimental study of wave propagation at 850 Mc," Proc. IRE, vol. 41, pp. 595-611, 1953.

[21] G. Millington, "Double Knife-Edge Diffraction in Field-Strength Predictions," The Institution of Electrical Engineers, Monograph No. 507E, Mar. 1962.

[22] C. L. Giovaneli, "An analysis of simplified solutions for multiple knife-edge diffractions," IEEE Trans on Antennas and Propagation., vol. 32, pp. 297-301, Mar. 1984.

[23] L. E. Vogler, "Radio wave diffraction by a rounded obstacle," Radio Sci., 1985, 20, pp. 582-590.

[24] “Propagation by diffraction” Recommendation ITU-R P.526-13, Nov. 2013. URL: http://www.itu.int.

[25] P.L. Rice, A.G. Longley, K.A. Norton, and A.P. Barsis, “Transmission loss predictions for tropospheric communications circuits,” Technical Note 101, revised 1/1/1967, U.S. Dept. of Commerce NTIA-ITS.

[26] NASA, “Shuttle Radar Topography Mission data,” Available on line at http://www2.jpl.nasa.gov/srtm/. The SRTM (3 arc-second) version V2 data can be obtained through the URL: https://dds.cr.usgs.gov/srtm/version2_1.

[27] G.A. Hufford, “The ITS Irregular Terrain Model, version 1.2.2, the Algorithm,” 1995, National Telecommunications and Information Administration, Institute for Telecommunications Sciences, 325 Broadway, Boulder, CO 80303-3328, U.S.A.

[28] G.A. Hufford, A.G. Longley, W.A. Kissick “A Guide to the Use of the ITS Irregular Terrain Model in the Area Prediction Mode,” April 1982, NTIA Report 82-100, U.S Department of Commerce.

[29] K. Ponnusamy, B. E. “Study on Wireless Channel Models,” A Thesis in Electrical Engineering, Texas Tech University, December, 2005.

[30] F. Ikegami, T. Takeuchi, and S. Yoshida, “Theoretical prediction of mean field strength for urban mobile radio,” IEEE Transactions on Antennas and Propagation, 39 (3), 299–302, 1991.

[31] R. Saunders and F. R. Bonar, “Explicit multiple building diffraction attenuation functions for mobile radio wave propagation,” Electronics Letters, 27 (14), 1276–77, 1991.

[32] R. Saunders and A. A. Zavala, Book “Antennas and Propagation for Wireless Communication Systems,” Second Edition, Wiley, p.171-178.

[33] Phillips, C., D. Sicker, and D. Grunwald, “A survey of wireless path loss prediction and coverage mapping methods,” IEEE Communications, Surveys, Tutorials, vol. 15, 1, pp.255-270, 2013.

CHAPTER 4

BASIC THEORY, PROPAGATION MODELS, AND SOFTWARE USED IN THIS STUDY

4.1 OVERVIEW

This chapter summarizes the propagation models used for simulations. Some basic theories and concepts, which are necessary for the understanding of the whole process, will also be presented in detail. Finally, a presentation and description of the programs created in MATLAB will be given**.**

4.2 PROPAGATION MODELS USED IN THIS STUDY

4.2.1 The NTIA-ITS Longley-Rice model, also known as the ITM (Irregular Terrain Model) coverage prediction model.

In all simulations and calculations that took place in this research, this model is compared with all the other models used. ITM [1-2] is a widely accepted model adopted by the Federal Communication Commission (FCC) of United States of America as a standard and is used for frequencies from 20 MHz to 20 GHz, antenna heights from 0.5 m to 3000 m and distances from 200 m to 500 km. The ITM software was developed by the NTIA (National Telecommunications & Information Administration) for point-to-point approach, and in combination with the freely available SRTM3 [3] (Shuttle Radar Mission Topography), 3-arc second resolution data with about 90m resolution (~3MB file size) data produce results of path loss of a reasonable accuracy. The SRTM1 [4] data, 1-arc second resolution data with about 30m resolution(~25MB file size) can be downloaded from NASA's Land Processes Distributed Active Archive Center (LP DAAC) located at the USGS Earth Resources Observation and Science (EROS) Center. In our research, Radio Mobile [5] and SPLAT! with ITM [6] software was used to run the ITM Longley-Rice model.

4.2.2 The ITWOM (Irregular Terrain with Obstructions Model) Model.

This model [7] is a combination of Longley-Rice model (Irregular Terrain Model) and ITU-R P.1546 Recommendation. SPLAT! software was used to run this model.

4.2.3 The Hata-Davidson model.

The Hata-Davidson [8] model is a modification to the Hata model. It was recommended by

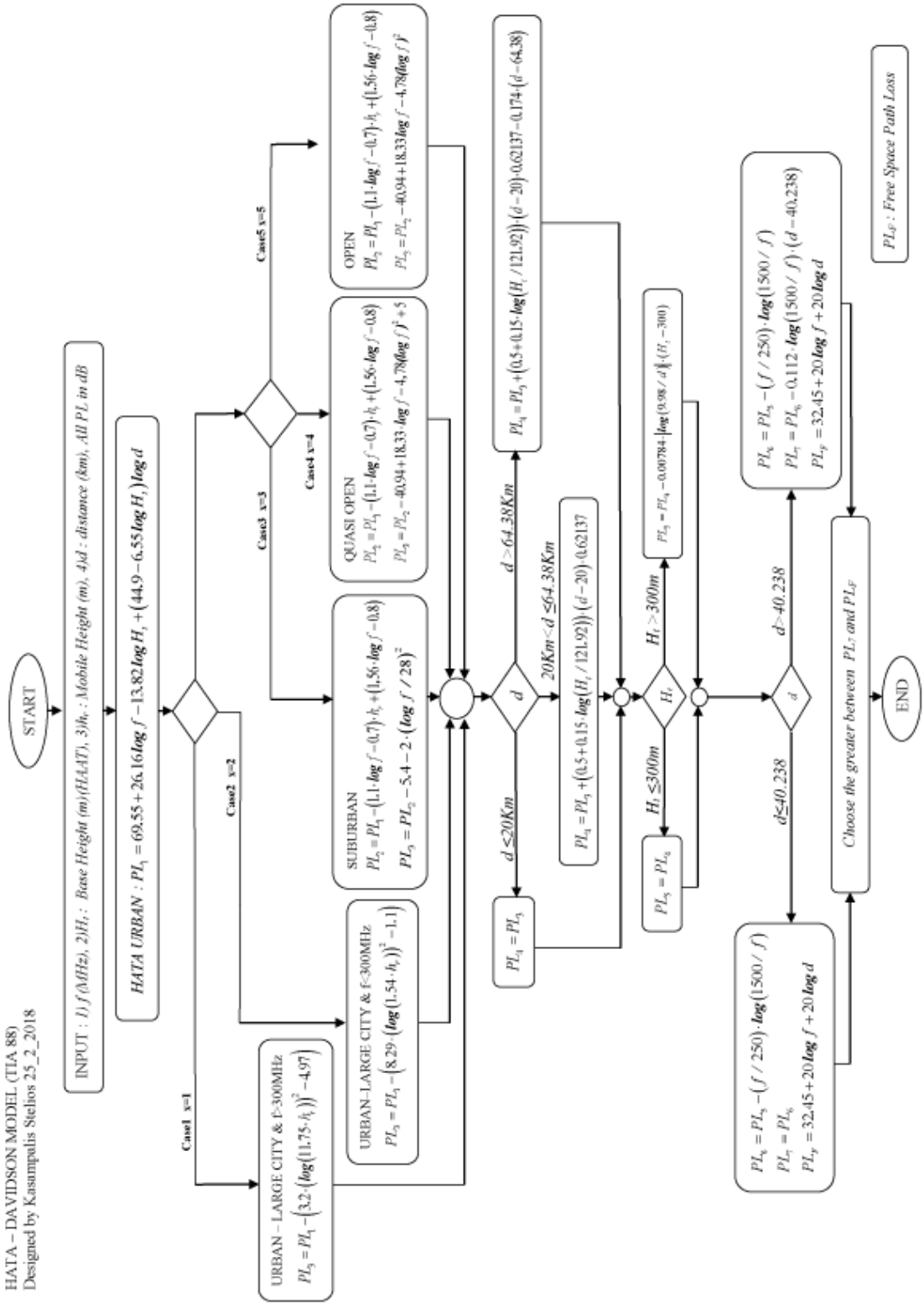

Figure 4-1: Flow Chart of Hata-Davidson model.

"The Telecommunications Industry Association (TIA)" [9], in order to cover a broader range of input parameters and distances than Hata's model and is used in our research. The Hata-Davidson model uses HAAT [10] (Height Average Above Terrain) in its calculations. A MATLAB program, derived from the equivalent FORTRAN program was written for this model. Program's flowchart is given in Figure 4-1.

4.2.4 The ITU-R P.1546 Recommendation.

In this research "Recommendation ITU-R P.1546" [11] proposed by The Radio Communication Sector of I.T.U also is used. A MATLAB program [12] named "ITU-R p. calculator" created by Jef Statham on 21 August 2009 and updated on 27 August 2009, was used for the simulation.

4.2.5 Deygout's Model

Analytical presentation of this model and its correction factor [13-14] is given in Chapter 3. A MATLAB program was written for this model.

4.2.6 Epstein-Peterson's Model

Analytical presentation of this model [15] is given in Chapter 3. Also, a MATLAB program was written for this model.

4.2.7 Giovaneli's Model

Analytical presentation of this model [16] is given in Chapter 3. Also, a MATLAB program was written for this model.

4.2.8 Recommendation ITU-R P.526-13

Models for "Double isolated edges and "rounded obstacles" presented by Recommendation ITU-R P.526-13 [17] which are identical to Epstein-Peterson's method (see Figure 11, Method for double isolated edges, page 22) and to Deygout's method (see Figure 12, Figure showing the main and the second obstacle, page 22) are also used.

4.3 FUNDAMENTAL CONCEPTS

4.3.1 PLOTTING THE FRESNEL ZONES – ELLIPSES

An **ellipse** is a geometric shape defined by two specific points (foci), each one called a focus, points $\boldsymbol{F_1}$ and $\boldsymbol{F_2}$ in Figure 4-2. The basic property of the ellipse is that the sum of the distances from any point ($\boldsymbol{P}$) on the ellipse to the focus points ($\boldsymbol{F_1, F_2}$) is constant, i.e., $\boldsymbol{PF_1+PF_2=2a}$. Ellipse has two axes, the major axis which is the line segment between the point labeled $\boldsymbol{-a}$ to the point labeled $\boldsymbol{a}$ and equals to $\boldsymbol{2a}$ and the minor axis

which is the line segment between the point labeled ***–b*** to the point labeled ***b*** and equals to ***2b***. ***C*** is the center of the ellipse

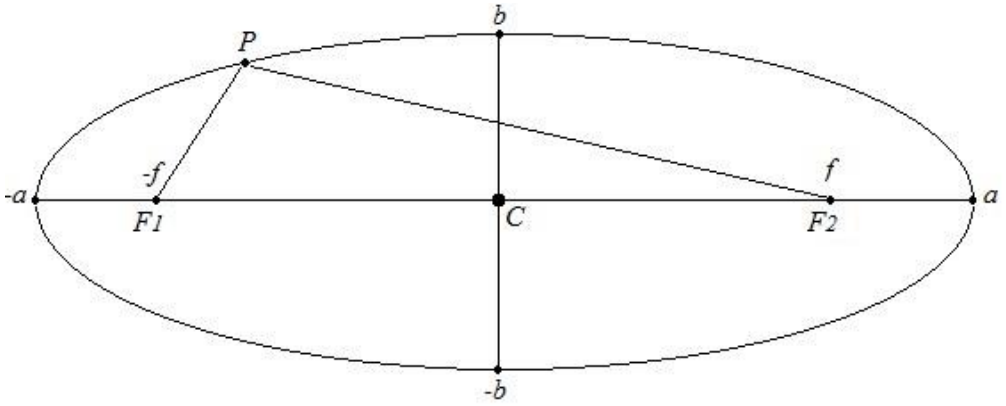

Figure 4-2: The ellipse and its characteristics.

One-half of the major axis is denoted by ***a*** and is called semi-major axis, and one-half of the minor axis is denoted by **b** and is called semi-minor axis. The four points ***a***, ***-a***, ***b***, and ***–b***, are called vertices.

The eccentricity of an ellipse, usually denoted by ***e***, equals to the distance between the two foci divided by the length of the major axis, i.e., e = 2*f*/2a = *f*/a.

If the major and minor axes of an ellipse coincide with the Cartesian axes, then the equation of this ellipse is given by equation (4.1)

$$\left(\frac{x^2}{a}\right)+\left(\frac{y^2}{b}\right)=1 \tag{4.1}$$

In our research, as many engineers do, Fresnel zones are used. They are concentric ellipsoids, which determine if the radio path is obstructed or not finding so the radio wave attenuation caused by obstacles between transmitter and receiver and by reflections which might be in phase or out of phase. The formula for calculating the Fresnel zone radius, $\boldsymbol{r_n}$ between the transmitter and the receiver at any point P, is given by equation (4.2)

$$r_n = \sqrt{\frac{n\lambda d_1 d_2}{d_1 + d_2}} \tag{4.2}$$

where,

r_n is the nth Fresnel zone radius, in meters

d_1 is the distance of point P from transmitter, in meters

d_2 is the distance of point P from receiver, in meters

λ is the wavelength of the transmitted electromagnetic wave, in meters

The Fresnel zone with other characteristic parameters is depicted in Figure 4-3.

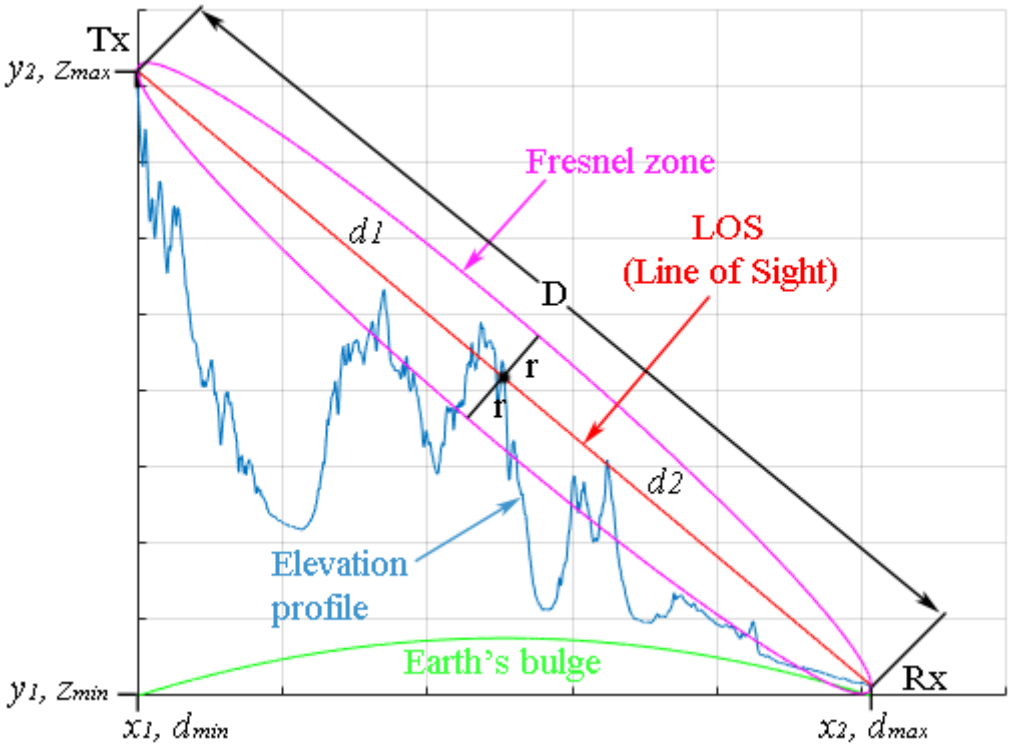

Figure 4-3: The first Fresnel zone.

From the Figure 4-3, setting $a=d_1=d_2=D/2$, $D = d_1+d_2$, and $\lambda=c/f$ and implementing Pythagoras' theorem parameter a (one half of the major axis of the ellipse) can be found.

$$a = \frac{D}{2} = d_1 = d_2 = \frac{1}{2}\sqrt{(x_2 - x_1)^2 + (y_2 - y_1)^2} = \\ = \frac{1}{2}\sqrt{(d_{max} - d_{min})^2 + (z_{max} - z_{min})^2} \tag{4.3}$$

and the radius of the 1st Fresnel zone, n=1 is calculated now as

$$r_1 = \sqrt{\frac{\lambda d_1 d_2}{d_1 + d_2}} = \sqrt{\frac{\lambda d_1^2}{2d_1}} = \sqrt{\lambda \cdot \frac{a}{2}} \tag{4.4}$$

Formula (4.4) is used to calculate the radius of the 1st Fresnel zone.

The formula (4.4), if f is in GHz, D in km, and $c=3\cdot10^8$m/s, turns into

$$r_1 = \sqrt{\lambda \cdot \frac{a}{2}} = \sqrt{\frac{c}{f} \cdot \frac{D}{4}} = \sqrt{\frac{300.000.000 m/s \cdot (D \cdot 1000) m}{(f \cdot 1.000.000.000) s^{-1} \cdot 4}} = \\ = \sqrt{75 \cdot \frac{D}{f}} = 8.66\sqrt{\frac{D}{f}} \tag{4.5}$$

In our simulations, the critical Fresnel zone, which defines the obstructed or unobstructed path, is the 0.6 times first Fresnel zone (this was explained in Chapter 1, page 6), which has radius $0.6r_1$.

$$r_{0.6} = 0.6 r_1 = 0.6\sqrt{\lambda \frac{a}{2}} \qquad (4.6)$$

The part of code, used in MATLAB, for the design of ellipses is shown below.

```
%=====================================================================
%                          PLOT THE ELLIPSES
%        1st FRESNEL ZONE (1F)- 0.6 OF FRESNEL ZONE (0.6F)
%=====================================================================
x1=dmin;
y1=zmin;
x2=dmax;
y2=zmax;
% Plot 1st Fresnel zone
fr=f*1000000;% f in Hz
c=300000000;% where, c is the light speed c=300000000m/s
l=c/fr; % l=wave length in meters
a = 1/2*sqrt((x2-x1)^2+(y2-y1)^2);
r = sqrt(l*a/2);% b=r
t = linspace(0,2*pi);
X = a*cos(t);
Y = r*sin(t);
w = atan2(y2-y1,x2-x1);
x = (x1+x2)/2 + X*cos(w) - Y*sin(w);
y = (y1+y2)/2 + X*sin(w) + Y*cos(w);
hold on, plot(x,y,'y')
grid on
% Plot the 0.6 Fresnel zone
r = 0.6*sqrt(l*a/2);% b=r
t = linspace(0,2*pi);
X = a*cos(t);
Y = r*sin(t);
w = atan2(y2-y1,x2-x1);
x = (x1+x2)/2 + X*cos(w) - Y*sin(w);
y = (y1+y2)/2 + X*sin(w) + Y*cos(w);
hold on, plot(x,y,'m')
```

4.3.2 FINDING ALL HEIGHTS BETWEEN TRANSMITTER AND RECEIVER, THE COMMAND zi.

To find all the heights between transmitter and receiver, the command z_i is coded in MATLAB.

The form of the command is: **zi=interp2(X.lon,X.lat,double(X.z),xi,yi,'linear'),** and the explanation of the its elements is given below.

1. The command **"interp2"** makes interpolation for 2-D gridded data in meshgrid format.

   Meshgrid→Rectangular grid in 2-D and 3-D space (see MATLAB)
2. X.lon, is a matrix created from readhgt.m and contains all the longitudes from long1 to long2 (21^0E (21.0000) to 25^0E (25.0000) in our research). You can see that if you create a matrix K=X.lon before executing command z_i.
3. X.lat, is a matrix created from readhgt.m and contains all the latitudes from lat1 to lat2 (39^0N (39.0000) to 42^0N (42.0000) in our research). You can see that if you create a matrix W=X.lat before executing command z_i.
4. double (X.z), the "double" command converts data to double precision, since SRTM elevation data are an int16 class (16bit).
5. "linear" is the default interpolation method of MATLAB. Cubic interpolation is another method of interpolation in MATLAB.
6. Finally, the above command gives all the heights from the transmitter to the receiver for all linespaces defined (if linespace = 4000, then 4000 heights (z_i) are created).

4.3.3 EQUIRECTANGULAR APPROXIMATION

(RHUMB LINE OR LOXODROME) OF THE GREAT CIRCLE

If it must be calculated the distance between two places, place1 and place2, located somewhere on Earth's surface, and whose longitudes and latitudes are known and defined as.

Place1: Latitude1 = lat1, Longitude1 = lon1,

Place2: Latitude2 = lat2, Longitude2 = lon2

Then the following procedure must be done:

- **The Haversine formula**

The "**Haversine**" formula calculates the great-circle distance between two points. That is the shortest distance over the earth's surface – giving an 'as-the-crow-flies' distance between the points.

$$\left.\begin{aligned} a &= sin^2\left((lat2-lat1)/2\right)+cos(lat1)\cdot cos(lat2)\cdot sin^2\left((lon2-lon1)/2\right) \\ c &= 2\cdot a\tan 2\left(\sqrt{|a|},\sqrt{|(1-a)|}\right) \\ d &= R\cdot c \end{aligned}\right] \quad (4.7)$$

R = Earth's radius (6370km=6370000m)

Angles must be in radians.

- **The equirectangular projection**

In many cases without significant errors, Pythagoras' theorem can be used on an equirectangular projection.

So, the distance between place1 and place2 now is given by the formula:

$$d = R\cdot\sqrt{((lon2-lon1)\cdot cos((lat1+lat2)/2))^2+(lat2-lat1)^2} \quad (4.8)$$

$$d = R\cdot sqrt(((lon2-lon1)\cdot cos((lat1+lat2)/2))^2+(lat2-lat1)^2) \quad (4.9)$$

For *R*=6370000m the result is in meters.

In our program, the distance *d* between place1 and place2 is given by:

$$d = \sqrt{((x(2)-x(1)).*cosd((y(1)+y(2))/2)).^2+(y(2)-y(1)).^2}\cdot 6370000\cdot pi/180 \quad (4.10)$$

In line 34 we find all the distances between pace1 and place2 and the formula should be:

$$di = \sqrt{((xi-x(1)).*cosd((y(1)+yi)/2)).^2+(yi-y(1)).^2}\cdot 6370000\cdot pi/180 \quad (4.11)$$

IMPORTANT NOTICE: the terms *((xi-x(1)), cosd((y(1)+yi)/2))* and *(yi-y(1))* are matrices which multiplied and added, and their dimensions must agree. To achieve this, a dot must be placed at the end of these matrices, otherwise MATLAB gives the error message "Inner matrix dimensions must agree", so the above terms must be written as *((xi-x(1)).*, *cosd((y(1)+yi)/2)).* and *(yi-y(1)).* The term *cosd* means *cos* in degrees that's why we multiply by pi/180 to convert in radians.

Finally, with quite no significant differences the simpler formula can be used:

$$di = \sqrt{((xi-x(1)).*cosd(yi)).^2+(yi-y(1)).^2}\cdot 6370000\cdot pi/180 \quad (4.12)$$

4.3.4 EARTH'S BULGE – THE K FACTOR

- **Radio Horizon**

The **Radio Horizon** is the locus of points where rays from a transmitting antenna are tangent to the surface of the Earth. If the Earth had no atmosphere and were a perfect sphere, the radio horizon would be a circle. This is depicted in Figure 4-4.

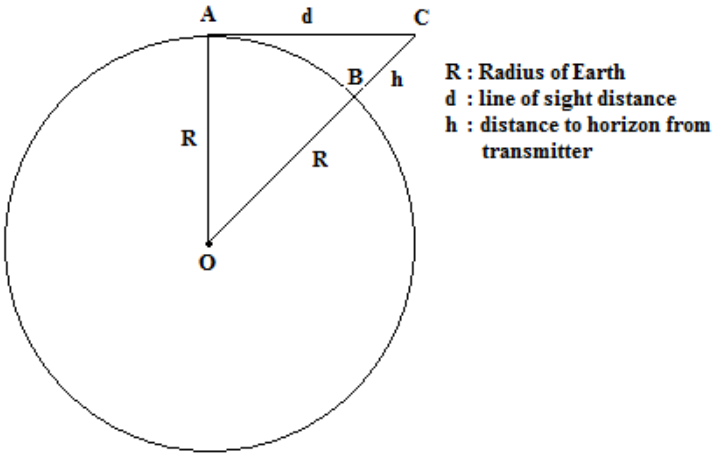

Figure 4-4: Earth as a perfect sphere.

The line of sight distance *d* (AC) can be calculated using Pythagorean Theorem:

$$\begin{aligned} (OC)^2 &= (OA)^2 + (AC)^2 \\ (R+h)^2 &= R^2 + h^2 \\ R^2 + 2\cdot R\cdot h + h^2 &= R^2 + d^2 \\ (2\cdot R + h)\cdot h &= d^2 \end{aligned} \tag{4.13}$$

Because $2\cdot R \gg h$ the above equation becomes:

$$2\cdot R\cdot h = d^2 \tag{4.14}$$

and finally:

$$d = \sqrt{2\cdot R\cdot h} \tag{4.15}$$

Solving equation (4.15) for *h*:

$$h = \frac{d^2}{2\cdot R} \tag{4.16}$$

Equation (4.16) is an equation of a parabola.

- **The K-factor**

Earth has an atmosphere, so the radio waves do not propagate in a straight line, but they are bending due to atmospheric refraction. This slight bending of the electromagnetic waves can be considered by assuming that the radius of the Earth is larger than its real value. This larger value of the Earth's radius is called the effective Earth radius. The effective Earth radius, R_e, can be calculated by multiplying the actual

Earth radius, R_0, by a factor K, the K-factor. Atmospheric refraction is also referred to as "the K-factor". This K-factor has a typical value of 4/3 of R_0 (R_0 =6370km). So, the effective Earth radius is given by:

$$R_e = K \cdot R_0 \tag{4.17}$$

- **Earth's Bulge**

As was mentioned above Earth has an effective radius and so an effective curvature. When dealing with path profiles and propagation models this effective curvature of the Earth, also called earth bulge, must be considered. This can be done by adding a parabolic approximation of the Earth's bulge to path profile. Equation (4.16) is such a parabolic approximation. Rearranging equation (4.16) at any point of a path that has a distance d_1 from the transmitter and d_2 from the receiver and considering the K-factor, the formula for the effective curvature h of Earth is given by:

$$h = \frac{d_1 \cdot d_2}{2 \cdot K \cdot R_0} \tag{4.18}$$

where,

h: effective Earth curvature in meters

d_1: distance of obstacle from the transmitter in meters

d_2: distance of obstacle from the receiver in meters

K = 4/3

R_0 = 6370000meters (actual Earth radius)

In MATLAB, all the parameters must be in meters, so equation (4.18) becomes:

$$h = \frac{d_1 \cdot d_2}{2 \cdot \frac{4}{3} \cdot 6.370.000} = \frac{d_1 \cdot d_2}{2 \cdot 1.333 \cdot 6370000} = 0.000000059 \cdot d_1 \cdot d_2 \tag{4.19}$$

In our MATLAB programs this value of the effective curvature h of Earth is used:

$$h = 0.000000059 \cdot d_1 \cdot d_2 \tag{4.20}$$

This effective curvature of Earth, *h*, should be added to all points of an elevation profile before determining Fresnel zone clearances or horizon points. This effective curvature h is added, in MATLAB programs. In Figure 4-5 Earth's bulge is shown.

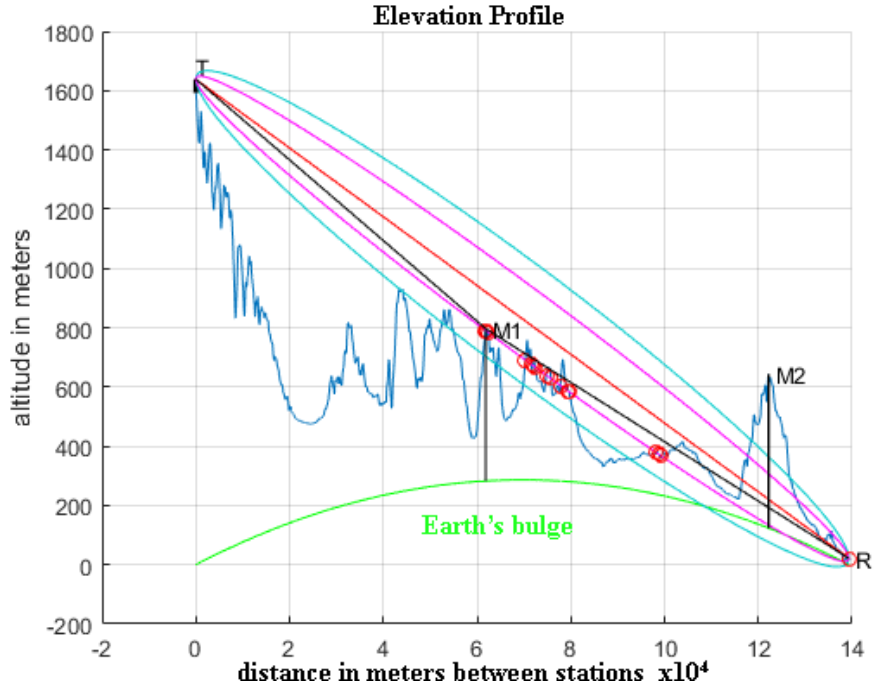

Figure 4-5: Earth's bulge.

4.3.5 FINDING THE INTERSECTION POINTS IN MATLAB BETWEEN TWO LINES USING AN ALGEBRAIC METHOD.

If the extensions of two lines in an elevation profile intersect we cannot use the command "polyxpoly" from the mapping Toolbox of MATLAB, because MATLAB gives the error message "empty matrix". In this case, an algebraic method to find the intersection points, is used. This method is described below.

Consider having the next two lines:

$$\begin{cases} 1st\ line \ : y - y_1 = \lambda_1 (x - x_1) \\ 2nd\ line : y - y_3 = \lambda_3 (x - x_3) \end{cases} \tag{4.21}$$

Solving the above linear system equations, the intersection points can be found.

- If 1st line passes through the points (x_1, y_1) and (x_2, y_2) then $\lambda_1=(y_2-y_1)/(x_2-x_1)$ and its equation becomes:

$$\begin{cases} y - y_1 = \left[(y_2 - y_1) / \ (x_2 - x_1) \right] \cdot (x - x_1) \ => \\ (y - y_1) \cdot (x_2 - x_1) \ = \ (y_2 - y_1) \cdot (x - x_1) \ => \\ (x_2 - x_1) \cdot y - \ (x_2 - x_1) \cdot y_1 = \ (y_2 - y_1) \cdot x - (y_2 - y_1) \cdot x_1 => \\ (y_2 - y_1) \cdot x \ - \ (x_2 - x_1) \cdot y = (y_2 - y_1) \cdot x_1 - \ (x_2 - x_1) \cdot y_1 \end{cases} \tag{4.22}$$

- If the 2nd line passes through the points (x_3, y_3) and (x_4, y_4), then $\lambda_3=(y_4-y_3)/(x_4-x_3)$ and its equation becomes:

$$\begin{cases} y - y_3 = \left[(y_4 - y_3) / \ (x_4 - x_3) \right] \cdot (x - x_3) \ => \\ (y - y_3) \cdot (x_4 - x_3) \ = \ (y_4 - y_3) \cdot (x - x_3) \ => \\ (x_4 - x_3) \cdot y - \ (x_4 - x_3) \cdot y_3 = \ (y_4 - y_3) \cdot x - (y_4 - y_3) \cdot x_3 => \\ (y_4 - y_3) \cdot x \ - \ (x_4 - x_3) \cdot y = (y_4 - y_3) \cdot x_3 - \ (x_4 - x_3) \cdot y_3 \end{cases} \quad (4.23)$$

The equations (4.24) is a linear system, and its solution gives the intersection point.

$$\begin{cases} (y_2 - y_1) \cdot x \ - \ (x_2 - x_1) \cdot y = (y_2 - y_1) \cdot x_1 - \ (x_2 - x_1) \cdot y_1 (3) \\ (y_4 - y_3) \cdot x \ - \ (x_4 - x_3) \cdot y = (y_4 - y_3) \cdot x_3 - \ (x_4 - x_3) \cdot y_3 (4) \end{cases} \quad (4.24)$$

It must be noted that:

The coefficients of x are: $(y_2-y_1), (y_4-y_3)$

The coefficients of y are: $-(x_2-x_1), -(x_4-x_3)$

The known terms are: $(y_2-y_1)\, x_1, -(x_2-x_1)\, y_1, (y_4-y_3)\, x_3, -(x_4-x_3)\, y_3$

In MATLAB to solve this system, the " \ " (backslash operator) is used to find the intersection point (2), because the "y coordinate" it is necessary and represents the height between Knife-Edge obstacle and the LOS (Line of Sight) line. This method is a general method and can be applied in both cases when the lines intersect, or their extensions intersect. The technique to solve it in MATLAB is given below:

1. A matrix A with x and y coefficients is created
   $A=[(y_2-y_1), -(x_2-x_1); (y_4-y_3), -(x_4-x_3)]$
2. A matrix b with x and y coefficients is created
   $b=[(y_2-y_1)\, x_1 -(x_2-x_1)\, y_1; (y_4-y_3)\, x_3 -(x_4-x_3)\, y_3]$
3. The intersection point is calculated using the backslash operator (\).
   Intersection point (2) $=A\backslash b$

Let's find the intersection point between line AB (Knife-Edge)) and LOS line CF, in Figure 4-6 below. Point A has coordinates (D1, maxheight1), where D1 is the horizontal distance from the transmitter TURTEL (point C) and maxheight1 is the height at this point. Point B has coordinates (D1, r1), where D_1 is the horizontal distance from the same transmitter and r_1 is the Earth's radius at this point, taking also into account the Earth's bulge at this point. Point C, transmitter has coordinates (dmin, zmin) and point F, receiver (NEGOTINO) has coordinates (dmax, zmax).

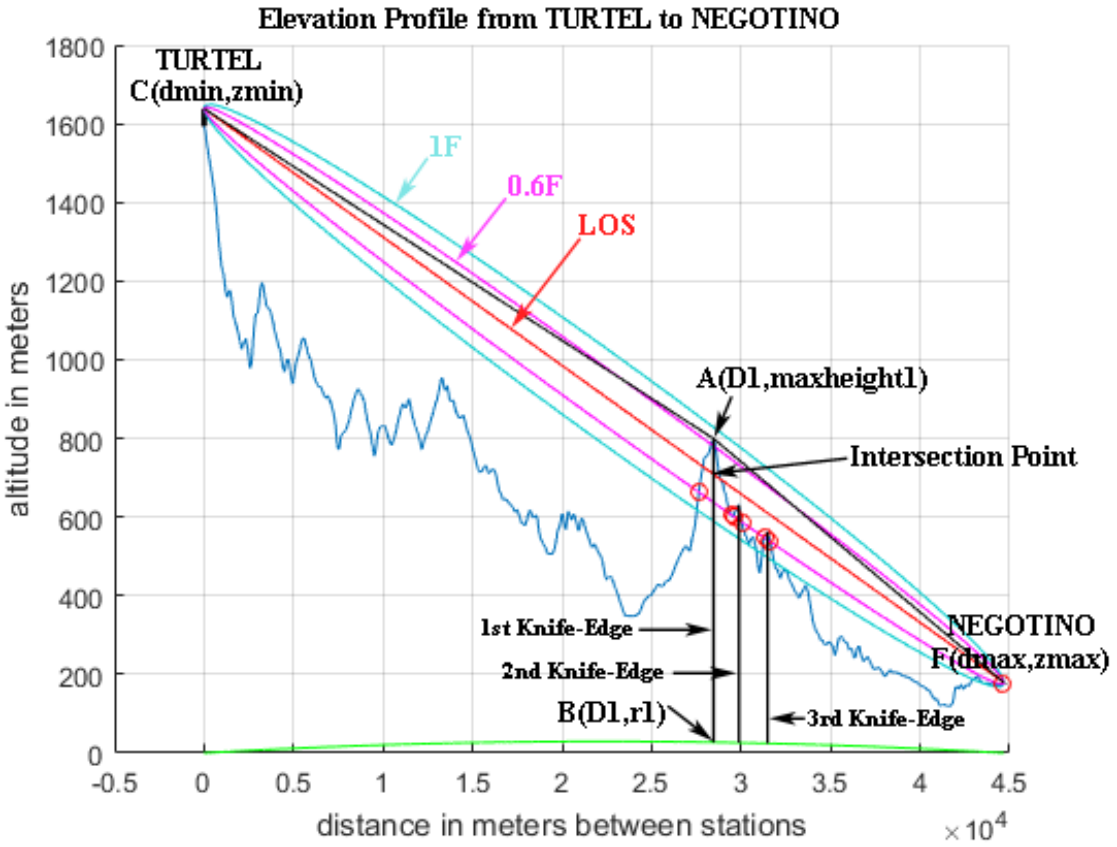

Figure 4-6: Coordinates for finding the intersections points.

Coordinates for line AB are: (D1, r1) →(x1, y1) and (D1, maxheight1)→(x2, y2).

Coordinates for line CF (LOS) are: (dmin, zmin) →(x3, y3) and (dmax, zmax)→(x4, y4)

4. A matrix A with x and y coefficients is created
   A=[(y_2-y_1), -(x_2-x_1); (y_4-y_3), -(x_4-x_3)], substituting with x and y with coordinates
   A=[(maxheight1-r_1), -(D_1-D_1); (zmax-zmin), -(dmax-dmin)]
5. A matrix b with x and y coefficients is created
   b=[(y_2-y_1) x_1 -(x_2-x_1) y_1; (y_4-y_3) x_3 -(x_4-x_3) y_3], substituting with coordinates
   b=[(maxheight1-r_1) D_1 -(D_1-D_1) r_1; (zmax-zmin) dmin -(dmax-dmin) zmin]
6. Finally, the intersection point is calculated using the backslash operator (\).
   Intersection point (2) =A\b

4.3.6 CALCULATING FIELD SIGNAL STRENGTH

The received power (P_r) *by* an isotropic antenna of a receiver at a specific location is given by [19]:

$$P_r(Watts) = \frac{\left[E(V/m)\right]^2 \left[effective\ antenna\ area\left(m^2\right)\right]}{\left(impedance\ of\ \ free\ space\right)} \qquad (4.25)$$

The impedance of free space has a value of 120π or 377Ω.

The effective antenna area is given by [20]:

$$A_e\left(m^2\right)=\frac{G_r\lambda^2}{4\pi} \tag{4.26}$$

where, A_e is the effective antenna area (m^2)

G_r is the antenna gain (numeric, not dB)

λ is the wavelength (m)

So, equation (4.25) with the use of equation (4.26) becomes:

$$P_r=\frac{E^2G_r\lambda^2}{377\cdot 4\pi} \tag{4.27}$$

It is well known that

$$c=\lambda\cdot f \tag{4.28}$$

where, c=3·10^8 m/s (light speed) and f = wave frequency (Hz), substituting λ from equation (4.28) and express P_r in milliwatts, E in μV/m and f in MHz the formula (4.27) becomes:

$$P_r\left(mW\right)=1.9\cdot 10^{-8}\frac{E(\mu V/m)^2\cdot G_r}{f^2(MHz)} \tag{4.29}$$

Converting to logarithmic units and simplifying:

$$\begin{aligned}10\log P_r\left(mW\right)=&\,10\log 1.9\cdot 10^{-8}+10\log E(\mu V/m)^2\\&+10\log G_r-10\log f^2(MHz)\end{aligned} \tag{4.30}$$

$$P_r(dBm)=-77.2+20\log E(\mu V/m)-20\log f(MHz)+10\log G_r \tag{4.31}$$

$$P_r(dBm)=-77.2+E(dB\mu V/m)-20\log f(MHz)+G_r(dBi) \tag{4.32}$$

Solving equation (4.32) for *E(dBμV/m)*:

$$E(dB\mu V/m)=P_r(dBm)+20\log f(MHz)-G_r(dBi)+77.2 \tag{4.33}$$

The received power is:

$$P_r(dBm) = P_t(dBm) - P_{TOTAL\ PATHLOSS}(dB) \quad (4.34)$$

where,

$P_t\,(dBm)$ is the transmitted power and equals to:

$$P_t\left(dBm\right) = P_{T.O.}\left(dBm\right) + G_t\left(dBi\right) \quad (4.35)$$

A. $P_{T.O}$ *Transmitted Power Output in dBm*

$G_t(dBi)$ *Transmitter antenna gain in dBi*

$G_r(dBi)$ *Receiver antenna gain in dBi*

$$P_{TL} = P_{TOTAL\,PATHLOSS} = P_{FREESPACE\ PATHLOSS} + P_{DIFRACTION\ \ PATHLOSS} \quad (4.36)$$

Finally, equation (4.33) considering equations (4.34), (4.35), (4.36) becomes:

$$E(dB\mu V/m) = P_t(dBm) - P_{TL}(dB) + 20\log f(MHz) - G_r(dBi) + 77.2 \quad (4.37)$$

In our simulations, we considered $G_r(dBi)=0$, so equation (4.37) becomes :

$$E(dB\mu V/m) = P_t(dBm) - P_{TOTAL\ PATHLOSS}(dB) + 20\log f(MHz) + 77.2 \quad (4.38)$$

Equation (4.38) was used for calculating field strength, in all our MATLAB programs and in all our simulations.

4.3.7 CONVERSIONS BETWEEN Watt, dBW, dBm, E.R.P, and E.I.R.P

- Converting Watt to dBW to dBm.

1) Assume the power output of the transmitter is P_0 = 1600 W

Then this power expressed in dBW (referenced to one Watt) is :

$$P_0 = 10 \cdot \log \frac{1600W}{1W} = 32\ dBW \quad (4.39)$$

The same power expressed in dBm (referenced to one milliwatt) is

$$P_0 = 10 \cdot \log \frac{1600000mW}{1mW} = 62.04\ dBm \quad (4.40)$$

- Finding ERP (Effective Radiated Power) and EIRP (Equivalent Isotropically Radiated Power) and making conversions between them.

1) Assume again that the power output of the transmitter is P_0 = 1600 W=62.04 dBm.
2) Assume that the gain of the transmitter's antenna is G_t =8.5 dBd or G_t = 10.65 dBi, the relation between dBi and dBd is : dBi=dBd+2.15.
3) Then, ERP in dBm, kW, dBW is given
   - ERP in dBm equals :

$$ERP_{dBm} = 62.04\ dBm + 8.5\ dBd = 70.54\ dBm \quad (4.41)$$

- ERP in kW equals :

$$dBm = 10 \cdot \log \frac{P_0}{1\ mW} \Rightarrow$$
$$70.54 = 10 \cdot \log \frac{P_0}{1\ mW} \Rightarrow$$
$$\frac{70.54}{10} = \log \frac{P_0}{1\ mW} \Rightarrow$$
$$P_0 = 10^{7.054} = 11{,}324{,}003.632\ mW \quad (4.42)$$
$$divide\ by\ 1000000\ to\ convert\ in\ kW$$
$$P_0 = 11.324\ kW\ \ i.e.$$
$$ERP_{KW} = 11.324\ kW$$

- ERP in dBW equals :

$$ERP_{dBW} = 10 \cdot \log \frac{11{,}324\ W}{1\ W} \Rightarrow \quad (4.43)$$
$$ERP_{dBW} = 40.54\ dBW$$

4) Then, EIRP in dBm, kW, dBW is given

- EIRP in dBm equals :

$$EIRP_{dBm} = 62.04\ dBm + 10.65\ dBi = 72.69\ dBm \quad (4.44)$$

- EIRP in kW equals :

$$dBm = 10 \cdot \log \frac{P_0}{1\ mW} \Rightarrow$$
$$72.69 = 10 \cdot \log \frac{P_0}{1\ mW} \Rightarrow$$
$$\frac{72.69}{10} = \log \frac{P_0}{1\ mW} \Rightarrow$$
$$P_0 = 10^{7.269} = 18{,}578{,}044.55\ mW \quad (4.45)$$
$$divide\ by\ 1000000\ to\ convert\ in\ kW$$
$$P_0 = 18.578\ kW\ \ i.e.$$
$$EIRP_{KW} = 18.578\ kW$$

- EIRP in dBW equals :

$$E.R.P_{dBW} = 10 \cdot \log \frac{18{,}578\ W}{1\ W} \Rightarrow \quad (4.46)$$
$$E.R.P_{dBW} = 42.69dB\ W$$

4.3.8 FINDING THE MAXIMUM HEIGHT (KNIFE-EDGE) OF AN OBSTACLE IN ELEVATION PROFILE

1) In our programs, there are two large matrices of which the number of elements depends upon the command "linespace". The command "linespace (4000)" interpolates 4000 elements between two given elements, first and last one. In our programs, the value of 4000 is used for the command "linespace". The two matrices are z_k and d_i, where z_k is the matrix of heights plus the Earth's bulge ($zk=z_i+r$, where z_i is the matrix of heights and r is the Earth's bulge at each point) and d_i is the matrix of distances. The development of matrices gives.

   $z_k=[z_k(1), \quad z_k(2), \quad z_k(3),\ldots\ldots l_i(1),\ldots\ldots l_i(2),\ldots\ldots\ldots z_k(3900), \quad z_k(4000)]$

   $d_i=[d_i(1), \quad d_i(2), \quad d_i(3),\ldots\ldots\ldots k_i(1),\ldots\ldots k_i(2),\ldots\ldots\ldots d_i(3900), \quad d_i(4000)]$

   The important thing here is that matrices z_k and d_i have the same number of elements and so the same number of indexes.

2) To find the intersection points between the 0.6 times of the first Fresnel zone and the elevation profile using the MATLAB command "polyxpoly" in the following form $[k_i, l_i]$=polyxpoly(x, y, d_i, z_k, 'unique'). Parameters are shown in Figure 4-7 .

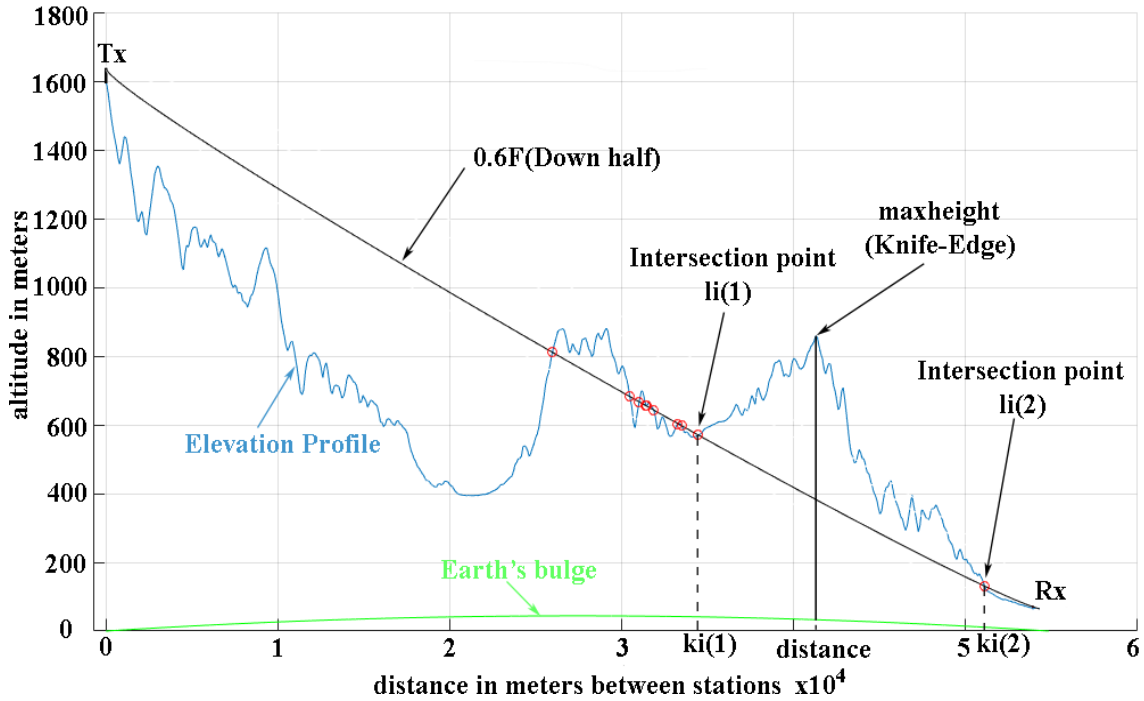

Figure 4-7: Intersection points.

Notice, that dividing intersection points by two, the number of obstacles is found. In the case of having eight intersection points, the number of obstacles is four.

3) In order to find the maximum height, "maxheight", between the intersection points ($k_i(1)$, $l_i(1)$) and ($k_i(2)$, $l_i(2)$) a certain procedure is used which is described below.

- First, the indices of the elements must be found, between intersection points $k_i(1)$ and $k_i(2)$ of the distances matrix d_i with the use of the following command: index=find($d_i<k_i(2)$ & $d_i>k_i(1)$)
- So, a matrix with the name "index" is created that includes all the indices of the elements from $k_i(1)$ to $k_i(2)$.
- Now the index of the first (1) and the last (end) element of the matrix "index" is found, using the following commands:

  f1=index(1)

  f2=index(end)
- Next a new matrix "m_i is created using the above f1, f2 indices which are the same in matrix z_k, using the command:

  $m_i=z_k$(f1:f2).

  The matrix m_i contains the elements (heights) of matrix z_k from f1 to f2.
- Next the element, in matrix m_i, with the maximum value element "maxheight" is found, which is the Knife-Edge of the specific obstacle, using the following command:

  maxheight=max(m_i)

  Well, the height of the Knife-Edge has been found, but its distance d_i from the transmitter, is still unknown and must be found.
- The index of the element "maxheight" is found (i.e. its place) in matrix m_i using the following command.

  index=find(abs(m_i-maxheight)<0.0001)

  In the case that there are two or more elements with the same index the first element is chosen with the use of the following command:

  f3=index(1)

  So, the element "maxheight" has the index f3.
- A matrix d1 with indices f1 and f2 from matrix d_i, is created using the following command:

  d1=di(f1:f2)
- The distance of "maxheight" from matrix d1 using the index f3 will now be found using the command:

  distance=d1(f3)

"distance" is named D1, and D1 is the distance between the specific obstacle and the transmitter and used in this form in all our MATLAB programs.

- Finally, the element "maxheight" which is the "Knife-Edge" has as coordinates : (distance, maxheight), i.e., its distance and its height are known from the transmitter.

4.4 EXPLANATION OF THE PROGRAM OPERATION

There will now be a presentation of the methodology developed to create the programs in MATLAB. All programs use the SRTM3 (Shuttle Radar Topography Mission), 3-arc second resolution data, around 90 m resolution (~3 MB file) and not the SRTM1, 1-arc second resolution data, around 30 m resolution(~25 MB file) because the differences in the produced elevations profiles are negligible.

Additionally, the site for downloading SRTM3 data is stable and easily accessible in contrast with the website that provides the SRTM1 data and which has some restrictions.

4.4.1 THE SINGLE KNIFE-EDGE PROGRAMS

Two programs were written in MATLAB for the calculation of the Single Knife-Edge. The SKEAD1D2.m which uses the inclined distances d_1 and d_2, between the transmitter (T) and receiver (R) and the SKEAHD1D2.m, which uses the horizontal distances d_1 and d_2, between the transmitter (T) and receiver (R). The inclined distances d_1 and d_2 are the actual distances between transmitter and receiver but the horizontal distances d_1 and d_2 are used by the engineers in path loss calculations without significant differences in results. The definitions of the distances d_1 and d_2 are shown in the Figure 4-8 and Figure 4-9. In this survey, the horizontal distances were used in MATLAB programs for simulations.

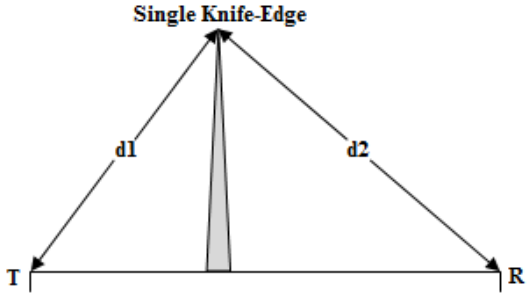

Figure 4-8: SKEAD1D2

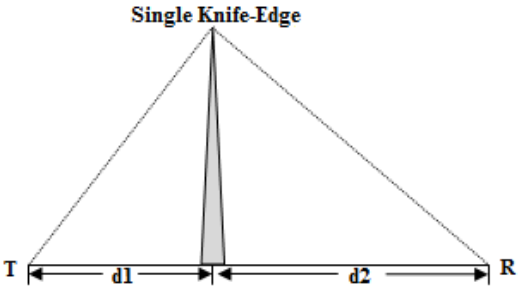

Figure 4-9: SKEAHD1D2

Both programs do the following:

- Accept the Input Data which are
  The frequency f in MHz of the transmitted signal, the transmitted power P in dBm, the height of the transmitter antenna Ht in m, the height of the receiver antenna Hr in m, the name of the transmitter, the name of the receiver, the Latitude, and Longitude of Transmitter and Receiver.
- Create
  The Geophysical Map of the area, the Elevation Profiles with Earth's bulge, the Fresnel Zones (1F, 0.6F) and the intersection points between obstacles and 0.6F
- Find the number of obstacles
  - If there are no obstacles, it calculates the free space path loss and the signal strength in dBμV/m.
  - If there are one or more obstacles makes the following :
    - Finds all obstacles that intersect with 0.6F.
    - Draws the respective Knife-Edges.
    - Implements Single Knife-Edge model for each Knife-Edge.
    - Calculates path loss for each of these Knife-Edges using **Lee formula**.
    - Finds the maximum Path Loss caused by a Single Knife-Edge.
    - Shows the position of the Single Knife-Edge that causes the maximum path loss (max v) and calculates the Signal Strength (dBμV/m).

Figure 4-10 shows Elevation profile, Fresnel zones 1F and 0.6F, Earth's bulge, intersection points (little red circles), Line of Sight (LOS), Single Knife-Edge obstacle and Transmitter (Tx) and Receiver (Rx).

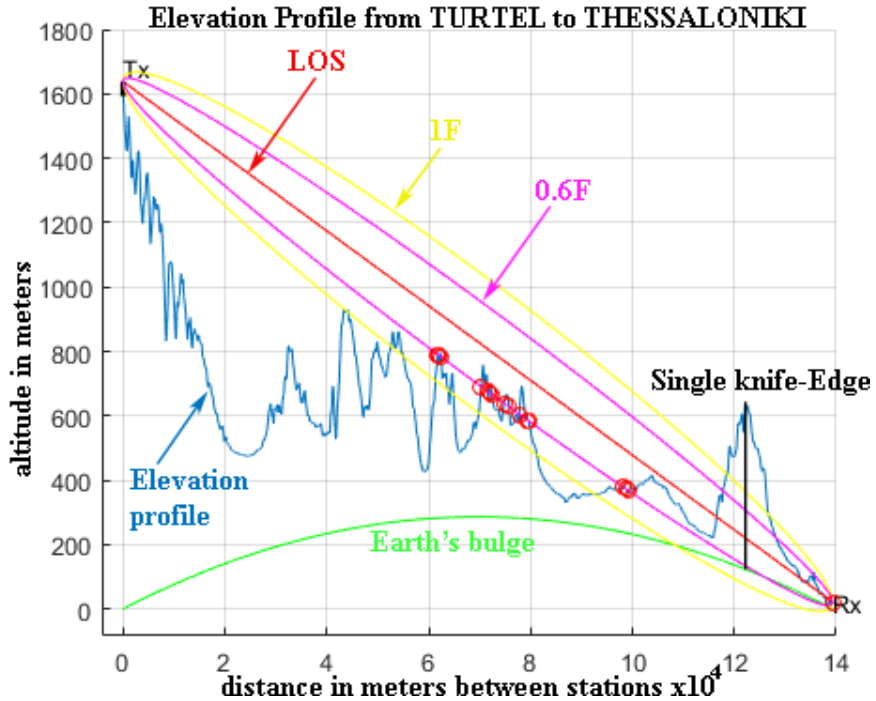

Figure 4-10: Detailed image derived from MATLAB for Single Knife-Edge.

The Flowchart of the Single Knife-Edge program is shown in Figure 4-11.

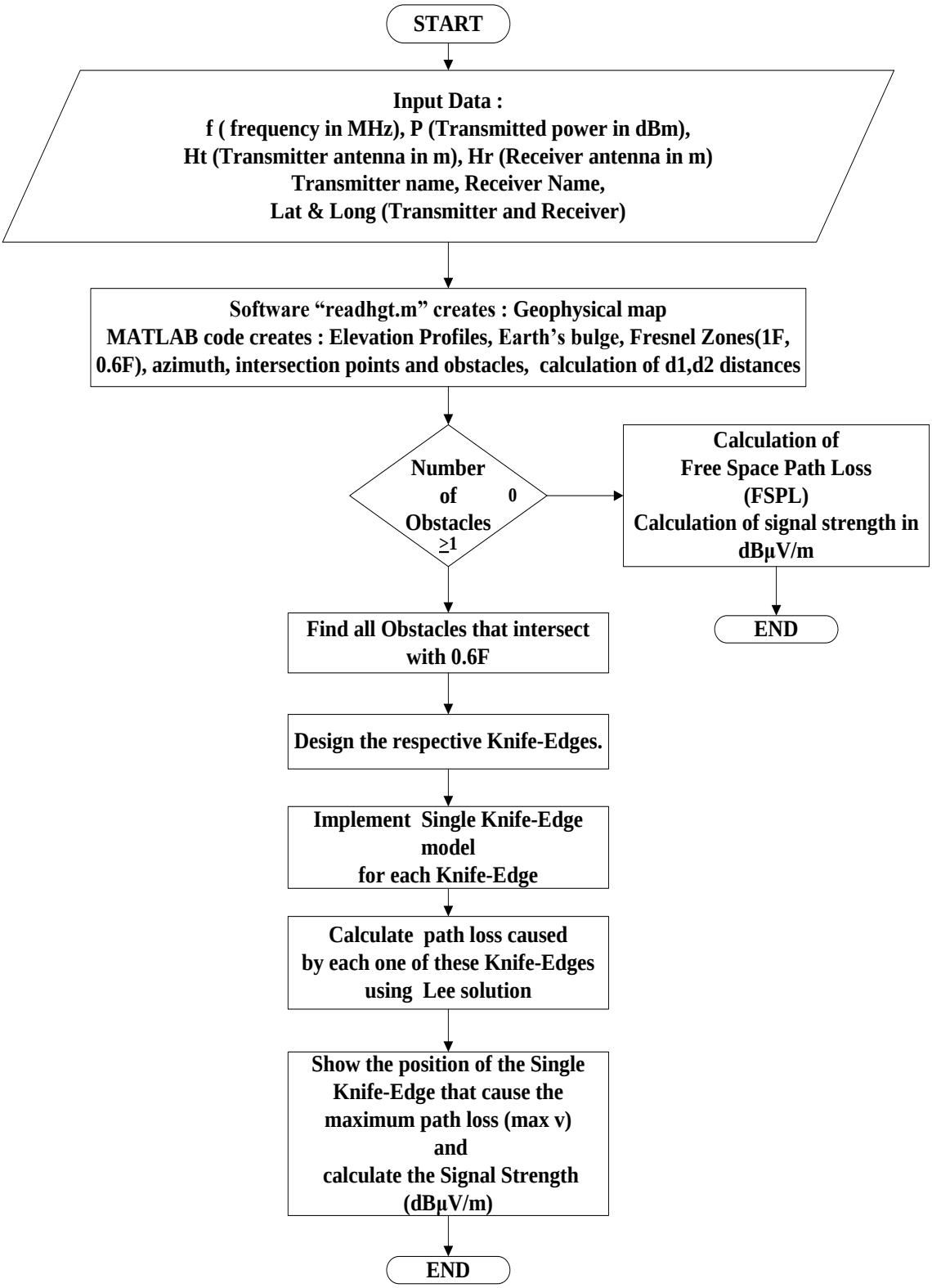

Figure 4-11: Single Knife-Edge flowchart.

Additionally, two more programs were written, the manual Single Knife-Edge program which shows all obstacles and allows the user to choose the Knife-Edge he wants to use and the SKEAFULL program that does the following:

- Finds the main Single Knife-Edge that causes the max loss (max v), and calculates the field strength, as the previous Single Knife-Edge programs do.

- Finds the total path loss (worst case – pessimistic value) by adding all the losses caused by all Single Knife-Edges and using as distances for each obstacle, its distance from the transmitter (D1) and receiver (D2) respectively. The operation of this program with all the calculated parameters is shown in Figure 4-12. The program is named "Cumulative Single Knife-Edge".

- Finds the path loss caused successively by each obstacle, reducing the receiving power at the next obstacle caused by the previous obstacle and using for each obstacle, as the distance (D_1) the distance between the previous and the next obstacle and as the distance (D_2) the distance between this obstacle and the receiver. The operation of this program with all the calculated parameters is shown in Figure 4-13. The program is named "Successive Single Knife-Edge".

Figures 4-12 and 4-13 are produced by MATLAB for a specific path with the following characteristics

- Transmitter name "Turtel", (analog TV station).
- Transmitting power, 79.18 dBm.
- Transmitting frequency, 217.25 MHz.
- Transmitter's antenna height, 45 m.
- Transmitter's longitude, 22.422550E.
- Transmitter's latitude, 41.802930N.
- Receiver located at position "Boskija".
- Boskija's longitude, 22.488190E.
- Boskija's latitude, 41.312160N.
- Receiver's antenna height, 2.5 m.

TURTEL and BOSKIJA are located at Former Yugoslav Republic of Macedonia (F.Y.R.O.M) state, north of Greece.

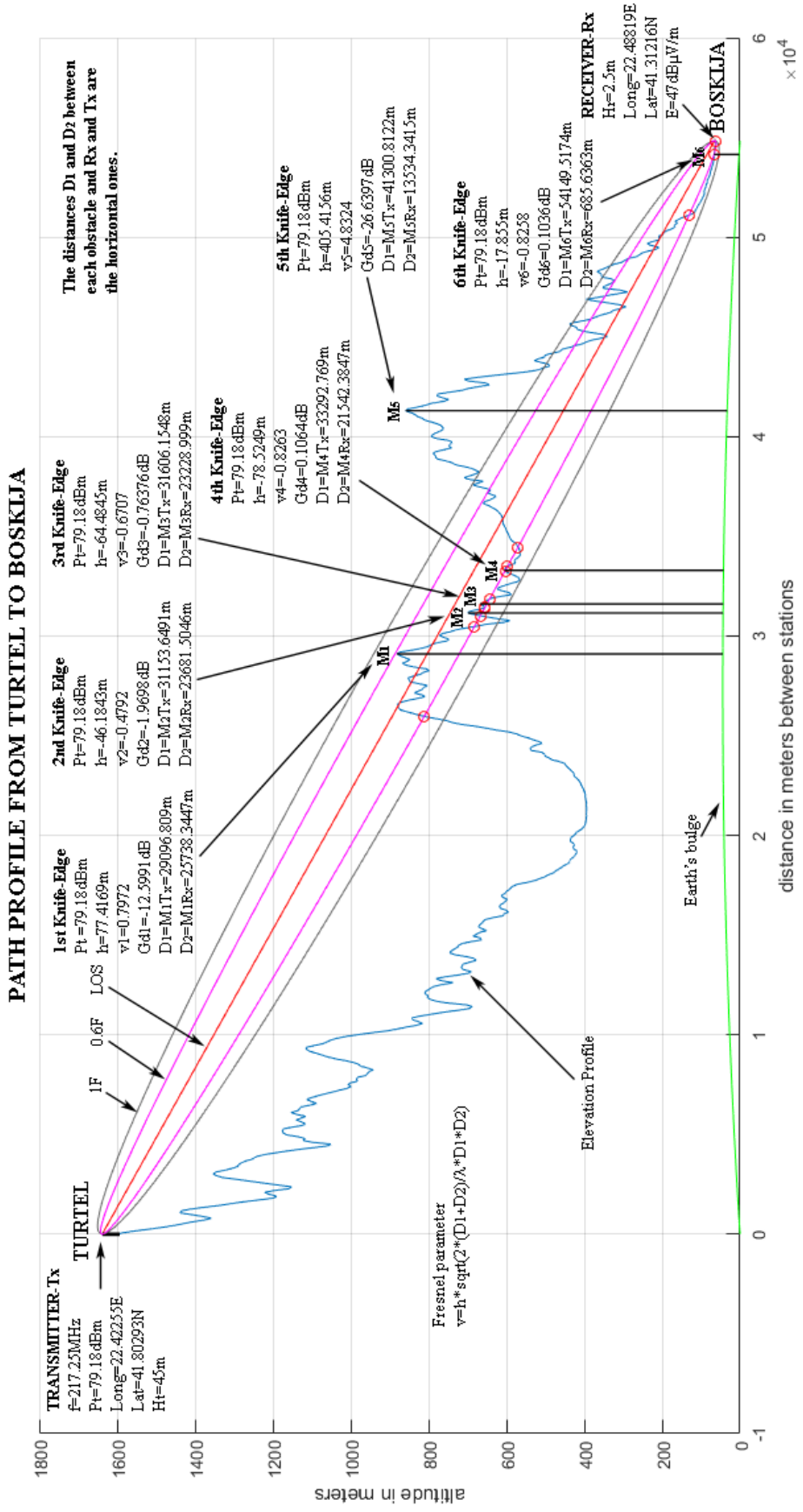

Figure 4-12: Worst case, adding all the losses caused by all Knife-Edges.

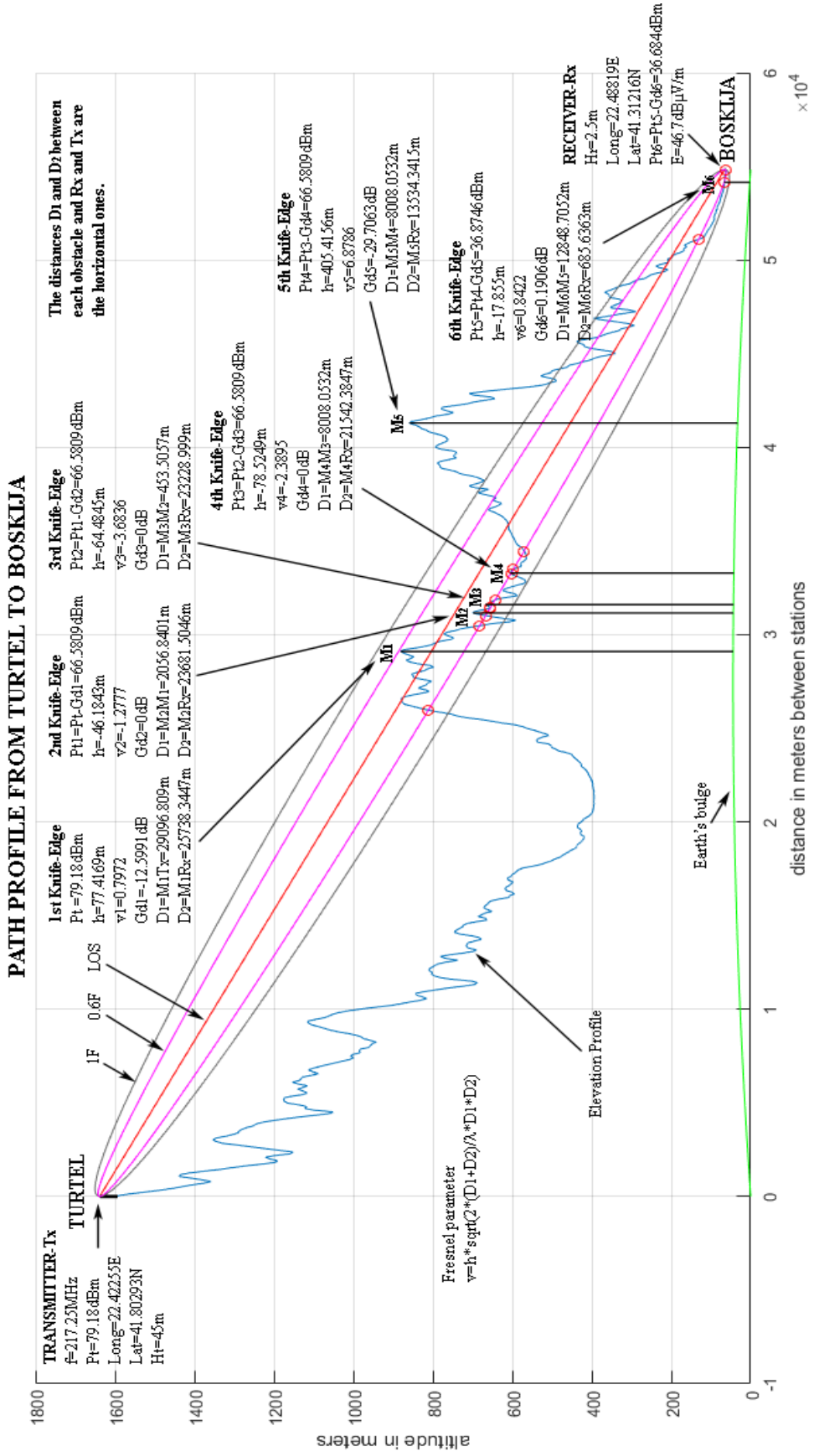

Figure 4-13: Path loss caused successively by each obstacle (each obstacle acts as a transmitter for the next obstacle).

4.4.2 THE DOUBLE KNIFE-EDGE PROGRAMS

The main programs that were written in MATLAB to calculate the double Knife-Edge path loss are :

The "Deygout.m" program that finds the primary (Deygout mentions it as "dominant") obstacle with the maximum Fresnel parameter v_1 and the secondary (Deygout mentions it as "predominant") obstacle with the second maximum Fresnel parameter v_2 (on the right or on the left of the main one) and implements the Deygout's model to calculate the path loss and the field strength at the specific receiving point. . Additionally, a program called "DeygoutTc.m" was written that involves the correction factor Tc proposed by Deygout.

The "Epstein-Peterson.m" program also finds the primary obstacle with the maximum Fresnel parameter v_1 and the secondary obstacle with the second maximum Fresnel parameter v_2 (on the right or on the left of the main one) and implements the Epstein-Peterson's model to calculate the path loss and the field strength at the specific receiving point. Additionally, a program called "EpsteinPetersonLc.m" was written that involves the correction factor Lc proposed by ITU-R P.526-23.

The "Giovaneli.m" program that works in the same way as Deygout's and Epstein-Peterson's programs but implements Giovaneli's model. For Giovaneli's model, two versions of the model were written. The classical model "GiovaneliFormula.m" which uses the formulas proposed by Giovaneli for path loss calculation and the geometrical model "GiovneliGTD.m" that calculates parameters using geometry. Both programs give the same results as it was expected.

All programs use the proper horizontal distances between transmitter, receiver and the obstacles, considering if the secondary obstacle lies on the left or on the right of the primary one. Two more programs were written, "Deygout3.m" that implements Deygout's model for 3 obstacles and "Deygout4.m" that implements Deygout's model for 4 obstacles. Finally, four more programs were written, the "manual Deygout.m", the "manual Epstein-Petesron.m," the "manual GiovaneliFormula.m" and the "manual GiovaneliGTD.m" which allow the user to select the desired two obstacles he wants to use. All programs calculate: a) Free space path loss and field strength if there are no obstacles. b) Single Knife-Edge path loss and field strength if there is one obstacle. c) Double Knife-Edge path loss and field strength if there are two or more obstacles.

The flowchart of the three main programs, i.e. "Deygout.m," "Epstein-Peterson.m" and "Giovaneli.m" is shown in Figure 4-14.

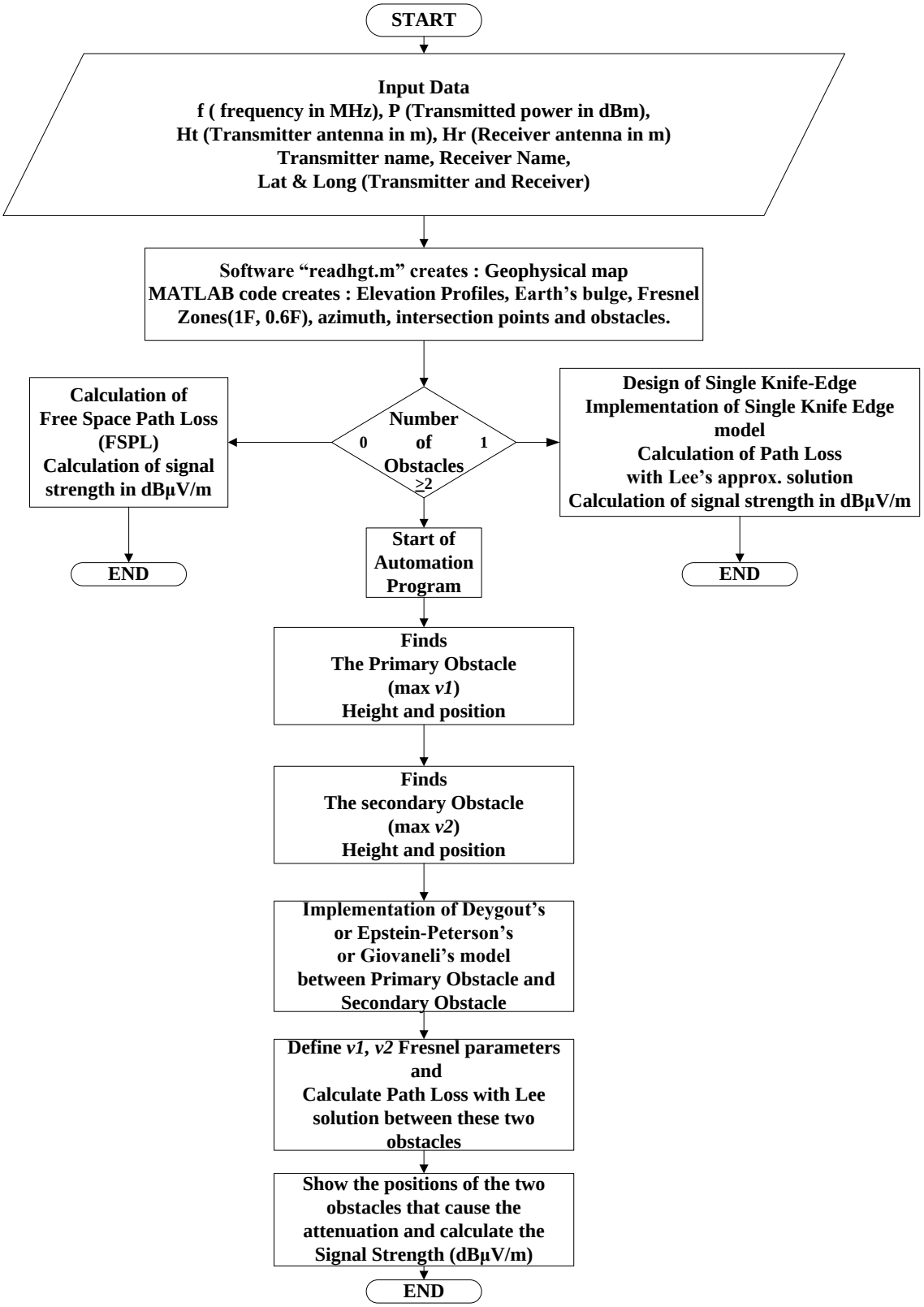

Figure 4-14: The Flow chart of the three main programs, i.e. Deygout.m, Epstein-Peterson.m and Giovaneli.m.

The MATLAB code of the "Deygout.m", "Epstein-Peterson.m" and "Giovaneli.m" programs is given in APPENDIX.

Path profile produced by MATLAB for Deygout's model in the case of double Knife-Edge is shown in Figure 4-15. The specific path has the following characteristics:

Transmitter located at position "TURTEL" with longitude of 22.42255^0E and latitude of 41.80293^0N, transmitting power of 79.18 dBm, transmitting frequency of 217.25 MHz (analog TV station), and transmitter's antenna height of 45 m.

Receiver located at position "PETROVEC" with longitude of 21.59649^0E, latitude of 41.95314^0N and receiver's antenna height of 2.5 m.

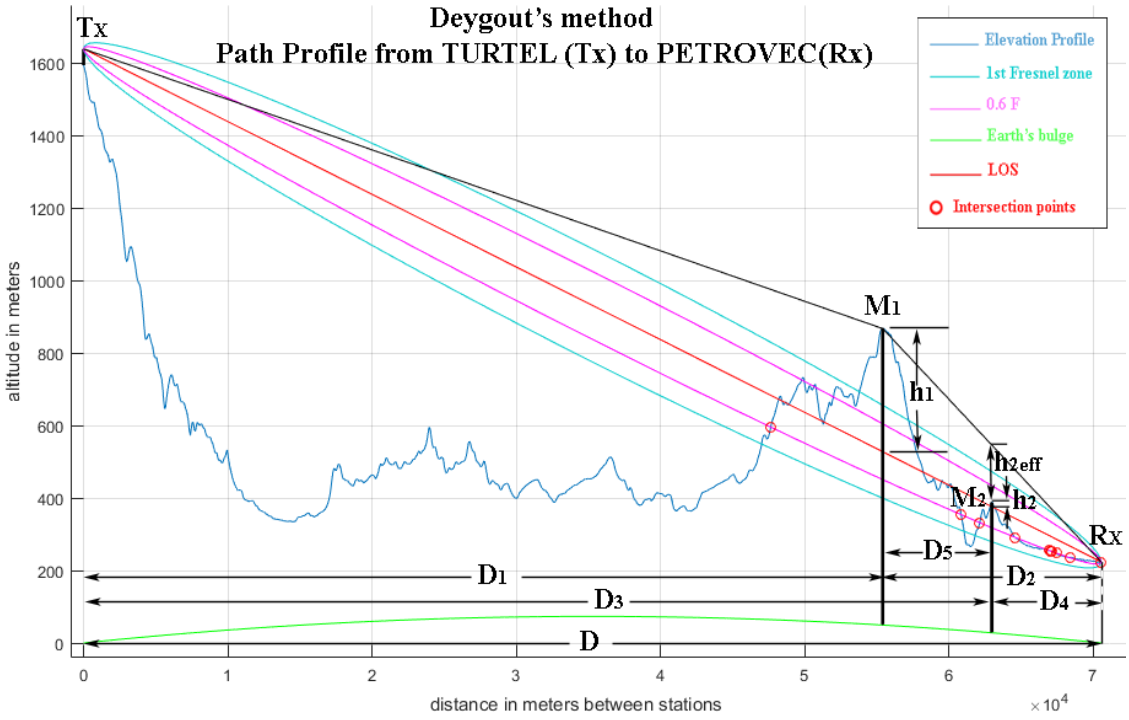

Figure 4-15: Deygout's method (double Knife-Edge).

All parameters depicted in Figure 4-15 are calculated by MATLAB and described below.

Totally, there are five obstacles.

M_1 is the primary obstacle, 1st Knife-Edge.

M_2 is the secondary obstacle, 2nd Knife-Edge.

Distance between Transmitter and Receiver, D = 70534.9987 m

1st Knife-Edge

Height of 1st Knife-Edge, maxheight1 = 866.9024 m

Height between 1st Knife-Edge and LOS, h_1 =339.4971 m

Distance between Transmitter and 1st Knife-Edge, D_1 =55397.0156 m

Distance between 1st Knife-Edge and Receiver, D_2=15137.9832 m

Fresnel Parameter v_1=3.7471

1st Knife-Edge Path Loss, Gd_1 =-24.4 dB

2nd Knife-Edge

Height of 2nd Knife-Edge=388.4096 m

Distance between Transmitter and 2nd Knife-Edge, D_3=62922.8532 m

Distance between Receiver and 2nd Knife-Edge, D_4=7612.1456 m

Distance between the Two Knife-Edges, D_5=7525.8376 m

Height between 2nd Knife-Edge and LOS, h_2 =11.919 m

Height between maxheight2 and line M_1Rx, h_{2eff}=-158.7973 m

Fresnel Parameter, v_2=-3.1066

2nd Knife-Edge Path Loss, Gd_2 =0 dB

Free Space Path Loss, 116.2 dB

Total Path Loss, $G_d = G_{d1}+G_{d2}$=-24.4dB+0dB=-24.4 dB

Double Knife-Edge Path Loss (Deygout) =140.6 dB

Field Strength =62.5 dBμV/m

Path profile produced by MATLAB for Epstein-Peterson's model in the case of double Knife-Edge for the same path, is shown in Figure 4-16 .

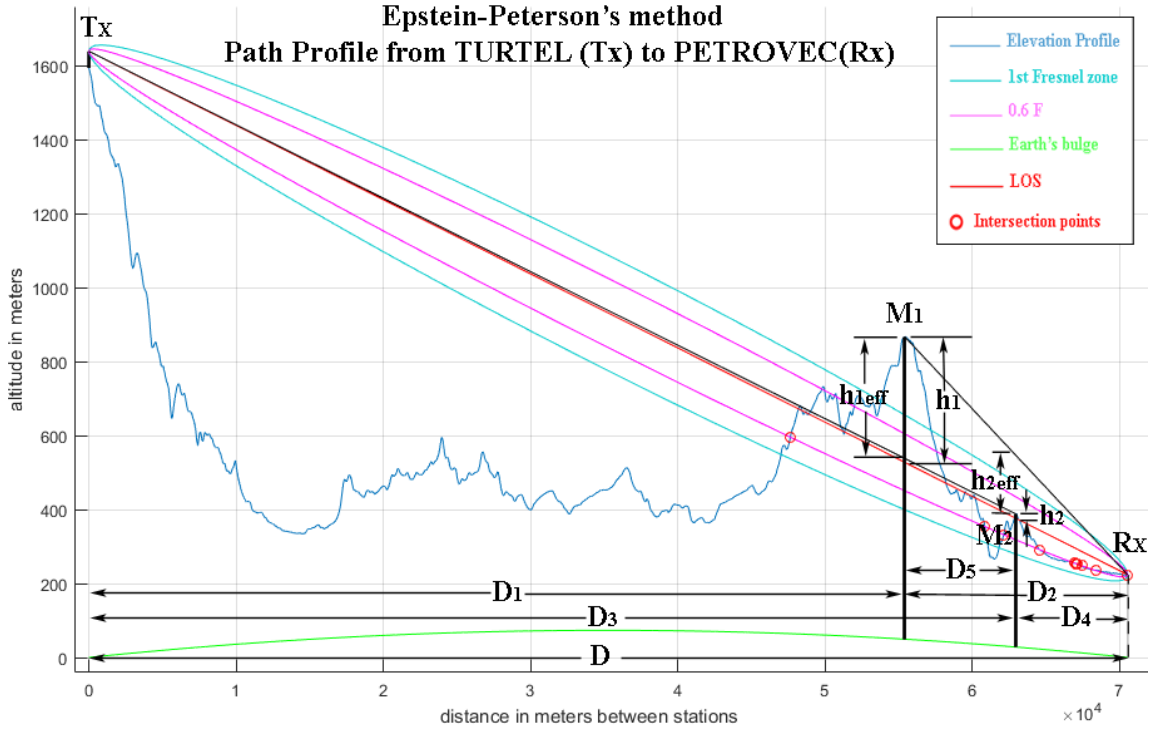

Figure 4-16: Epstein-Peterson's method (Double Knife-Edge).

All parameters depicted in Figure 4-16 are calculated by MATLAB and described below.

There are total five obstacles.

M_1 is the primary obstacle, 1st Knife-Edge.

M_2 is the secondary obstacle, 2nd Knife-Edge.

Distance between Transmitter and Receiver, D = 70534.9987 m

1st Knife-Edge

Height of 1st Knife-Edge, maxheight1=866.9024 m

Height between 1st Knife-Edge and LOS, h_1 =339.4971 m

Horizontal distance between Transmitter and 1st Knife-Edge, D_1=55397.0156 m

Horizontal distance between 1st Knife-Edge and Receiver, D_2=15137.9832 m

2nd Knife-Edge

Height of 2nd Knife-Edge, maxheight2=388.4096 m

Distance between Transmitter and 2nd Knife-Edge D_3=62922.8532 m

Distance between Receiver and 2nd Knife-Edge D_4=7612.1456 m

Distance between the Two Knife-Edges D_5=7525.8376 m

Height between 2nd Knife-Edge and LOS, h_2 =11.919 m

Height between maxheight1 and line M_2Tx, h_{1eff}=329.0036 m

Fresnel Parameter v_1=4.8643

1st Knife-Edge Path Loss G_{d1} =-26.6967 dB

Height between maxheight2 and line M_1Rx, h_{2eff}=-158.7973 m

Fresnel Parameter v_2=-3.1066

2nd Knife-Edge Path Loss, G_{d2} =0 dB

Free Space Path Loss, 116.2 dB

Total Path Loss, $G_d = G_{d1}+G_{d2}$=-26.7dB+0dB=-26.7 dB

Double Knife-Edge Path Loss (Epstein-Peterson) =142.9 dB

Field Strength =60.3 dBμV/m.

Path profile produced by MATLAB for Giovaneli's model in the case of double Knife-Edge, for the same path, is shown in Figure 4-17.

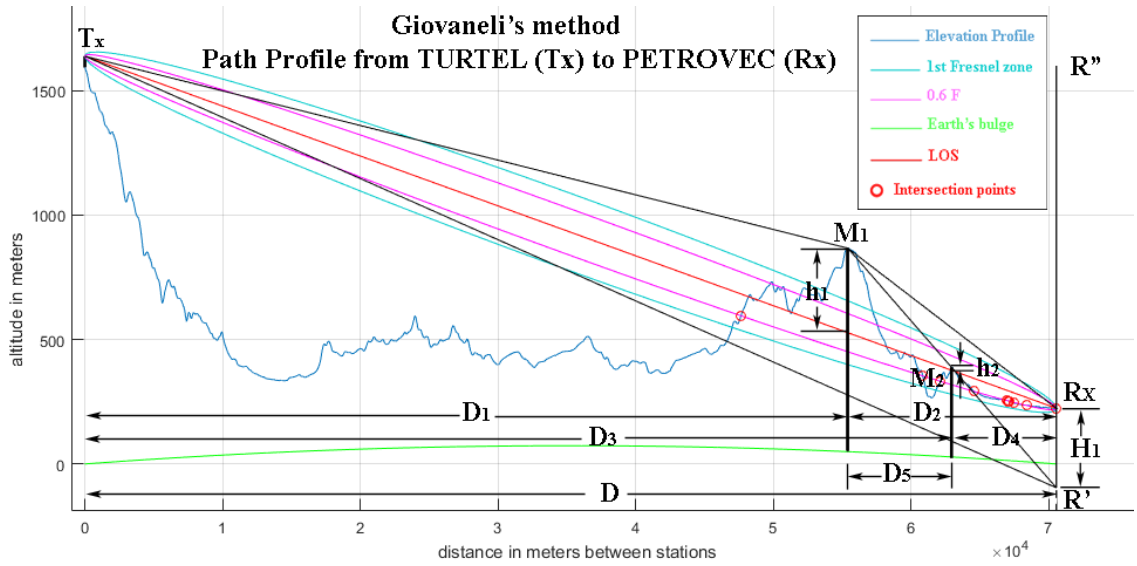

Figure 4-17: Giovaneli's method (double Knife-Edge).

All parameters depicted in Figure 4-17 are calculated by MATLAB and described below.

There are total five obstacles.

M_1 is the primary obstacle, 1st Knife-Edge.

M_2 is the secondary obstacle, 2nd Knife-Edge.

Distance between Transmitter and Receiver, D =70534.9987 m

1st Knife-Edge

Height of 1st Knife-Edge, maxheight1=866.9024 m

Height between 1st Knife-Edge and LOS, h_1 =339.4971 m

Distance between Transmitter and 1st Knife-Edge, D_1=55397.0156 m

Distance between 1st Knife-Edge and Receiver, D_2=15137.9832 m

2nd Knife-Edge

Height of 2nd Knife-Edge, maxheight2=388.4096 m

Distance between Transmitter and 2nd Knife-Edge, D_3= 62922.8532 m

Distance between Receiver and 2nd Knife-Edge, D_4=7612.1456 m

Distance between the Two Knife-Edges, D_5=7525.8376 m

Height between 2nd Knife-Edge and LOS, h_2 =11.919 m

H_1=-319.4158 m

h_{1eff}=590.361 m

Fresnel Parameter, v_1=6.5159

1st Knife-Edge Path Loss, Gd_1 =-29.2 dB

h_{2eff}=-158.7973 m

Fresnel Parameter v_2=-3.1066

2nd Knife-Edge Path Loss, G_{d2} =0 dB

Free Space Path Loss =116.2 Db

Total Path Loss, $G_d = G_{d1}+G_{d2}$=-29.2dB+0dB=-29.2dB

Double Knife-Edge Path Loss (Giovaneli) =145.4 dB

Field Strength =57.7 dBμV/m

The same methodology is used for Deygout's model that considers three, four, five or more obstacles. The main difference is the position of the obstacles in relation with the primary obstacle. Two study cases for three and four obstacles are presented.

4.4.3 CASE STUDY FOR THREE OBSTACLES WITH DEYGOUT'S METHOD

Initial parameters

In this study, the three obstacles M_1, M_2 and M_3 with heights h_1, h_2, h_3 respectively from line TxRx (LOS) are shown in Figure 4-18.

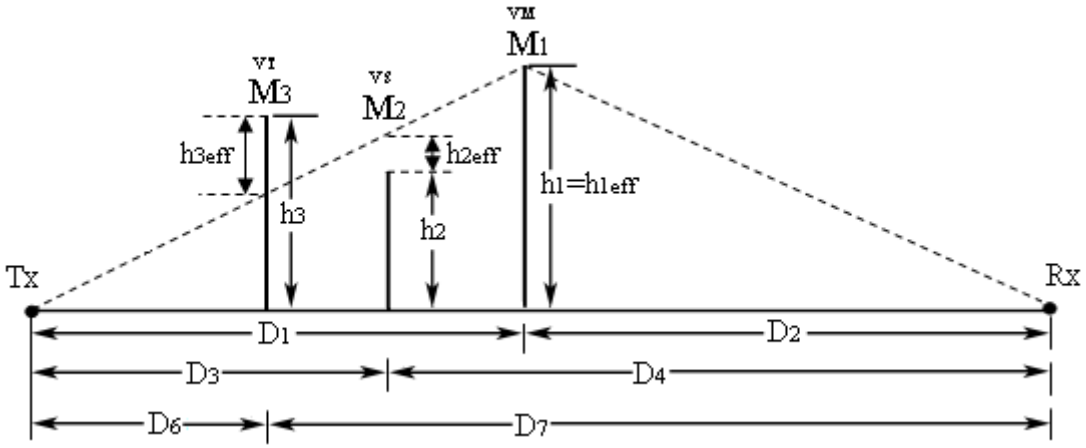

Figure 4-18: Deygout's method for three obstacles M_1, M_2, M_3, their heights h_1, h_2, h_3, and their effective heights h_{1eff}, h_{2eff}, h_{3eff}.

First, individual Fresnel parameters v_M, v_S, v_T are calculated. These will be used in this study for defining main obstacle, secondary obstacle, and third obstacle.

So, parameters v_M, v_S, v_T are calculated with the use of equation (4.47):

$$v_M = h_1\sqrt{\frac{2}{\lambda}\left(\frac{1}{D_1}+\frac{1}{D_2}\right)} \quad v_S = h_2\sqrt{\frac{2}{\lambda}\left(\frac{1}{D_3}+\frac{1}{D_4}\right)} \quad v_T = h_3\sqrt{\frac{2}{\lambda}\left(\frac{1}{D_6}+\frac{1}{D_7}\right)} \qquad (4.47)$$

Where, f is the frequency of the transmitting signal in MHz and λ is the wavelength of it in meters.

The analysis described in this study is used in a proper program, named "Deygout3.m", written in MATLAB. This program calculates individual Fresnel parameters v_M, v_S, v_T and always classifies $v_M>v_S>v_T$ which means that M_1 is the main obstacle (primary or dominant), M_2 is the secondary obstacle (predominant), and M_3 is the third obstacle.

Distances D_3, D_6 comparing with distance D_1 determine the position of the obstacles M_2, M_3 in relation to the main obstacle M_1. If they are on the right of the main obstacle M_1 intersect with line M_1R and if they are on the left of the main obstacle M_1 intersect with the line TM_1.

In our calculations, parameters (effective heights) h_{2eff} (M_2), h_{3eff} (M_3), defined as the height between the top of M_2, M_3 obstacles and lines TM_1, M_1R, obeying so in Deygout´s model. Distances between obstacles are shown in the figure above. Distances of obstacle M_3 are calculated in relation to the main obstacle M_1 and the secondary obstacle M_2. For all distances and their differences, the absolute values (abs) were used. The following cases are examined.

CASE 1: If $D_3<D_1$ && $D_6<D_3$ (Obstacles M_3, M_2 are located on the left of the main edge M_1 in the following order: **T**, M_3, M_2, **M_1**, **R**.

- Fresnel parameters v_1, v_2, v_3, are calculated as a function of :

  $v_1=f(\lambda, h_1, D_1, D_2)$, $v_2=f(\lambda, h_{2eff}, D_3, D_1-D_3)$, $v_3=f(\lambda, h_{3eff}, D_6, D_3-D_6)$

CASE 2: If $D_6<D_1$ && $D_3<D_6$ (Obstacles M_2, M_3 are located on the left of the main edge M_1 in the following order: **T**, M_2, M_3, **M_1**, **R**.

- Fresnel parameters v_1, v_2, v_3, are calculated as a function of :

  $v_1=f(\lambda, h_1, D_1, D_2)$, $v_2=f(\lambda, h_{2eff}, D_3, D_1-D_3)$, $v_3=f(\lambda, h_{3eff}, D_6-D_3, D_1-D_6)$

CASE 3: If $D_3<D_1$ && $D_6>D_1$ (Obstacle M_2 is located on the left of the main edge M_1 and M_3 is located on the right of the main edge M_1 in the following order: **T**, M_2, **M_1**, M_3, **R**.

- Fresnel parameters v_1, v_2, v_3, are calculated as a function of :

  $v_1=f(\lambda, h_1, D_1, D_2)$, $v_2=f(\lambda, h_{2eff}, D_3, D_1-D_3)$, $v_3=f(\lambda, h_{3eff}, D_6-D_1, D_7)$

CASE 4: If $D_6<D_1$ && $D_3>D_1$ (Obstacle M_3 is located on the left of the main edge M_1 and M_2 is located on the right of the main edge M_1 in the following order: **T**, M_3, **M_1**, M_2, **R**.

- Fresnel parameters v_1, v_2, v_3, are calculated as a function of :

  $v_1=f(\lambda, h_1, D_1, D_2)$, $v_2=f(\lambda, h_{2eff}, D_3-D_1, D_4)$, $v_3=f(\lambda, h_{3eff}, D_1-D_6, D_6)$

CASE 5: If $D_3>D_1$ && $D_6<D_3$ (Obstacles M_2, M_3 are located on the right of the main edge M_1 in the following order: **T**, M_3, **M_1**, M_2, **R**.

- Fresnel parameters v_1, v_2, v_3, are calculated as a function of :

  $v_1=f(\lambda, h_1, D_1, D_2)$, $v_2=f(\lambda, h_{2eff}, D_3-D_1, D_4,)$, $v_3=f(\lambda, h_{3eff}, D_6-D_3, D_7)$

CASE 6: If $D_6>D_1$ && $D_3>D_6$ (Obstacles M_3, M_2 are located on the right of the main edge M_1 in the following order: **T**, **M_1**, M_3, M_2, **R**.

- Fresnel parameters v_1, v_2, v_3, are calculated as a function of :

  $v_1=f(\lambda, h_1, D_1, D_2)$, $v_2=f(\lambda, h_{2eff}, D_3-D_1, D_4)$, $v_3=f(\lambda, h_{3eff}, D_6-D_1, D_3-D_6)$

Figure 4-19 produced by MATLAB for the case of three obstacles is shown below. The path is the same as the double Knife-Edge.

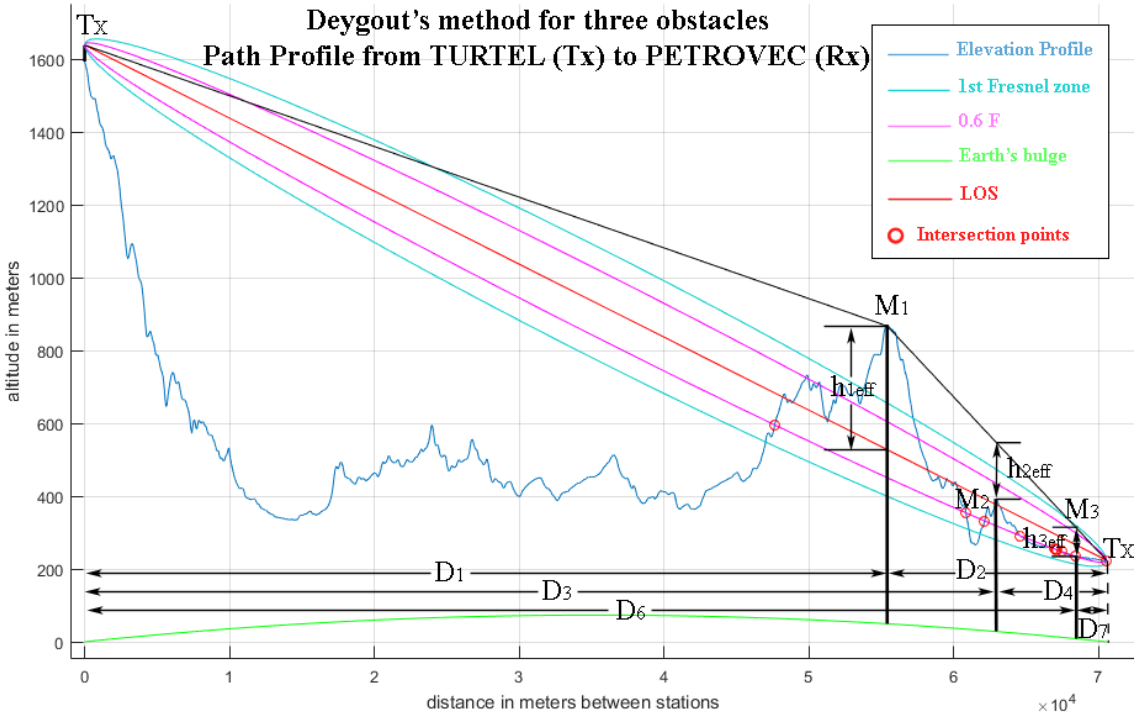

Figure 4-19: Deygout's method for three obstacles by MATLAB.

All parameters are calculated by MATLAB and depicted in Figure 4-19.

There are total five obstacles.

M_1 is the primary obstacle, 1st Knife-Edge.

M_2 is the secondary obstacle, 2nd Knife-Edge.

M_3 is the third obstacle, 3rd Knife-Edge.

Fresnel parameter v is calculated for each obstacle as if it was alone.

Height of Knife-Edge=866.9024 m

Horizontal distance of Knife-Edge from transmitter =55397.0156 m

Height between Knife-Edge line and LOS, h =339.4971 m

LOS length =70549.179 m

Horizontal distance between Transmitter and Knife-Edge =55397.0156 m

Horizontal Distance between Knife-Edge and Receiver =15137.9832 m

Fresnel Parameter v=3.7471

Height of Knife-Edge=388.4096 m

Horizontal distance of Knife-Edge from transmitter =62922.8532 m

Height between Knife-Edge line and LOS, h =11.919 m

LOS length =70549.179 m

Horizontal distance between Transmitter and Knife-Edge =62922.8532 m

Horizontal Distance between Knife-Edge and Receiver =7612.1456 m

Fresnel Parameter v=0.17407

Height of Knife-Edge=255.3306 m

Horizontal distance of Knife-Edge from transmitter =66958.2227 m

Height between Knife-Edge line and LOS, h =-40.2391 m

LOS length =70549.179 m

Horizontal distance between Transmitter and Knife-Edge =66958.2227 m

Horizontal Distance between Knife-Edge and Receiver =3576.776 m

Fresnel Parameter v=-0.83107

Height of Knife-Edge=253.0619 m

Horizontal distance of Knife-Edge from transmitter =67169.669 m

Height between Knife-Edge line and LOS, h =-38.2678 m

LOS length =70549.179 m

Horizontal distance between Transmitter and Knife-Edge =67169.669 m

Horizontal Distance between Knife-Edge and Receiver =3365.3297 m

Fresnel Parameter v=-0.81352

Height of Knife-Edge=236.4724 m

Horizontal distance of Knife-Edge from transmitter =68455.9367 m

Height between Knife-Edge line and LOS, h =-29.0639 m

LOS length =70549.179 m

Horizontal distance between Transmitter and Knife-Edge =68455.9367 m

Horizontal Distance between Knife-Edge and Receiver =2079.0621 m

Fresnel Parameter v=-0.77867

The first max Fresnel parameter v_1 =3.7471 and it is caused by obstacle 1 which is M_1

The second max Fresnel parameter v_2 =0.17407 and it is caused by obstacle 2 which is M_2

The third max Fresnel parameter v_3 =-0.77867 and it is caused by obstacle 5 which is M_3

Height of 1st Knife-Edge, M_1=866.9024 m

Height between 1st Knife-Edge and LOS, h_{1eff} =339.4971 m

LOS length =70549.179 m

Horizontal distance between Transmitter and 1st Knife-Edge D_1 =55397.0156 m

Horizontal distance between 1st Knife-Edge and Receiver D_2=15137.9832 m

---

Height of 2nd Knife-Edge, M_2=388.4096 m

Distance between Transmitter and 2nd Knife-Edge D_3=62922.8532 m

Distance between Receiver and 2nd Knife-Edge D_4=7612.1456 m

Height between 2nd Knife-Edge and LOS, h_2 =11.919 m

Height of 3rd Knife-Edge, M_3=236.4724 m

Distance between Transmitter and 3rd Knife-Edge D_6=68455.9367 m

Distance between Receiver and 3rd Knife-Edge D_7=2079.0621 m

Height between 3rd Knife-Edge and LOS, h_3 =-29.0639 m

The Main Hill M_1 has v_M=3.7471

The Secondary Hill M_2 has v_S=0.17407

The Third Hill M_3 has v_T=-0.77867

CASE 3

Height between maxheight2 and line M_1Rx, h2eff=-158.7973 m

Height between maxheight3 and line M_1Rx, h3eff=-448.5917 m

1st Knife-Edge v_1 =3.7471 dB

2nd Knife-Edge v_2 =-3.1066 dB

3rd Knife-Edge v_3 =-13.8874 dB

1st Knife-Edge (Main Hill) Path Loss G_{d1} =-24.4 dB

2nd Knife-Edge Path Loss G_{d2} =0 dB

3rd Knife-Edge Path Loss G_{d3} =0 dB

FINAL RESULT

Free Space Path Loss =116.2 dB

Four Knife-Edge Path Loss (DEYGOUT), $G_d = G_{d1}+G_{d2}+G_{d3}$ = -24.4+0+0 = -24.4 dB

Field Strength =62.5 dBμV/m

4.4.4 CASE STUDY FOR FOUR OBSTACLES WITH DEYGOUT'S METHOD

Deygout in his paper [13] gives ten various examples. An example for calculating path loss for five obstacles placed in specific locations is shown in Figure 4-20. The assumptions for estimating path loss, at this particular case, are described below.

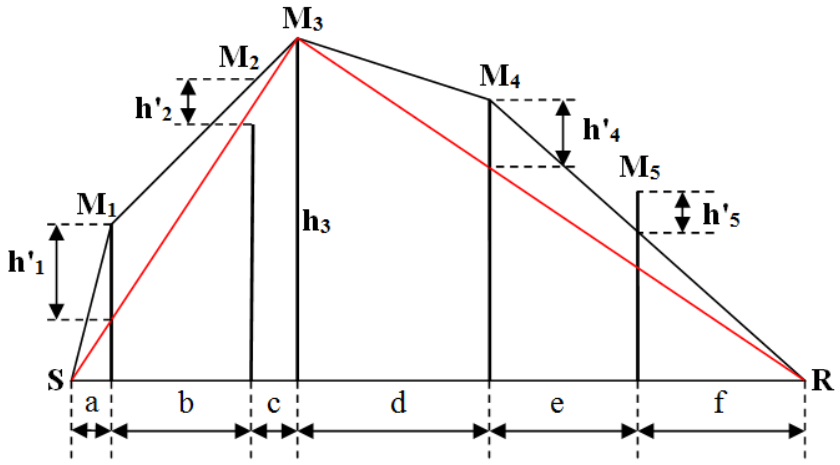

Figure 4-20: Multiple Knife-Edge approximations. Reproduced from Deygout's paper.

- The main obstacle (Deygout mentions it as "main hill") is found, M_3 is the main obstacle (maximum v Fresnel parameter).
- The red line SM_3 between S (Station) and M_3 and the red line M_3R between M_3 and R (Receiver) are plotted.
- The red line SM_3 (Line of Sight between S and M_3) intersects with the obstacle M_1 in a positive height of h_1'(above the LOS line SM_3) and with the obstacle M_2 in a negative height of h_2'(below the LOS line SM_3 and between the top of obstacle M_2 and line M_1M_3). So, M_1 is the main obstacle between S και M_3. Considering the above, the lines SM_1 and M_1M_3 are plotted, defining so heights $h_1'$and h_2' that must be calculated to find path loss.
- The red line M_3R (Line of Sight between M3 and R) intersects with the obstacle M_4 in a positive height of h_4'(above the LOS line M_3R) and with the obstacle M_5 also in a positive height of h_5'(above the LOS line M_3R and between the top of obstacle M_5 and line M_4R), but $h_4' > h_5'$. So M_4 is the main obstacle between M_3 και R. Considering the above, the lines M_3M_4 and M_4R are plotted, defining so heights $h_4'$and h_5' that must be calculated to find path loss.
- Finally, the whole calculation will be done with the use of the Table 4-1:

Table 4-1. Parameters for five obstacles. Reproduced from Deygout's paper.

Parameter	M_1	M_2	M_3	M_4	M_5
Distance1	a	b	a+b+c	d	E
Distance2	b+c	c	d+e+f	e+f	f
Effective height	h'_1	h'_2	h_3	h'_4	h'_5

Taking into consideration all the above and the ten various examples described in Deygout's paper, the case of four obstacles is investigated.

Initial parameters

In this study, there are four obstacles M1, M2, M3, M4 with heights h_1, h_2, h_3, h_4 respectively from line TxRx (LOS). Figure 4-21 depicts these data.

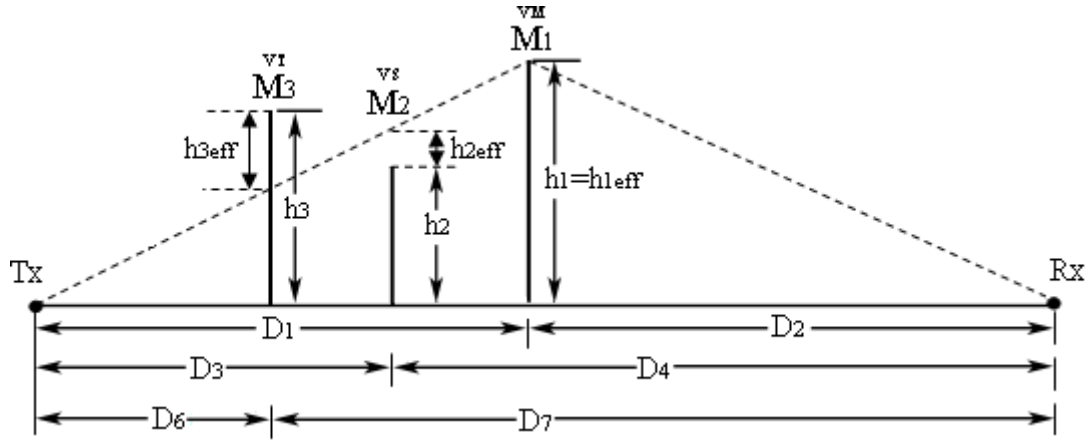

Figure 4-21: Deygout's method for four obstacles M_1, M_2, M_3, M_4, their heights h_1, h_2, h_3, h_4 and their effective heights h_{1eff}, h_{2eff}, h_{3eff}, h_{4eff}.

First, individual Fresnel parameters v_M, v_S, v_T, v_F, are calculated which will be used in our study for defining primary obstacle (main or dominant), secondary obstacle (predominant), third obstacle and fourth obstacle.

These parameters are calculated using equations (4.48):

$$v_M = h_1\sqrt{\frac{2}{\lambda}\left(\frac{1}{D_1}+\frac{1}{D_2}\right)} \qquad v_S = h_2\sqrt{\frac{2}{\lambda}\left(\frac{1}{D_3}+\frac{1}{D_4}\right)}$$
$$v_T = h_3\sqrt{\frac{2}{\lambda}\left(\frac{1}{D_6}+\frac{1}{D_7}\right)} \qquad v_F = h_4\sqrt{\frac{2}{\lambda}\left(\frac{1}{D_8}+\frac{1}{D_9}\right)} \tag{4.48}$$

Where, f is the frequency of the transmitting signal in MHz and λ is the wavelength in meters. The analysis described in this study is used in a program, named "Deygout4.m", written in MATLAB. This program calculates individual Fresnel parameters v_M, v_S, v_T, v_F and always classifies $v_M>v_S>v_T>v_F$ which means that M_1 is the main obstacle, M_2 is the second obstacle, M_3 is the third obstacle and M_4 is the fourth obstacle.

In the case of five obstacles, the program becomes complicated enough, so it is not studied here.

Distances D_3, D_6, D_8 comparing with distance D_1 determine the position of the obstacles M_2, M_3, M_4 in relation to the main obstacle M_1. If they are on the right of the main obstacle M_1 intersect with line M_1R and if they are on the left of the main obstacle M_1 intersect with the line TM_1.

In our calculations, parameters (effective heights) h_{2eff} (M_2), h_{3eff} (M_3), h_{4eff} (M_4) defined as the height between the top of M_2, M_3, M_4 obstacles and lines TxM_1, M_1Rx, obeying so in Deygout´s model. Distances between obstacles are shown in the figure above. Distances of obstacles M_3 and M_4 are calculated in relation to the main obstacle M_1 and the secondary obstacle M_2. For all distances and their differences, absolute values (abs) are used. Figure 4-22, produced MATLAB program depicts the case of four obstacles.

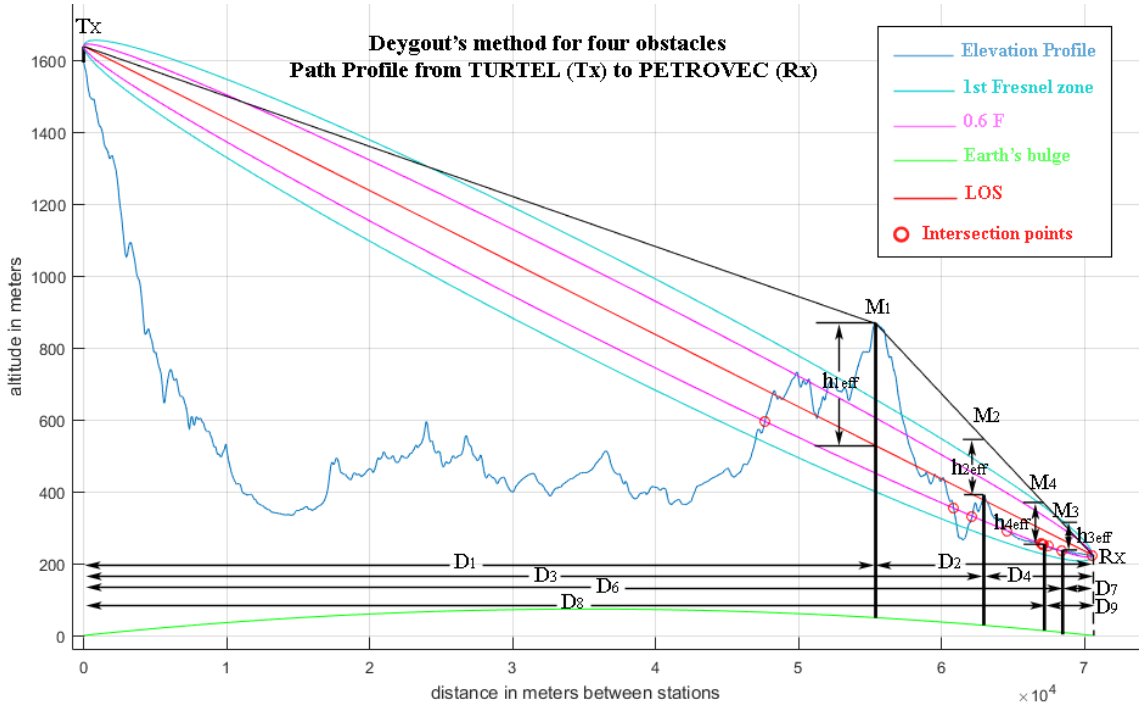

Figure 4-22: Deygout's method for four obstacles.

All parameters are calculated by MATLAB and depicted in Figure 4-22.

Deygout model for four obstacles

There are total five obstructions.

M_1 is the primary obstacle, 1st Knife-Edge.

M_2 is the secondary obstacle, 2nd Knife-Edge.

M_3 is the third obstacle, 3rd Knife-Edge.

M_4 is the fourth obstacle, 4th Knife-Edge.

Fresnel parameter v is calculated, for each obstacle as if it were alone.

Height of Knife-Edge=866.9024 m

Horizontal distance of Knife-Edge from transmitter =55397.0156 m

Height between Knife-Edge line and LOS, h =339.4971 m

LOS length =70549.179 m

Horizontal distance between Transmitter and Knife-Edge =55397.0156 m

Horizontal Distance between Knife-Edge and Receiver =15137.9832 m

Fresnel Parameter v=3.7471

Height of Knife-Edge=388.4096 m

Horizontal distance of Knife-Edge from transmitter =62922.8532 m

Height between Knife-Edge line and LOS, h =11.919 m

LOS length =70549.179 m

Horizontal distance between Transmitter and Knife-Edge =62922.8532 m

Horizontal Distance between Knife-Edge and Receiver =7612.1456 m

Fresnel Parameter v=0.17407

Height of Knife-Edge=255.3306 m

Horizontal distance of Knife-Edge from transmitter =66958.2227 m

Height between Knife-Edge line and LOS, h =-40.2391 m

LOS length =70549.179 m

Horizontal distance between Transmitter and Knife-Edge =66958.2227 m

Horizontal Distance between Knife-Edge and Receiver =3576.776 m

Fresnel Parameter v=-0.83107

Height of Knife-Edge=253.0619 m

Horizontal distance of Knife-Edge from transmitter =67169.669 m

Height between Knife-Edge line and LOS, h =-38.2678 m

LOS length =70549.179 m

Horizontal distance between Transmitter and Knife-Edge =67169.669 m

Horizontal Distance between Knife-Edge and Receiver =3365.3297 m

Fresnel Parameter v=-0.81352

Height of Knife-Edge=236.4724 m

Horizontal distance of Knife-Edge from transmitter =68455.9367 m

Height between Knife-Edge line and LOS, h =-29.0639 m

LOS length =70549.179 m

Horizontal distance between Transmitter and Knife-Edge =68455.9367 m

Horizontal Distance between Knife-Edge and Receiver =2079.0621 m

Fresnel Parameter v=-0.77867

The first max Fresnel parameter v_M =3.7471 and it is caused by obstacle 1 which is M_1

The second max Fresnel parameter v_S =0.17407 and it is caused by obstacle 2 which is M_2

The third max Fresnel parameter v_T =-0.77867 and it is caused by obstacle 5 which is M3

The fourth max Fresnel parameter v_F =-0.81352 and it is caused by obstacle 4 which is M_4

Height of 1st Knife-Edge, M_1=866.9024 m

Height between 1st Knife-Edge and LOS, h_{1eff} =339.4971 m

LOS length =70549.179 m

Horizontal distance between Transmitter and 1st Knife-Edge D_1 =55397.0156 m

Horizontal distance between 1st Knife-Edge and Receiver D_2=15137.9832 m

---

Height of 2nd Knife-Edge, M_2=388.4096 m

Distance between Transmitter and 2nd Knife-Edge D_3=62922.8532 m

Distance between Receiver and 2nd Knife-Edge D_4=7612.1456 m

Height between 2nd Knife-Edge and LOS, h_2 =11.919 m

Height of 3rd Knife-Edge, M_3=236.4724 m

Distance between Transmitter and 3rd Knife-Edge D_6=68455.9367 m

Distance between Receiver and 3rd Knife-Edge D_7=2079.0621 m

Height between 3rd Knife-Edge and LOS, h_3 =-29.0639 m

Height of 4th Knife-Edge, M_4=253.0619 m

Distance between Transmitter and 4th Knife-Edge D_8=67169.669 m

Distance between Receiver and 4th Knife-Edge D_9=3365.3297 m

Height between 4th Knife-Edge and LOS, h_4 =-38.2678 m

The Main Hill M_1 has v_M=3.7471, the secondary Hill M_2 has v_S=0.17407

The Third Hill M_3 has v_T=-0.77867, the Fourth Hill M_4 has v_F=-0.81352

CASE 8

Height between maxheight2 and line M_1Rx, h2eff=-158.7973 m

Height between maxheight3 and line M_1Rx, h_{3eff}=-448.5917 m

Height between maxheight4 and line M_1Rx, h_{4eff}=-449.9128 m

1st Knife-Edge v_1 =3.7471 dB

2nd Knife-Edge v_2 =-3.1066 dB

3rd Knife-Edge v_3 =-13.8874 dB

4th Knife-Edge v_4 =-12.496 dB

1st Knife-Edge (Main Hill) Path Loss, G_{d1} =-24.4 dB

2nd Knife-Edge Path Loss G_{d2} =0 dB

3rd Knife-Edge Path Loss G_{d3} =0 dB

4rth Knife-Edge Path Loss G_{d4} =0 dB

FINAL RESULT

Free Space Path Loss = 116.1573 dB

Four Knife-Edge Path Losses (Deygout),

$G_d = G_{d1}+G_{d2}+G_{d3}+G_{d4}$ = -24.4+0+0 = -24.4 dB

Field Strength =62.5 dBμV/m

All programs also produce the geophysical map of the area where transmitter and receiver are located. Such a map from transmitter “TURTEL” to receiver “PETROVEC’ is shown in Figure 4-23.

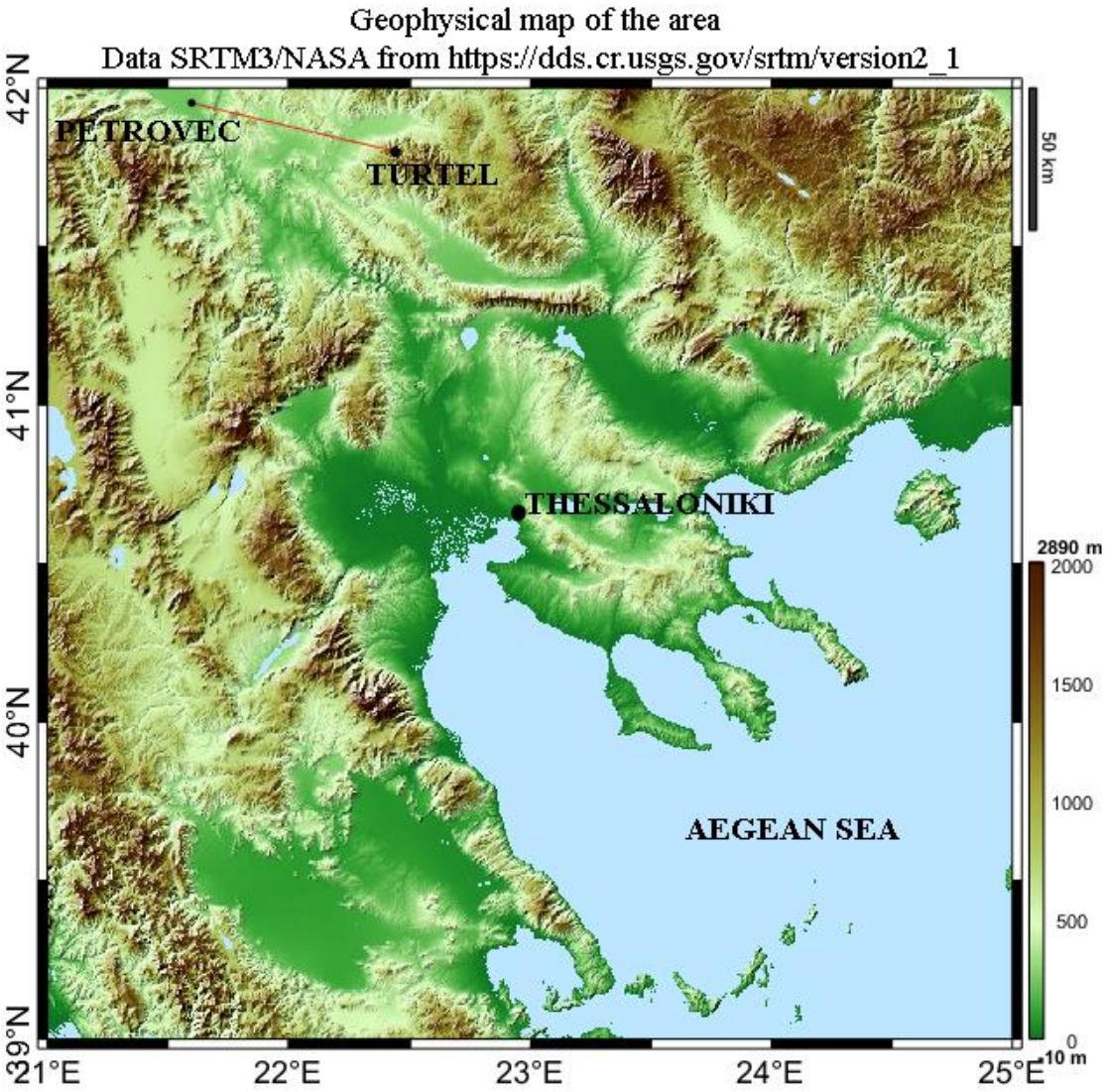

Figure 4-23: Geophysical map of the specific path.

4.5 ASSUMPTIONS

In this research and in the MATLAB programs of Deygout, Epstein-Peterson and Giovaneli, the following were not considered :

- Antenna pattern for the transmitter and cable losses for transmitter and receiver.
- The shape of the obstacles (rounded, cylindrical, etc.).
- Time percentage (i.e. 50%).
- Vegetation (a value of additional height for vegetation must be added)
- The main obstacles were defined using Fresnel parameter v instead of the ratio *h/r*. Parameter *h* is the height between the top of the obstacle and the line of sight (L.O.S – the straight-line joins transmitter and receiver) and *r* is the radius of the first Fresnel zone at the position of the obstacle Parameters v and *h/r* differs only with the numerical factor of √2.

- Ground reflection (2-ray) model (reflection coefficient for bare ground, forest, fresh water, sea water, marsh, urban, suburban).
- Path loss due to tropospheric scatter.
- Location variability (based on terrain roughness, frequency and nearby trees and buildings).

4.6 SUMMARY

This chapter describes in detail the propagation models used for simulations in this survey. It also presents fundamental theories and concepts, which are necessary for the understanding of the whole process. Finally, it gives and describes the programs that were coded in MATLAB and used for the simulations in this survey**.**

4.7 REFERENCES

[1] NTIA, National Telecommunications & Information Administration, Available on line at https://www.ntia.doc.gov/home

[2] P.L. Rice, A.G. Longley, K.A. Norton, and A.P. Barsis, "Transmission loss predictions for tropospheric communications circuits", Technical Note 101, revised 1/1/1967, U.S. Dept. of Commerce NTIA-ITS.

[3] NASA, "Shuttle Radar Topography Mission data," SRTM3. Available on line at http://www2.jpl.nasa.gov/srtm/.

[4] NASA, "Shuttle Radar Topography Mission data," SRTM1. Available on line at https://e4ftl01.cr.usgs.gov/SRTM/SRTMGL1.003/2000.02.11/.

[5] Roger Coud Coudé, Webpage of Radio Mobile, a site for downloads and How to http://www.cplus.org/rmw/english1.html, freeware by VE2DBE.

[6] SPLAT! A Terrestrial RF Path Analysis Application for Linux/Unix. Available on line at http://www.qsl.net/kd2bd/splat.html.

[7] S. E. Shumate, "Longley-Rice and ITU-P.1546 combined: A new international terrain-specific propagation model," in *Proc. 2010 IEEE 72nd Vehicular Technology Conference Fall (VTC 2010-Fall),* Sept. 2010, pp.1-5.

[8] Hata/Davidson, "A Report on Technology Independent Methodology for the Modeling, Simulation and Empirical Verification of Wireless Communications System Performance in Noise and Interference Limited Systems Operating on Frequencies between 30 and 1500MHz," TIA TR8

Working Group, IEEE Vehicular Technology Society Propagation Committee, May 1997.

[9] TIA, "The Telecommunications Industry Association," Advancing Global Communications. Available at http://www.tiaonline.org/.

[10] Federal Communication Commission's terrain database calculator. Available at https://www.fcc.gov/media/radio/haat-calculator

[11] "Method for point-to area prediction for terrestrial services in the frequency range 30 MHz to 300MHz," Recommendation ITU-R P.1546-5, 2013. Available at http://www.itu.int

[12] Jef Statham, "ITU-R p. calculator". An implementation of the ITU-R P.1546-3 model. Created on 21 August 2009 and updated on 27 August 2009. Available at https://www.mathworks.com/MATLABcentral/fileexchange/25099-itu-r-p-1546-calculator?requestedDomain=www.mathworks.com

[13] J. Deygout, "Multiple Knife-Edge Diffraction of Microwaves," IEEE Trans on Antennas and Propagation. vol. 14, pp. 480-489, Apr. 1966.

[14] J. Deygout, "Correction Factor for Multiple Knife-Edge Diffraction," IEEE Trans on Antennas and Propagation. vol. 39, No. 8, pp. 1256-1258, August 1991.

[15] J. Epstein and D. W. Peterson, "An experimental study of wave propagation at 850 Mc," Proc. IRE, vol. 41, pp. 595-611, 1953.

[16] C. L. Giovaneli, "An analysis of simplified solutions for multiple knife- edge diffraction," IEEE Trans. on Antennas and Propagation., vol. 32, pp. 297-301, Mar. 1984.

[17] "Propagation by diffraction," Recommendation ITU-R P.526-13, 11/2013, P Series, Radiowave propagation. Available at www.itu.int/rec/R-REC-P.526-13-201311-I

[18] François Beauducel, "READHGT: Import/download NASA SRTM data files (.HGT). Created on 25 August 2012 and updated on 27 December 2016. Available on line at URL:https://www.mathworks.com/MATLABcentral/fileexchange/36379-readhgt-import-download-nasa-srtm-data-files---hgt-

[19] R. L. Freeman, Radio System Design for Telecommunications, 3rd edition, John Wiley & Sons, ISBN: 978-0-471-75713-9, 2007

[20] C. A. Balanis, Antenna Theory: analysis and design, 3rd edition, John Wiley & Sons, ISBN 0-471-66782-X, 2005

CHAPTER 5

LONGLEY-RICE MODEL PREDICTION INACCURACIES IN THE UHF AND VHF TV BANDS IN MOUNTAINOUS TERRAIN.

5.1 INTRODUCTION

The necessity of accurate point-to-area prediction tools arises from the huge demand in designing broadcasting systems for digital TV and cellular communications. Up to now, a considerable number of coverage prediction models for radio coverage has been developed. In electromagnetic wave propagation theory three are the main types of propagation models. The empirical models that are based on a large quantity of measurement data are very simple but not very accurate. The semi-deterministic models that are based on measurement data and electromagnetic theory of propagation, which are more accurate. Finally, the deterministic models based on theoretical physics, like diffraction theory and Fresnel theory, which require a significant amount of geometrical data about the propagation terrain profile but are the most accurate, and preferred.

In nowadays, coverage prediction is of prime importance for TV broadcasting. A classic model used for TV coverage prediction is the Longley-Rice model (ITM- Irregular Terrain Model). Other well-known multiple knife-edge diffraction models are those of Epstein-Peterson, Deygout, and Giovaneli. In this study, comparisons are made between field precision measurements, taken from a Rohde & Schwarz FSH-3 portable spectrum analyser using precision calibrated antennas and Longley-Rice model simulations, and multiple knife-edge models combined with the 3-arc-second SRTM (Satellite Radar Topography Mission) terrain data. Calculations are limited to the main two Knife-Edges of the propagation path. The Longley-Rice model predicts received field strength accurately in most cases even in mountainous terrain with multiple diffracting obstacles in the VHF and UHF TV Bands. However, in some long-distance reception areas field-strength is underestimated by the Longley-Rice model, while it is accurately calculated by the multiple knife-edge diffraction models.

In this study, coverage prediction results, for VHF and UHF TV broadcasting in the region of Thessaloniki – Greece are compared, with accurate field measurements taken by our measurement equipment. Longley-Rice simulations in this chapter are carried with the use of Radio Mobile. It is presented as a Radio Propagation and Virtual Mapping Freeware, [1] [2]. It is a program based on the Irregular Terrain Model (known

as the Longley-Rice Model) [3] and uses the 3-arc-second SRTM maps [4]. The classical approach for single Knife-Edge diffraction and the calculation of path loss over a single sharp obstacle is based on the Fresnel-Kirchhoff's theory of optics.

This theory was discussed in previous chapters. Also, Epstein-Peterson's [5], Deygout's [6] [7], and Giovaneli's [8] models were presented in detail in previous chapters. For all our calculations, the approximate solution provided by Lee [9] is used.

Free Space Loss is calculated from the well-known formula (5.1)

$$PL_{FREE\ SPACE} = 32.44 + 20 \cdot log_{10}\ f_{MHz} + 20 \cdot log_{10}\left(d_{km}\right) \quad (5.1)$$

and total Path Loss is estimated adding path losses of Free Space and Diffraction.

$$PL(dB) = PL_{FREESPACE} + PL_{DIFFRACTION} \quad (5.2)$$

In general, the field strength as a function of Path Loss (PL), E.R.P (Effective Radiated Power) and frequency f (MHz), is calculated using the formula (5.3)

$$E\left(dB\mu V / m\right) = ERP\left(dBW\right) - PL\left(dB\right) + 20 log_{10}\ f_{MHz} + 109.35 \quad (5.3)$$

If E.I.R.P (Equivalent Isotropically Radiated Power) is used and consider that $G_r(dBi)=0$ (receiver antenna gain), the equation (5.3) becomes

$$E\left(dB\mu V / m\right) = P_t\left(dBm\right) - P_{TOTAL\ PATHLOSS}\left(dB\right) + 20 log_{10}\ f_{MHz} + 77.2 \quad (5.4)$$

Equation (5.4) is used in all our simulations.

In this study, the "Sample Standard Deviation" was calculated between measured path loss values and those predicted by Radio Mobile and SPLAT! by the following very commonly used equation with Bessel's correction:

$$s = \sqrt{\frac{1}{N-1}\sum_{i=1}^{N}(x_i - \mu)^2} \quad (5.5)$$

where,

s is the Simple Standard Deviation

N is the number of measurement data points,

x_i is the error between the predicted and the measured field-strength for data point i, and

μ is the average value of error (dB).

5.2 MEASUREMENTS AND COMPARISONS

The propagation of electromagnetic waves over irregular terrain with obstacles includes diffraction attenuation of the received signal. It is essential to determine the diffraction losses over such obstructions. Therefore, to measure the signal strength of UHF DVB-T and VHF ATV transmissions, a measurement campaign was carried out around the city

of Thessaloniki [10-16] located in the north of Greece and the neighboring FYR of Macedonia (F.Y.R.O.M). A Rohde & Schwarz FSH-3 portable spectrum analyser with tracking generator (100 kHz – 3 GHz), and a ± 0.7 dB accuracy (factory calibrated) was used in our measurements. Also, two high-precision biconical antennas, Schwarzbeck SBA 9113 and Schwarzbeck BBVU 9135, with ± 1.0 dB accuracy (factory calibrated) were used. A precision log-periodic Schwarzbeck USLP9143 with approximately 6-7 dBi gain, a commercial Iskra P20 UHF-TV Band log-periodic with a 6-7 dBi gain, and a low-loss, 1.8meters long, cable Suhner GX-07272-D 50 Ohm, with N-type connectors were also used.

For simulations, the Longley-Rice model (ITM) incorporated into the Radio Mobile software was used. The Epstein-Peterson, Deygout, and Giovaneli methods coded in MATLAB were also used for comparison purposes. Parameters h, h_1, h_2 in some cases were negative because the Line of Sight (LOS) line did not intersect with the obstacles, which means that the LOS line was clear, but the 0.6 of Fresnel zones (0.6F) intersected with the obstacles. Ground reflections were ignored in our Knife-Edge calculations. Separation distances between obstacles were much larger compared to the wavelength.

A program, which calculates diffraction losses from the above mentioned multiple diffraction methods and uses the SRTM terrain was coded in MATLAB. If there are no intersection points between the 0.6 of first Fresnel zone (0.6F) and obstacles, it calculates Free Space Loss. If there is one obstacle it estimates diffraction loss using single Knife-Edge theory. Finally, if there are two obstacles it computes diffraction losses using Epstein-Peterson's, Deygout's, and Giovaneli's approach.

A point-to-point analysis took place for analog TV "TURTEL", which is located at the state of Former Yugoslav Republic of Macedonia (F.Y.R.O.M), with the following characteristics.

- Transmitter's name: TURTEL
- Transmission Channel: VHF 11
- Transmission frequency: 217.25 MHz
- $P_{o:}$ 8 kW or 39 dBW or 69.03 dBm
- Net Antenna Gain: 8.0 dBd, or 10.15 dBi
- E.R.P: 50.4 kW or 47 dBW or 77.03 dBm
- E.I.R.P: 82.8 kW or 49.18 dBW or 79.18 dBm
- Transmitter Antenna Height Ht: 45 m

- Receiver Antenna Height Hr: 2.5 m
- Altitude: 1590 m
- Longitude: 22.42255E and Latitude: 41.80293N

Measurements and simulations are shown in Table 5-1.

Table 5-1. Measurement Points and Results for "TURTEL" VHF-ATV.

No.	Measurements Points	LAT(N)/ LONG(E)	E (dBμV/m)				
			FSH-3 Measurements	Longley-Rice	Double Knife-Edge		
					Deygout	Epstein-Peterson	Giovaneli
1	NEGOTINO (44.6 km/215.6 degs)	41.47592 22.10990	70.8	76.5	76.5	65.9	76.5
2	VELES (51 km/258.3 degs)	41.70822 21.82033	70.6	66.0	74.1	69.7	68.6
3	BOSKIJA (54.8 km/174.3 degs)	41.31216 22.48819	65.4	56.1	62.5	61.4	60.3
4	CRN VRV (58.4 km/275.4 degs)	41.85039 21.72081	55.3	38.2	57.4	57.4	57.4
5	OKTA (64.6 km/280.3 degs)	41.90413 21.65462	55.5	55.6	52.2	53.3	64.4
6	PETROVEC (70.6 km/283.9 degs)	41.95314 21.59469	55.4	58.0	62.5	60.3	57.7
7	VODNO 1051m (87 km/282 degs)	41.96507 21.39452	86.9	84.8	81.1	81.1	81.1
8	EKO-POLYKASTRO (94.1 km/170 degs)	40.96926 22.62205	59.8	62.0	64.2	63.6	60.9
9	POLYKASTRO-2 (101 km/169 degs)	40.90833 22.65187	62.0	70.0	71.9	68.0	58.8
10	AG. ATHANASIOS-4 (109 km/169.1 degs)	40.83807 22.66864	62.3	72.5	73.6	63.7	54.5
11	POLYKASTRO-3 (112 km/169.2 degs)	40.80907 22.67319	73.3	74.4	72.9	67.9	64.9
12	POLYKASTRO (117 km/169 degs)	40.79522 22.68180	76.0	78.0	76.3	68.7	75.5
13	AG. ATHANASIOS-6 (130 km/169 degs)	40.65207 22.71910	57.4	62.7	66.9	67.0	69.3

14	THESSALONIKI (139 km/161.2 degs)	40.61582 22.95573	54.5	41.1	55.7	54.7	54.3
15	PROFITIS ELIAS (140 km/158 degs)	40.64032 23.04020	79.8	75.3	77.4	77.4	77.4

Differences between measurements (FSH-3) and simulations from various models, with average error and standard deviation, are shown in Table 5-2. It is observed from Tables 5-1 and 5-2 that the Longley-Rice model can lead to large negative and positive differences from measured results (e.g. points 4, 7, 10, and 14 where the differences are around 10 dB or larger).

Diffraction attenuation is mostly overestimated by the Longley-Rice model and this can be easily seen at measurement points 7 and 14, where the three other models used in this study are very near to the measured result. Epstein-Peterson method (both classical and modified approach) has the best accuracy in this VHF TV case study with the lowest standard deviation, followed closely by Deygout. Longley-Rice in this case study has the biggest standard deviation than other methods.

Table 5-2. Differences, average, and standard deviation between measurements and simulation results for "TURTEL" VHF-ATV.

No.	Measurements Points	Differences (dB) between			
		FSH-3 & ITM	FSH-3 & Deygout	FSH-3 & Epstein-Peterson	FSH-3 & Giovaneli
1	NEGOTINO (44.6 km/215.6 degs)	+5.7	+5.7	-4.9	-13.6
2	VELES (51 km/258.3 degs)	-4.6	+3.5	-0.9	-2.0
3	BOSKIJA (54.8 km/174.3 degs)	-9.3	-2.9	-4.0	-5.1
4	CRN VRV (58.4 km/275.4 degs)	-17.1	+2.1	+2.1	+2.1
5	OKTA (64.6 km/280.3 degs)	+0.1	-3.3	-2.2	+8.9
6	PETROVEC (70.6 km/283.9 degs)	+2.6	+7.1	+4.9	+2.3
7	VODNO 1051m (87 km/282 degs)	-2.1	-5.8	-5.8	-5.8
8	EKO-POLYKASTRO (94.1 km/169.8 degs)	+2.2	+4.4	+3.8	+1.1

9	POLYKASTRO-2 (101 km/169 degs)	+8.0	+9.9	+6.0	-3.2
10	AG. ATHANASIOS-4 (109 km/169.1 degs)	+10.2	+11.3	+1.4	-7.8
11	POLYKASTRO-3 (112 km/169.2 degs)	+1.1	-0.4	-5.4	-8.4
12	POLYKASTRO (117 km/169 degs)	+2.0	+0.3	-7.3	-0.5
13	AG. ATHANASIOS-6 (130 km/169 degs)	+5.3	+9.5	+9.6	+11.9
14	THESSALONIKI (139 km/161.2 degs)	-13.4	+1.2	+0.2	-0.2
15	PROFITIS ELIAS (140 km/158 degs)	-4.5	-2.4	-2.4	-2.4
	Average	-0.9	+2.7	-0.3	-0.8
	Standard Deviation	7.7	5.3	4.9	7.4

Differences between the measurements and the simulations resulting from the comparison of the Longley-Rice, Deygout, Epstein-Peterson, and Giovaneli models, are shown in Figure 5-1, in a bar diagram.

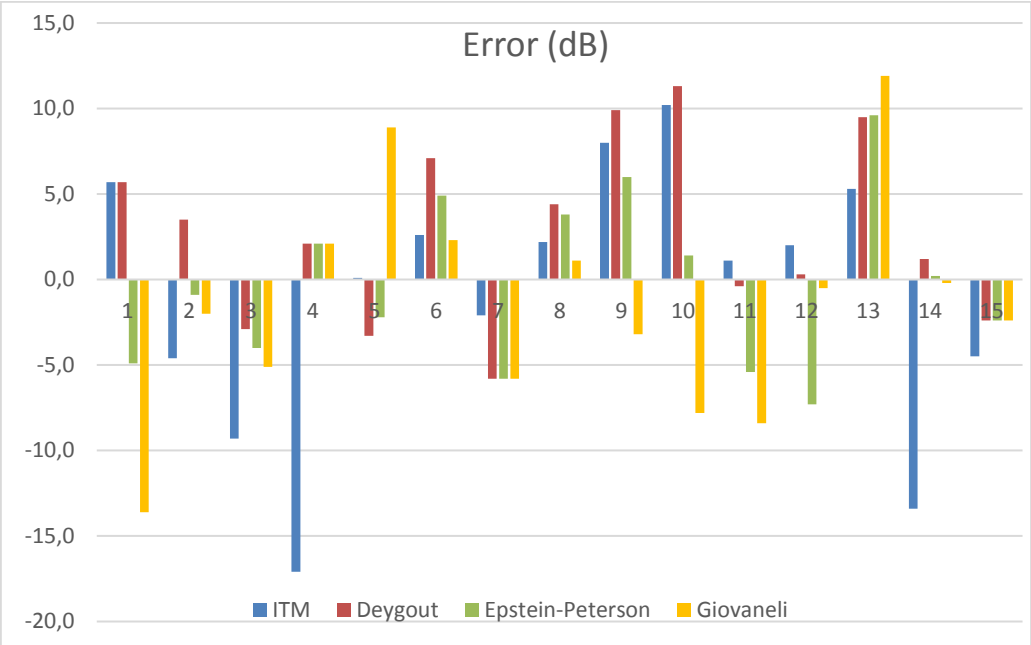

Figure 5-1: Errors between measurements and simulations (ITM, Deygout, Epstein-Peterson, and Giovaneli models) for "TURTEL" VHF-ATV.

A geophysical map that depicts the analog TV transmitter "TURTEL" and all the places our measurements took place, is shown in Figure 5-2. The places with the name, OKTA, BOSKIJA, VELES, PETROVEC, CRN-VRV, NECOTINO, VODNO, are in FYROM, and the places with the name, EKO-POLYKASTRO, POLYKASTRO-2, AG. ATHANASIOS-4, POLYKASTRO-3, POLYKASTRO, THESSALONIKI, AG-ATHANASIOS-6, are in Greece.

Figure 5-2: Geophysical map of the "TURTEL" net.

In Figure 5-3, elevation profile between transmitter "TURTEL" located in FYROM and receiver located at place "AG.ATHANASIOS-4" in Greece, with double Knife-Edge obstacles and Fresnel zones for Deygout's approach, is depicted. In this approach, the second obstacle, as can be seen from the intersection points (little red circles), has the maximum value of Fresnel parameter v_1 and is the main obstacle M1 and the third obstacle with the second maximum value of Fresnel parameter v_2 is the secondary one M2. Lines TxM1 and M1Rx define the Deygout model. In Figure 5-4 a geophysical map between transmitter "TURTEL" located in FYROM and receiver located at place "AG.ATHANASIOS-4" in Greece.

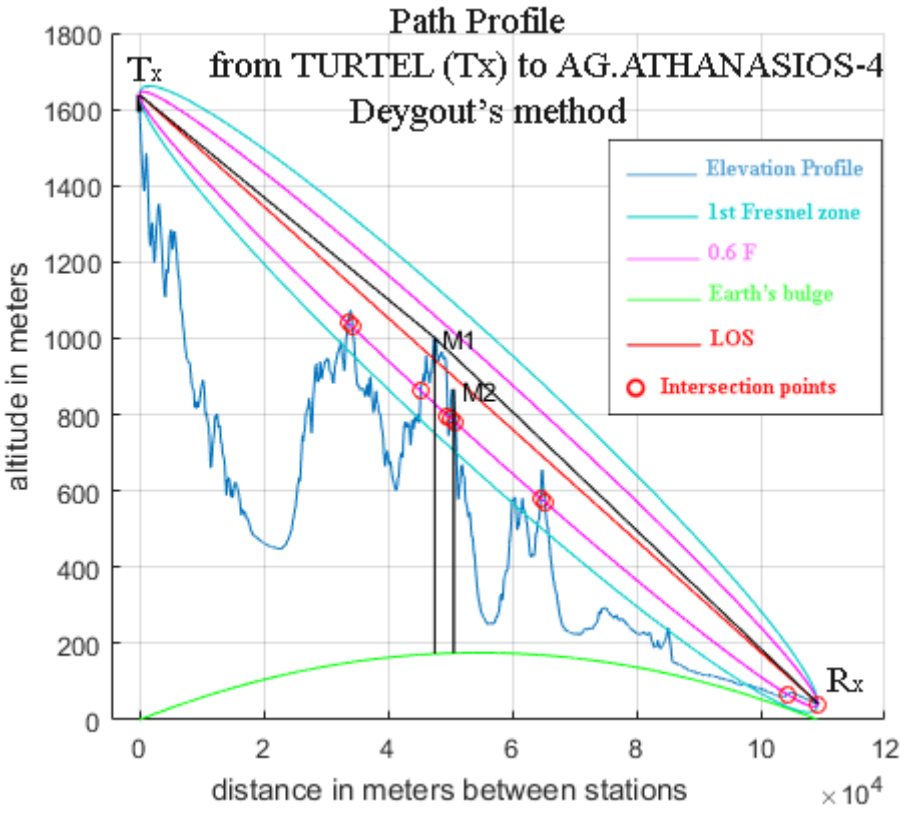

Figure 5-3: Path profile between transmitter "TURTEL" and receiver located at place "AG.ATHANASIOS-4", with Double Knife-Edges obstacles (M1 is the main obstacle and M2 is the second one) and Fresnel zones for Deygout's approach.

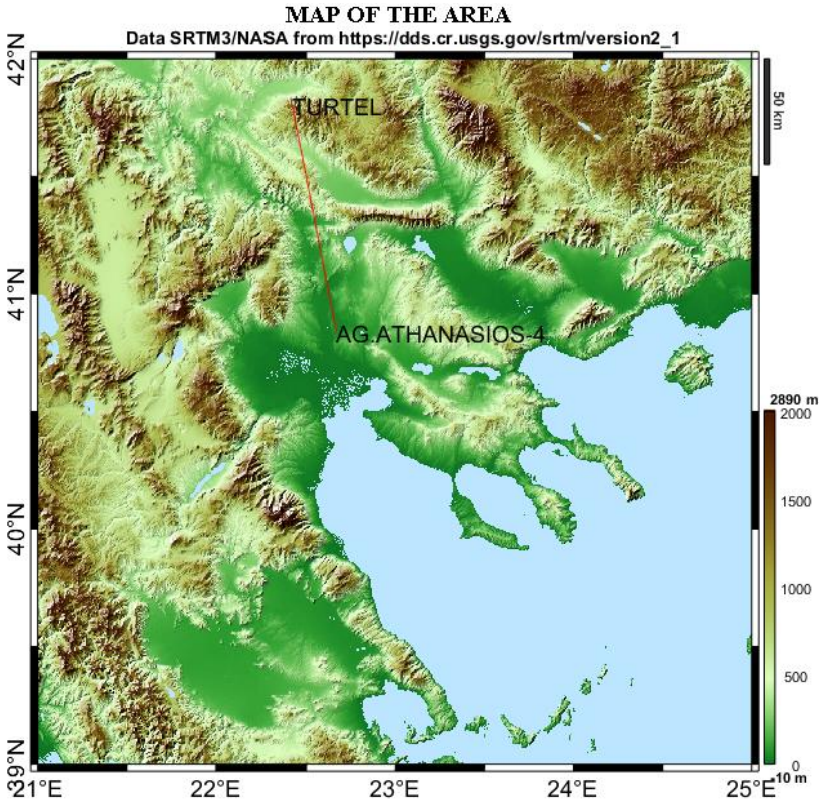

Figure 5-4: A geophysical map of the area between transmitter "TURTEL" and place "AG.ATHANASIOS-4".

In Figure 5-5, elevation profile between transmitter "TURTEL" and receiver located at place "AG.ATHANASIOS-4", with Double Knife-Edge obstacles and Fresnel zones for Epstein-Peterson's approach is depicted. Second and third obstacles are the main M1 and secondary M2 obstacles respectively. Lines TxM2 and M1Rx now define Epstein-Peterson's method.

The geophysical map of the area is the same as in Figure 5-4.

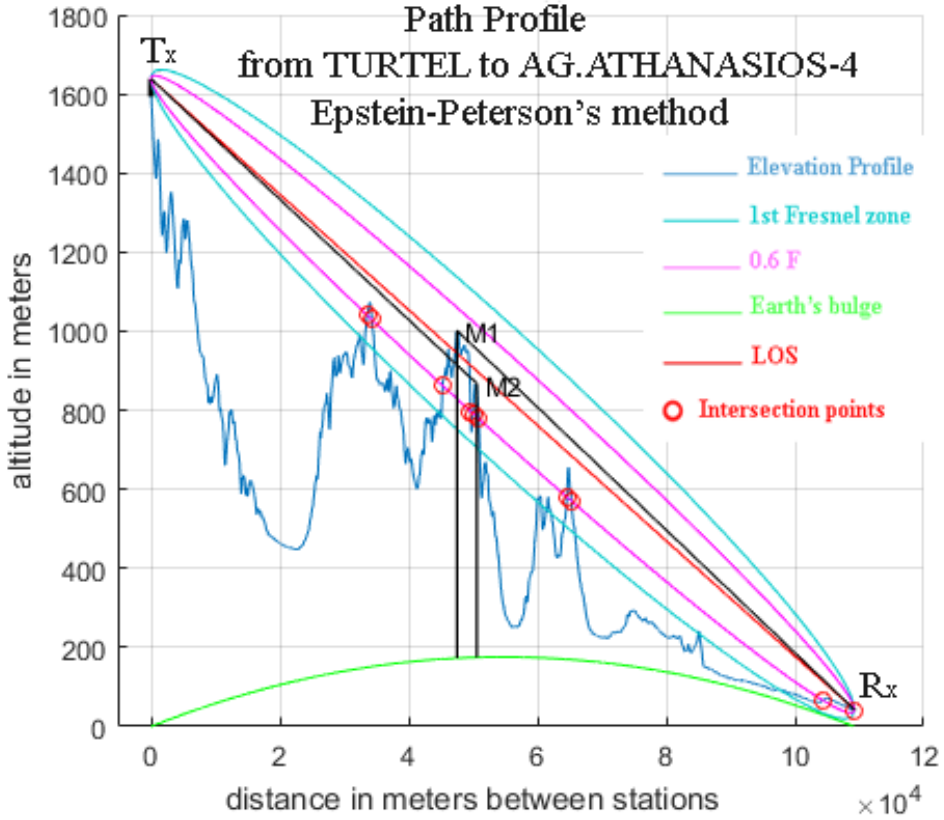

Figure 5-5: Path profile between transmitter "TURTEL" and receiver located at place "AG.ATHANASIOS-4", with Double Knife-Edges obstacles (M1 is the main obstacle and M2 is the second one) and Fresnel zones for Epstein-Peterson's approach.

In Figure 5-6, elevation profile between transmitter "TURTEL", located in F.Y.R.O.M and receiver located at place "AG.ATHANASIOS-4" in Greece, with double Knife-Edge obstacles and Fresnel zones for Giovaneli's approach is depicted.

Lines TxM1, M1Rx, TxR' and M1M2R' and plane R'R" now define Giovaneli's method. Second and third obstacles are the main (primary) M1 and secondary M2 obstacles respectively.

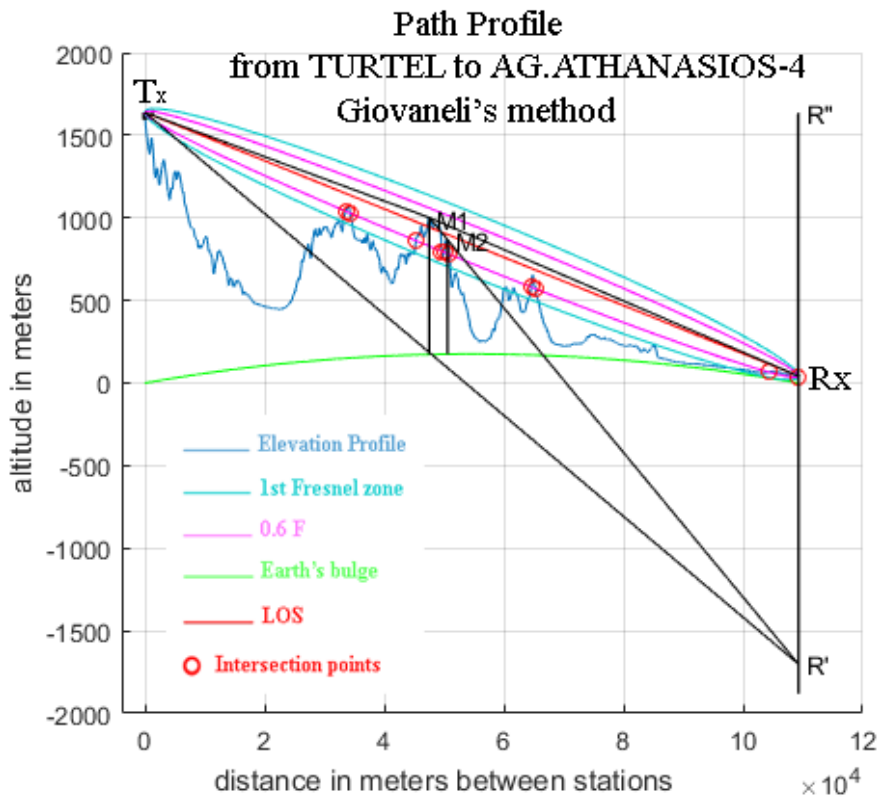

Figure 5-6: Path profile between transmitter "TURTEL" and receiver located at place "AG-ATHANASIOS-4", with Double Knife-Edges obstacles (M1 is the main obstacle, and M2 is the second one) and Fresnel zones for Giovaneli's approach.

Comparing now the "Deygout.m" program which considers only the two main obstacles ("Deygout.m" is the main program which is used in all our research), with the "Deygout3.m" and the "Deygout4.m" programs, it is found that there are insignificant errors between the simulation results. The "Deygout3.m" considers the three main obstacles and the "Deygout4.m" program considers the four main obstacles.

A further comparison between FSH-3 measurements and Longley-Rice (Irregular Terrain Model) simulation results on the one hand and Single Knife-Edge programs on the other are shown in Table 5-3 below.

A complete description of the three programs, "Single Knife-Edge," "Successive Sigle Knife-Edge," and "Cumulative Single Knife-Edge," was given in Chapter Four. It must be reminded, that the "Single Knife-Edge" program finds the obstacle with the maximum Fresnel parameter v that causes the biggest attenuation and calculates the field strength. The "Successive Single Knife-Edge" program finds the final path loss caused successively by each obstacle, reducing the receiving power at the next obstacle caused by the previous obstacle. The "Cumulative Single Knife-Edge" program adds all the path losses caused by each obstacle (pessimistic case).

Table 5-3. Measurement Points and simulation results for "TURTEL" VHF-ATV, using Single Knife-Edge, Successive Single Knife-Edge , and Cumulative Single Knife-Edge.

No.	Measurement points	LAT(N)/ LONG(E)	E(dBμV/m)				
			FSH-3 Measurements	Longley-Rice (Radio-Mobile)	Single Knife-Edge		
					Single Knife-Edge	Successive Single Knife-Edge	Cumulative Single Knife-Edge (pessimistic case)
1	NEGOTINO (44.6 km/215.6 degs)	41.47592 22.10990	70.8	76.5	76.5	76.5	72.7
2	VELES (51 km/ 258.3degs)	41.70822 21.82033	70.6	66.0	74.1	74.1	73.9
3	BOSKIJA (54.8 km/174.3 degs)	41.31216 22.48819	65.4	56.1	62.5	46.7	47.0
4	CRN VRV (58.4 km/275.4 degs)	41.85039 21.72081	55.3	38.2	57.4	57.4	57.4
5	OKTA (64.6 km/280.3 degs)	41.90413 21.65462	55.5	55.6	67	45.6	47.3
6	PETROVEC (70.6 km/283.9 degs)	41.95314 21.59469	55.4	58.0	62.5	54.6	54.8
7	VODNO 1051m (87 km/282 degs)	41.96507 21.39452	86.9	84.8	81.1	81.1	81.1
8	EKO-POLYKASTRO (94.1 km/170 degs)	40.96926 22.62205	59.8	62.0	64.2	51.8	50.7
9	POLYKASTRO-2 (101 km/169 degs)	40.90833 22.65187	62.0	70.0	71.8	43.3	52.2
10	AG. ATHANASIOS-4 (109 km/169.1 degs)	40.83807 22.66864	62.3	72.5	73.7	66.0	63.4
11	POLYKASTRO-3 (112 km/169.2 degs)	40.80907 22.67319	73.3	74.4	72.9	69.1	69.2
12	POLYKASTRO (117 km/169 degs)	40.79522 22.68180	76.0	78.0	76.3	73.0	69.6
13	AG. ATHANASIOS-6 (130 km/169 degs)	40.65207 22.71910	57.4	62.7	73.1	56.2	57.4
14	THESSALONIKI (139 km/161.2 degs)	40.61582 22.95573	54.5	41.1	55.7	53.8	47.7
15	PROFITIS ELIAS (140 km/158 degs)	40.64032 23.04020	79.8	75.3	77.4	77.4	77.4

Differences between measurements and simulations are shown in Table 5-4.

Table 5-4. Differences, average and standard deviation, for VHF TV "TURTEL", using Single Knife-Edge, Successive Single Knife-Edge , and Cumulative Single Knife-Edge.

No.	Measurement points	Errors (dB) between measurements and simulations			
		FSH-3 & ITM	FSH-3 & Single Knife-Edge	FSH-3 & Successive Single Knife-Edge	FSH-3 & Cumulative Single Knife-Edge
1	NEGOTINO (44.6 km/215.6 degs)	+5.7	+5.7	+5.7	+1.9
2	VELES (51 km/258.3 degs)	-4.6	+3.5	+3.5	+3.3
3	BOSKIJA (54.8 km/174.3 degs)	-9.3	-2.9	-18.7	-18.4
4	CRN VRV (58.4 km/275.4 degs)	-17.1	+-2.1	+2.1	+2.1
5	OKTA (64.6 km/280.3 degs)	+0.1	+11.5	-9.9	-8.2
6	PETROVEC (70.6 km/283.9 degs)	+2.6	+7.1	-0.8	-0.6
7	VODNO 1051m (87 km/282 degs)	-2.1	-5.8	-5.8	-5.8
8	EKO-POLYKASTRO (94.1 km/170 degs)	+2.2	+4.4	-8.0	-9.1
9	POLYKASTRO-2 (101 km/169 degs)	+8.0	-9.8	18.7	9.8
10	AG. ATHANASIOS-4 (109 km/169.1 degs)	+10.2	+11.4	+3.7	+1.1
11	POLYKASTRO-3 (112 km/169.2 degs)	+1.1	-0.4	-4.2	-4.1
12	POLYKASTRO (117 km/169 degs)	+2.0	+0.3	-3.0	-6.4
13	AG. ATHANASIOS-6 (130 km/169 degs)	+5.3	+15.7	-1.2	0.0
14	THESSALONIKI (139 km/161.2 degs)	-13.4	+1.2	-0.7	-6.8
15	PROFITIS ELIAS (140 km/158 degs)	-4.5	-2.4	-2.4	-2.4
Average		-0.9	+4.1	-3.9	-4.2
Standard Deviation		7.7	6.1	7.4	5.9

Figure 5-7, shows the differences between the measurements and the simulations resulting from the comparison of the models, in a bar diagram.

Figure 5-7. Errors between measurements and Single Knife-Edge simulations for the net "TURTEL".

Another point-to-point analysis took place for analog TV CRN-VRV, FYR of Macedonia (F.Y.R.O.M), with the following characteristics

- Transmitter's name: CRN-VRV
- Transmission Channel: VHF 6
- Transmission frequency: 182.25 MHz
- $P_{o:}$ 10 kW or 40 dBW or 70 dBm
- Net Antenna Gain: 8.5 dBd, or 10.65 dBi
- E.R.P: 70.8 kW or 48.45 dBW or 78.5 dBm
- E.I.R.P: 116.14 kW or 50.64 dBW or 80.65 dBm
- Transmitter Antenna Height Ht: 80 m
- Receiver Antenna Height Hr = 2.5 m
- Altitude: 772 m
- Longitude: 21.73846E and Latitude: 41.85931N

Some of the presented measurement paths are selected to contain diffracting obstacles. So, in Table 5-5 and in column 'Number of Obstacles' 0 means Free Space propagation, 1 means one obstacle and Single Knife-Edge propagation, and 2+ means two or more obstacles and Double Knife-Edge diffraction calculations.

Measurements and simulation results are shown in Table 5-5, which includes Deygout, Epstein-Peterson and Giovaneli models.

Table 5-5. Measurement Points and Results for "CRN-VRV" VHF-ATV.

No	Measurement points	LAT(N)/ LONG(E)	E(dBμV/m)						
			Number of Obstacles	Type of Path Loss	FSH3-Measurements	Longley-Rice (Radio Mobile)	Deygout	Epstein-Peterson	Giovaneli
1	PETROVEC 1 (15.8 km/311.3 degs)	41.953140 21.594690	1	SKE	94.3	103.6	98.8	98.8	98.8
2	VELES (18.1 km/158.0 degs)	41.708220 21.820330	1	SKE	95.0	96.8	99.8	99.8	99.8
3	VODNO 1051m (30.8 km/292.5 degs)	40.838070 22.668640	0	FS	95.7	95.8	95.6	95.6	95.6
4	NEGOTINO (52.5 km/144.0 degs)	41.475920 22.109900	2+	DKE	67.4	81.4	81.3	81.2	80.9
5	BOSKIJA (86.9 km/134.0 degs)	41.312160 22.488190	2+	DKE	51.9	44.4	60.1	59.4	59.0
6	POLYKASTRO (141.7 km/146.0 degs)	40.795220 22.681800	2+	DKE	52.8	38.2	50.7	48.4	50.4^{M}
7	PROFITIS ELIAS (173.1 km/140.8 degs)	40.640320 23.040200	2+	DKE	64.3	42.3	56.4	56.3	55.9

FS = Free Space, SKE = Single Knife-Edge, DKE = Double Knife-edge
M = Giovaneli Manual program using obstacles 5 and 6

In our calculations, only the double Knife-Edge models were used, although in some cases there were more than two obstacles. This was done to get equivalent comparisons between our code and the Longley-Rice model because the latter uses only the Double and Single Knife-Edge models. Refraction was considered by using the effective earth radius coefficient k = 1.33.

Average errors and standard deviations between measurements (FSH-3) and simulations produced by Longley-Rice, Deygout, Epstein-Peterson and Giovaneli models are shown

in Table 5-6 below.

Table 5-6. Differences between measurements and propagation models, ITM, Deygout, Epstein-Peterson, and Giovaneli for "CRN-VRV" VHF-ATV.

No.	Measurements Points	Differences (dB) between			
		FSH-3 & ITM	FSH-3 & Deygout	FSH-3 & Epstein-Peterson	FSH-3 & Giovaneli
1	PETROVEC 1 (15.8 km/311.3 degs)	+9.3	+4.5	+4.5	+4.5
2	VELES (18.1 km/158.0 degs)	+1.8	+4.8	+4.8	+4.8
3	VODNO 1051m (30.8 km/292.6 degs)	+0.1	-0.1	-0.1	-0.1
4	NEGOTINO (52.5 km/144.0 degs)	+14.0	+13.9	+13.8	+13.5
5	BOSKIJA (86.9 km/134.0 degs)	-7.5	+8.2	+7.5	+7.1
6	POLYKASTRO (141.7 km/146.0 degs)	-14.6	-2.1	-4.4	-2.4
7	PROFITIS ELIAS (173.1 km/140.8 degs)	-22.0	-7.9	-8.0	-8.4
	Average	-2.7	+3.0	+2.6	+2.7
	Standard Deviation	12.8	7.1	7.4	7.1

It is observed from Tables 5-5 and 5-6 that the Longley-Rice model can lead to significant negative and positive differences from measured results (e.g., points 4, 6, and 7) where the differences are larger than 10 dB). Generally speaking, diffraction attenuation is mostly overestimated by the Longley-Rice model, especially at very large distances, and this can be easily seen at measurement points 6 and 7, where the three other models used in this study are nearer to the measured result. In this case study in the VHF-TV Band, the classical multiple diffraction models of Deygout, Epstein- Peterson,

and Giovaneli are more accurate than the Longley-Rice model, especially at very large distances from the transmitter.

Figure 5-8, shows the differences between the measurements and the simulations resulting from the comparison of the Longley-Rice model and the classical models of Deygout, Epstein-Peterson, and Giovaneli, in a bar diagram.

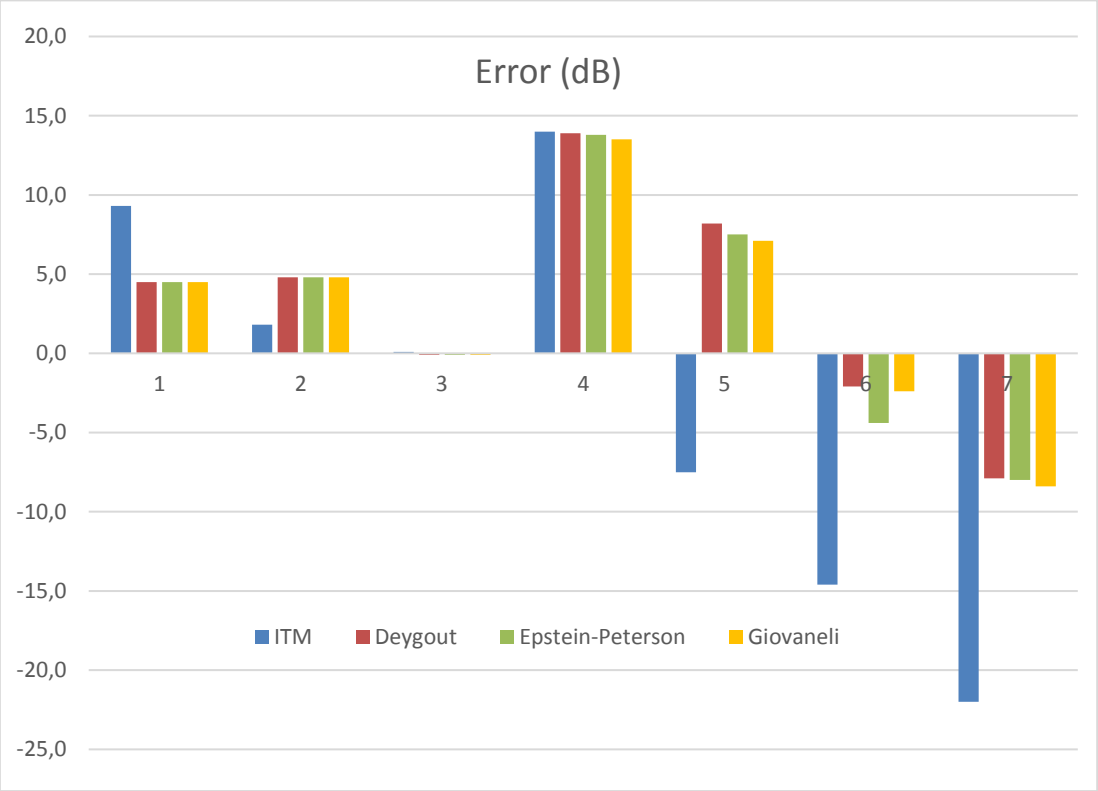

Figure 5-8: Errors between measurements taken by FSH-3 and simulations produced by ITM and Deygout, Epstein-Peterson and Giovaneli models, for VHF TV "CRN-VRV".

A geophysical map that depicts the analogue TV transmitter "CRN-VRV" and all the places our measurements took place is shown in the Figure 5-9.

The places with the name, BOSKIJA, VELES, PETROVEC 1, NECOTINO, VODNO, are in the state of FYROM (Former Yugoslav Republic of Macedonia).

The places with the name, POLYKASTRO and PROFITIS ELIAS are located in Greece.

Figure 5-9: Geophysical map of the "CRN-VRV" net

A point-to-point propagation from CRN-VRV to BOSKIJA with the use of Deygout's model, produced by our MATLAB program, with all obstacles, is shown in Figure 5-10.

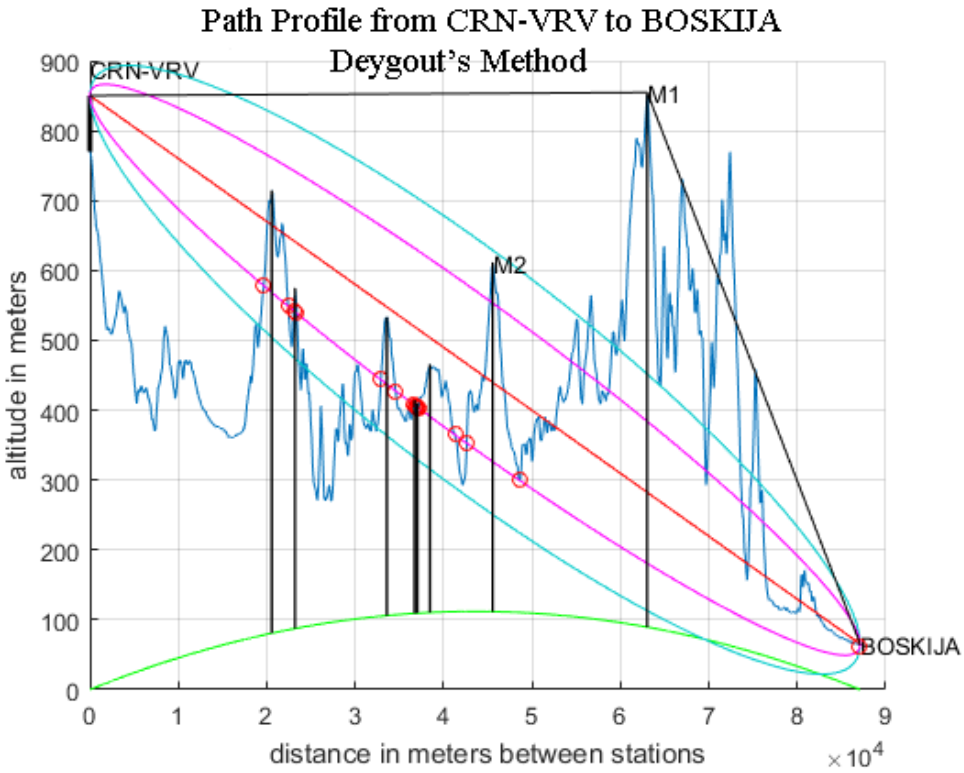

Figure 5-10: Path profile between "CRN-VRV" to 'BOSKIJA", all the Knife-Edges are shown, M1 is the main obstacle while M2 on its left, is the secondary one.

Comparing again, the "Deygout.m" program with the "Deygout3.m" program and the "Deygout4.m" program it can be seen, that there are insignificant differences in simulated results.

A further comparison for "CRN-VRV" VHF-ATV between FSH-3 measurements and ITM and Single Knife-Edge programs on the other is shown in Table 5-7 below. A complete description of the programs, "Single Knife-Edge", "Successive Single Knife-Edge" and "Cumulative Single Knife-Edge", is given in Chapter Four.

Table 5-7. Measurements and simulations between FSH-3, ITM, and Single Knife-Edge programs for "CRN-VRV" VHF-ATV.

No.	Measurements Points	LAT(N)/ LONG(E)	Number of Obstacles	Type of Path Loss	E(dBμV/m)				
					FSH3 Measurements	Longley-Rice (Radio Mobile)	Single Knife-Edge	Successive Single Knife-Edge	Cumulative Single Knife-Edge
1	PETROVEC 1 (15.8km/311.3degs)	41.953140 21.594690	1	SKE	94.3	103.6	98.8	98.8	98.8
2	VELES (18.1km/158.0degs)	41.708220 21.820330	1	SKE	95.0	96.8	99.8	99.8	99.8
3	VODNO 1051m (30.8km/292.5degs)	40.838070 22.668640	0	FS	95.7	95.8	95.6	95.6	95.6
4	NEGOTINO (52.5km/144.0degs)	41.475920 22.109900	2+	DKE	67.4	81.4	85.6	78.5	77.1
5	BOSKIJA (86.9km/134.0degs)	41.312160 22.488190	2+	DKE	51.9	44.4	60.1	23.0	25.0
6	POLYKASTRO (141.7km/146.0degs)	40.795220 22.681800	2+	DKE	52.8	38.2	50.7	47.8	48.6
7	PROFITIS ELIAS (173.1km/140.8degs)	40.640320 23.040200	2+	DKE	64.3	42.3	57.0	21.6	27.4
FS = Free Space, SKE = Single Knife-Edge, DKE = Double Knife-edge									

As can be seen from the above Table 5-7, Single Knife-Edge gives satisfactory simulation results, while at the same time “Successive Single Knife-Edge ” program and “Cumulative Single Knife-Edge” program give in two cases (cases 5 and 7) very

pessimistic simulation results. A Table with errors for the above Table 5-7 is not presented.

Figure 5-11 depicts a point-to-point propagation from site “TURTEL” to site “EKO-POLYKASTRO”, using Deygout’s method for three obstacles, and the “Deygout3.m” MATLAB program.

As can be seen in Figure 5-11, M1 is the main obstacle, M2 on its right is the second one and M3 also on the right, is the third significant obstacle.

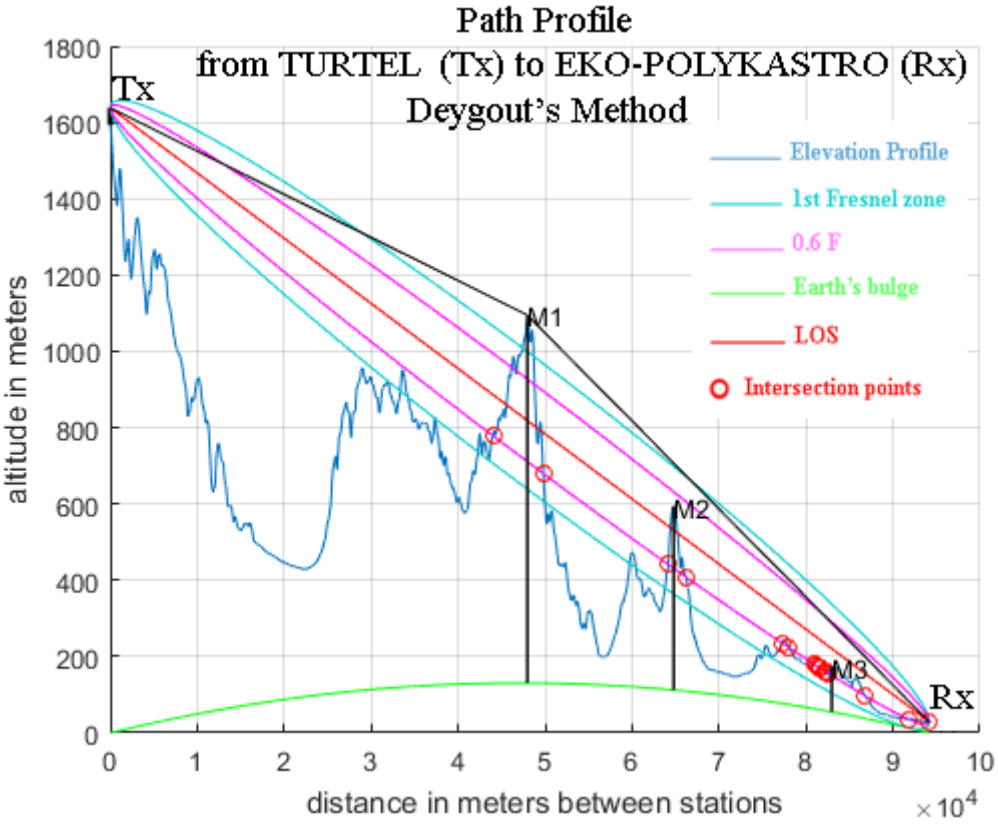

Figure 5-11: Path profile, LOS (Line of Sight), Fresnel zones (1F, 0.6F), three obstacles (three Knife-Edges) and Deygout’s method between transmitter’s site "TURTEL" and receiver’s site "EKO-POLYKASTRO".

Figure 5-12 depicts a point-to-point propagation from site “TURTEL” to site “AG-ATHANASIOS-4”, using Deygout’s method for four obstacles, and the “Deygout4.m” MATLAB program respectively.

As can be seen in Figure 5-12, M1 is the main obstacle, M2 on its right is the second one and M3 also, on the right is the third significant obstacle and finally, M4 on the left is the fourth significant obstacle.

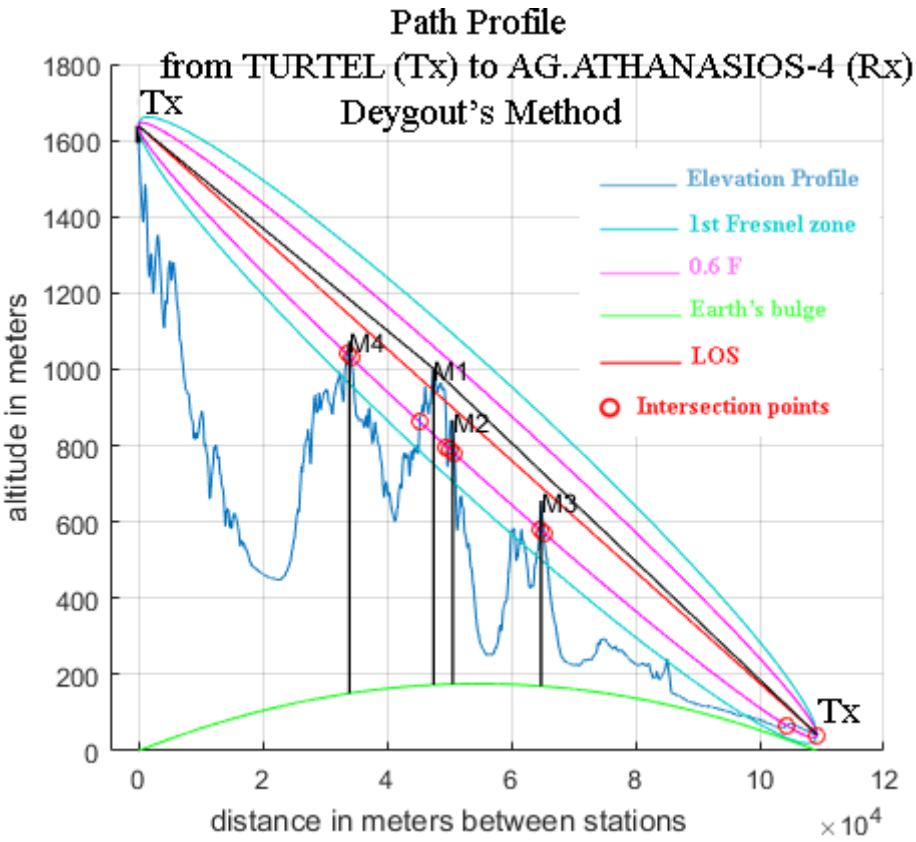

Figure 5-12: Path profile, LOS (Line of Sight), Fresnel zones (1F, 0.6F), four obstacles (four Knife-Edges) and Deygout's method between transmitter's site "TURTEL" and receiver's site "AG. ATHANASIOS-4".

5.3 SUMMARY

Classical propagation prediction models have been compared in this study for the VHF and UHF TV broadcasting frequencies. This study was focused on propagation in mountainous terrain, and in long propagation paths. Two different broadcasting sites have been used Turtel and CRN-VRV that cover neighboring geographical areas. The Longley-Rice model (ITM) with worldwide SRTM 3-arc-second data, incorporates single Knife-Edge and double Knife-Edge models and produces satisfactory results in comparison to measurements in most cases. However, the Longley-Rice model is overestimating diffraction attenuation at very large distances from the transmitter, especially in the VHF TV Band. Deygout, Epstein-Peterson and Giovaneli approaches are approximating multiple Knife-Edge diffractions using geometrical constructions. All the three of them give satisfactory results, and they are classic well-established models [17-18]. Their relative accuracy was found to be comparable in the case studies of this paper. They proved to be more accurate than the Longley-Rice model over long paths including diffracting obstacles in the VHF-TV Band. The main finding is that in most

cases the single Knife-Edge approach gives very satisfactory results. The double Knife-Edge programs, of course, provide better results, while the programs for three and four obstacles do not deliver better results except in very few cases. A further improvement in diffracting loss calculation accuracy is expected from Vogler's rigorous method [19].

5.4 REFERENCES

[1] Roger Coudé, Webpage of Radio Mobile, a site for downloads and How to http://www.cplus.org/rmw/english1.html, freeware by VE2DBE.

[2] Salamanca L. Murillo-Fuentes J.J. Olmos P. "Review of the Radio Mobile Software as a teaching tool for Radio planning" IEEE Multidisciplinary Engineering Education Magazine, Vol. 6, No. 2, June 2011.

[3] P.L. Rice, A.G. Longley, K.A. Norton, and A.P. Barsis. "Transmission loss predictions for tropospheric communications circuits", Technical Note 101, revised 1/1/1967, U.S. Dept. of Commerce NTIA-ITS.

[4] NASA, "Shuttle Radar Topography Mission data". Available on line at http://www2.jpl.nasa.gov/srtm/.

[5] J. Epstein and D. W. Peterson, "An experimental study of wave propagation at 850 Mc," Proc. IRE, vol. 41, pp. 595-611, 1953.

[6] J. Deygout, "Transmissions Multivoies par Faisceaux Hertziens", E.A.T. (Montargis), titre III, Fasc. 1, 1961, and titre I, pp. 139-141, 1964.

[7] J. Deygout, "Multiple Knife-Edge Diffraction of Microwaves," IEEE Trans on Antennas and Propagation. vol. 14, pp. 480-489, Apr. 1966.

[8] C. L. Giovaneli, "An analysis of simplified solutions for multiple knife-edge diffractions," IEEE Trans on Antennas and Propagation., vol. 32, pp. 297-301, Mar. 1984.

[9] W. C. Y. Lee, "Mobile Cellular Telecommunications: Analog and Digital Systems," McGraw-Hill, 1995.

[10] S. Kasampalis, P. Lazaridis, Z. Zaharis, S. Zettas, J. Cosmas, "Comparison of ITM and ITWOM propagation models for DVB-T coverage prediction", IEEE BMSB 2013 conference, London, June 2013.

[11] S. Kasampalis, P. Lazaridis, Z. Zaharis, S. Zettas, J. Cosmas, "Comparison of Longley-Rice, ITM, and ITWOM propagation models for DTV and FM broadcasting", WMPC 2013 conference, Atlantic city, New Jersey, USA, June 24-27, 2013.

[12] S. Kasampalis, P. Lazaridis, Z. Zaharis, S. Zettas, J. Cosmas, "Comparison of Longley-Rice, ITU-R P.1546 and Hata-Davidson propagation models for DVB-T coverage prediction", IEEE BMSB 2014, International Symposium on Broadband Multimedia Systems and Broadcasting, June 25-27, 2014, Beijing, China.

[13] P. I. Lazaridis, S. Kasampalis, Z. D. Zaharis, J. Cosmas, A. Bizopoulos, P. Latkoski, L. Gavrilovska, O. Fratu, R. Prasad, "UHF TV band spectrum and field-strength measurements before and after analog switch-off," Global Wireless Summit, Aalborg, Denmark, May 11-14, 2014.

[14] A. Bizopoulos, P. I. Lazaridis, E. Paparouni, D. Drogoudis, S. Kasampalis, I. Dalis, L. Gavrilovska, "Coverage Prediction and Validation for DVB-T Services," ETAI, Ohrid, Sep. 2011.

[15] P. I. Lazaridis, A. Bizopoulos, S. Kasampalis, J. Cosmas, Z.D. Zaharis, "Evaluation of Prediction Accuracy for the Longley-Rice model in the FM and TV bands," ETAI, Ohrid, Sep. 2013.

[16] P. I. Lazaridis, S. Kasampalis, Z. D. Zaharis, J. P. Cosmas, L. Paunovska, I. Glover, "Longley-Rice model precision in case of multiple diffracting obstacles," URSI Atlantic Conference, Canary Islands, May 2015.

[17] T.L. Rusyn, "A study of the 'slack-string' knife-edge diffraction model," The 3rd European Conference on Antennas and Propagation, 2009.

[18] D. A. Bibb, J. Dang, Z. Yun, M. F. Iskander, "Computational Accuracy and Speed of Some Knife-Edge Diffraction Models," Antennas and Propagation Society International Symposium (APSURSI), IEEE 2014, Memphis, TN, 6-11 July 2014, pp. 705-706.

[19] L. E. Vogler, "An attenuation function for multiple knife-edge diffraction," Radio Sci., vol. 17, pp. 1541-1546, Nov.-Dec. 1982.

CHAPTER 6

COMPARISON OF LONGLEY-RICE, ITU-R P.1546, AND HATA-DAVIDSON PROPAGATION MODELS FOR DVB-T COVERAGE PREDICTION (MODELS DEYGOUT, EPSTEIN-PETERSON, AND GIOVANELI ARE ALSO INCLUDED)

6.1 INTRODUCTION

The massive increase in designing broadcast systems for digital TV and cellular systems necessitates the development of accurate point-to-area prediction tools. In electromagnetic wave propagation theory there is a large number of coverage prediction models for DVB-T coverage. More specifically, there are three main types of propagation models. Empirical models that are based on measurement data, they are simple and use statistical data but they are not very accurate, semi-deterministic models that are based on empirical data and deterministic aspects, and deterministic models that are based on theory and require a lot of geometrical information about the site and the terrain, need a very significant computational effort, but they are more accurate.

In this study precision field-strength measurements are taken by a Rohde & Schwarz FSH-3 portable spectrum analyser. Simulation results are derived from the ITM (Longley-Rice model) coverage prediction model, in conjunction with the 3-arc-second SRTM (Satellite Radar Topography Mission) geographical data. Propagation predictions of ITU-R Recommendation P.1546 and those of the empirical Hata-Davidson model using HAAT also derived. Finally, in this paper comparisons between measurements and ITM, P.1546 and Hata-Davidson models take place. Models ITU-R P.1546 and Hata-Davidson exhibit higher errors at longer distances, and therefore necessary corrections should be introduced in the models to increase propagation prediction accuracy. Especially, measurements results show that ITU-R P.1546, on average, underestimates the field strength at distances longer than 50 km. The Longley-Rice model using the digital terrain elevations is more accurate, as expected, and its results are closer to the measurement data.

This research aims to provide coverage prediction results for DVB-T services, in the region of Thessaloniki – Greece, and compare the simulation results produced by the propagation prediction software with field measurements taken by our measurement equipment. It is well known that the use of prediction models becomes a necessity because making on-site measurements costs in time and money.

The Radio Mobile program [1-2] (Radio Propagation and Virtual Mapping Freeware) is based on the Longley-Rice Model ITM [3] and uses the 3-arc-second Satellite Radar Terrain Mission SRTM maps, [4]. The Radio Communication Sector of ITU proposed the Recommendation ITU-R P.1546 [5]. It is a method for point-to-area-prediction for terrestrial services in the frequency range 30 MHz to 3 GHz. This method is based on empirically derived field-strength curves and has replaced the older ITU-R 370 Recommendation. These curves are functions of frequency, antenna height, distance and time percentage. Extrapolation and interpolation methods are used to derive data from these empirical curves. The field strength (dBμV/m) is calculated for 1 kW ERP (Effective Radiated Power). The latest version is ITU-R P.1546-5, Sept. 2013.

The empirical Hata model [6], on the other hand, uses mathematical equations that involve antenna heights of transmitter and receiver, frequency 150 MHz to 1500 MHz, distance from the base station ranges from 1 km to 20 km in urban, suburban and open area environments. It is an extension of Okumura's method, and it is based on Okumura's field test results for the city of Tokyo, Japan [7-9].

The Telecommunications Industry Association (TIA) recommended a modification to the Hata model to cover a broader range of input parameters and distances. The model is known as Hata-Davidson model and provides corrections for links up to 300 km distance and transmitters at an altitude up to 2500 m. It was published in TSB-88A [10]. The formulas of the Hata-Davidson model are described in detail in Chapter 3.

Field strength is calculated from the equation (5.4), and Free Space Path Loss is derived from the well-known equation (5.1). Field-strength is not allowed to assume values higher than the free-space values.

6.2 MEASUREMENTS AND COMPARISONS

A measurement campaign, to measure the signal strength of DVB-T transmissions, was carried out around the city of Thessaloniki [11-12], located in the north of Greece.

A point-to-point analysis for Greek public TV ERT, Channel UHF 23 is made of the measurement points shown in Table 6-1.

- Transmitter's name: ERT
- Transmission Channel: CH23
- Transmission frequency: 490 MHz
- P_o: 1600 W or 32 dBW or 62 dBm

- Net Antenna Gain: 10 dBd, or 12.15 dBi
- E.R.P: 15.8 kW or 42 dBW or 72 dBm
- E.I.R.P: 26 kW or 44.14 dBW or 74.15 dBm
- Transmitter Antenna Height Ht: 70 m
- Receiver Antenna Height Hr: 2.5 m
- Altitude: 898.5 m
- Longitude: 23.099793E and Latitude: 40.597648N

One of main correction factors that Davidson added to Hata's formulas is the HAAT factor (antenna **H**eight **A**bove **A**verage **T**errain). In the Hata model formulas are limited in their applicability to:

- Range from Base, 1-20 km.
- Frequency Range, 150-1500 MHz.
- Base HAAT, 20-200 meters.

In the Hata-Davidson model, these limits are extended to:

- Range from Base, 1-300 km.
- Frequency Range, 30-1500 MHz.
- Base HAAT, 20-2500 meters.

Table 6-1. Measurement points and HAAT for "ERT" net.

No.	Measurement Points	d(km)	LAT	LONG	DEGS	HAAT (m)
1	PROFITIS ELIAS	7	40.640411	23.039927	313	487.2
2	THESSALONIKI	12.3	40.615822	22.955735	279	784.8
3	LAKE VOLVI	14.3	40.707102	23.188914	31	788.8
4	PEREA	16.7	40.513489	22.937471	236	815.5
5	METHONI	47	40.469402	22.574711	252	799.7
6	KORINOS	52	40.307130	22.618620	232	810.7
7	BORDER EVZONI	68.8	41.081410	22.588160	321	479.5
8	POLYKASTRO	69	41.081190	22.588360	320	475.9
9	SOUMELA	86	40.410086	22.116606	256	789.8

10	LOUTRAKI	107	40.966160	21.923630	293	629.4

Many programs can calculate HAAT. Radio Mobile software (that uses the Longley-Rice model) is also one of them. In this chapter, HAAT was computed using NAD83/WGS84, FCC's terrain database, and the GLOBE 1 km database [13]. It should be clarified that the term "HAAT" refers to the HAAT in the direction of the radial under consideration and not to the overall site HAAT. HAAT values are shown in Table 6-1 and Figure 6-1 respectively, for the ten measurements points.

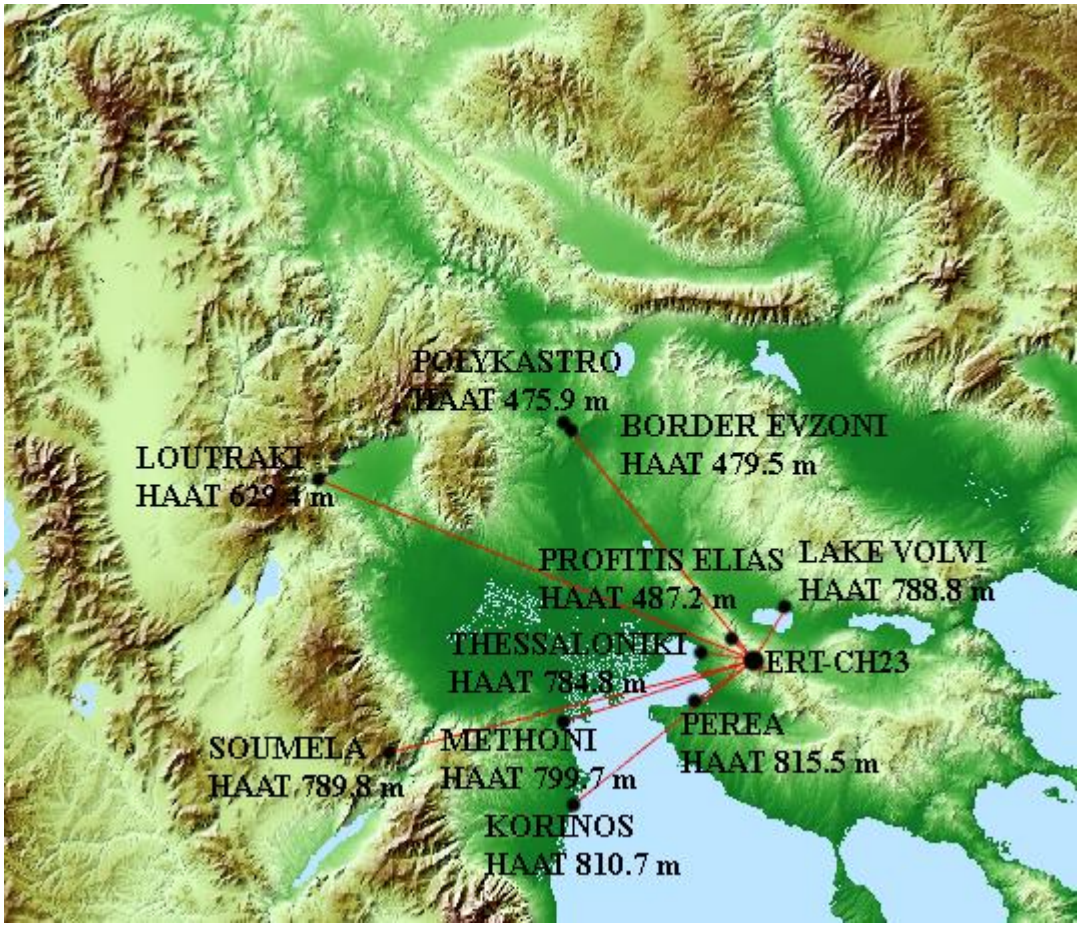

Figure 6-1: Measurement points and HAAT for "ERT-CH23" net.

Propagation curves of Recommendation ITU-R P.1546 that are used for the calculation of field strength, with the proper interpolations, is shown in Figure 6-2. These curves and the appropriate equations were used, to obtain our calculated results.

The propagation curves of Recommendation ITU-R P.1546, are designed for 1 kW effective radiated power (ERP) which is 60 dBm. The ERP power of the transmitter under study (ERT – CH23) is 1600 W which is 62 dBm, and the transmitter's antenna

has a gain of 10 dBd, so the total transmitted ERP power is 72 dBm. Consequently, a value of 12 dB (72 dBm-60 dBm=12 dB) must be added to the values of field strength produced by the ITU-R P.1546 propagation curves.

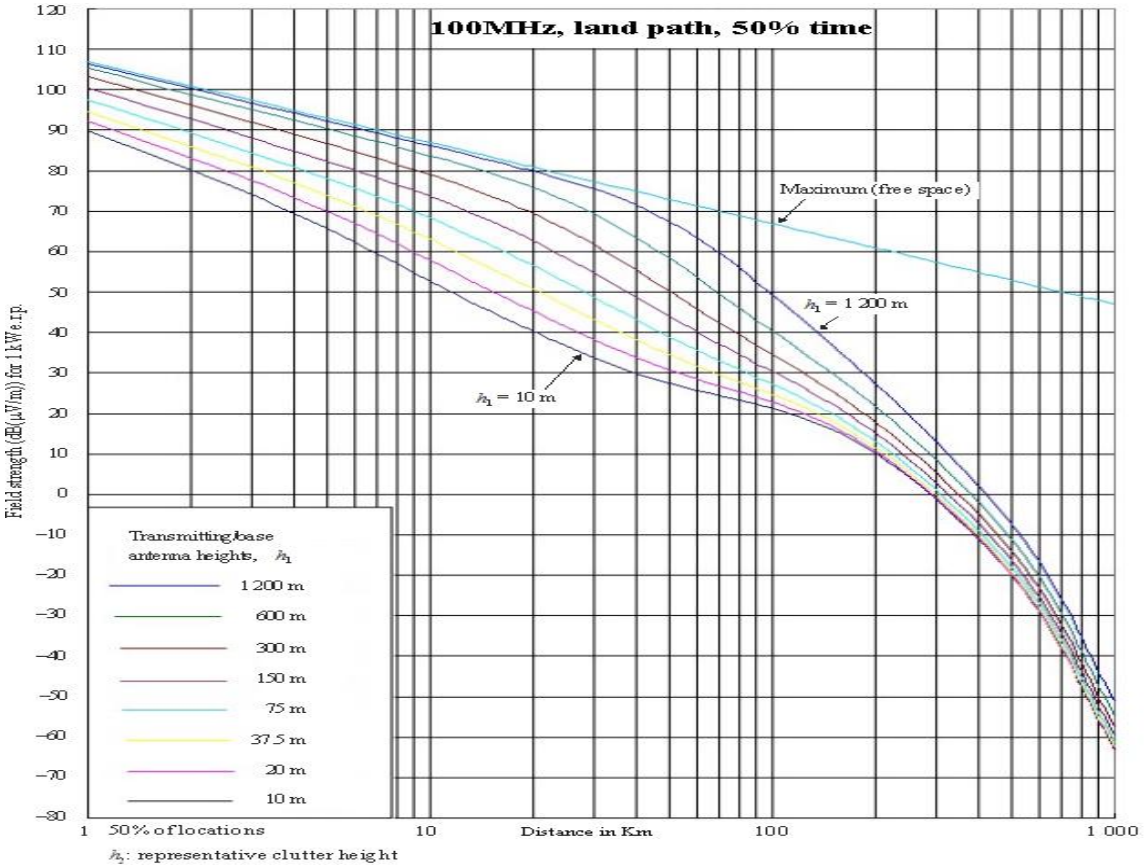

Figure 6-2: Sample propagation curves of Recommendation ITU-R P.1546.

The transmitting antenna height h_1 depends on the length and type of the specific path and the height information available. For sea paths, h_1 is the height above sea level. For land paths shorter than 15 km and if there is not any info on terrain morphology and path length d is less than or equal to 3 km ($d \leq 3$ km), $h_1 = h_a$ (m), else if path length d is between 3 km and 15 km ($3 \text{ km} < d < 15 \text{ km}$), $h_1 = h_a + (h_{eff} - h_a)(d-3)/12$ (m), where h_a is the antenna height above ground, and h_{eff} is the effective height of the transmitting antenna, and for land paths is defined as its height in meters over the average level of the ground between distances of 3 and 15 km from the transmitting antenna in the direction of the receiving antenna.

If there is information on terrain morphology $h_1 = h_b$, where h_b is the height of the antenna above terrain height averaged between 0.2d and d (km). For land paths of 15 km or longer $h_1 = h_{eff}$. In Figure 6-3, calculation of h_b is depicted for transmitter ERT (CH23) and a receiver located in the city of Thessaloniki.

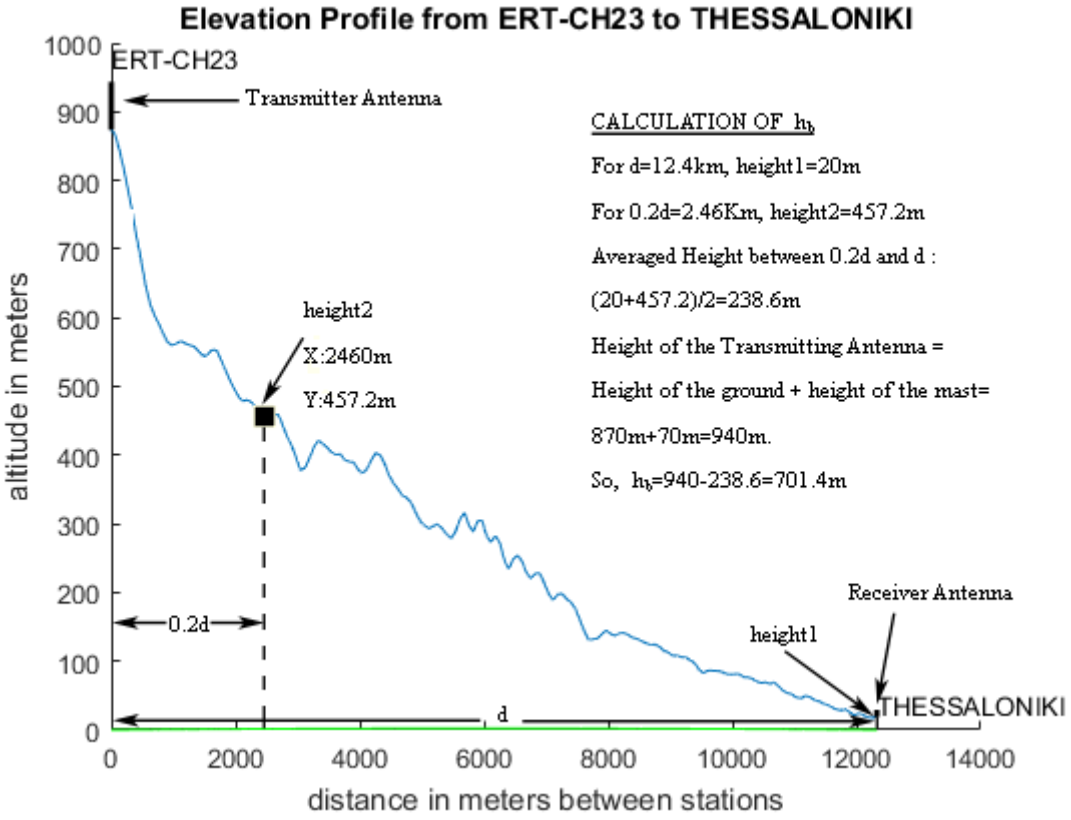

Figure 6-3: Calculation of h_b.

In our data, produced by the ITU-R P.1546 curves, paths and elevation profiles from our MATLAB programs were used to compute the height h_b (m). The time percentage is assumed to be 50%, and the receiver antenna altitude (Hr) is 10 m by default.

This effective height, EFFHGT (eff_hgt) can be calculated online at the site of the ITU (International Telecommunication Union) at the URL: www.itu.int/SRTM3 [14], with the use of the SRTM3 Database. Giving the longitude, latitude and antenna height, the values shown in Table 6-2 are taken.

Table 6-2. Values of eff_hgt taken from ITU for the transmitter "ERT-CH23".

www.itu.int/SRTM3 **BRTSD eff_hgt de/from SRTM3** Date: Mon Jul 3 17:23:41 CEST 2017 Adm ERT-CH23 Site GREECE t_long=+0230559 t_lat=+403551 t_hgt_agl = 70 t_site_alt = 880 t_eff_hgtmax = 851 <ANT_HGT>		
t_eff_hgt@azm000 = 793	t_eff_hgt@azm120 = 248	t_eff_hgt@azm240 = 851
t_eff_hgt@azm010 = 805	t_eff_hgt@azm130 = 192	t_eff_hgt@azm250 = 824

t_eff_hgt@azm020 = 812	t_eff_hgt@azm140 = 373	t_eff_hgt@azm260 = 792
t_eff_hgt@azm030 = 809	t_eff_hgt@azm150 = 561	t_eff_hgt@azm270 = 820
t_eff_hgt@azm040 = 795	t_eff_hgt@azm160 = 683	t_eff_hgt@azm280 = 799
t_eff_hgt@azm050 = 773	t_eff_hgt@azm170 = 719	t_eff_hgt@azm290 = 707
t_eff_hgt@azm060 = 758	t_eff_hgt@azm180 = 713	t_eff_hgt@azm300 = 574
t_eff_hgt@azm070 = 731	t_eff_hgt@azm190 = 713	t_eff_hgt@azm310 = 556
t_eff_hgt@azm080 = 669	t_eff_hgt@azm200 = 788	t_eff_hgt@azm320 = 468
t_eff_hgt@azm090 = 627	t_eff_hgt@azm210 = 810	t_eff_hgt@azm330 = 560
t_eff_hgt@azm100 = 566	t_eff_hgt@azm220 = 826	t_eff_hgt@azm340 = 700
t_eff_hgt@azm110 = 393	t_eff_hgt@azm230 = 839	t_eff_hgt@azm350 = 760

Data for heff (effective eight), ha (has no value because there is no terrain information), hb, and Path Type are shown in Table 6-3.

Table 6-3. Values of heff, ha, hb, and Path Type.

No.	Measurements Points	d (km)	DEGS	heff(m)	ha(m)	hb(m)	Path Type
1	PROFITIS ELIAS	7	313	529.6	-	392	Land
2	THESSALONIKI	12.3	279	801.1	-	701.4	Land
3	LAKE VOLVI	14.3	31	807.6	-	618.5	Cold Sea
4	PEREA	16.7	236	846.2	-	-	Cold Sea
5	METHONI	47	252	817.6	-	-	Cold Sea
6	KORINOS	52	232	841.4	-	-	Cold Sea
7	BORDER EVZONI	68.8	321	477.2	-	-	Land
8	POLIKASTRO	69	320	468.0	-	-	Land
9	SOUMELA	86	256	804.8	-	-	Cold Sea
10	LOUTRAKI	107	293	667.1	-	-	Land+ Cold Sea

Measurements and simulations are shown in Table 6-4. It must be mentioned that for all measurements our equipment consisted of a Rohde & Schwarz FSH-3, a portable spectrum analyser with tracking generator (100 kHz – 3 GHz), factory calibrated with

± 0.7 dB accuracy, two high-precision calibrated biconical antennas by Schwarzbeck, SBA 9113 (500 MHz – 3 GHz) and BBVU 9135 (30 MHz – 1000 MHz), a log-periodic precision calibrated Schwarzbeck antenna (0.25 – 6 GHz), all factory calibrated to within ± 1.0 dB accuracy, low-loss cable Huber-Suhner GX-07272-D 50 Ohm, 1.8 m long, with N-type low-loss connectors.

Table 6-4. Measurements (FSH3) and simulations between ITM, ITU-R P.1546 and Hata-Davidson with HAAT (Hr = Receiver antenna height) for "ERT CH-23" net.

No.	Measurements Points	LAT(N)/ LONG(E)	E(dBμV/m)			
			FSH-3 Hr 2.5 m	ITM Longley-Rice Hr 2.5 m	ITU-R P.1546 Hr 10 m	Hata-Davidson with HAAT Hr 2.5 m
1	PROFITIS ELIAS (7 km/313 degs)	40.640411 23.039927	101.9	95.3	96.1	100.8
2	THESSALONIKI (12.3 km/279 degs)	40.615822 22.955735	94.7	98.2	93.5	97.1
3	LAKE VOLVI (14.3 km/31 degs)	40.707102 23.188914	98.2	97.0	95.8	95.8
4	PEREA (16.7 km/236 degs)	40.513489 22.937471	98.2	94.8	94.4	94.5
5	METHONI (47 km/252 degs)	40.469402 22.574711	89.1	82.4	84.2	75.2
6	KORINOS (52 km/232 degs)	40.307130 22.618620	83.5	80.4	82.8	72.8
7	BORD. EVZONI (68.8 km/321 degs)	41.081410 22.588160	64.1	72.3	55.4	76.0
8	POLYKASTRO (69 km/320 degs)	41.081190 22.588360	71.9	72.4	55.3	75.0
9	SOUMELA (86 km/256 degs)	40.410086 22.116606	77.9	77.9	71.5	80.2
10	LOUTRAKI (107 km/293 degs)	40.966160 21.923630	77.3	74.7	61.0	78.3

The receiving antenna height was 2.5 m, for all our measurements, so in Longley-Rice and Hata-Davidson models the same height for the receiving antenna is used. The default antenna height for ITU-R P.1546 model is 10 m and can't be changed. The loss computed by Hata-Davidson model is not allowed to be less than the Free-Space loss, and the same criterion is applied to all models.

Errors between measurements (FSH-3) and simulations from the Longley-Rice ITM model (Radio Mobile), from the ITU-R P.1546-5 model and the Hata-Davidson model

with average error, average absolute error, and standard deviation are shown in Table 6-5 and Figure 6-4.

Table 6-5. Errors, mean error, mean absolute error and standard deviation between FSH-3, ITM, ITU-R P.1546 and Hata-Davidson for "ERT CH-23" net.

No.	Measurements Points	Error (dB) FSH-3 & Longley-Rice	Error (dB) FSH-3 & P.1546	Error (dB) FSH-3 & Hata - Davidson
1	PROFITIS ELIAS (7 km/313 degs)	-6.6	-5.8	-1.1
2	THESSALONIKI (12.3 km/279 degs)	+3.5	-1.2	+2.4
3	LAKE VOLVI (14.3 km/31 degs)	-1.2	-2.4	-2.4
4	PEREA (16.7 km/236 degs)	-3.4	-3.8	-3.7
5	METHONI (47 km/252 degs)	-6.7	-4.9	-13.9
6	KORINOS (52 km/232 degs)	-3.1	-0.7	-10.7
7	BORDER EVZONI (68.8 km/321 degs)	+8.2	-8.7	+11.9
8	POLYKASTRO (69 km/320 degs)	+0.5	-16.6	+3.1
9	SOUMELA (86 km/256 degs)	0.0	-6.4	+2.3
10	LOUTRAKI (107 km/293 degs)	-2.6	-16.3	+1.0
	Mean	-1.1	-6.7	-1.1
	Mean absolute	3.6	6.7	5.3
	Standard Deviation	4.5	5.7	7.3

The same errors between measurements taken by an FSH-3 spectrum analyser and simulations produced by the Longley-Rice ITM model (Radio Mobile), the ITU-R P.1546-5 model and the Hata-Davidson model are depicted in the bar graph Figure 6-4.

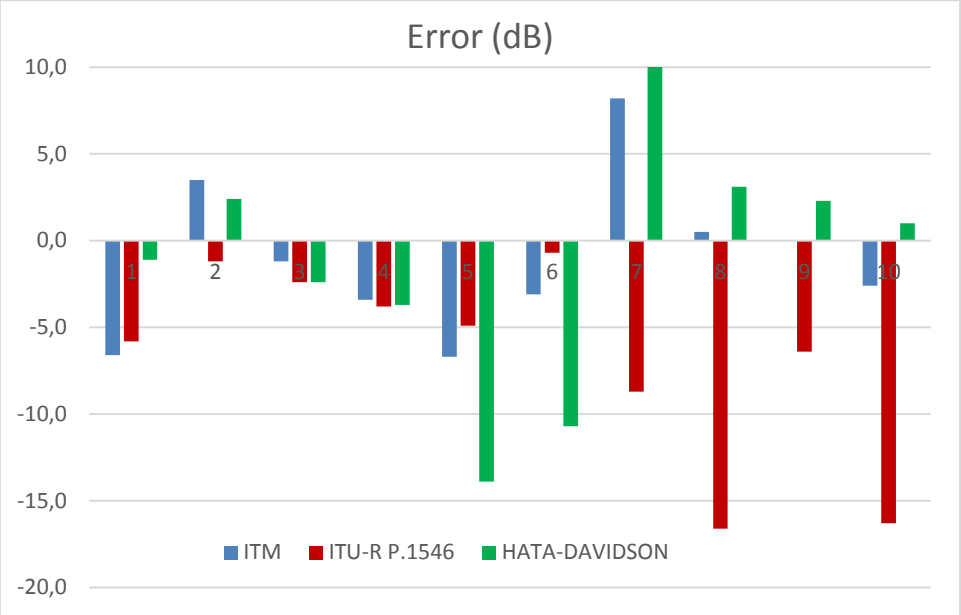

Figure 6-4: Errors between measurements taken by FSH-3 and simulations produced by ITM, ITU-R P.1546 and Hata-Davidson.

Observing the above tables, it is concluded that the Longley-Rice (ITM) model, using accurate terrain elevation data, is the most accurate but also the most computationally intensive, [11-12]. The ITU-R 1546-5 model while it is very precise for shorter distances below 50 km, it becomes increasingly inaccurate for longer distances, severely underestimating the received signal strength, [15-19]. It must be mentioned that an optimization method for tuning the parameters of ITU-R P.1546 was recently proposed [20]. Finally, the Hata-Davidson model using HAAT, while being quite simple to implement and based on approximate analytical equations, is accurate enough, and on average more accurate than the ITU-R 1546 model. It could also be significantly improved by using different approximations for land paths and sea paths as in the ITU model. Models proposed by Deygout, Epstein-Peterson, and Giovaneli [21-24] are also used in this study.

Another measurement campaign was carried in the region of Northern Greece and the area of Southern FYROM (Former Yugoslavian Republic of Macedonia).

A point-to-point analysis for Analog FYROM public TV "TURTEL", UHF Channel 11 took place for the measurement points shown in Table 6-6.

- Transmitter's name: TURTEL
- Transmission Channel: VHF 11
- Transmission frequency: 217.25 MHz

- P_o: 8 kW or 39 dBW or 69.03 dBm
- Net Antenna Gain: 8.0 dBd, or 10.15 dBi
- E.R.P: 50.4 kW or 47 dBW or 77.03 dBm
- E.I.R.P: 82.8 kW or 49.18 dBW or 79.18 dBm
- Transmitter Antenna Height Ht: 45 m
- Receiver Antenna Height Hr: 2.5 m
- Altitude: 1590 m
- Longitude: 22.42255E and Latitude: 41.80293N

Measurements and simulations of models ITM (Irregular Terrain Model)), Deygout, Epstein-Peterson, Giovaneli, ITU-R P.1546 with EFFHGT and Hata-Davidson with HAAT are shown in Table 6-6.

Table 6-6. Measurements and simulations of models ITM, Deygout, Epstein -Peterson, Giovaneli, ITU-R P.1546 with EFFHGT and Hata-Davidson with HAAT for Analog TV "TURTEL".

No	Measurement Points	LAT(N)/ LONG(E)	FSH3 Hr = 2.5 m	Longley-Rice Hr = 2.5 m	Double Knife-Edge Hr =2.5 m			ITU-R P.1546 with EFFHGT (m) Hr = 10 m	Hata – Davidson with H.A.A.T Hr = 2.5 m
					Deygout	Epstein-Peterson	Giovaneli		
1	NEGOTINO (44.6 km/215.6 degs)	41.47592 22.10990	70.8	76.2	76.5	66.0	57.2	80.4	68.3
2	VELES (51 km/258.3 degs)	41.70822 21.82033	70.6	65.8	74.1	69.7	68.6	81.4	61.4
3	CRN-VRV (58.4 km/275.4 degs)	41.85032 21.72081	55.3	38.1	57.4	57.4	57.4	79.1	58.9
4	OKTA (64.6 km/280.3 degs)	41.90413 21.65462	55.5	55.4	52.2	53.3	64.4	76.8	74.1
5	PETROVEC (70.6 km/283.9 degs)	41.95314 21.59469	55.4	57.8	62.5	60.3	57.7	74.3	79.7

6	VODNO 1051m (87 km/282 degs)	41.96501 21.39452	86.9	84.9	84.6	84.6	84.6	67.1	88.5
7	EKO-POLYKASTRO (94.1 km/170 degs)	40.96926 22.62205	59.8	61.6	64.2	63.6	60.9	57.2	70.3
8	POLYKASTRO-2 (101 km/169 degs)	40.90833 22.65187	62.0	69.4	71.8	68.1	59.0	54.1	71.7
9	AG.ATHANASIOS-4 (109 km/169.1 degs)	40.83807 22.66864	62.3	71.7	73.7	63.9	54.6	51.2	73.8
10	POLYKASTRO-3 (112 km/169.2 degs)	40.80907 22.67319	73.3	73.4	72.9	68.0	64.9	50.1	73.6
11	POLYKASTRO (117 km/169 degs)	40.79522 22.68180	76.0	77.5	76.3	68.8	59.8	48.3	74.5
12	AG.ATHANASIOS-6 (130 km/169 degs)	40.65207 22.71910	57.4	62.6	66.9	67.0	69.3	44.1	76.9
13	PROFITIS ELIAS (140 km/158 degs)	40.64032 23.04020	79.8	75.7	77.4	77.4	77.4	38.0	81.0

Height Average Above Terrain (H.A.A.T) was calculated using NAD83/WGS84, FCC's terrain database, and the GLOBE 1 km database. It is available online at https://www.fcc.gov/media/radio/haat-calculator. Measurement points with HAAT parameter are shown in Table 6-7.

Table 6-7. Measurement points and HAAT for "TURTEL" net.

No.	Measurement Points	d(km)	LAT	LONG	DEGS	HAAT (m)
1	NEGOTINO	44.6	41.47592	22.10990	215.6	720.0
2	VELES	51.0	41.70822	21.82033	258.3	1023.3
3	CRN-VRV	58.4	41.85.032	21.72081	275.4	1090.5
4	OKTA	64.6	41.90413	21.65462	280.3	1093.1
5	PETROVEC	70.6	41.95314	21.59469	283.9	1085.4
6	VODNO	87	41.96501	21.39452	282	1089.2
7	EKO-POLYKASTRO	94.1	40.96926	22.62205	170	683.3
8	POLYKASTRO-2	101	40.90833	22.65187	169	692.9

9	AG.ATHANASIOS-4	109	40.83807	22.66864	169.1	691.9
10	POLYKASTRO-3	112	40.80907	22.67319	169.2	691.0
11	POLYKASTRO	117	40.79522	22.68180	169	692.9
12	AG.ATHANASIOS-6	130	40.65207	22.71910	169	692.9
13	PROFITIS ELIAS	140	40.64032	23.04020	158	542.7

The Recommendation ITU-R P.1546 uses the effective height of the transmitting antenna. It is defined as the height of the transmitting antenna above terrain height averaged between distances of 3 to 15 km in the direction of the receiving antenna. The data is available for the American Eurasian and African continents and up to 60 degrees North only. The Data holes were filled by interpolation or with DTED0 data.

This effective height, EFFHGT (eff_hgt) can be calculated online at the site of the International Telecommunication Union (ITU) at the URL, www.itu.int/SRTM3, with the use of the SRTM3 Database.

The longitude and latitude magnitudes must be provided in degrees, minutes and seconds. For west longitude and south latitude, a minus in front of them respectively must be placed. Transmitter's antenna height must be in meters. So, giving for the transmitter "TURTEL" longitude of 22^0 25' 21"E (22.42255E in decade form) and latitude of 41^0 48' 10"N (41.80293N in decade form), the values are shown in Table 6-8. To take the exact values of eff_hgt for the specific measurement points, proper calculations must be done, with the use of Table 6-8.

Table 6-8. Values of eff_hgt taken from ITU for "TURTEL" net.

www.itu.int/SRTM3

BRTSD eff_hgt de/from SRTM3

Date: Thu Oct 19 15:21:25 CEST 2017

Adm TURTEL Site FYROM
t_long=+0222521
t_lat=+414810
t_hgt_agl = 45
t_site_alt = 1592
t_eff_hgtmax = 1237
<ANT_HGT>

t_eff_hgt@azm000 = 1217	t_eff_hgt@azm120 = 383	t_eff_hgt@azm240 = 872
t_eff_hgt@azm010 = 1199	t_eff_hgt@azm130 = 335	t_eff_hgt@azm250 = 927
t_eff_hgt@azm020 =	t_eff_hgt@azm140 =	t_eff_hgt@azm260 =

1171	349	1037
t_eff_hgt@azm030 = 1153	t_eff_hgt@azm150 = 476	t_eff_hgt@azm270 = 1063
t_eff_hgt@azm040 = 1029	t_eff_hgt@azm160 = 615	t_eff_hgt@azm280 = 1104
t_eff_hgt@azm050 = 934	t_eff_hgt@azm170 = 750	t_eff_hgt@azm290 = 1130
t_eff_hgt@azm060 = 907	t_eff_hgt@azm180 = 677	t_eff_hgt@azm300 = 1148
t_eff_hgt@azm070 = 740	t_eff_hgt@azm190 = 751	t_eff_hgt@azm310 = 1156
t_eff_hgt@azm080 = 502	t_eff_hgt@azm200 = 739	t_eff_hgt@azm320 = 1198
t_eff_hgt@azm090 = 410	t_eff_hgt@azm210 = 748	t_eff_hgt@azm330 = 1237
t_eff_hgt@azm100 = 353	t_eff_hgt@azm220 = 773	t_eff_hgt@azm340 = 1202
t_eff_hgt@azm110 = 228	t_eff_hgt@azm230 = 809	t_eff_hgt@azm350 = 1209

As mentioned earlier, the propagation curves of Recommendation ITU-R P.1546, are designed for 1 kW Effective Radiated Power (ERP). Converting this power into dBm,

$$dBm = 10\log\frac{P_{OUT}}{1\ mW} = 10\log\frac{1\ kW}{1\ mW} = 10\log\frac{1000000\ mW}{1\ mW} = 60\ dBm \quad (6.1)$$

The ERP power of the transmitter under study "TURTEL" is 8 kW. Converting this power into dBm,

$$dBm = 20\log\frac{P_{OUT}}{1\ mW} = 10\log\frac{8\ kW}{1\ mW} = 10\log\frac{8000000\ W}{1\ mW} = 69.03\ dBm \quad (6.2)$$

The antenna of the transmitter has a gain of 8.0dBd. Adding this gain to the transmitter's ERP power, the total ERP transmitted power is calculated.

$$ERP_{TOTAL} = ERP_{TRANSMITTER} + dBd_{ANTENNA} \quad (6.3)$$

So, the total ERP transmitted power from transmitter "TURTEL" in dBm equals to

$$ERP_{TOTAL} = 69.03\ dBm + 8.0\ dBd = 77.03\ dBm \quad (6.4)$$

In order to obtain the right simulations results, a value must be added to the values of the field strength, produced by the default propagation curves of Recommendation ITU-R P.1546. So, the result of the equation (6.1) must be deducted from the result of the equation (6.4) , i.e., 77.03 dBm - 60 dBm=17.03 dB.

Consequently, a value of 17.03 dB must be added to the values of the field strength produced by the ITU-R P.1546 propagation curves to get the real values for the "TURTEL" net.

Table 6-9, shows the effective height "h_{eff}" (EFFHGT) in meters and the parameters "h_a" and "h_b". Parameter "h_a" has no value because there is terrain information and parameter "h_b" also have no value because all the measurement points are at distances greater than 15 km. Transmitting antenna height h_1, for distances greater than 15 km, equals $h_1 = h_{eff}$. For further details see ITU-R P.1546 Recommendation. The time percentage is assumed to be 50%, and the receiver antenna altitude (Hr) is 10 m by default.

Table 6-9. Values of heff (EFFHGT), ha, hb for "TURTEL" net.

No.	Measurement Points	LAT(N)/ LONG(E)	ITU-R P.1546			
			h_{eff} EFFHGT (m) From 3 km to 15 km	Path distance d>15 km		E(dBμV/m) +17.03 dB
				h_a	h_b	
1	NEGOTINO (44.6 km/215.6 degs)	41.47592 22.10990	777.0	----	----	82.1
2	VELES (51 km/258.3 degs)	41.70822 21.82033	1033.3	----	----	83.1
3	CRN-VRV (58.4 km/275.4 degs)	41.85032 21.72081	1100.1	----	----	80.8
4	OKTA (64.6 km/280.3 degs)	41.90413 21.65462	1119.8	----	----	78.5
5	PETROVEC (70.6 km/283.9 degs)	41.95314 21.59469	1129.1	----	----	75.9
6	VODNO 1051m (87 km/282 degs)	41.96501 21.39452	1124.0	----	----	68.9
7	EKO-POLYKASTRO (94.1 km/170 degs)	40.96926 22.62205	765.0	----	----	59.0
8	POLYKASTRO-2 (101 km/169 degs)	40.90833 22.65187	751.5	----	----	56.0
9	AG.ATHANASIOS-4 (109 km/169.1 degs)	40.83807 22.66864	752.9	----	----	53.0
10	POLYKASTRO-3 (112 km/169.2 degs)	40.80907 22.67319	754.2	----	----	52.0
11	POLYKASTRO (117 km/169 degs)	40.79522 22.68180	751.5	----	----	50.1
12	AG.ATHANASIOS-6 (130 km/169 degs)	40.65207 22.71910	751.5	----	----	45.8
13	PROFITIS ELIAS (140 km/158 degs)	40.64032 23.04020	602.2	----	----	39.6

Errors between measurements taken by FSH-3 and simulations produced by models ITM, Deygout, Epstein -Peterson, Giovaneli, ITU-R P.1546 with EFFHGT and Hata – Davidson with HAAT are shown in Table 6-10 and Figure 6-5 in a bar graph mode respectively.

Table 6-10. Errors between measurements taken by FSH-3 and simulations produced by models ITM, Deygout, Epstein -Peterson, Giovaneli, ITU-R P.1546 with EFFHGT and Hata-Davidson with HAAT for the "TURTEL" broadcasting site.

No.	Measurement Points	LAT(N)/ LONG(E)	Differences (dB) between FSH-3 &					
			Longley-Rice	Deygout	Epstein-Peterson	Giovaneli	ITU-R P.1546	Hata-Davidson
1	NEGOTINO (44.6 km/215.6 degs)	41.47592 22.10990	+5.4	+5.7	-4.8	-13.6	+9.6	-2.5
2	VELES (51 km/258.3 degs)	41.70822 21.82033	-4.8	+3.5	-0.9	-2.0	+10.8	-9.2
3	CRN-VRV (58.4 km/275.4 degs)	41.85032 21.72081	-17.2	+2.1	+2.1	+2.1	+23.8	+3.6
4	OKTA (64.6 km/280.3 degs)	41.90413 21.65462	-0.1	-3.3	-2.2	+8.9	+21.3	+18.6
5	PETROVEC (70.6 km/283.9 degs)	41.95314 21.59469	+2.4	+7.1	+4.9	+2.3	+18.9	+24.3
6	VODNO 1051m (87 km/282 degs)	41.96501 21.39452	-2.0	-2.3	-2.3	-2.3	-19.8	-1.7
7	EKO-POLYKASTRO (94.1 km/170 degs)	40.96926 22.62205	+1.8	+4.4	+3.8	+1.1	-2.6	+10.5
8	POLYKASTRO-2 (101 km/169 degs)	40.90833 22.65187	+7.4	+9.8	+6.1	-3.0	-7.9	+9.7
9	AG.ATHANASIOS-4 (109 km/169.1 degs)	40.83807 22.66864	+9.4	+11.4	+1.6	-7.7	-11.1	+11.5
10	POLYKASTRO-3 (112 km/169.2 degs)	40.80907 22.67319	+0.1	-0.4	-5.3	-8.4	-23.2	+0.3
11	POLYKASTRO (117 km/169 degs)	40.79522 22.68180	+1.5	+0.3	-7.2	-16.2	-27.7	-1.5
12	AG.ATHANASIOS-6 (130 km/169 degs)	40.65207 22.71910	+5.2	+9.5	+9.6	+11.9	-13.3	+19.5

13	PROFITIS ELIAS (140 km/158 degs)	40.64032 23.04020	-4.1	-2.4	-2.4	-2.4	-41.8	+1.2
Mean			+0.4	+3.5	+0.2	-2.3	-4.8	+6.5
Standard Deviation			+6.8	+5.0	+4.9	+8.0	+20.6	+10.1

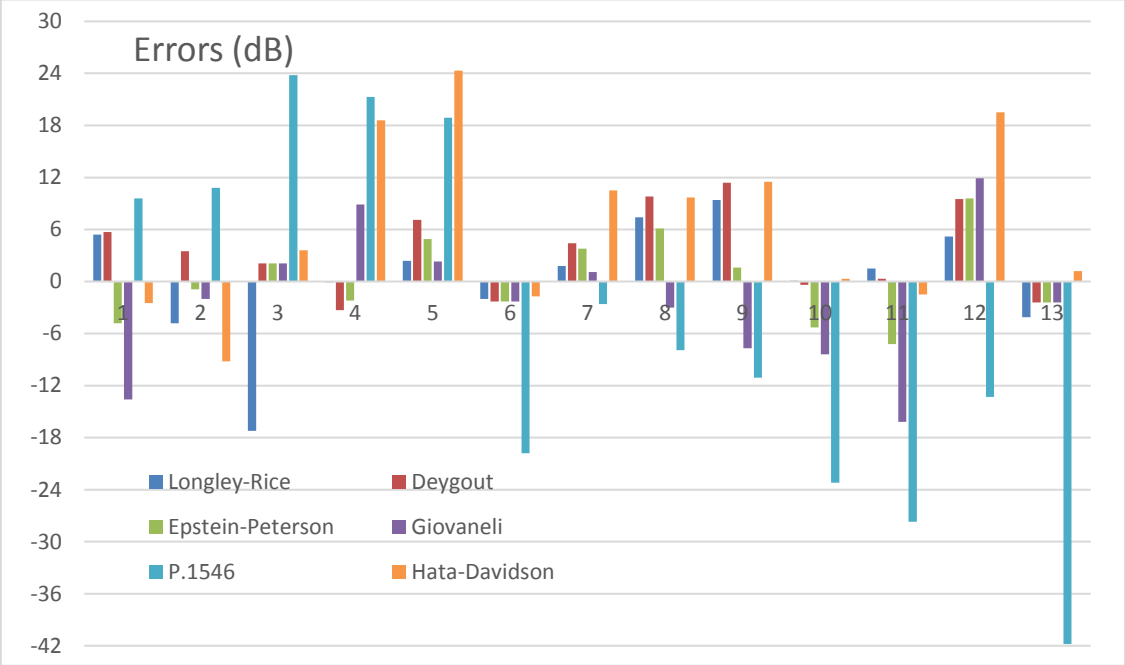

Figure 6-5: Errors between measurements taken by FSH-3 and simulations produced by models ITM, Deygout, Epstein -Peterson, Giovaneli, ITU-R P.1546 with EFFHGT and Hata – Davidson with HAAT for "TURTEL".

The loss computed by all models is not allowed to be less than the Free-Space loss.

6.3 SUMMARY

The Longley-Rice (ITM) model using worldwide SRTM 3-arc-second data for terrain elevation gives satisfactory results in comparison to the measurements but is more computationally intensive than simple empirical models. The propagation curves in Recommendation ITU-R P.1546 give significant errors, mainly at distances longer than 50 km and need corrections, and the Hata-Davidson model with HAAT, despite being an elementary model, gives in some cases reasonable results and certainly better than the ITU-R P.1546 model. Deterministic models of Deygout, Epstein-Peterson, and Giovaneli give quite accurate simulations results.

6.4 REFERENCES

[1] Roger Coudé, webpage of Radio Mobile, a site for downloads and How to http://www.cplus.org/rmw/english1.html, freeware by VE2DBE.

[2] Salamanca L. Murillo-Fuentes J.J. Olmos P. "Review of the Radio Mobile Software as a teaching tool for Radio planning" IEEE Multidisciplinary Engineering Education Magazine, Vol. 6, No. 2, June 2011.

[3] P.L. Rice, A.G. Longley, K.A. Norton, and A.P. Barsis, "Transmission loss predictions for tropospheric communications circuits," Technical Note 101, revised 1/1/1967, U.S. Dept. of Commerce NTIA-ITS.

[4] NASA, "Shuttle Radar Topography Mission data." Available online at http://www2.jpl.nasa.gov/srtm/

[5] "Method for point-to-area prediction for terrestrial services in the frequency range 30 MHz to 300MHz," Recommendation ITU-R P.1546-5, 2013. http://www.itu.int.

[6] M. Hata, "Empirical Formula for Propagation Loss in Land Mobile Radio Services," IEEE Transactions on Vehicular Technology, Vol. VT-29, No. 3, August 1980.

[7] Z. Nadir, N. Elfadhil, F. Tounti, "Path loss Determination Using Okumura-Hata Model and Spline Interpolation For Missing Data For Oman," Proceedings of the World Congress on Engineering, Vol. I WCE 2008, July 2-4, 2008, London, U.K.

[8] V. Armoogum, K.M.S., N. Mohamudally, T. Fogarty, "Propagation Models and their Applications in Digital Television Broadcast Network Design and Implementation.", Book "Trends in Telecommunications Technologies," ISBN 978-953-307-072-8, Mar. 2010.

[9] N. Faruk, Y.A. Adediran, A.A. Ayeni, "Optimization of Davidson Model based on RF measurement conducted in UHF/VHF bands," ICIT 2013, The 6th International Conference on Information Technology, May 8, 2013.

[10] Hata/Davidson "A Report on Technology Independent Methodology for the Modeling, Simulation and Empirical Verification of Wireless Communications System Performance in Noise and Interference Limited Systems Operating on Frequencies between 30 and 1500MHz", TIA TR8 Working Group, IEEE Vehicular Technology Society Propagation Committee, May 1997.

[11] S. Kasampalis, P. Lazaridis, Z. Zaharis, S. Zettas, J. Cosmas, "Comparison of ITM and ITWOM propagation models for DVB-T coverage prediction," IEEE BMSB 2013 conference, London, June 2013.

[12] S. Kasampalis, P. Lazaridis, Z. Zaharis, S. Zettas, J. Cosmas, "Comparison of Longley-Rice, ITM, and ITWOM propagation models for DTV and FM broadcasting," WMPC 2013 conference, Atlantic City, New Jersey, USA, June 24-27, 2013.

[13] FCC's terrain database calculator, https://www.fcc.gov/media/radio/haat-calculator

[14] International Telecommunication Union, Calculation of effective antenna heights (eff_hgt) using the SRTM3 Terrain database, available on the Internet at URL : www.itu.int/SRTM3

[15] C.H. Lee, N.R. Jeon, S.C. Kim, J. Lim, "Comparison of Measurement and Prediction of ITU-R Recommendation P.1546", The 4th IEEE VTS Asia Pacific Wireless Communications Symposium (APWCS2007), 2007-2008, http://hdl.handle.net/10371/7748.

[16] K.W. Suh, H. Jung, J. H. Lee, J.S. Jang, "The Calculation of Field Strength for DTV Receiver by Rec. ITU-R P.1546", Applied Electromagnetics (APACE), 2010 IEEE Asia-Pacific Conference on, 9-11 Nov. 2010, pp. 1-4.

[17] E. Ostlin, H. Suzuki, H.J. Zepernick, "Comparison and Evaluation of ITU-R Recommendation P.1546 Versions". 2006 IEEE 63rd Vehicular Technology Conference, 2006, ISBN 1780393929, Vol. 1, pp. 2896 – 2900.

[18] E. Ostlin, H. Suzuki, H.J.Zepernick, "Evaluation of the Propagation Model Recommendation ITU-R P.1546 for Mobile Services in Rural Australia*", IEEE Transactions on Vehicular Technology*, vol. 57, no. 1, Jan. 2008.

[19] B. A. Witvliet, P. W. Wijninga, E. van Maanen, B. Smith, M. J. Bentum R. Schiphorst, C. H. Slump, "Mixed-Path Trans-Horizon UHF Measurements for P.1546 Propagation Model Verification," Antennas and Propagation in Wireless Communications (APWC), 2011, IEEE-APS, Topical conference in Torino, Italy 12-16 Sept.2011.

[20] K.Paran, N. Noori. "Tuning of the propagation model ITU-R P.1546 recommendation". Progress in Electromagnetics Research B, Vol. 8, 243-255, 2008.

[21] J. Deygout, "Multiple Knife-Edge Diffraction of Microwaves," IEEE Trans on Antennas and Propagation. vol. 14, pp. 480-489, Apr. 1966.

[22] J. Deygout, “Correction Factor for Multiple Knife-Edge Diffraction,” IEEE Trans on Antennas and Propagation. vol. 39, No. 8, pp. 1256-1258, August 1991.

[23] J. Epstein and D. W. Peterson, “An experimental study of wave propagation at 850 Mc,” Proc. IRE, vol. 41, pp. 595-611, 1953.

[24] C. L. Giovaneli, “An analysis of simplified solutions for multiple knife-edge diffraction,” IEEE Trans on Antennas and Propagation., vol. 32, pp. 297-301, Mar. 1984.

CHAPTER 7

COMPARISON OF ITM AND ITWOM PROPAGATION MODELS FOR DVB-T COVERAGE PREDICTION.

7.1 INTRODUCTION

With the rapid deployment of digital TV, there is an increasing need for accurate point-to-area prediction tools. There is a lot of propagation models for coverage prediction of DTV. Some of them are pure empirical models; others are mixed, empirical-analytical models, based on measurement campaigns and electromagnetic theory and others are deterministic models. The aim of this paper is to compare accurate measurements taken by a Rohde & Schwarz FSH-3 portable spectrum analyser and precision antennas (biconical and log-periodic), with simulation results derived from coverage prediction models, like the NTIA-ITS Longley-Rice model, the ITM (Irregular Terrain Model) using the 3-arc-second SRTM (Satellite Radar Topography Mission) data that is available freely, and the newer ITWOM (Irregular Terrain with Obstructions Model) model which combines equations from ITU-R P.1546 model with Beer's law and Snell's law. Furthermore, measurements for analog FM broadcasting are compared to predictions from the models mentioned above.

To take full advantage of DTV services and characteristics and to obtain a satisfactory coverage, measurement campaigns are required, as well as field trials, comparing simulation and laboratory results with measurements. The scope of this research is to provide coverage prediction maps for DTV and FM radio services, in the region of Thessaloniki – Greece, and to validate simulation results with field measurements. It is well known that the coverage of a transmitter can only be obtained by extensive measurement campaigns. However, on-site measurements are inconvenient, because they cost in time and money. Therefore, the use of a prediction model becomes a necessity. There is a vast number of prediction models, like Egli, Longley-Rice, Okumura-Hata, COST 231, Lee, Bullington, the ITU model P.1546-3 [1], and others. The literature on this subject is enormous [2-3]. From all the above models, Longley-Rice is by far the most widely used. There are commercial software programs for coverage prediction based on the propagation mentioned above models, but they are expensive, and the use of their demonstration versions is very restricted. Fortunately, there are some excellent freeware programs, such as Radio Mobile (Windows-based

software) and SPLAT! (Linux based software). Both are based on the NTIA's original Longley-Rice Technical Note 101 (TN101) [4].

The Radio Mobile program, [5-7] (Radio Propagation and Virtual Mapping Freeware is based on the Longley-Rice Model-ITM and uses the 3-arc-second Satellite Radar Terrain Mission SRTM maps [8]. Radio Mobile performs a wide range of simulations, it is user-friendly and can be used instead of the costly commercial applications giving satisfactory simulation results.

The SPLAT! [9] program (an RF **S**ignal **P**ropagation, **L**oss, **A**nd **T**errain analysis tool) for the spectrum between 20MHz and 20GHz is an excellent open-source, Linux based program. For Windows users, there are two versions, freely available [10-11]. SPLAT! is also based on the Longley-Rice Model-ITM and uses SRTM maps.

In the latest version of SPLAT! ITM is replaced by the ITWOM [12-13]. The ITWOM involves empirical data from ITU-R P.1546 as well as Beer's law and Snell's law and promises higher accuracy over the older ITM. To get the Simulation results produced by ITWOM, we used a Linux program, Ubuntu 12.10 [14]. In a similar study, the path loss is calculated with the use of the Longley-Rice Irregular Terrain Model (ITM), the NASA SRTM terrain database and the SPLAT! software [15].

7.2 HOW ''splat-1.2.3-win32 (ITM model)'' WORKS

It is SPLAT that runs on windows, the result of John McMellen’s [10] efforts, a senior broadcast engineer at KMSU at Missouri State University. It is a command line program (windows-cmd) as in Linux, and it is freely available under the GNU GPL. To run this program, the following procedures must be followed to run this program on Windows.

- Unzip the downloaded zip file and install “splat-1.2.3-win32”, preferably on path C:\splat-1.2.3-win32.
- Download the SRTM3 maps [8] from NASA’s website; these maps have an extension of ".hgt"
- Use the conversion tool "srtm2sdf.exe" , which is in path C:\splat-1.2.3-win32\utils\srtm2sdf.exe, to convert the maps form ".hgt" to ".sdf" extension. Splat can use the maps only in ".sdf" format (Splat data Files).
- Create the ".qth" files (Site Location Files), with the use of notepad, which imports site location information of transmitter and receiver. QTH files contain the site’s name, the site’s longitude (West longitude from 0 to 360 degrees, East longitude from 0 to -360 degrees), the site’s latitude (positive for North latitude

and negative for South latitude), and the site's antenna height above ground level (AGL). The ".qth" files for the transmitter and all the receiving sites is created.

A ".qth" file for the ERT-CH23 transmitter is shown below.

ERT_CH23.qth	
ERT_CH23	Transmitter's name
40.597648	Transmitter's latitude, North
-23.099793	Transmitter's longitude, East
70m	Transmitter's antenna height

A ".qth" file for the PROFITIS-ELIAS receiver is shown below.

PROFITIS_ELIAS.qth	
PROFITIS_ELIAS	Transmitter's name
40.640411	Transmitter's latitude, North
-23.039927	Transmitter's longitude, East
2.5m	Transmitter's antenna height

- Create the ".lrp" files (Site Location Files), with the use of notepad. LRP files are the Irregular Terrain Model parameter files and are required for SPLAT! to determine path loss, field strength, in either area prediction mode or point-to-point mode. LRP files have the same base name as the transmitter QTH file, but with a ".lrp" extension.

  A ".lrp" file for the ERT-CH23 transmitter is shown below.

ERT_CH23.lrp	
15.000	Earth Dielectric Constant (Relative permittivity)
0.005	Earth Conductivity (Siemens per meter)
301.000	Atmospheric Bending Constant (N-units)
490.000	Frequency in MHz (20 MHz to 20 GHz)
5	Radio Climate (5 = Continental Temperature
0	Polarization (0 = Horizontal, 1 = Vertical)
0.50	Fraction of situations (50% of locations)
0.90	Fraction of time (90% of the time)
15,848.9	Effective Radiated Power (ERP) in Watts (optional)

After creating the two-necessary type of files (.qth and .lrp) and converting the maps to ".sdf" format, The SPLAT! program is ready to run. The"-metric" switch means that the results are in the metric system.

For further and detailed information refer to SPLAT! guide.

- **Coverage maps and signal meter**
  - To get the coverage map for transmitter ERT-CH23 with an antenna height of 70 m in a radius of 150 km, the next command must be typed in "cmd" mode.
    C:\splat-1.2.3-win32>splat -t ERT_CH23.qth -L 70 -o ERT_CH23.ppm -R 150 -kml -metric
  - Typing now the next command in cmd (console mode in Windows), the signal meter is depicted on the coverage map.
    C:\splat-1.2.3-win32>splat -t ERT_CH23.qth -L 70 -o ERT_CH23.ppm -R 150 -plo ERT_CH23.txt -o path_loss_map -metric
- **Point-to-point analysis**
  - To get the point-to-point analysis between transmitter ERT- CH23 and receiver site PROFITIS ELIAS, the next command must be typed in "cmd" mode..
    C:\splat-1.2.3-win32>splat -t ERT_CH23.qth -r PROFITIS_ ELIAS.qth -kml -metric
- **Elevation profiles**
  - To get the Elevation Profile between transmitter ERT- CH23 and receiver site PROFITIS ELIAS, the next command must be typed in "cmd" mode.
    C:\splat-1.2.3-win32>splat -t ERT_CH23.qth -r PROFITIS_ELIAS.qth -p terrain_profile.png -metric
- **Elevation profiles with Fresnel zones**
  - To get the Elevation Profile between transmitter ERT- CH23 and receiver site PROFITIS ELIAS and the 1st Fresnel and the 0.6F, the next command must be typed in "cmd" mode.
    C:\splat-1.2.3-win32>splat -t ERT_CH23.qth -r PROFITIS_ELIAS.qth -f 490.000 -H normalized_height_profile.png -metric

7.3 HOW ''SPLAT! v1.4.0 (ITWOM model)'' WORKS

This version of SPLAT runs only on LINUX. The same files must be created (.qth, .lrp) as in the case of splat-1.2.3-win32 (windows), the same conversion of SRTM3 maps from ".hgt" format to ".sdf" format and the same procedure must be followed. In this survey, Ubuntu 12.10, a Linux operating system for personal computers, was used to run SPLAT! v1.4.0.

7.4 MEASUREMENTS AND COMPARISONS

A measurement campaign was carried out around the city of Thessaloniki, located in the north of Greece to measure the signal strength of DVB-T transmissions. Our measurements equipment consists of a Rohde & Schwarz FSH-3 portable spectrum analyser with tracking generator (100kHz – 3GHz), factory calibrated with ±0.7dB accuracy, two high-precision calibrated biconical antennas by Schwarzbeck, SBA 9113 (500MHz – 3GHz), and BBVU 9135 (30MHz – 1GHz), a log-periodic precision calibrated Schwarzbeck antenna (0.25 GHz – 6GHz), all factory calibrated with ±1.0dB accuracy, and low-loss cable Suhner GX-07272-D, 50 Ohm, 1.8 meters long with N-type connectors. For the simulation purposes, an Omni type transmitting antenna has been used.

A point-to-point analysis took place for Greek public TV ERT, Channel UHF 23 with the following characteristics.

- Transmitter's name: ERT
- Transmission Channel: CH23
- Transmission frequency: 490 MHz
- P_o: 1600 W or 32 dBW or 62 dBm
- Net Antenna Gain: 10 dBd, or 12.15 dBi
- E.R.P: 15.8 kW or 42 dBW or 72 dBm
- E.I.R.P: 26kW or 44.14 dBW or 74.15 dBm
- Transmitter Antenna Height Ht: 70 m
- Receiver Antenna Height Hr: 2.5 m
- Altitude: 898.5 m
- Longitude: 23.099793E and Latitude: 40.597648N

Measurement points taken by FSH-3 spectrum analyser and simulation results produced by ITM and ITWOM models are presented in Table 7-1. Observing simulation results No. 3, 4, 7, 8, 9 and 10, it is concluded that are better for Radio Mobile than those of SPLAT! for Windows, and simulation results No. 1, 2, 5, and 6 are better for SPLAT! (ITM). The main conclusion for the above measurement points is that the Radio Mobile gives overall better simulation results with the lower standard deviation (SD = 4.6 dB) than SPLAT! for Windows (SD = 6.4 dB), though both programs are based on the same propagation model, i.e., ITM (Longley-Rice model).

Table 7-1. A point-to-point analysis for Greek public DTV "ERT-CH23" with the use of FSH-3, ITM (Radio Mobile), SPLAT! with ITM and SPLAT! with ITWOM.

No.	Measurements Points	LAT(N)/ LONG(E)	E(dBμV/m)			
			FSH-3 Measure-ments	ITM Radio Mobile (Windows)	ITM SPLAT! v1.2.3 for Windows	ITWOM SPLAT! v1.4.0 (Ubuntu 12.10)
1	PROFITIS ELIAS (7 km/313 degs)	40.640411 23.039927	101.9	95.3	100.1	94.7
2	THESSALONIKI (12.3 km/279 degs)	40.615822 22.955735	94.7	98.2	95.0	93.8
3	LAKE VOLVI (14.3 km/31 degs)	40.707102 23.188914	98.2	97.0	93.7	90.7
4	PEREA (16.7 km/236 degs)	40.513489 22.937471	98.2	94.8	92.4	89.4
5	METHONI (47 km/252 degs)	40.469402 22.574711	89.1	82.4	82.8	65.0
6	KORINOS (52 km/232 degs)	40.307130 22.618620	83.5	80.4	81.6	61.6
7	BORDER EVZONI (68.8 km/321 degs)	41.081410 22.588160	64.1	72.3	78.4	59.0
8	SOUMELA (86 km/256 degs)	40.410086 22.116606	77.9	77.9	77.0	57.4
9	LOUTRAKI (107 km/293 degs)	40.966160 21.923630	77.3	74.7	73.7	54.2
10	POLYKASTRO (69 km/320 degs)	41.081190 22.588360	71.9	72.4	78.4	59.0

It is important to note that the original Longley-Rice model used in the Radio Mobile program has undergone some minor modifications to improve its accuracy and to avoid discontinuities of the predicted field-strength. So, the changes were made to the original code of ITM model used in Radio Mobile, give better simulation results. SPLAT! for Windows uses the original code of Longley-Rice model without any modifications and provides worse simulation results. It can be noticed from the above measurements and simulation results, that ITWOM model gives worse simulation results than those of ITM model produced by SPLAT! for Windows and Radio Mobile software. Parameter "Attenuation due to terrain effects" in reports that SPLAT! v1.2.3 for Windows produces using ITM model, varies in logical values. At the same time parameter "Attenuation due to terrain shielding" in reports that SPLAT! v1.4.0 for Linux produces using ITWOM

model, in most cases, varies in high values, even where there are no obstacles. In these cases, ITWOM model produce significant path losses. The two parameters are depicted in Table 7-2. Most probably, SPLAT! with ITWOM overestimates the attenuation by obstacles. Additionally, for distances larger than around 40 km the simulation results are much worse.

Table 7-2. Attenuation due to terrain for ITM and ITWOM models.

No.	Measurements Points	LAT(N)/ LONG(E)	Number of Obstacles	ITM SPLAT!v1.2.3 For Windows	ITWOM SPLAT!v1.4.0 (Ubuntu 12.10)
				Attenuation due to terrain effects (dB)	Attenuation due to terrain shielding (dB)
1	PROFITIS ELIAS (7 km/313 degs)	40.640411 23.039927	1	-0.12	+7.42
2	THESSALONIKI (12.3 km/279 degs)	40.615822 22.955735	0	+0.01	+3.37
3	LAKE VOLVI (14.3 km/31 degs)	40.707102 23.188914	0	-0.00	+5.19
4	PEREA (16.7 km/236 degs)	40.513489 22.937471	0	+0.04	+5.21
5	METHONI (47 km/252 degs)	40.469402 22.574711	0	+0.69	+20.60
6	KORINOS (52km/232degs)	40.307130 22.618620	0	+0.90	+23.06
7	BORDER EVZONI (68.8 km/321 degs)	41.081410 22.588160	1	+1.70	+23.26
8	SOUMELA (86 km/256 degs)	40.410086 22.116606	0	+1.14	+22.92
9	LOUTRAKI (107 km/293 degs)	40.966160 21.923630	5	2.61	+24.16
10	POLYKASTRO (69 km/320 degs)	41.081190 22.588360	1	+1.70	+23.26

For all our simulations and measurements, the sample standard deviation was calculated between measured path loss values and those predicted by Radio Mobile and SPLAT! using the well-known formula (5.5) with Bessel's correction.

Errors (differences) between measurements taken by FSH-3 and simulations derived from ITM model with the use of Radio Mobile and SPLAT! v1.2.3 for Windows and

ITWOM model using SPLAT! v1.4.0 for Ubuntu 12.10, with average error and standard deviation, are shown in Table 7-3 and bar graph in Figure 7-1, respectively.

Table 7-3. Errors between FSH-3 measurements and simulations results produced by ITM (Radio Mobile and SPLAT! for Windows) and by ITWOM (SPLAT! - Ubuntu 12.10) for Greek DTV "ERT-CH23".

No.	Measurements Points	Error (dB)		
		FSH-3 & Radio Mobile	FSH-3 & SPLAT! ITM (WINDOWS)	FSH-3 & ITWOM SPLAT! v 1.4.0 (Ubuntu 12.10)
1	PROFITIS ELIAS (7 km/313 degs)	-6.6	-1.8	-7.2
2	THESSALONIKI (12.3 km/279 degs)	3.5	0.3	-0.9
3	LAKE VOLVI (14.3 km/31 degs)	-1.2	-4.5	-7.5
4	PEREA (16.7 km/236 degs)	-3.4	-5.8	-8.8
5	METHONI (47 km/252 degs)	-6.7	-6.3	-24.1
6	KORINOS (52 km/232 degs)	-3.1	-1.9	-21.9
7	BORDER EVZONI (68.8 km/321 degs)	8.2	14.3	-5.1
8	SOUMELA (86 km/256 degs)	0.0	-0.9	-20.5
9	LOUTRAKI (107km/293degs)	-2.6	-3.6	-23.1
10	POLYKASTRO (69 km/320 degs)	0.5	6.5	-12.2
	Average	-0.6	0.5	-13.2
	Standard Deviation	4.6	6.4	8.5

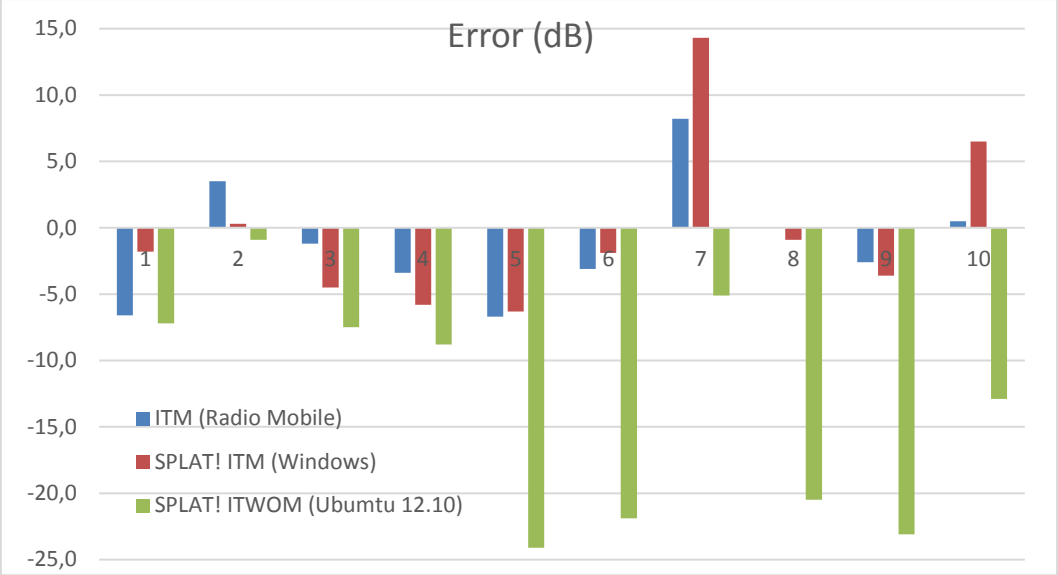

Figure 7-1: Error between measurements (FSH-3) and simulations results produced by ITM (Radio Mobile and SPLAT! for Windows) and by ITWOM (SPLAT! - Ubuntu 12.10) for Greek DTV "ERT-CH23".

A coverage map produced by Radio Mobile that uses the ITM model for the Greek public DTV "ERT-CH23" is depicted in Figure 7-2 below.

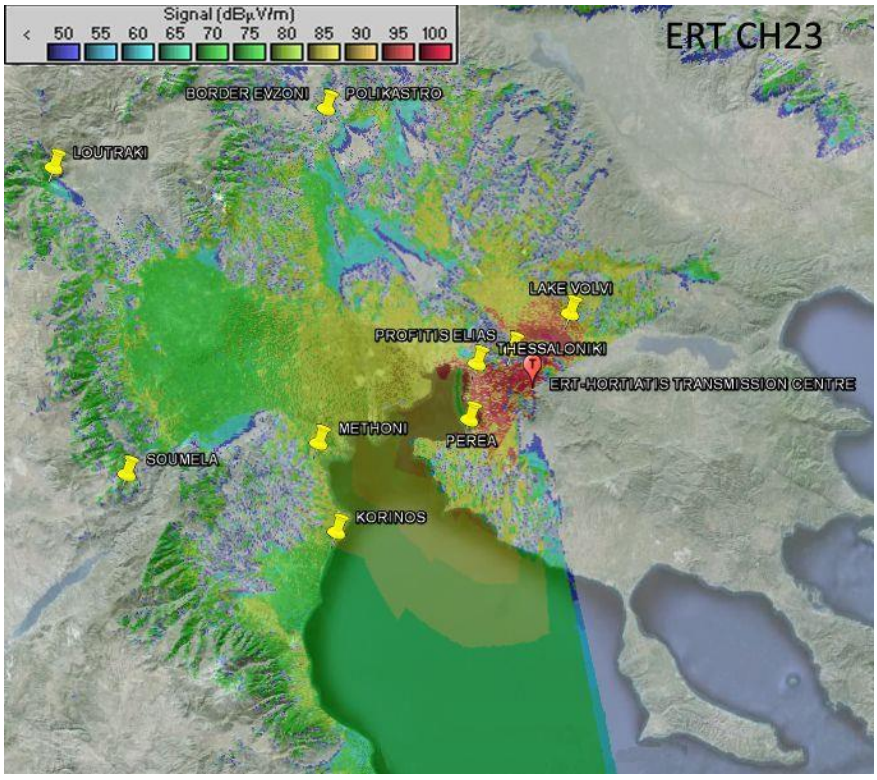

Figure 7-2: Coverage map produced by Radio Mobile for Greek DTV "ERT-CH23".

The point-to-point analysis (ERT_CH23 to PROFITIS_ELIAS.txt) between the ERT-CH23 transmitter and the receiver at place PROFITIS_ELIAS, produced by SPLAT! v1.2.3 for Windows which uses the ITM model is presented.

--==[SPLAT! v1.2.3 Path Analysis]==--

Transmitter site: ERT_CH23
Site location: 40.5976 North / 336.9002 West (40° 35' 51" N / 336° 54' 0" W)
Ground elevation: 880.00 meters AMSL
Antenna height: 70.00 meters AGL / 950.00 meters AMSL
Distance to PROFITIS_ELIAS: 6.94 kilometers
Azimuth to PROFITIS_ELIAS: 313.28 degrees
Depression angle to PROFITIS_ELIAS: -3.2077 degrees
Depression angle to the first obstruction: -3.1661 degrees

Receiver site: PROFITIS_ELIAS
Site location: 40.6404 North / 336.9601 West (40° 38' 25" N / 336° 57' 36" W)
Ground elevation: 563.00 meters AMSL
Antenna height: 2.50 meters AGL / 565.50 meters AMSL
Distance to ERT_CH23: 6.94 kilometers
Azimuth to ERT_CH23: 133.24 degrees
Elevation angle to ERT_CH23: +3.1454 degrees

Longley-Rice path calculation parameters used in this analysis:
Earth's Dielectric Constant: 15.000
Earth's Conductivity: 0.005 Siemens/meter
Atmospheric Bending Constant (N-units): 301.000 ppm
Frequency: 490.000 MHz
Radio Climate: 5 (Continental Temperate)
Polarization: 0 (Horizontal)
Fraction of Situations: 50.0%
Fraction of Time: 90.0%
Transmitter ERP: 15.849 kilowatts

Summary for the link between ERT_CH23 and PROFITIS_ELIAS:
Free space path loss: 103.10 dB
Longley-Rice path loss: 102.98 dB
Attenuation due to effects of terrain: -0.12 dB
Field strength at PROFITIS_ELIAS: 100.08 dBuV/meter
Voltage produced by a terminated 50 ohms 0 dBd gain antenna: 8081.73 uV
Voltage produced by a terminated 75 ohms 0 dBd gain antenna: 9898.06 uV
Mode of propagation: Line-Of-Sight Mode

Between PROFITIS_ELIAS and ERT_CH23, SPLAT! detected obstructions at:
40.6398 N, 336.9592 W, 0.10 kilometers, 576.00 meters AMSL
Antenna at PROFITIS_ELIAS must be raised to at least 7.68 meters AGL
to clear all obstructions detected by SPLAT!
Antenna at PROFITIS_ELIAS must be raised to at least 15.61 meters AGL
to clear the first Fresnel zone.
Antenna at PROFITIS_ELIAS must be raised to at least 12.56 meters AGL
to clear 60% of the first Fresnel zone.

The point-to-point analysis for the same path ERT-CH23 to PROFITIS_ELIAS given

by SPLAT!v1.4.0 (ITWOM) is shown.

```
                --==[ SPLAT! v1.4.0 Path Analysis ]==--
-------------------------------------------------------------------------------------------------
Transmitter site: ERT_CH23
Site location: 40.5976 North / 336.9002 West (40° 35' 51" N / 336° 54' 0" W)
Ground elevation: 880.00 meters AMSL
Antenna height: 70.00 meters AGL / 950.00 meters AMSL
Distance to PROFITIS_ELIAS: 6.94 kilometers
Azimuth to PROFITIS_ELIAS: 313.28 degrees
Depression angle to PROFITIS_ELIAS: -3.2078 degrees
Depression angle to the first obstruction: -3.1661 degrees
-------------------------------------------------------------------------------------------------
Receiver site: PROFITIS_ELIAS
Site location: 40.6404 North / 336.9601 West (40° 38' 25" N / 336° 57' 36" W)
Ground elevation: 563.00 meters AMSL
Antenna height: 2.50 meters AGL / 565.50 meters AMSL
Distance to ERT_CH23: 6.94 kilometers
Azimuth to ERT_CH23: 133.24 degrees
Elevation angle to ERT_CH23: +3.1455 degrees
-------------------------------------------------------------------------------------------------
ITWOM Version 3.0 Parameters Used In This Analysis:
Earth's Dielectric Constant: 15.000
Earth's Conductivity: 0.005 Siemens/meter
Atmospheric Bending Constant (N-units): 301.000 ppm
Frequency: 490.000 MHz
Radio Climate: 5 (Continental Temperate)
Polarization: 0 (Horizontal)
Fraction of Situations: 50.0%
Fraction of Time: 90.0%
Transmitter ERP: 16.000 kilowatts (+72.04 dBm)
Transmitter EIRP: 26.189 kilowatts (+74.18 dBm)
-------------------------------------------------------------------------------------------------
Summary For The Link Between ERT_CH23 and PROFITIS_ELIAS:
Free space path loss: 103.10 dB
ITWOM Version 3.0 path loss: 110.51 dB
Attenuation due to terrain shielding: 7.42 dB
Field strength at PROFITIS_ELIAS: 94.73 dBuV/meter
Signal power level at PROFITIS_ELIAS: -36.33 dBm
Signal power density at PROFITIS_ELIAS: -51.05 dBW per square meter
Voltage across a 50-ohm dipole at PROFITIS_ELIAS: 4364.69 uV (72.80 dBuV)
Voltage across a 75-ohm dipole at PROFITIS_ELIAS: 5345.63 uV (74.56 dBuV)
Mode of propagation: Line of Sight
ITWOM error number: 0 (No error)
-------------------------------------------------------------------------------------------------
Between PROFITIS_ELIAS and ERT_CH23, SPLAT! detected obstructions at:
40.6398 N, 336.9592 W,  0.10 kilometers, 576.00 meters AMSL
Antenna at PROFITIS_ELIAS must be raised to at least 7.68 meters AGL
to clear all obstructions detected by SPLAT!
```

Antenna at PROFITIS_ELIAS must be raised to at least 15.61 meters AGL to clear the first Fresnel zone.
Antenna at PROFITIS_ELIAS must be raised to at least 12.56 meters AGL to clear 60% of the first Fresnel zone.

A coverage map produced by SPLAT! v 1.2.3 for Windows that uses the ITM model, for the Greek Public DTV, "ERT-CH23" (490 MHz), is shown in Figure 7-3. The Longley-Rice analysis range has been set to a radius of 150 km.

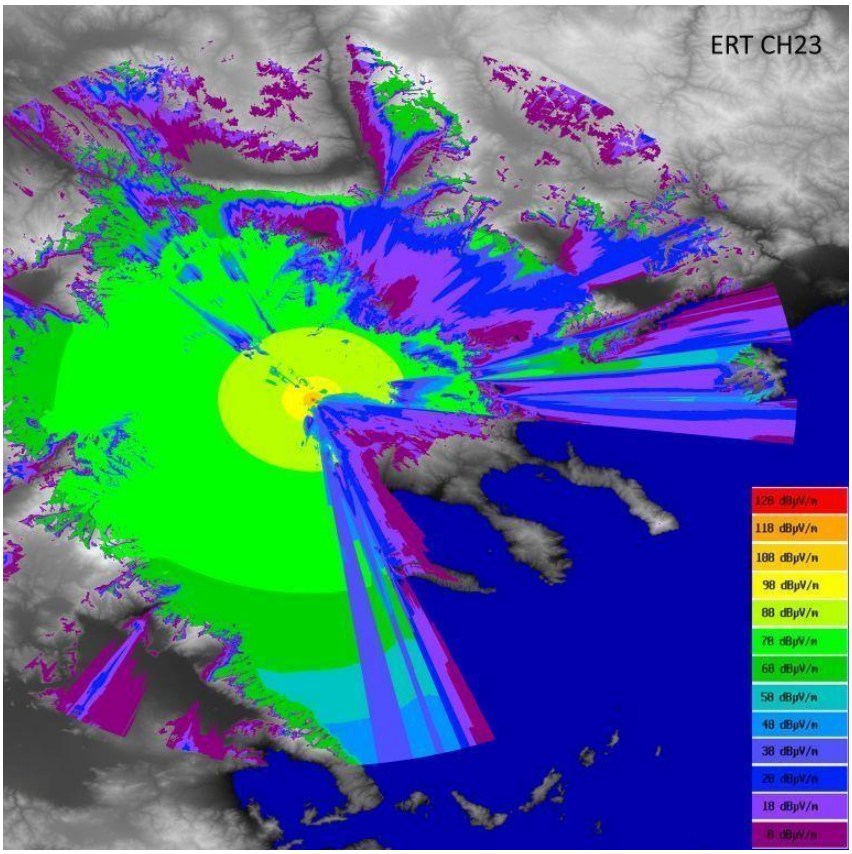

Figure 7-3: Coverage map produced by SPLAT! v1.2.3 for Windows for Greek DTV "ERT CH-23". Coverage radius is 150 km.

Also, a coverage map produced by SPLAT! v 1.4.0 operating in Ubuntu 12.10 that uses ITWOM model for the Greek Public TV, "ERT-CH23" (490 MHz), is shown in Figure 7-4. The Longley-Rice analysis range has also been set to a radius of 150 km. Topographic maps display elevations using a logarithmic grayscale. Higher elevations represented through brighter shades of gray. Only the sea-level is represented using the blue color. Both coverage maps include a legend at the right bottom. Each color of the legend corresponds to a signal strength in decibels over one microvolt per meter (dBµV/m).

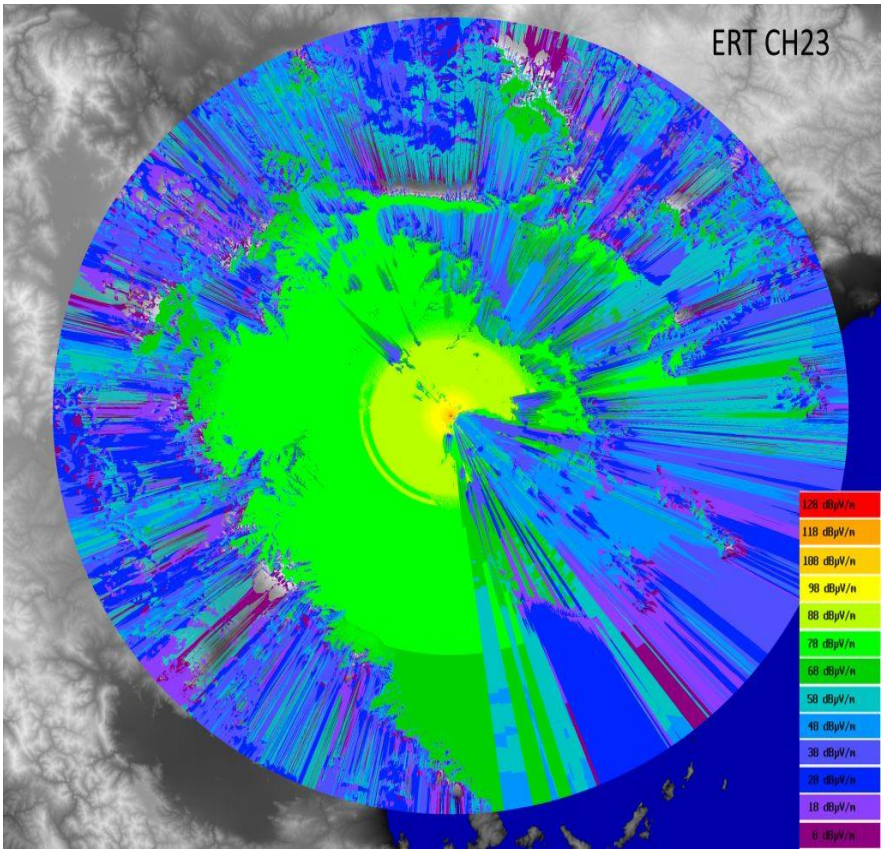

Figure 7-4: Coverage map produced by SPLAT! v1.4.0 for Greek DTV "ERT CH-23". Coverage radius is 150 km.

Path profile produced by Radio Mobile which use ITM model with minor modifications is shown in Figure 7-5.

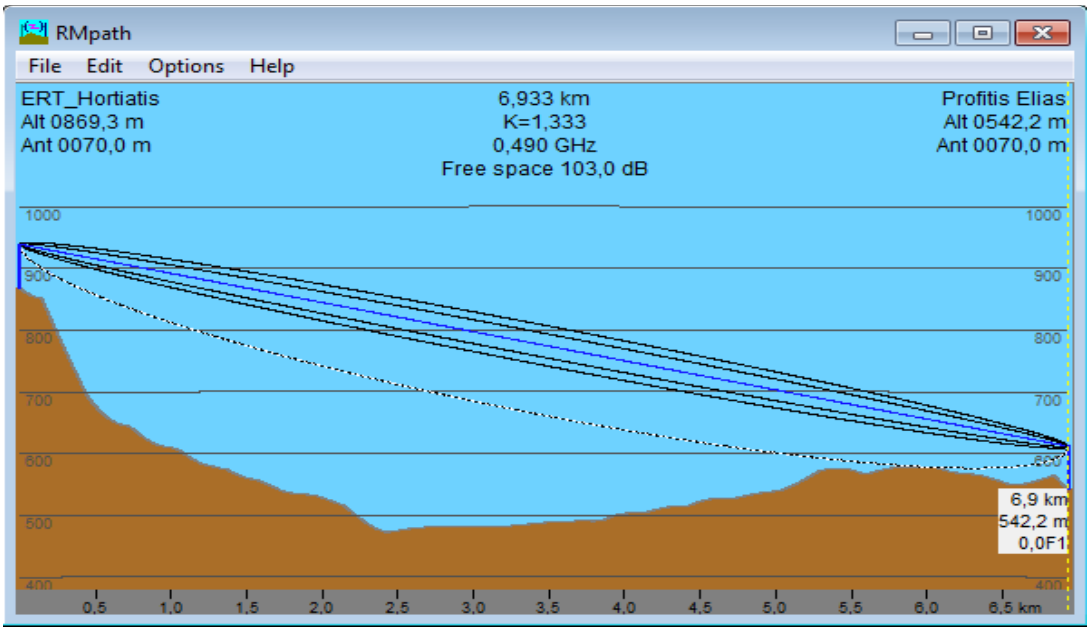

Figure 7-5: Path profile produced by Radio Mobile between transmitter "ERT-CH23" and place "PROFITIS ELIAS".

Path profiles produced by SPLAT! v1.2.3 for Windows, that uses the ITM model (SPLAT! v1.4.0 with ITWOM model generates the same path profiles) are depicted in Figure 7-6, and Figure 7-7 respectively.

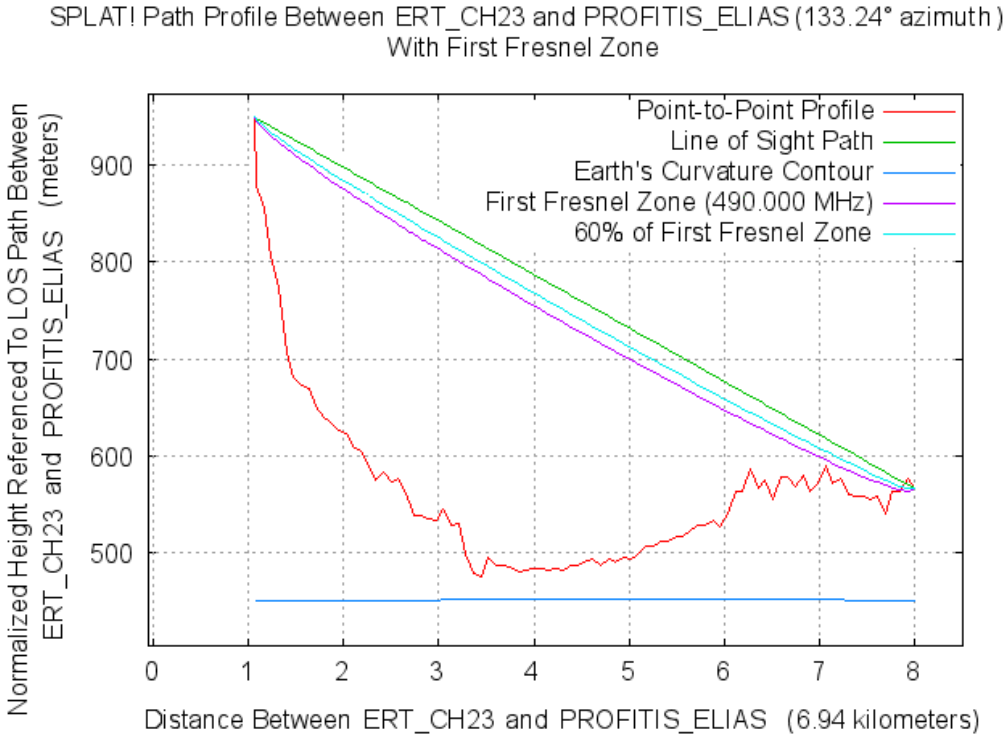

Figure 7-6: Path profile produced by SPLAT! v1.2.3 (Windows) between "ERT-CH23" and "PROFITIS ELIAS".

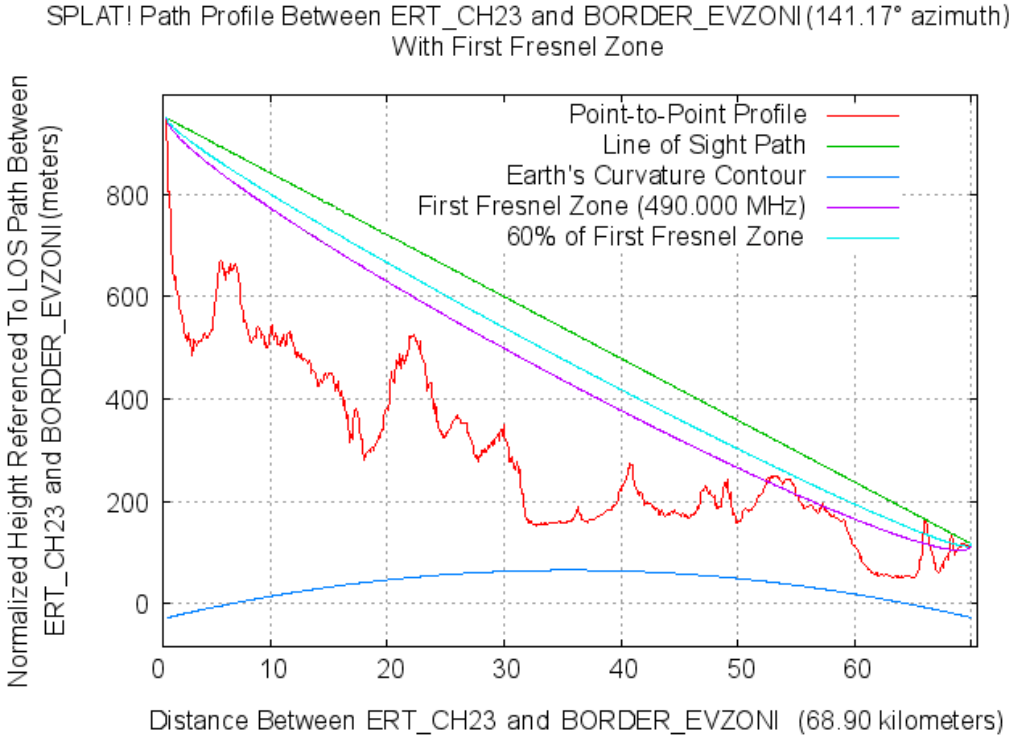

Figure 7-7: Path profile produced by SPLAT! v1.2.3 (Windows) between "ERT-CH23" and "BORDER EVZONI".

All measurements were made with the reception antenna at an altitude of 2.5 meters above ground. The simulation results generated by ITM & ITWOM models using Radio Mobile and SPLAT! Software, use the same 2.5-meter antenna height for more accurate comparisons.

Another Point-to-Point analysis for Public Greek DTV "ERT-CH 56" (754MHz) with the following characteristics, is presented in Table 7-4.

- Transmitter's name: ERT
- Transmission Channel: CH56
- Transmission frequency: 754 MHz
- P_o: 1250 W or 30.97 dBW or 60.97 dBm
- Net Antenna Gain: 10 dBd, or 12.15 dBi
- E.R.P: 12.5 kW or 40.97 dBW or 70.97 dBm
- E.I.R.P: 20.51 kW or 43.12 dBW or 73.12 dBm
- Transmitter Antenna Height Ht: 70 m
- Receiver Antenna Height Hr: 2.5 m
- Altitude: 864.5 m
- Longitude: 23.099793E and Latitude: 40.597648N

Table 7-4. A point-to-point analysis for Greek Public DTV "ERT-CH56" (754 MHz)

No.	Measurements Points	LAT(N)/ LONG(E)	E(dBμV/m)			
			FSH-3 Measure-ments	ITM Radio Mobile (Windows)	ITM SPLAT! (Windows)	ITWOM SPLAT! v1.4.0 (Ubuntu 12.10)
1	PROFITIS ELIAS (7 km/313 degs)	40.640411 23.039927	101.6	96.4	99.0	93.8
2	THESSALONIKI (12.3 km/279 degs)	40.615822 22.955735	95.9	97.0	93.9	92.8
3	LAKE VOLVI (14.3 km/31 degs)	40.707102 23.188914	98.9	97.0	92.7	89.5
4	PEREA (16.7 km/236 degs)	40.513489 22.937471	96.7	95.8	91.3	88.4
5	METHONI (47 km/252 degs)	40.469402 22.574711	84.0	84.0	81.7	63.1
6	KORINOS (52 km/232 degs)	40.307130 22.618620	82.3	84.3	80.6	60.6

7	BORDER EVZONI (68.8 km/321 degs)	41.081410 22.588160	65.3	73.8	77.4	58.0
8	SOUMELA (86 km/256 degs)	40.410086 22.116606	75.6	77.2	76.0	56.4
9	LOUTRAKI (107 km/293 degs)	40.966160 21.923630	75.8	77.8	72.8	53.3
10	POLYKASTRO (69 km/320 degs)	41.081190 22.588360	71.9	73.9	77.4	58.0

Errors between measurements taken by FSH-3 spectrum analyser instrument and simulations results produced by ITM model using Radio Mobile and SPLAT! v1.2.3 for Windows software, with average error and standard deviation, are shown in Table 7-5.

Table 7-5. Errors between FSH-3 measurements and simulations by models ITM (Radio Mobile), ITM (SPLAT! for windows) and ITWOM (SPLAT! v1.4.0-Ubuntu 12.10) with Average Error and Standard Deviation for DTV, "ERT-CH56".

No.	Measurements Points	Errors (dB)		
		FSH-3 & Radio Mobile	FSH-3 & SPLAT! ITM (WINDOWS)	FSH-3 & ITWOM SPLAT! v 1.4.0 (Ubuntu 12.10)
1	PROFITIS ELIAS (7 km/313 degs)	-5.2	-2.6	-7.8
2	THESSALONIKI (12.3 km/279 degs)	1.1	-2.0	-3.1
3	LAKE VOLVI (14.3 km/31 degs)	-1.9	-6.2	-9.4
4	PEREA (16.7 km/236 degs)	-0.9	-5.4	-8.3
5	METHONI (47 km/252 degs)	0.0	-2.3	-20.9
6	KORINOS (52 km/232 degs)	2.0	-1.7	-21.7
7	BORDER EVZONI (68.8 km/321 degs)	8.5	12.1	-7.3
8	SOUMELA (86 km/256 degs)	1.6	0.4	-19.2
9	LOUTRAKI (107 km/293 degs)	2.0	-3.0	-22.5
10	POLIKASTRO (69 km/320 degs)	2.0	5.5	13.9

	Average	0.9	-0.5	-13.4
	Standard Deviation	3.5	5.5	7.1

Errors between measurements (FSH-3) and simulations results produced by ITM model using Radio Mobile & SPLAT! (Windows) and ITWOM model (Ubuntu 12.10) are shown in the bar graph below, in Figure 7-8.

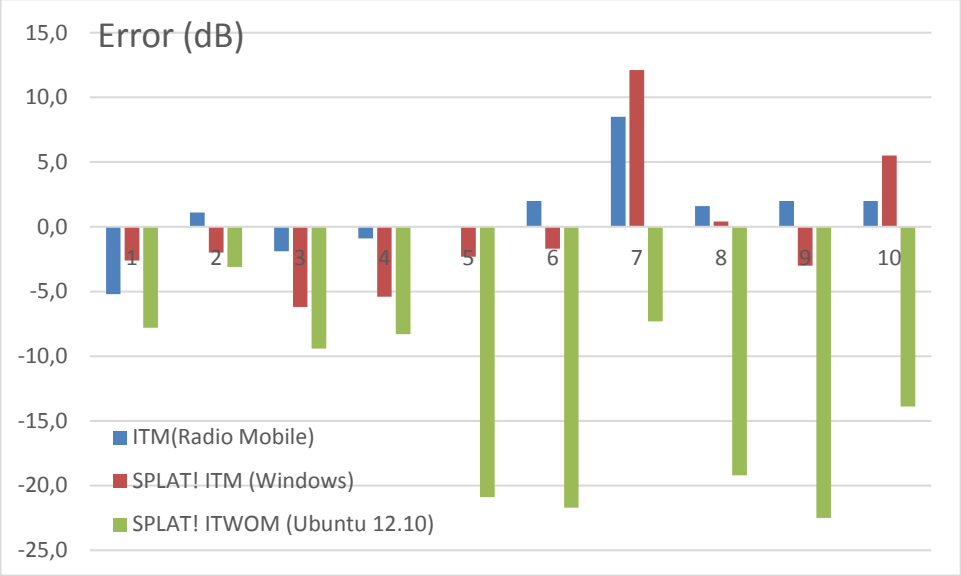

Figure 7-8: Errors between measurements (FSH-3) and simulations using ITM model (Radio Mobile & SPLAT! for Windows) and ITWOM model (Ubuntu 12.10).

The No. 2, 4, 5, 7, 9, and 10 simulations results are better for Radio Mobile than those of SPLAT! for Windows, and No. 1, 6, and 8 simulation results are better for SPLAT! (ITM) than those for Radio Mobile. The main conclusion for the above measurement points is that Radio Mobile gives overall better simulation results with the lower standard deviation (S.D. = 3.5 dB) than SPLAT! for Windows (S.D. = 5.5 dB), though both software uses the same propagation model, i.e., ITM.

The above measurements and simulation results show that, ITWOM model produced by SPLAT! v1.4.0, gives worse simulation results than ITM model produced by SPLAT! v1.2.3 for Windows and by Radio Mobile. Additionally, in distances bigger than 40km the simulation results are much worse. Most probably, ITWOM model overestimates the attenuation by obstacles and this is currently under investigation. All the antennas of the FM radio and TV stations are located on Hortiatis mountain nearby the city of Thessaloniki. A coverage map produced by Radio Mobile that uses the ITM model for

Greek public Digital TV station "ERT-CH56" (754 MHz), is shown in Figure 7-9. A signal meter at the right corner of the map correlates each color with a specific signal strength in decibels over one microvolt per meter (dBμV/m). Longley-Rice analysis range has been set to a radius of 150 km. Topographic maps display elevations using a logarithmic grayscale. Higher elevations represented through brighter shades of gray. The sea-level is represented using a light blue color .

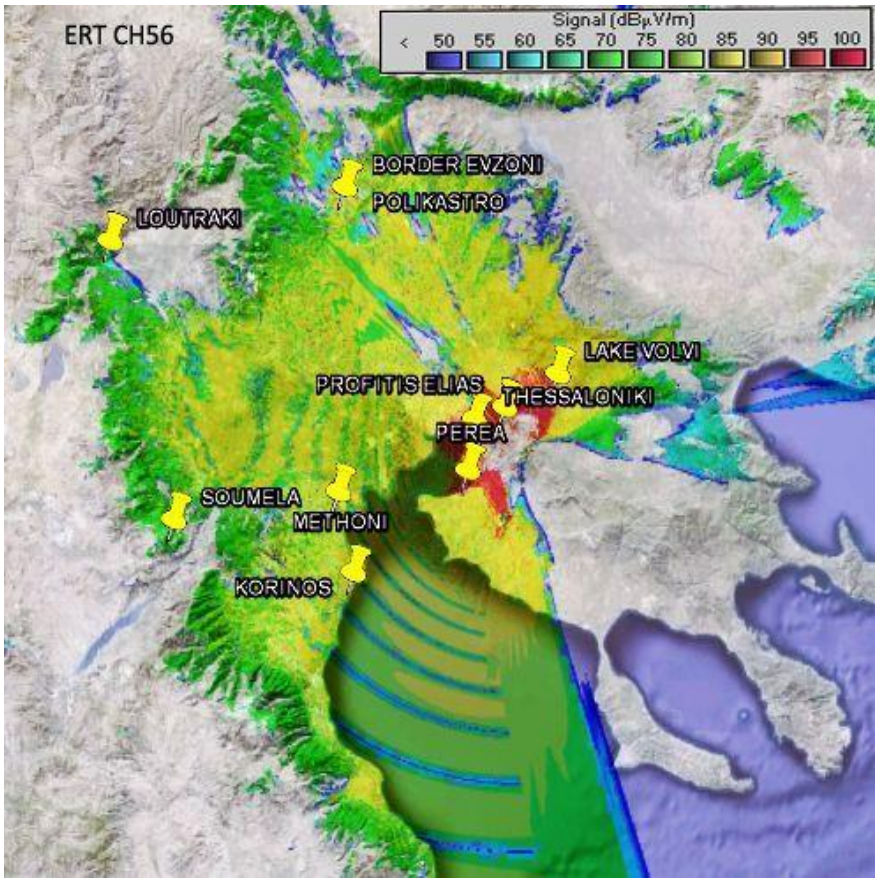

Figure 7-9: Coverage map produced by Radio Mobile for Greek DTV "ERT-CH56". Coverage radius is 150 km.

Another coverage map produced by SPLAT! for Windows using ITM model, for the Greek public Digital TV station , "ERT-CH56" (754 MHz), is shown in Figure 7-10. Topographic maps produced by SPLAT! display elevations using a logarithmic grayscale. Higher elevations represented through brighter shades of gray. Only the sea-level is represented using the colour blue. The coverage map includes a legend at the right top. Each color of the legend corresponds to signal strength in decibels over one microvolt per meter (dBμV/m).

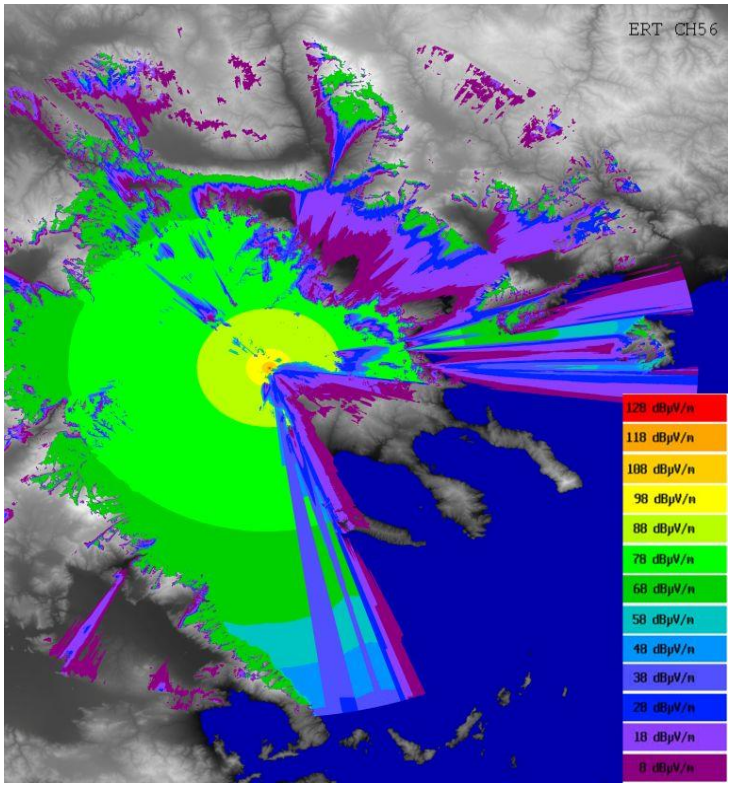

Figure 7-10: Coverage map produced SPLAT! (Windows) for Greek TV "ERT-CH56". Coverage radius is 150 km.

A coverage map produced by SPLAT! v.1.4.0 (Ubuntu 12.10) using ITWOM model for the Greek public DTV "ERT-CH56" is shown in Figure 7-11.

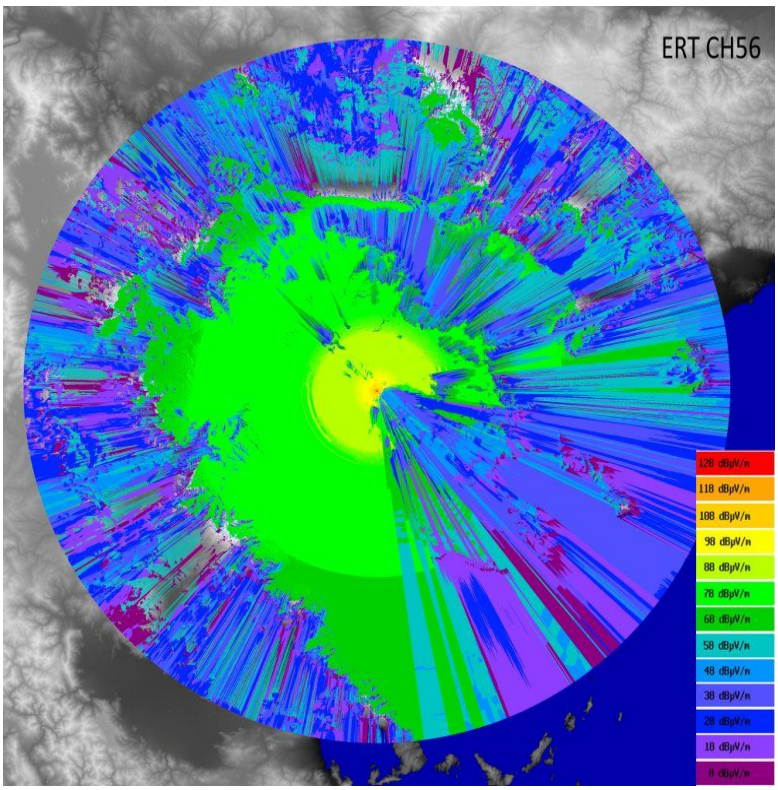

Figure 7-11: Coverage map produced by SPLAT! v1.4.0 (ITWOM model) for Greek TV station "ERT-CH56". Coverage radius is 150 km.

All measurements were made keeping the receiving antenna to 2.5 meters height. The simulation results generated by ITM & ITWOM models using Radio Mobile and SPLAT! software respectively, use the same 2.5-meter antenna height for an accurate comparison of results.

Although DAB (Digital Audio Broadcasting), was developed in the early nineties, it is still not in use in many countries. Recently, in February 2013 at Geneva, EBU released recommendation r138 for Digital Radio Distribution in Europe [18]. In Greece DAB is currently not in use, and all radio stations are still analog.

There is, however, a necessity for measurements and predictions in radio broadcasting, especially in the VHF frequencies. Using the same equipment and software, as above for the DTV case, measurements were made for the Greek public FM radio station "ERA-102".

This station is also located on Hortiatis Mountain (it is the highest mountain nearby Thessaloniki and so the best transmitting point), next to the city of Thessaloniki. The coordinates are the same as before (same antenna tower), the transmit power is 20 kW, frequency is 102 MHz, the antenna type is 6 bays in 3 directions of FM panel antennas (dipoles in front of reflector) with a total gain minus cable losses of 5 dBd, the average antenna height is 50 m, and the azimuth is 285 degs. Analytically this radio station has the following characteristics.

- Transmitter's name: "ERA-102", FM Stereo
- Transmission frequency: 102 MHz
- P_o: 20 kW or 43.01 dBW or 73 dBm
- Net Antenna Gain: 5 dBd, or 7.15 dBi
- E.R.P: 63.09 kW or 47.99 dBW or 78 dBm
- E.I.R.P: 103.5 kW or 50.15 dBW or 80.15 dBm
- Transmitter Antenna Height Ht: 50 m
- Transmitter Antenna type: 6 bays in 3 directions (dipoles in front of reflector)
- Receiver Antenna Height Hr: 2.5 m
- Altitude: 864.5 m
- Longitude: 23.0997993E and Latitude: 40.597648N

A Point-to-Point analysis for the Greek public FM Stereo radio station "ERA-102" is shown in Table 7-6.

Table 7-6. A point-to-point analysis for the Greek Public FM radio station "ERA-102".

No.	Measurements Points	LAT/ LONG	E(dBμV/m)			
			FSH-3 Measure-ments	ITM Radio Mobile (Windows)	ITM SPLAT! (Windows)	ITWOM SPLAT! v1.4.0 (Ubuntu 12.10)
1	KOURI (5.2 km/319 degs)	40.632814 23.058840	108.8	110.0	100.8	96.6
2	METHONI (47 km/252 degs)	40.469402 22.574711	96.7	91.7	94.0	76.1
3	KORINOS (52 km/232 degs)	40.307130 22.618620	71.9	81.5	92.9	73.0
4	BORDER EVZONI (68.8 km/321 degs)	41.081410 22.588160	63.0	76.3	88.8	70.3
5	LOUTRAKI (107 km/293 degs)	40.966160 21.923630	65.7	76.7	82.7	65.8
6	POLIKASTRO (69 km/320 degs)	41.081190 22.588360	56.1	67.7	88.8	70.3

Errors between FSH-3 measurements and simulations produced by ITM model using Radio Mobile and SPLAT! v1.2.3 for Windows, with average error and standard deviation, for Greek FM radio station "ERA-102", are shown in Table 7-7.

Table 7-7. Errors between FSH-3 measurements and simulations by ITM model (Radio Mobile & SPLAT! for windows), with Average Error and Standard Deviation for the Greek FM Stereo radio station "ERA-102".

No.	Measurements Points	Errors (dB)		
		FSH-3 & Radio Mobile	FSH-3 & SPLAT! For Windows	FSH-3 & SPLAT! ITWOM (Ubuntu 12.10)
1	KOURI (5.2 km/319 degs)	1.2	-8.0	-12.2
2	METHONI (47 km/252 degs)	-5.0	-2.7	-20.6
3	KORINOS (52 km/232 degs)	9.6	21.0	1.1
4	BORDER EVZONI (68.8 km/321 degs)	13.3	25.8	7.3

5	LOUTRAKI (107 km/293 degs)	11.0	17.0	0.1
6	POLIKASTRO (69 km/320 degs)	11.6	32.7	14.2
	Average	7.0	14.3	-1.7
	Standard Deviation	7.2	16.2	12.7

Errors between measurements taken by FSH-3 instrument and simulations produced by ITM model using Radio Mobile and SPLAT! v1.2.3 for Windows and, by ITWOM model using SPLAT! v1.4.0 for Linux, are shown in Figure 7-12.

Observing Figure 7-12 or Table 7-7, it is concluded that simulation results No. 1, 3, 4, 5, and 6 are better for ITM model used by Radio Mobile than these of ITM model used by SPLAT! for Windows, and only No. 2 simulation result is better for ITM model used by SPLAT! than ITM model used by Radio Mobile. Consequently, Radio Mobile with ITM model gives better simulation results with a lower standard deviation (S.D. = 7.2dB) than SPLAT! for Windows with ITM model (S.D.= 16.2 dB). That proves that the modifications made in the original ITM code in Radio Mobile are in the right direction giving improved simulation results while SPLAT! v1.2.3 for Windows using the original ITM code without changes produces worse simulation results. It can also be seen in the FM case that the simulations results produced by SPLAT! for Windows are worse than Radio Mobile results and getting worse as distance increases above around 40km. The simulation results are, in general, worse for VHF FM radio frequencies than those for UHF DVB-T frequencies.

In Figure 7-12 or Table 7-7, it also can be noticed that simulation results for No. 3 4, 5, and 6 measurement points produced by ITWOM model using SPLAT! v1.4.0 are better than those produced by ITM model using SPLAT! v1.2.3 for Windows, which in turn gives better results for No. 1 and 2 measurement points.

It is observed that for frequencies in the VHF FM range, ITWOM model (SPLAT! v1.4.0) gives better simulation results than ITM model (SPLAT! for Windows). It is concluded so, that changes, and additions made by the author in the code of ITM model to produce ITWOM model work better in lower frequencies overestimating the path loss of obstacles in higher frequencies.

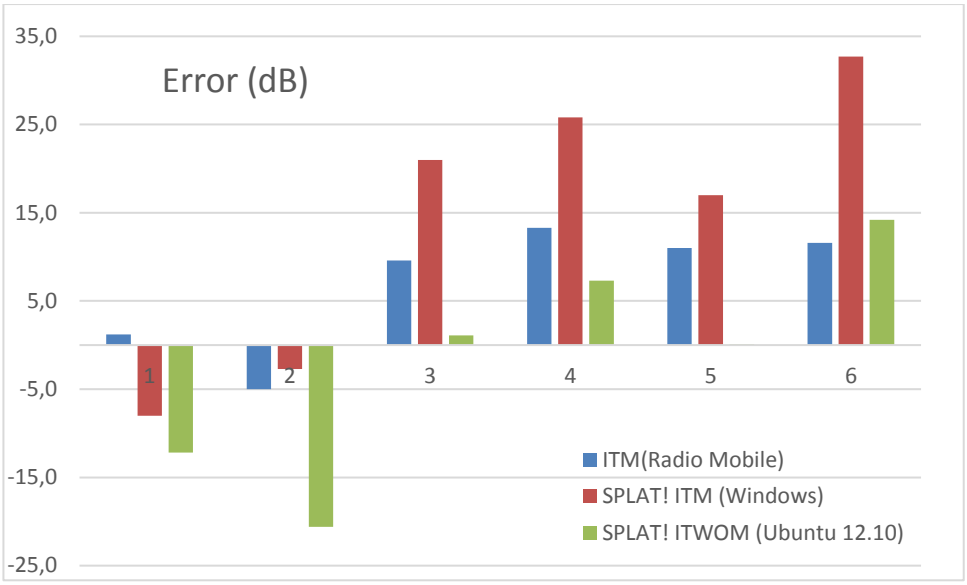

Figure 7-12: Errors between measurements (FSH-3) and simulations using ITM model (Radio Mobile & SPLAT! for Windows) and ITWOM model (Ubuntu 12.10), for the Greek FM stereo radio station "ERA-102".

A coverage map produced by Radio Mobile using ITM (Longley-Rice) model with some minor modifications for Greek public FM stereo radio station "ERA-102" is shown in Figure 7-13.

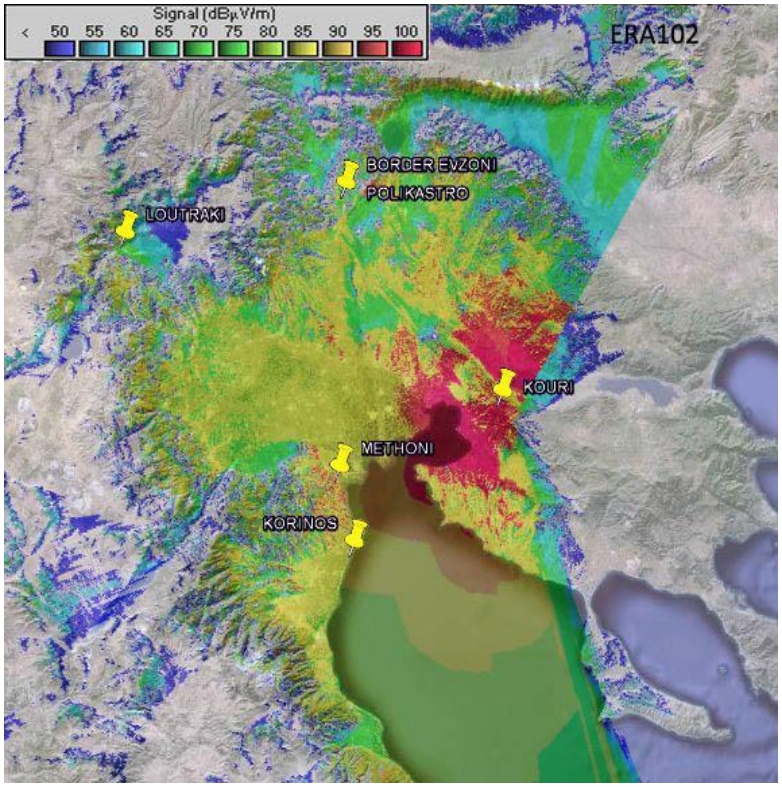

Figure 7-13: Coverage map produced by Radio Mobile for Greek FM stereo radio station "ERA-102". Coverage radius is 150 km.

Coverage maps produced by SPLAT! v1.2.3 for Windows (ITM model) and SPLAT! v1.4.0 (ITWOM model) for the Greek public FM stereo radio station, "ERA-102" are shown in Figures 7-14 and 7-15.

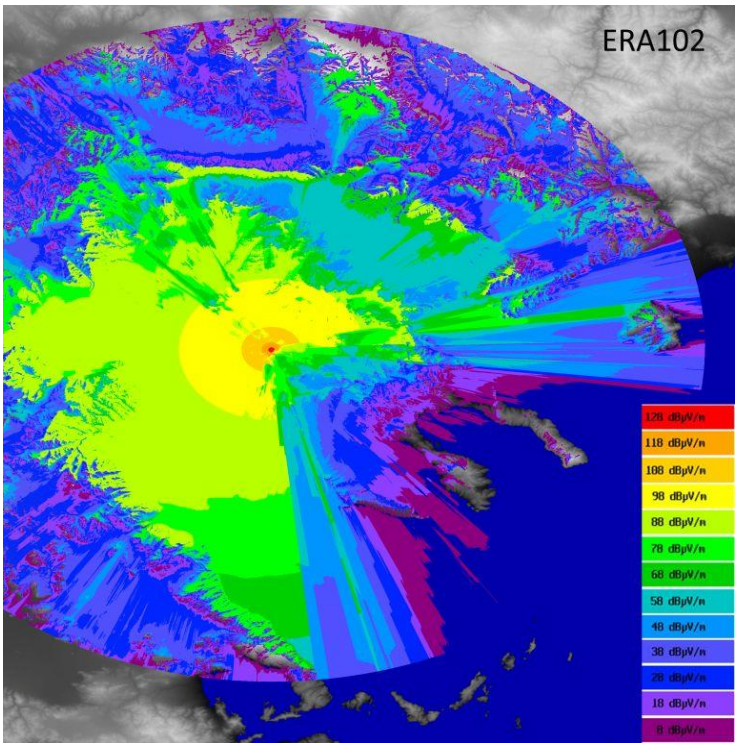

Figure 7-14: Coverage map produced by SPLAT! v1.2.3 for Windows, Greek FM stereo radio station "ERA-102". Coverage radius is 150 km.

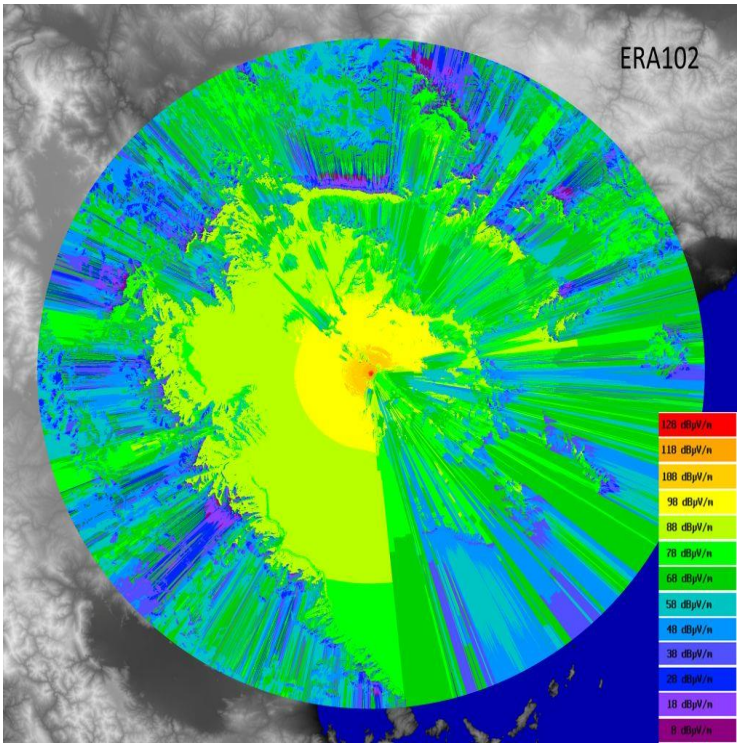

Figure 7-15: Coverage map produced by SPLAT! v1.4.0 for Greek FM stereo radio station "ERA-102". Coverage radius is 150 km.

7.5 SUMMARY

The Longley-Rice (ITM) model, that Radio Mobile and SPLAT! (splat-1.2.3-win32) use in conjunction with global Shuttle Mission Satellite Radar 3-arc-second data (SRTM3) produces, in some cases, big errors compared to measurements results. The Longley-Rice model does not work quite well in the line-of-sight mode and the early diffraction range. Furthermore, the Longley-Rice model does not use more detailed terrain information as other more sophisticated models do. The ITWOM (SPLAT! v1.4.0 for Linux) propagation model was recently proposed, claiming an improved accuracy over the older ITM model. However, new simulation results and measurements in point-to-point path analysis with ITWOM model do not verify these claims. The ITWOM model has a somewhat better accuracy for distances smaller than 20 km, but vast differences for distances larger than 40 km.

7.6 REFERENCES

[1] ITU-R, "Method for point-to-area predictions for terrestrial services in the frequency range 30MHz to 3.000 MHz (p.1546-3)," 2007.

[2] T. Rappaport, "Wireless Communications: Principles and Practice." Prentice Hall, 2002.

[3] J.S. Seybold. "Introduction to RF Propagation," John Wiley & Sons, Inc, 2005.

[4] P.L. Rice, A.G. Longley, K.A. Norton, and A.P. Barsis. "Transmission loss predictions for tropospheric communications circuits," Technical Note 101, revised 1/1/1967, U.S. Dept. of Commerce National Telecommunications & Information Administration, Institute for Telecommunications Sciences(NTIA-ITS).

[5] Roger Coudé, Web page of Radio Mobile, downloads and How to http://www.cplus.org/rmw/english1.html, Freeware by VE2DBE.

[6] Webpage of G3TVU about Radio Mobile applications and possibilities. http://www.g3tvu.co.uk.Radio_Mobile.htm.

[7] Salamanca L. Murillo-Fuentes J.J. Olmos P. "Review of the Radio Mobile Software as a teaching tool for Radio planning" IEEE multidisciplinary engineering education magazine, vol. 6, no. 2, June 2011.

[8] NASA, "Shuttle Radar Topography Mission data." Available online at URL: http://www2.jpl.nasa.gov/srtm/. The SRTM (3 arc-seconds) version V2 can be obtained through the URL: https://dds.cr.usgs.gov/srtm/version2_1.

[9] Magliacane J**. SPLAT!** An RF **S**ignal **P**ropagation, **L**oss, **A**nd **T**errain analysis tool for the spectrum between 20 MHz and 20 GHz. Available online at URL http://www.qsl.net/kd2bd/splat.html.

[10] McMellen, J. RF propagation modeling (Longley-Rice) with SPLAT! for windows. Available online at URL http://blog.gearz.net/2007/09/rf-propagation-modeling-with-splat-for.html.

[11] Austin W. RF propagation modeling with SPLAT! for windows. Available online at URL http://www.ve3ncq.ca/wordpress/?page_id=62.

[12] Sid Shumate, 'Deterministic Equations for Computer Approximation of ITU-R P.1546-2', International Symposium on Advanced Radio Technologies and The Working Party Meetings for ITU-R WP3J,3K,3L and 3M hosted by National Institute of Standards and Technology, June 2/4, 2008.

[13] S.E. Shumate. 'Longley-Rice and ITU-P.1546 combined A new international terrain-specific propagation model'. In Vehicular Technology Conference Fall (VTC 20102-Fall), 2010 IEEE 72nd, Sept 2012.

[14] Ubuntu 12.10. Available on line. http://www.ubuntu.com.

[15] A. Achtzehn, J. Riihijärvi, G. Martínez Vargas, M. Petrova, and P. Mähönen, "Improving coverage prediction for primary multi-transmitter networks operating in the TV whitespaces," in Proc. 2012 9th Annual IEEE Communications Society Conference on Sensor, Mesh and Ad Hoc Communications and Networks (SECON), 2012, pp.623-631.

[16] Available on line at URL: http://tech.ebu.ch/docs/r/r138.pdf.

CHAPTER 8

UHF TV BAND SPECTRUM AND FIELD-STRENGTH MEASUREMENTS BEFORE AND AFTER ANALOG SWITCH-OFF (ASO).

8.1 INTRODUCTION

The radio-frequency spectrum is a limited natural resource with great economic and social impact. Most countries around the world have already abandoned the traditional analog broadcasting of TV signals in favor of the digital broadcasting techniques. In Europe DVB-T and DVB-T2 are used with great success and most European countries have already concluded the Analog Switch-off (ASO). The modulation and coding gains of DTV combined with the compression gains of the MPEG-4 type of video compression algorithms result in a significantly reduced spectrum usage and to higher transmitting bit rates Furthermore, the principle of SFN (Single Frequency Network) broadcasting, where a single frequency channel is used in a whole geographical region or allotment, leads to even more efficient spectrum utilisation. Moreover, digital receivers are much more sensitive than the analog ones, requiring less than 25-30 dBμV input, in the absence of reflections, for a blocking-free picture, while, on the contrary, analog receivers needed at least 50 dBμV input for the snow-free reception. Consequently, lower field-strengths and lower transmitter powers are in general required for the same geographical coverage.

8.2 FREQUENCY PLANS AND ALLOTMENTS

The Regional Radiocommunication Conference held in Geneva in 2006 (RRC 06) is the most important ITU (International Telecommunications Union) event in the process of digital broadcasting planning [1].

According to the ITU, the transitional period with simultaneous analog and digital broadcasting should end on 17/05/2015 for the whole of the world. In Greece, the digital transition should be completed by the end of 2014.

However, in the region of Thessaloniki, the ASO already took place in the end of 2012 and only DTV signals are being used since then. Allotment zones in Greece are shown in Figure 1 and definitions are given in Table 8-1 [2].

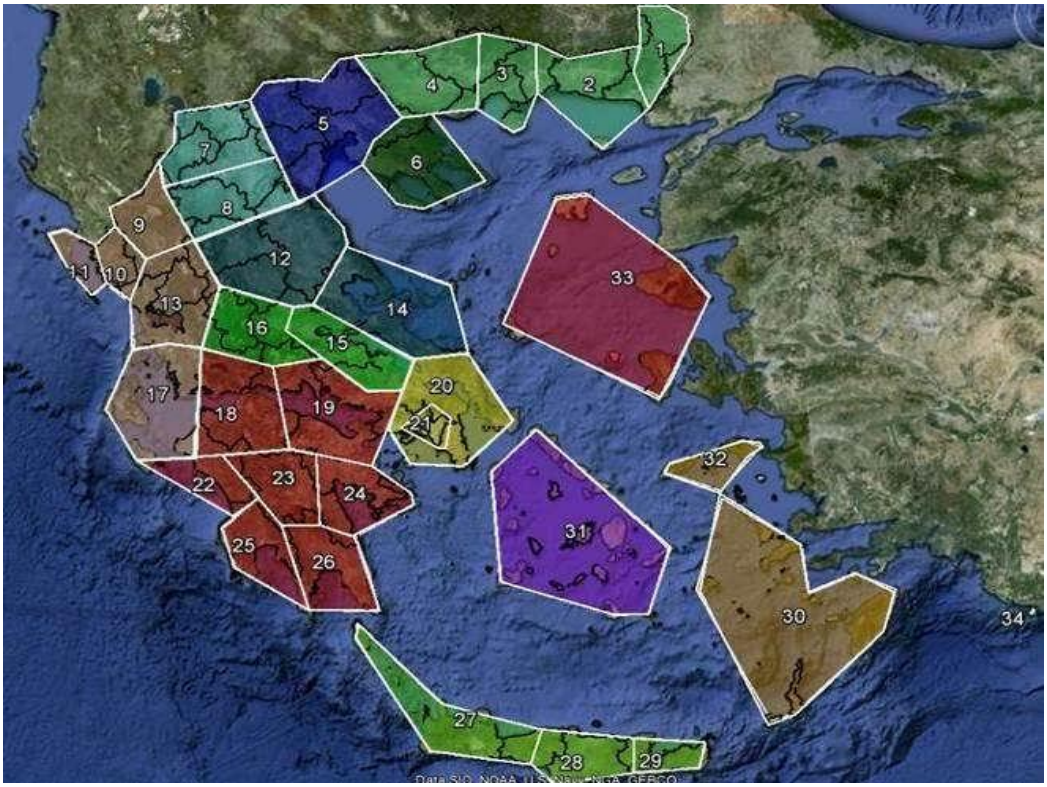

Figure 8-1: Allotment zones in Greece.

Table 8-1. Definitions of allotment zones in Greece.

ALLOTMENT	AREA	ALLOTMENT	AREA
1	EVROS	19	KORINTHOS
2	PLAKA	20	ATTIKH(SFN-1)
3	THASSOS	21	ATHINA(SFN-2)
4	PAGGAIO	22	PYRGOS
5	THESSALONIKI	23	TRIPOLI
6	XALKIDIKI	24	NAFPLIO
7	FLORINA	25	KALAMATA
8	METAKSAS	26	SPARTI
9	IOANNINA	27	WEST CRETE
10	THESPROTIA	28	CENTRAL CRETE
11	KERKYRA	29	EAST CRETE
12	LARISSA	30	DODEKANISA
13	AKARNANIKA	31a	KYKLADES(SFN-1)
14	VOLOS	31b	KYKLADES(SFN-2)
15	LAMIA	32	SAMOS
16	KARPENISI	33	LESVOS
17	AINOS	34	KASTELLORIZO
18	PATRA		

According to the ITU, allotments are geographical areas whose main purpose is less interference between them, when transmitting digital signals. To set an allotment, the allotment boundaries must be defined, and a maximum acceptable interference level among the allotments must be fixed. Greece is in the Southeastern Europe and has a population of around 11 million people. The terrain morphology of Greece is extremely diverse, with mountains, covering almost 60 percent of its land, with 16.300 km coast line and 6000 islands of which only 117 are inhabited. The Greek Ministry of Transport and Communications is the responsible authority for the country's representation in the ITU. Greece is divided into 34 allotment zones for DVB-T broadcasting purposes, in order to achieve full national coverage. Modulations of 16 QAM and 64 QAM types are used, 8K carriers, FEC 2/3 and 3/4 and guard interval (GI) that varies from 1/4 to 1/16 are used [3]. For the video compression, the standard MPEG-4 part 10-AVC (also known as ISO/IEC 14496-10 or ITU H.264) is used [4] while some local TV broadcasters still use the MPEG-2 standard for video compression. The allotment zones for Greece are shown in Figure 8-1.

8.3 SPECTRUM MEASUREMENTS PRE- AND POST-ASO

Measurements of UHF-TV band spectra and field-strength levels in the pre- and post-analog switch-off periods in the cities of Thessaloniki (a seaside town of Northern Greece) and Skopje (capital of Former Yugoslav Republic of Macedonia – F.Y.R.O.M) clearly demonstrate the much reduced spectrum occupancy, the lower signal levels, and the feasibility of digital dividend phase 1 allocations to cellular operators in the 800 MHz band, digital dividend phase 2 allocations in the 700 MHz band, as well as the feasibility of opportunistic secondary spectrum utilisation in extensive parts of the spectrum. The risk of LTE-4G interference to TV services and vice-versa is also pointed out and clearly observed from spectrum measurements near a cellular base station.

The measurements equipment consists of a Rohde & Schwarz FSH-3 portable spectrum analyser, factory calibrated with ± 0.7 dB accuracy, two high-precision calibrated biconical antennas by Schwarzbeck, SBA 9113 (500 MHz – 3 GHz) and BBVU 9135 (30 MHz – 1000 MHz), a log-periodic precision calibrated Schwarzbeck antenna USLP 9143 (0.25 – 6 GHz), factory calibrated with ± 1.0 dB accuracy, and low-loss cable Suhner GX-07272-D, 1.8 meters long with N-type connectors, [5-6]. Also, a commercial Iskra P20 log-periodic antenna is used in some measurements. This

low-cost short 10 dipole antenna has, in the UHF-TV band, similar gain as the professional USLP9143 at around 6-7 dBi, relatively flat across the whole band.

In Figure 8-2 the UHF-TV band spectrum before the Analog Switch-off and during the simulcast period of analog and digital TV is depicted. The spectrum occupancy is seen to be very dense with a very limited number of free TV channels (TVWS – TV White Spaces).

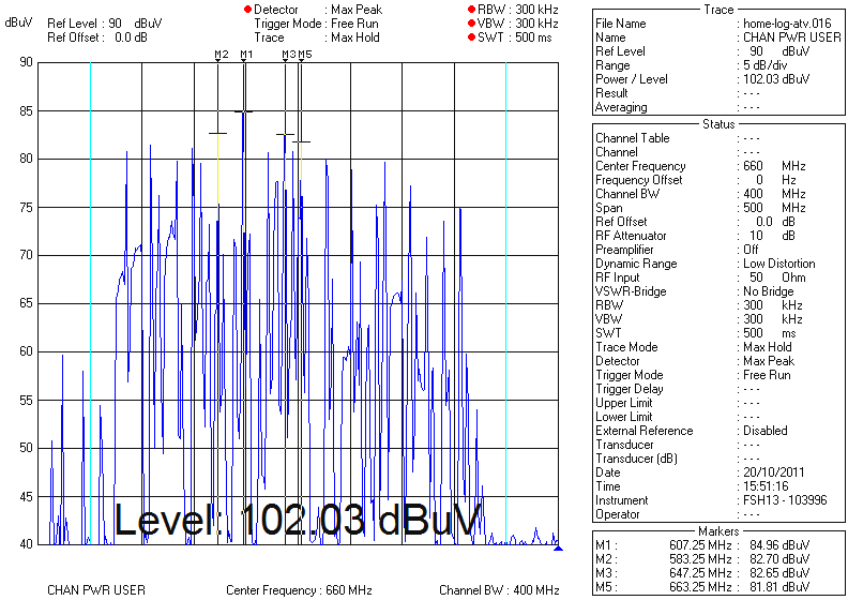

Figure 8-2: UHF-TV Band spectrum during the simulcast period, Thessaloniki center, date 20/10/2011.

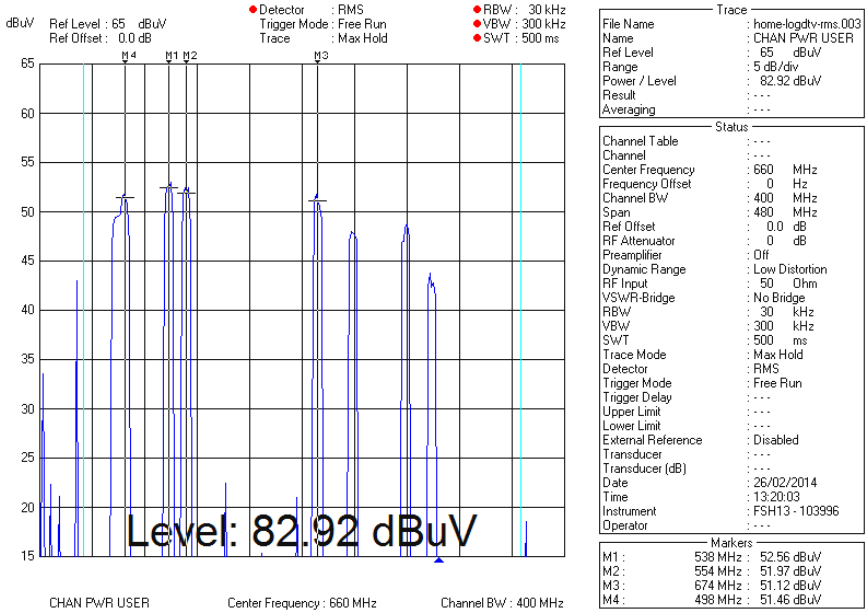

Figure 8-3: UHF-TV Band spectrum after the ASO (14/12/2012),Thessaloniki center, date 26/02/2014.

However, as seen in Figure 8-3, the situation post-ASO (after the 14th of December 2012) changes dramatically. Now, there are plenty of unoccupied TV channels. In fact,

the only occupied channels are 8 (8 MUXs-Multiplexes) which carry all previous TV Broadcasting programs. These 8 UHF-Channels are: 23, 24, 29, 31, 46, 50, 56, 59. The digital dividend frequencies 790-862 MHz (UHF, Channels 61-69) are unoccupied and are going to be used by LTE 4G cellular network operators. Apart from the freeing of the vast majority of TV channels, another very important characteristic of the post-ASO period is the much lower signal levels used by DTV. The 10 kW PEP (Peak Envelope Power) analog transmitters were replaced by 1-2.5 kW RMS DVB-T transmitters, leading to 8-10 dB lower signal strengths that are sufficient for the more sensitive digital receivers [7]. In figure 8-4 UHF-TV Band plus GSM900 spectrum after the ASO at the center of Thessaloniki is depicted.

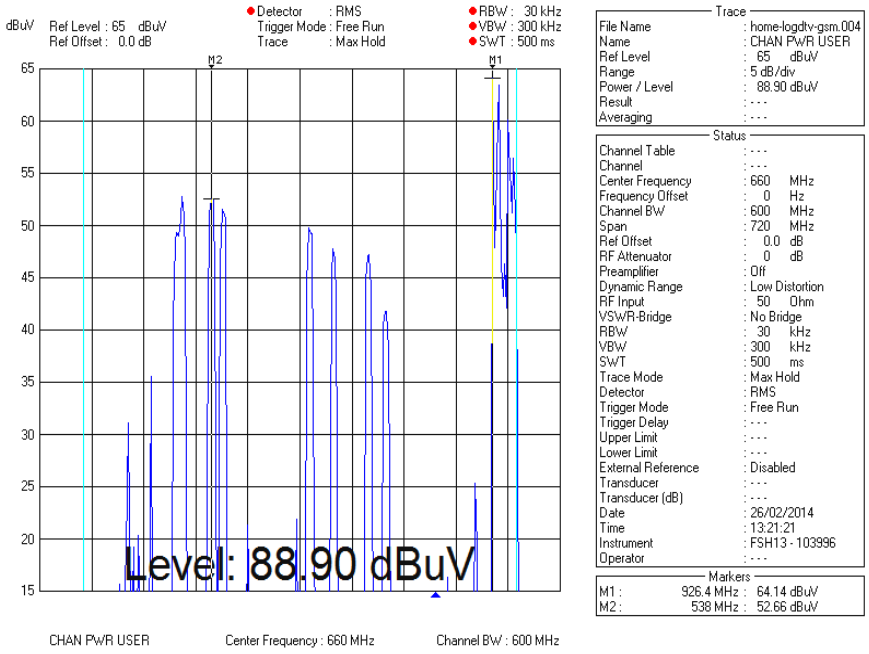

Figure 8-4: UHF-TV Band plus GSM900 spectrum after the ASO (14/12/2012), Thessaloniki center, date 26/02/2014.

Another, important detail that could potentially create interference, is the vicinity of the cellular frequency bands to the top of the UHF-TV band. In Figure 4, the spectrum of the UHF-TV band is depicted together with the GSM 900 MHz cellular frequency band. The measurement was performed with a directional log-periodic antenna pointed to the direction of the TV antenna park on Hortiatis mountain at a distance of approximately 12 km, East – Southeast of the city center. However, in the close vicinity of the reception point at a distance of 100 m and at an angle of approximately 60 degrees there is a GSM base station. Although a minimum of 16 dB signal reduction is expected at that angle, due to the directivity (and polarization) discrimination of the TV reception

antenna [8] the downlink GSM signal in the range of 920-960 MHz is very strong, at least 10 dB above the TV signals. This kind of strong signal could easily overload some reception preamplifiers, distribution amplifiers, or even TV receiver front-ends. In Tables 8-2 and 8-3, measured field strengths are shown before and after ASO.

Table 8-2. Measured field-strength in Thessaloniki center before ASO.

No.	TV Station Name	UHF TV Channel	Frequency (MHz)	Field Strength Measured (dBμV/m)
1	m.TV	38	607.25	104.8
2	SKAI	35	583.25	102.3
3	ALPHA	45	663.25	102.3
4	ALTER	41	631.25	100.7
5	ET-3	27	519.25	100.0
6	STAR	51	711.25	99.6
7	MEGA	24	495.25	99.0
8	NET	30	543.25	98.8
9	TV-100	33	567.25	98.7

Table 8-3. Measured field-strength in Thessaloniki center after ASO.

No.	TV Station Name	UHF TV Channel	Frequency (MHz)	Field Strength Measured (dBμV/m)
1	DT MUX1	23	490	90.8
2	Digea MUX1	24	498	93.1
3	Digea MUX2	29	538	95.0
4	PERTHO	31	554	94.6
5	DP	46	618	94.5
6	DBS	50	706	90.6
7	DT MUX2	56	754	92.0
8	DU	59	778	86.9

The situation is expected to become even worse when LTE 4G transmissions begin in the digital dividend frequency 800 MHz band of 790-862 MHz where no filtering was foreseen in older TV reception equipment and amplifiers. In Table II the 9 strongest TV

signals are depicted in the pre-ASO period in the center of Thessaloniki. The reception is performed on the rooftop of a 6-floor building with a clear unobstructed view to Hortiatis mountain antenna park. The field-strength values are quite high (in the range of 105 - 100 dBμV/m) and in any case much higher than the 70 dBμV/m value that was recommended for adequate analog TV coverage. Almost all TV channels were used at that time, thus eliminating the notion of TV white spaces. On the contrary, in the post-ASO era, only 8 TV channels are occupied, as seen in Figure 8-3, and their field-strength values are much lower (in the range of 95 - 87 dBμV/m), *cf.* Table 8-3. Notably, there is a big white space of 112 MHz from 558 to 670 MHz, situated between Ch 31 and 46. Furthermore, the total received signal power in the UHF-TV band post-ASO is 19 dB lower than in the simulcast period (83 dBμV instead of 102 dBμV).

Furthermore, with the future introduction of phase 2 digital dividend, or equivalently the '700 MHz' Band for mobile communications, some migration of TV services from UHF Bands IV-V (470-790 MHz) back to broadcasting VHF Band III (174-230 MHz) could be expected.

Similar spectrum measurements were likewise performed in the city of Skopje (F.Y.R.O.M), that is of comparable size and population as Thessaloniki [9]. The measurements were performed in the center of the city of Skopje (Boulevard Partizanski Odredi) in clear unobstructed view of the antenna park of Mount Vodno that is situated around 4 km to the South of the measurement point. The receiving antenna is placed 10 m above ground level and is a directional log-periodic antenna. Also, in this case, it is seen from Figure 8-5 and Table 8-4 that during the simulcast period most of the TV channels were occupied and there were scarce opportunities for secondary spectrum usage. On the contrary, in the post-ASO era, only 6 TV channels are occupied: Ch 23, 26, 28, 30, 33, and 52, *cf*. Figure 8-6 and Table 8-5. Channels 23 and 52 are being used by public TV and the rest for the private and subscriber TV networks. The field-strength levels are lower in the post-ASO period for the public broadcaster, but somewhat higher for the other broadcasters, as depicted in Tables IV and V., In this case, there is an even bigger white space of 144 MHz between the frequencies 574 and 718 MHz, i.e. between Ch 33 and Ch 52, that could advantageously be used for secondary opportunistic transmissions. It is also clearly observed that the digital dividend 800 MHz band from 790 to 862 MHz (former TV Channels 61-69) is unoccupied and ready to be used by cellular operators.

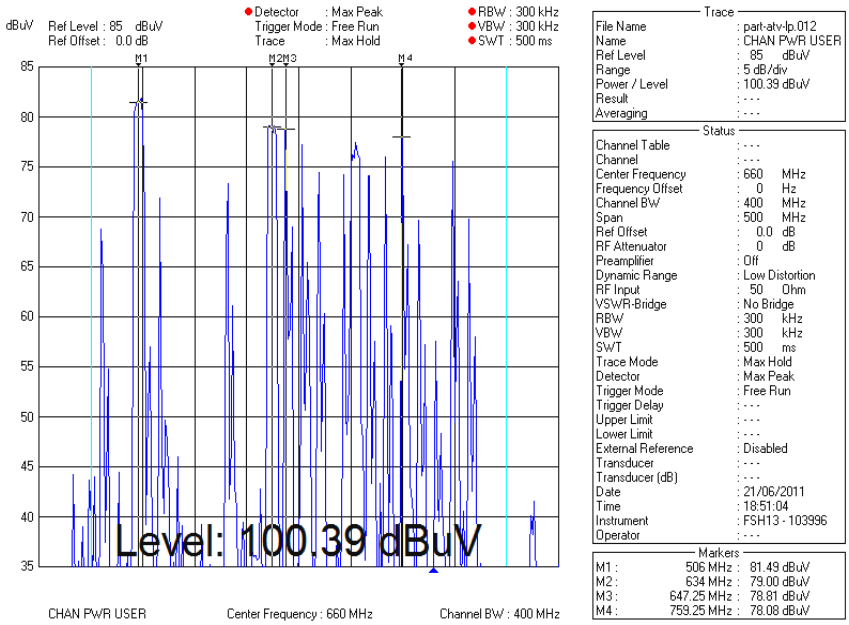

Figure 8-5: UHF-TV Band spectrum during the simulcast period, Skopje center, date 21/06/2011.

Table 8-4. Measured field-strength in Skopje center before ASO.

No.	TV Station Name	UHF TV Channel	Frequency (MHz)	Field Strength Measured (dBμV/m)
1	Sitel	57	759.25	99.7
2	Telma	43	647.25	99.1
3	TV	63	807.25	98.1
4	Mak Spot	55	743.25	97.3
5	ERA	53	727.25	95.2
6	A1	47	679.25	95.1
7	Kanal 5	50	703.25	95.0
8	MTB-3	36	591.25	92.9
9	MTM	28	527.25	90.6

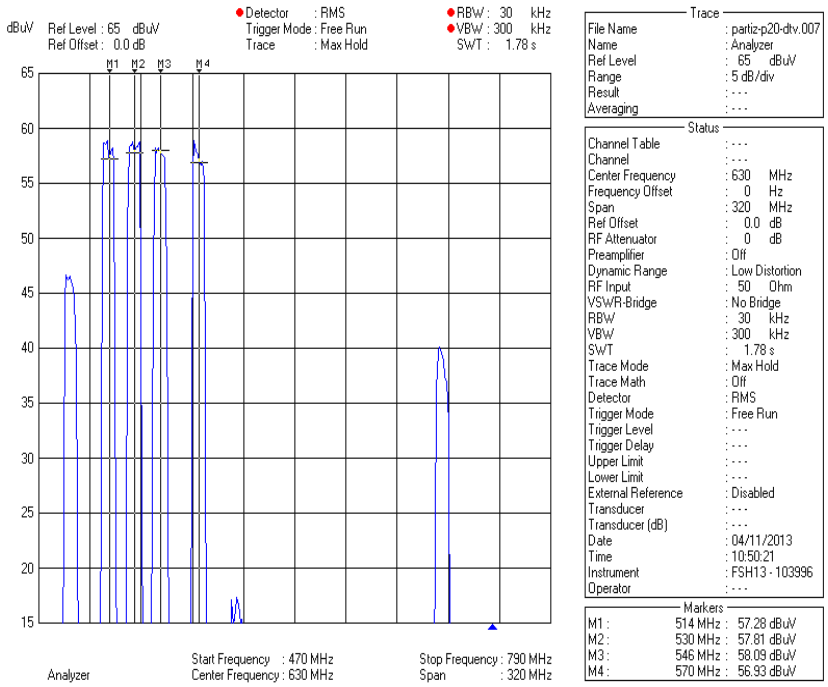

Figure 8-6: UHF-TV Band spectrum after the ASO (31/05/2013), Skopje center, date 04/11/2013.

Table 8-5. Measured field-strength in Skopje center after ASO.

No.	TV Station Name	UHF TV Channel	Frequency (MHz)	Field Strength Measured (dBμV/m)
1	MRT	23	490	87.5
2	ONE	26	514	101.1
3	ONE	28	530	101.5
4	ONE	30	546	101.2
5	ONE	33	570	101.0
6	MRT	52	722	84.7

8.4 SECONDARY SPECTRUM AVAILABILITY

A quantitative assessment of the TV White Space (TVWS) potential to support WiFi-like usage, prior and after the DSO in the city of Skopje was made. The analysis focused on one particular geographical point located within the premises of the Faculty of Electrical Engineering and Information Technologies in Skopje. The measurement setup involved an Anritsu MS2690A spectrum analyser and a Schwarzbeck SBA9113

biconical antenna. Similar studies have been performed around the world, e.g. in Germany, USA, New Zealand, and South Africa [10].

To calculate the real usable frequency chunks for secondary communication that will not degrade the operation of the primary TV reception, the analysis firstly determines the maximum received power for each TV channel. These values represent an input to the calculation process which implements the ECC rules for the operation of White Space Devices (WSD) in TV band based on the SE43 Report 154 [11]. According to the SE43, the implementation of any WSD should not violate certain limits in degradation of the TV reception location probability. Additionally, the calculation of secondary spectrum availability needs a precise specification of the WSD regarding its transmission power and required channel bandwidth. One important input parameter in the calculation is the number of adjacent TV channels, which will be protected from the WSD transmissions. The requirement to protect a higher number of adjacent TV channels reduces the secondary spectrum availability.

The calculation of the secondary spectrum availability presented here assumes introduction of WiFi-like WSD with a transmission power of 15 dBm, located indoors where the wall penetrating loss is 5 dB. The aim is to calculate the allowable transmission power of the WSD according to the ECC rules before and after the DSO, respectively. Both cases assume protection of TV receivers operating on the same channel as the WSD, as well as ±1 adjacent channels. Only the TV channels where the allowable transmission power is equal or higher than the assumed WSD transmission power, are eligible for the operation of the secondary devices.

A quantitative study on TVWS availability prior and after DSO would require a comparison of the secondary system performance in terms of the throughput that will be achieved by the WSDs. Figure 7 presents the achievable combined throughput of the secondary system using 8 and 16 MHz chunks prior and after the DSO and protecting ±1 channel. This calculation assumes that the secondary system comprises a WiFi-like access point (APs) operating on differently available frequency chunks, without creating interference towards the primary receivers, nor between each other. This idealized case can be achieved if the number of secondary APs is a controllable parameter and there is also a resource manager that regulates the operational frequency of each AP. In this way, the results presented in Figure 8-7 represent the upper boundary of the achievable throughput by the secondary system. Furthermore, the results give the combined MAC

layer throughput from all APs, as the calculation considers the known performance of the Distributed Coordinating Function (DCF) for the current Wi-Fi technology.

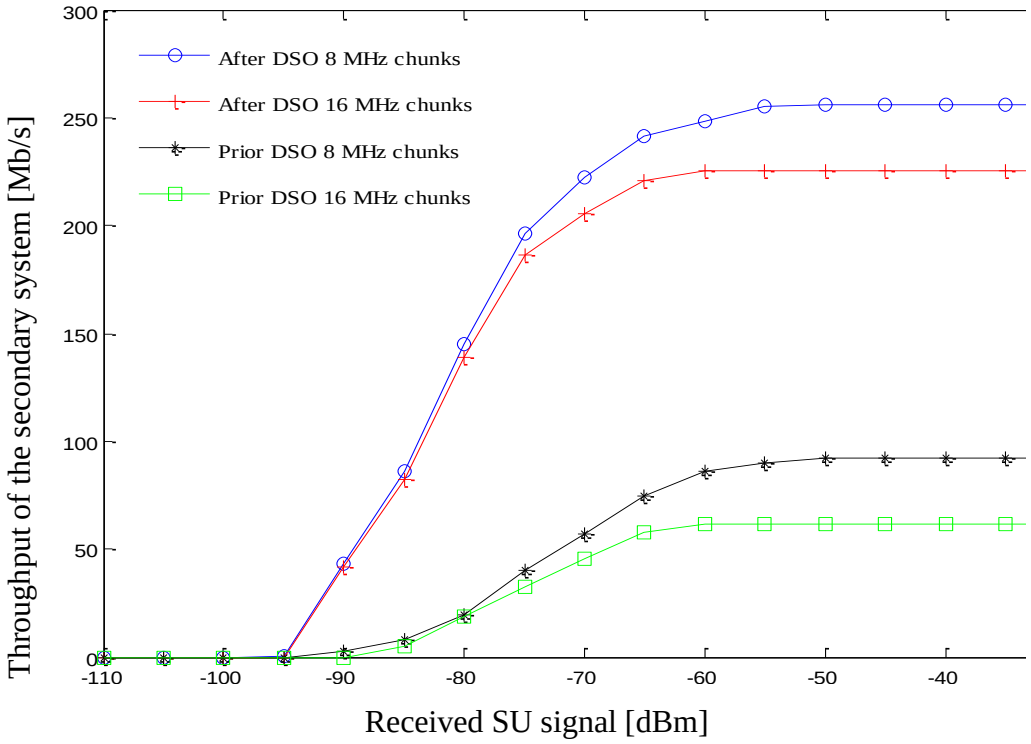

Figure 8-7: Combined throughput of the secondary system using 8 and 16 MHz chunks prior and after DSO protecting ±1 channel.

The results presented in Figure 8-7 reveal that the scenario involving the TV band after the DSO, where the secondary system operates on 8 MHz frequency chunks, provides the best performance in terms of achievable throughput. The organization in 16 MHz chunks is less efficient as there are available frequency chunks with an odd number of 8 MHz-channels. The achievable throughput prior to the DSO is much lower for both cases (8 MHz and 16 MHz frequency chunks operation).

8.5 SUMMARY

The measured UHF-TV band spectra in the cities of Thessaloniki and Skopje pre- and post-ASO clearly demonstrate the economies made on spectrum occupation by the passage to digital television. Additionally, for the same coverage area, lower field-strength values are required, thus leading to lower transmitted powers. Furthermore, a study for the city of Skopje reveals that TVWS availability is much higher in the post-ASO era leading to an increased potential throughput of the secondary system in Mbits/s.

8.6 REFERENCES

[1] ITU, "Final Acts of the Regional Radiocommunication Conference for the planning of the digital terrestrial broadcasting service in parts of Regions 1 and 3, in the frequency bands 174-230 MHz and 470-862 MHz (RRC-06), " Geneva, 2006.

[2] D. A. Kateros, D. A. Zarbouti, D. C. Tsilimantos, C. I. Katsigiannis, P. K. Gkonis, I. E. Foukarakis, et al., "DVB-T network planning: a case study for Greece," IEEE Antennas and Propagation Magazine, vol. 51, No. 1, pp. 91-101, Feb. 2009.

[3] ETSI EN 300 744 V. 1.5.1, "Digital Video Broadcasting (DVB); Framing structure, channel coding, and modulation for digital terrestrial television," June 2004.

[4] Recommendation ITU-T, "H.264-Advanced video coding for generic audiovisual services," Geneva, May 2003.

[5] S. Kasampalis P. Lazaridis, Z. Zaharis, A. Bizopoulos, S. Zettas, and J. Cosmas, "Comparison of ITM and ITWOM propagation models for DVB-T coverage prediction", IEEE BMSB 2013 conference, London, June 2013.

[6] S. Kasampalis, P. Lazaridis, Z. Zaharis, A. Bizopoulos, S. Zettas, and J. Cosmas, "Comparison of Longley-Rice, ITM, and ITWOM propagation models for DTV and FM broadcasting", WPMC 2013 conference, Atlantic City, NJ, June 2013.

[7] Recommendation ITU-R BT.1368-2, "Planning criteria for digital terrestrial television in the VHF/UHF bands, " 2000.

[8] Recommendation ITU-R BT.419-3, "Directivity and polarization discrimination of antennas in the reception of television broadcasting," 1992.

[9] L. Paunovska, P. Ivanoski, D. Vucikevik, P. Latkoski, V. Atanasovski, L. Gavrilovska, "Digital Switchover (DSO) in Macedonia: background, case study, and future," Proc. Of the XI International Conference ETAI, Ohrid, 26th -28th Sep. 2013.

[10] M. Ferreira and A. Helberg, "White space and digital dividends: the case for dynamic spectrum access in South Africa," IEEE Africon 2011 Conference, Zambia, 13th-15th Sep. 2011.

[11] ECC Report 159, "Technical and operational requirements for the possible operation of cognitive radio systems in the 'White Spaces' of the frequency band 470-790 MHz".

CHAPTER 9

EVALUATION OF PREDICTION ACCURACY FOR THE LONGLEY-RICE MODEL IN THE FM AND TV BANDS

9.1 INTRODUCTION

As mentioned many times in previous chapters, accurate geographical coverage predictions maps for FM and TV are needed for channel and frequency allocations and to avoid unwanted interferences.

The analog switch-off (ASO) is now a reality in all European countries, in the United States and in many countries, all over the world but the question of accurate coverage prediction is still open. Digital TV (DTV) makes the demand for accurate coverage prediction more important as operators of digital TV stations must ensure that their transmissions do not cause interference to other stations or to mobile telephony operators in nearby frequency channels (digital dividend). All these issues make the accurate coverage prediction and DTV transmitter distribution critical facts for the proper deployment of digital terrestrial television [1-10]. Furthermore, the accurate prediction of FM radio coverage is also very important to FM broadcasters in order to impose them the correct maximum ERP (Effective Radiating Power) and to avoid long-distance (DX) interferences between stations using the same frequencies.

In order to correctly evaluate the accuracy of a propagation model, and more specifically in this case, of the Longley-Rice model, extensive field measurements are required, and their comparison to simulation results obtained by propagation models [1-4]. This is exactly the scope of this study, i.e. to compare accurate field-strength measurements with simulation results in the Thessaloniki-Greece area and evaluate the precision of the propagation model in various circumstances. Also, in [4] some comparisons between measurements and the Longley-Rice model have been presented in the case of UHF DVB-T and, in a limited number of points, FM broadcasting. In this study, the coverage prediction maps and field-strength calculations were produced by the Radio Mobile software [10] using the classic Longley – Rice ITM (Irregular Terrain Model) [1]. Consequently, the measurements equipment and their precision will be described, followed by Tables comparing measured to simulated results, their statistical analysis, and, finally, the conclusions about the relative accuracy of the Longley-Rice model in the VHF-FM radio band and in the UHF-TV band.

The Longley–Rice model is a radio propagation model for predicting the attenuation of radio signals for a telecommunication link in the frequency range of 20 MHz to 20 GHz. It is also known as the Irregular Terrain Model (ITM) because it considers the terrain elevation and irregularities, (hills, mountains, etc.). It was created for the needs of frequency planning in television broadcasting in the United States in the 1960s and 1970s and was extensively used for preparing the tables of channel allocations for VHF/UHF broadcasting. The Longley-Rice model has been used for this purpose over the last four decades and still being used almost exclusively by the FCC in the United States. The Longley-Rice model originally used for the planning of analog TV broadcasting and channel allocation in the US in the 1960s is still being used to date [1]. In fact, it is the method of choice in the United States, and almost exclusively used in FCC (Federal Communications Commission) calculations. The FCC's Office of Engineering and Technology (OET) has recently released an updated version of the model to calculate TV station coverage and potential interference to repack the TV stations coverage areas.

The Longley-Rice model has two calculation modes: a mode for predictions over an area and a mode for point-to-point link predictions. Like all other propagation models (e.g. ITU-R P.1546-4 [5-7]) the Longley-Rice model requires the input of certain general parameters needed for the propagation calculations. The model is described in detail in Chapter 3.

The Longley – Rice model is implemented within the Radio Mobile software. Radio Mobile is a freeware able to calculate a wireless coverage map and point-to-point propagation loss, [10].

The program obtains data for the terrain elevation from databases that are freely accessible through the internet. The main database is the STRM (Shuttle Radar Topography Mission) which has two versions, SRTM3 version with data of a 3 arc-seconds resolution, which is 1/1200 of a degree of latitude and longitude, or about 90 meters (295 feet) and SRTM1 version with data of a 1 arc-second resolution, or about 30 meters (98 feet) [11-13].

9.2 MEASUREMENTS AND SIMULATIONS RESULTS

In this work, a comparison is presented between the relative accuracy of the Longley-Rice model in the VHF-FM and UHF-TV frequency bands. Simulations were made with accurate and up to date input data (antenna height, location, gain, transmit power, etc.)

for the FM-TV stations provided by the ERT S.A. public broadcaster in the region of Thessaloniki – Greece. Finally, the calculated – simulated results were confronted to field measurements using a Rohde & Schwarz FSH3 portable spectrum analyser and high precision calibrated biconical and log-periodic antennas, and the errors between predictions and measurements were statistically analysed in the two frequency bands. It has been found in this study that the Longley-Rice model, in general, overestimates field-strength values, but this overestimation is much higher in the VHF – FM radio band (88-108 MHz) than in the UHF-TV band (470-790 MHz).

The basic idea of this study is to compare simulated results with measurements at 11 points around the broadcasting site and at varying distances and angles. The measurements points are chosen in order to be representative of all kinds of propagation conditions from short to long distance and from Line-Of-Sight (LOS) unobstructed to severely obstructed. The signal-strength measurements were performed during the second half of 2012, and before the analog TV switch-off of the Hortiatis mountain broadcasting site, that is serving the region of the city of Thessaloniki in northern Greece. The analog TV stations were used in this study because their signal strength was much higher than the corresponding DTV signals (due to much higher ERP), and so the measurements results are more accurate.

Details for the Greek analog public TV station "ET-3" are given below.

- Transmitter's name: ET-3
- Transmission frequency: CH 27 - 519.25 MHz
- P_o: 10kW or 40dBW or 70dBm
- Net Antenna Gain: 12.6 dBd, or 14.75 dBi
- E.R.P: 181.97 kW or 52.59 dBW or 72.6 dBm
- E.I.R.P: 298.54 kW or 54.74 dBW or 84.75 dBm
- Transmitter Antenna Height Ht: 70 m
- Transmitter Antenna type: 6 bays – 3 directions UHF panel arrangement in horizontal polarization.
- Receiver Antenna Height Hr = 2.5 m
- Altitude: 864.5 m
- Longitude: 23.0997993E and Latitude: 40.597648N

Measurements points and simulations for the Greek analog public TV station "ET-3" are presented in Table 9-1.

Table 9-1. A point-to-point analysis for Greek Public Analog TV "ET-3", CH27 (519.25 MHz). Comparison between measurements and Longley-Rice model.

No.	Measurements Points	LAT.(N)/ LONG.(E)	R&S FSH-3 Measure-ments	Longley-Rice	Error (dB)
1	KOURI-642m (5.2 km/319 degs)	40.632814 23.058840	116.9	108.7	–8.2
2	CARREFOUR-90m (15.2 km/307degs)	40.680266 22.956606	91.8	93.5	+1.7
3	SHOLARI-225m (17.5 km/207 degs)	40.457970 23.004350	102.9	102.7	-0.2
4	TEI-2m (25.6 km/285 degs)	40.655267 22.805703	101.5	98.0	-3.5
5	PROHOMA-64m (43 km/303 degs)	40.809070 22.673190	66.9	52.7	-14.2
6	METHONI-30m (47 km/252 degs)	40.469402 22.574711	97.4	93.6	-3.8
7	KORINOS-1m (52 km/232 degs)	40.307130 22.618620	91.3	90.5	-0.8
8	EVZONI-114m (69 km/321 degs)	41.081410 22.588160	72.4	79.8	+7.4
9	VERIA-305m (75 km/259 degs)	40.467249 22.225950	67.3	55.5	-11.8
10	PLATAMONAS-2m (78 km/213 degs)	40.008522 22.598672	83.3	76.9	-6.4
11	LOUTRAKI-354m (107 km/293 degs)	40.966160 21.923630	84.6	84.4	-0.2
Average error = +3.6 Db					
Standard deviation = +6.2 Db					

Differences between FSH-3 measurements and Longley-Rice simulations are shown in Figure 9-1 below.

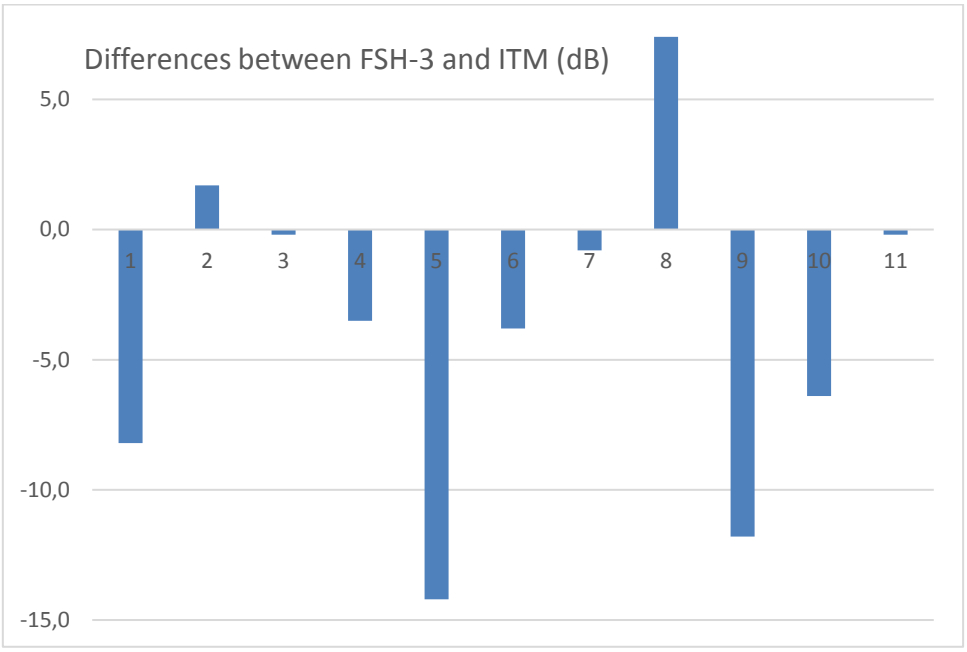

Figure 9-1: Differences between FSH-3 measurements and ITM simulations for the Greek TV station "ET-3".

Details for the Greek FM Station “ERA-102 MHz” station is given below.

- Transmitter’s name: ERA-102 MHz
- Transmission frequency: 102 MHz
- P_o: 20 kW or 43 dBW or 73 dBm
- Net Antenna Gain: 5 dBd, or 7.15 dBi
- E.R.P: 63.09 kW or 47.99 dBW or 78 dBm
- E.I.R.P: 103.51 kW or 50.15 dBW or 80.15 dBm
- Transmitter Antenna Height Ht: 50 m
- Transmitter Antenna type: The FM antenna system is a 6 bay – 3 directions FM panel arrangement in mixed (horizontal-vertical) polarizations.
- Receiver Antenna Height Hr = 2.5 m
- Altitude: 824.5 m
- Longitude: 23.0997993E and Latitude: 40.597648N

Measurements points and simulations for the Greek FM "ERA-102 MHz" radio station is presented in Table 9-2

Table 9-2. A point-to-point analysis for Greek Public FM Radio Station "ERA-102". Comparison between measurements by FSH-3 & the Longley-Rice Model

No.	Measurements Points	LAT.(N)/ LONG.(E)	R&S FSH-3 Measure-ments	Longley-Rice	Error (dB)
1	KOURI-642m (5.2 km/319 degs)	40.632814 23.058840	108.8	110.4	1.6
2	CARREFOUR-90m (15.2 km/307degs)	40.680266 22.956606	76.3	81.1	4.8
3	SHOLARI-225m (17.5 km/207 degs)	40.457970 23.004350	98.8	96.1	-2.7
4	TEI-2m (25.6 km/285 degs)	40.655267 22.805703	87.7	93.6	5.9
5	PROHOMA-64m (43 km/303 degs)	40.809070 22.673190	56.1	63.6	7.5
6	METHONI-30m (47 km/252 degs)	40.469402 22.574711	96.7	91.9	-4.8
7	KORINOS-1m (52 km/232 degs)	40.307130 22.618620	71.9	81.4	9.5
8	EVZONI-114m (69 km/321 degs)	41.081410 22.588160	63.0	72.3	9.3
9	VERIA-305m (75 km/259 degs)	40.467249 22.225950	63.2	67.5	4.3
10	PLATAMONAS-2m(78km/213degs)	40.008522 22.598672	72.1	81.8	9.7
11	LOUTRAKI-354m (107 km/293 degs)	40.966160 21.923630	65.7	75.9	10.2
Average error = -5.0 Db					
Standard deviation = +5.1 Db					

Differences between FSH-3 measurements and Longley-Rice simulations are shown in Figure 9-2 below.

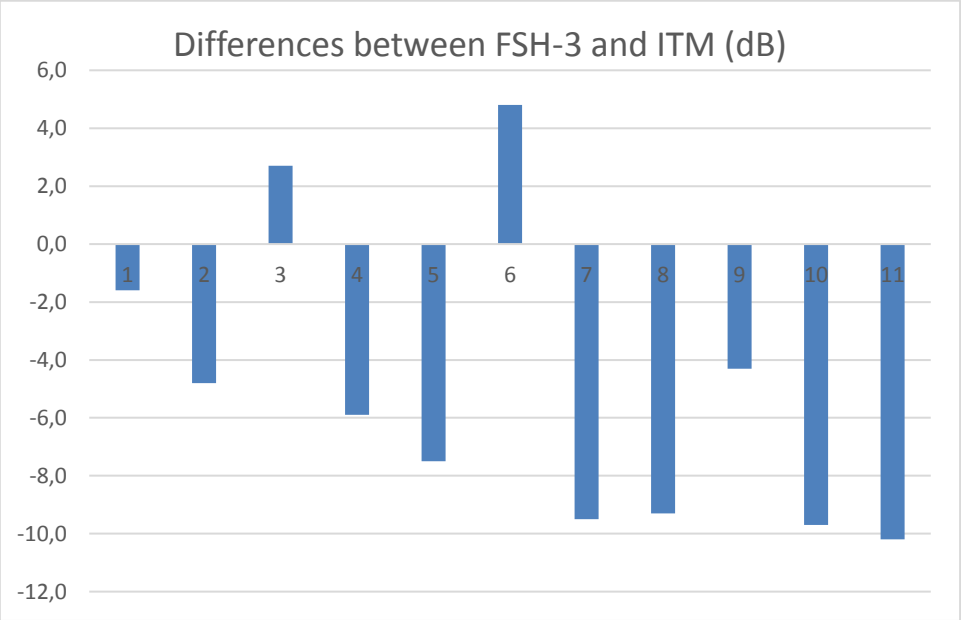

Figure 9-2: Differences between FSH-3 measurements and ITM simulations for the Greek Public Radio Station "ERA-102 MHz".

In Tables 9-1 and 9-2, the simulations and measurements results for eleven different locations in the region around the city of Thessaloniki are presented. In all cases, the broadcasting site was at the Hortiatis mountain antenna park, and more specifically the ERT S.A. public broadcaster's antenna tower (N 40.597648 - E 23.099793), around 13 km southeast of Thessaloniki city center at an altitude of 868 m. Both TV and FM stations transmit from an antenna tower that has a height of 80 m.

The TV antenna UHF panels are located at the top of the tower at an average height of 70 m on the tower while the VHF-FM panels are below them at an average height of around 50 m on the same tower. The TV antenna system is a 6 bay – 3 directions UHF panel arrangement in horizontal polarization with a net gain of 14 dBd (after cable losses have been subtracted). The FM antenna system is a 6 bay – 3 directions FM panel arrangement in mixed (horizontal-vertical) polarizations with a net gain of 5 dBd in each polarization. Both antenna's main lobe is at an azimuth of 285^{o} towards the city center. The TV transmitter has a power of 10 kW and an ERP of 52.5 dBW (182 kW), and the FM transmitter has a power of 20 kW and an ERP of 48 dBW (63 kW).

The simulation results are compared with highly accurate field measurements in Table I for TV and Table II for FM radio. The measurement equipment consists of a Rohde &

Schwarz FSH-3 portable spectrum analyser, factory calibrated with ± 0.7 dB accuracy, two high-precision calibrated biconical antennas by Schwarzbeck, SBA 9113 (500 MHz – 3 GHz) and BBVU 9135 (30 MHz – 1000 MHz), a log-periodic precision calibrated Schwarzbeck antenna USLP 9143 (0.25 – 6 GHz), factory calibrated with ± 1.0 dB accuracy, and low-loss cable Suhner GX-07272-D, 1.8 meters long with N-type connectors.

The sample standard deviation was calculated between measured field-strength values and those predicted by the Longley-Rice model using the well-known formula (5.5) with Bessel's correction:

In all presented simulations, the antenna height was varied from 0.5 m to 2.5 m and the value where the signal is maximum was held. The measurements with the spectrum analyser were made with the MAX-HOLD option on and a corresponding change in the height of the receiving antenna, between 0.5 and 2.5 m from the ground, to have a correct correspondence between measurements and simulations procedures. This option is the simplest and fastest to implement, and it is also like the approach of a user moving his antenna trying to maximize his received FM-TV signal.

For the above results, we considered the operating frequencies, the transmission power P (kW), the Effective Radiated Power (ERP), the height of the antenna mast (m) and the type and gain of the transmitting antenna system (dBd or dBi).

Minimum signal levels according to for satisfactory coverage of analog TV and average signal levels for DVB-T and FM Stereo are shown in Table 9-3.

Table 9-3. Minimum Signal Levels for Satisfactory Reception

Analog UHF-TV	70 dBμV/m
Digital UHF-TV, DVB-T	47 dBμV/m
RADIO-FM STEREO	54 dBμV/m

9.3 COVERAGE MAPS

Coverage maps were created using the “Single Polar Coverage” option of the software with 0.01^{o} step size and with the correct antenna radiation pattern, as interpolated from the antenna manufacturer’s data, and with an azimuth of 285^{o}, thus directed to the city center. The ‘Cartesian Coverage’ option was not used because it was found to result in inaccuracies depending on the software version utilized. Figure 9-3 shows the coverage

map for the “ET-3” public Greek TV station and Figure 9-4 shows the coverage map for the “ERA-102 MHz” public Greek radio station.

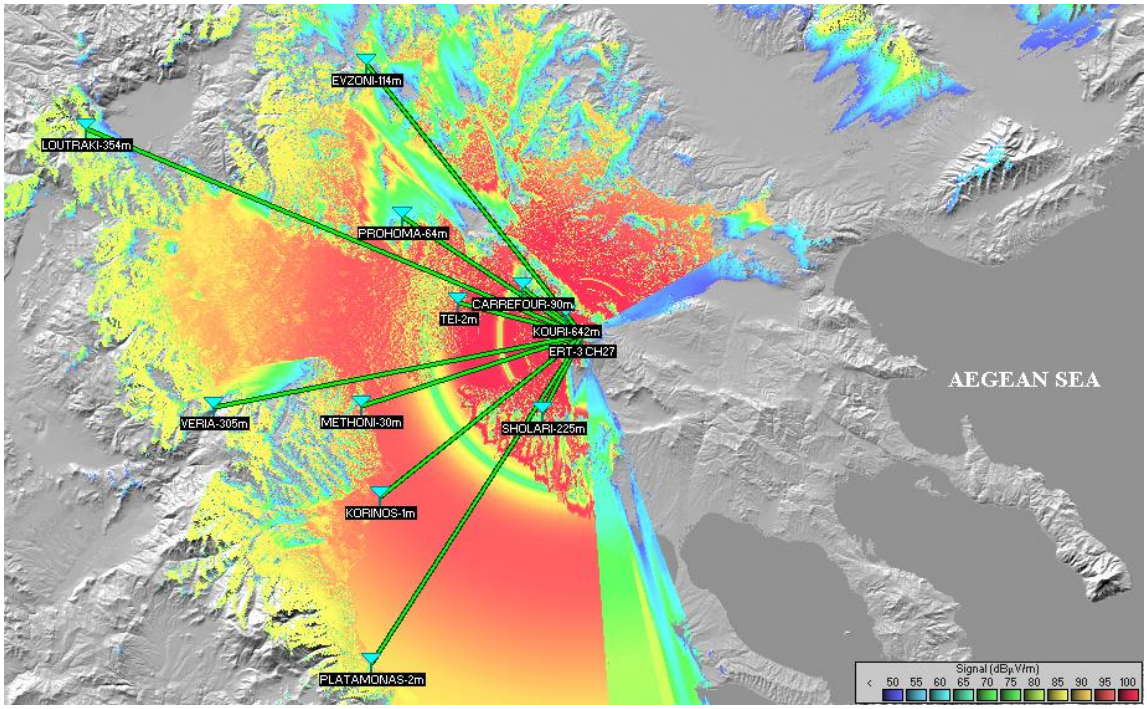

Figure 9-3: ET-3 TV station coverage map (for a receiving antenna height of 10 m) from the Longley-Rice model along with the 11 measurements points.

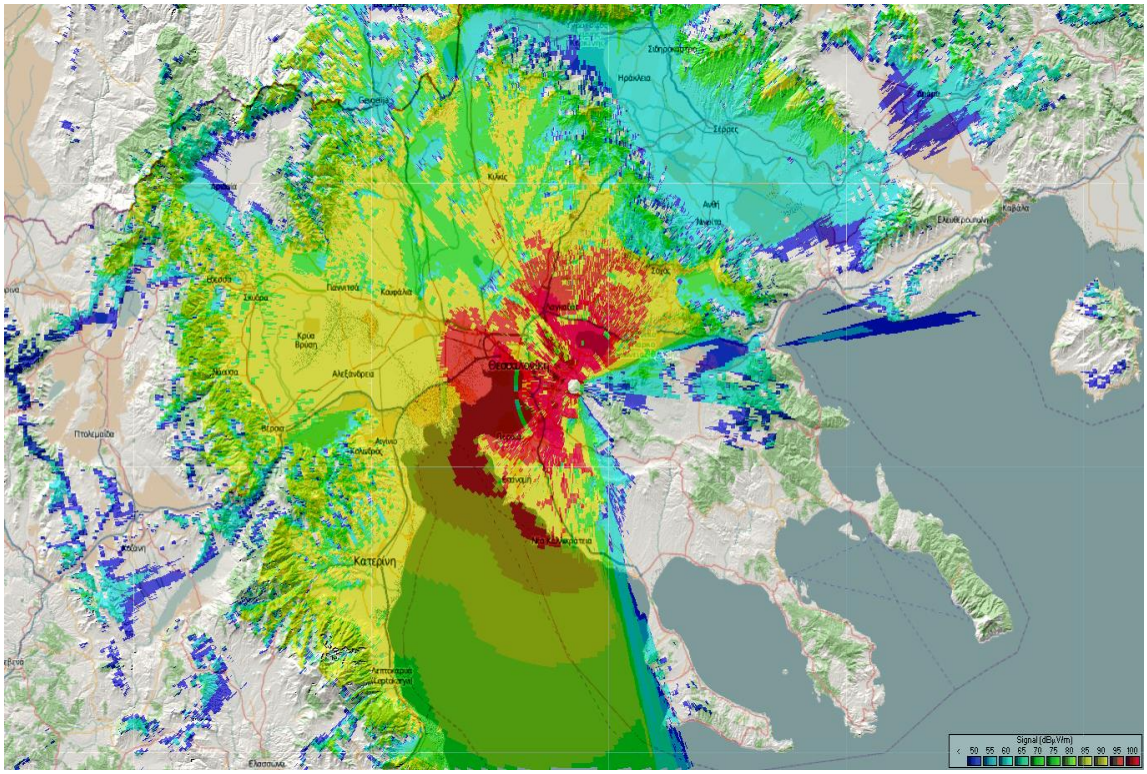

Figure 9-4: Coverage map of ERT FM Station 102 MHz, from Hortiatis mountain) for a receiving antenna height of 10 m.

A much broader coverage area is predicted by the Longley-Rice model for the FM station transmitting from the same tower as the TV station. However, this prediction seems overly optimistic and could be misleading in the case of long-range (DX) interference studies. It should be noted that the colors in the two figures above do not correspond to the same field-strength values. Thus, the figures are just indicative of the general coverage area in the two cases.

9.4 DISCUSSION

Comparing the point measurements made with the spectrum analyser and the simulation results, it is seen that the simulation is very near to the measured results (to within 2 dB) in the very short distance and unobstructed Line-of-Sight (LOS) point 1 for FM and points 2, 3, 7, for TV station that is also unobstructed LOS but at a larger distance. In these cases, the free-space propagation model is applicable. For TV station Point 1, Longley-Rice model greatly underestimates the Field strength though it is in a very short distance and unobstructed. Points 2, 4, 7, 10 are, progressively, longer distance but unobstructed LOS points. At these points, it is seen that the Longley-Rice model clearly overestimates field-strength in the FM case, and this cannot be due to the calculation of diffraction losses. Most probably, this is due to the much stronger reflection of lower frequency FM radio signals leading to destructive vector addition at the measurement points, after a certain distance.

It also is clearly seen by the statistical analysis of the results presented in the Tables above that the Longley-Rice model overestimates, in general, the measured field-strength (positive average values). However, the overestimation is much bigger for the lower frequencies of the VHF-FM band (much bigger average values of error than in the UHF-TV band). The standard deviation values are slightly higher in the UHF-TV band, most probably due to the higher diffraction losses in this case.

9.5 SUMMARY

The measurements and simulation results using the Longley-Rice propagation model indicate that, when there is no significant obstruction of the Fresnel ellipsoid in the propagation path the model, that in this case is reduced to essentially the simple free-space propagation model, accurately predicts the field-strength values, at least at relatively short distances. As the distance increases, the accuracy gradually gets worse, especially for point 11, where an overestimation of the order of 10 dB by the model in

the FM band shows the shortcomings of the free-space model for long distances at lower VHF frequencies. A 2-ray model with a break-point distance depending upon the antenna heights would be preferable in this case. On the other hand, for propagation paths with large obstructions of the Fresnel ellipsoid leading to substantial attenuations of the order of 10 – 20 dB (measurement points 5, and 9 for TV) the Longley-Rice model seems again to underestimate the obstruction loss in the vast majority of cases (and mainly in the FM long distance cases). Consequently, there is a need for correcting the model, especially in the large-distance (DX) mode, and in the coverage limit zone, because as it is, its behaviour is overly optimistic and particularly in the FM band where, even in the absence of obstructions and in longer distances, the calculated values can be 10 dB higher than the measured field-strength values.

9.6 REFERENCES

[1] P. L. Rice, A. G. Longley, K. A. Norton, and A. P. Barsis, "Transmission loss predictions for tropospheric communications circuits," Technical Note 101, U.S. Dept. of Commerce NTIA-ITS, 1967.

[2] C. Phillips, D. Sicker, and D. Grunwald, "A survey of wireless path loss prediction and coverage mapping methods', IEEE Communications, Surveys, Tutorials, vol. 15, 1, pp. 255-270, 2013.

[3] "Comparison of UHF measurements with the propagation model of Recommendation ITU-R P.1546," the Radiocommunications Agency Netherlands, 2010.

[4] S. Kasampalis, P.I. Lazaridis, Z.D. Zaharis, A. Bizopoulos, S. Zettas, and J. Cosmas, "Comparison of Longley-Rice, ITM, and ITWOM propagation models for DTV and FM broadcasting," GWS-2013 conference, Atlantic City, NJ, USA, June 2013.

[5] ITU-R Recommendation P.1546-4 (10/2009), "Method for point-to-area predictions for terrestrial services in the frequency range 30 MHz to 3000 MHz,".

[6] ITU-R Report BT.2137, 'Coverage prediction methods and planning software for digital terrestrial television broadcasting (DTTB) networks', 2008.

[7] Dariusz Więcek and Dariusz Wypior, "New SEAMCAT Propagation Models: Irregular Terrain Model and ITU-R P. 1546-4," National Institute of

Telecommunications, Wrocław, Poland, Journal of Telecommunications and Information Technology, 3/2011, pp. 131-140.

[8] BBC R&D White Paper WHP 048, 'UK planning model for digital terrestrial television coverage', P.G. Brown, K. Tsioumparakis, M. Jordan, and A. Chong, Sept. 2002.

[9] Bachir Belloul and Simon Saunders, "Accurate coverage prediction and optimization for digital broadcasting," EBU technical review, April 2004.

[10] Radio Mobile software. Available on line at URL: http://www.cplus.org/rmw.

[11] NASA, "Shuttle Radar Topography Mission data". Available on line at http://www2.jpl.nasa.gov/srtm/.

[12] The SRTM (3 arc-seconds) version V2 data can be obtained through this URL: https://dds.cr.usgs.gov/srtm/version2_1

[13] The SRTM (1 arc-second) data can be downloaded from USGS EROS Data Center and can be obtained, under some restrictions, through this URL: https://e4ftl01.cr.usgs.gov/SRTM/SRTMGL1.003/2000.02.11/

CHAPTER 10

COVERAGE PREDICTION AND VALIDATION FOR DVB-T SERVICES

10.1 INTRODUCTION

Digital terrestrial broadcasting services are now a reality in Europe, and elsewhere in the world, as improved service quality, lower set-up costs and increased content offered by the broadcasters attract more viewers and listeners to these new platforms [1-2]. So, the accurate coverage prediction and DVB-T transmitter distribution are critical facts for the proper deployment of digital terrestrial television [3-5].

In September 2009 ETSI released the first version of the DVB-T2 standard [6] which is focused primarily but not exclusively to High Definition Television (HDTV) broadcasting over terrestrial networks. Its predecessor DVB-T [7] is still concentrated on Standard Definition Television (SDTV) broadcasting and will be the leading standard for several years to come. Both DVB-T systems, as most of the modern terrestrial transmission systems, use the COFDM modulation to have a robust signal that can deal with very severe channel conditions. Moreover, DVB-T offers a large variety of technical parameters, like 2k or 8k subcarriers, variable channel bandwidth (6,7 or 8MHz), three modulation options (QPSK, 16-QAM, 64QAM), 5 FEC rates and four-guard intervals options. Adjusting the above parameters each operator can find a balance between the minimum required field-strength for adequate reception and content capacity in Mbps. DVB-T2 offers, even more, options and improved performance.

To take full advantage of DVB-T services and characteristics field trials are required, comparing simulation and laboratory results with measurements, [8-10]. The scope of this study is to provide coverage prediction maps for DVB-T services, in the region of Thessaloniki – Greece, and validate the simulation results with field measurements. The coverage prediction maps were produced by the Radio Mobile software [11] using the Longley-Rice model [12]. This study was done in 2011, and thus analog and digital TV channels co-existed. Problems that are arising from the coexistence of analog and digital TV stations will be discussed. Our measurements and simulations included both types of TV stations.

The Longley–Rice model is a radio propagation model for predicting the attenuation of radio signals for a telecommunication link in the frequency range of 20 MHz to 20 GHz. The Longley-Rice model is also known as the Irregular Terrain Model (ITM) because it

takes into account terrain elevation and irregularities, (hills, mountains, etc.). It was created for the needs of frequency planning in television broadcasting in the United States in the 1960s and was extensively used for preparing the tables of channel allocations for VHF/UHF broadcasting. The Longley-Rice model has two calculation modes: a mode for predictions over an area and a mode for point-to-point link predictions. Like all other propagation models (e.g., Bullington [13], Okumura [14], etc.), the Longley-Rice model requires the input of specific general parameters needed for the propagation calculations. These are the operating frequency, the length of the path, the polarization of antennas (the model considers that both antennas, transmit and receive, have the same polarization, vertical or horizontal), the heights of the antennas, the refractivity of the atmosphere, the effective earth curvature, the conductivity of the soil, the relative permittivity or dielectric constant of the ground and the climatic conditions. These parameters are sufficient for the calculation of the free-space loss, the ground reflection coefficients, the Fresnel-Kirchhoff parameters of diffraction and thus the total electric field. The Longley-Rice model is described in detail in Chapter 3.

The Longley – Rice model is implemented within the Radio Mobile software [15]. Radio Mobile is a freeware that uses the following input parameters and can calculate and present a coverage map.

The inputs are:

- Transmitter's location
- Transmitted output power
- Operating Frequency
- Antenna type
- Radiation pattern
- Antenna Gain
- Transmission line losses, including filters and dividers
- Data for the terrain elevation of the specific coverage calculation area.

The program gets data for the elevation of the terrain from databases that are freely accessible on the internet. The main database is the STRM (Shuttle Radar Topography Mission) with a resolution of approximately 90 meters, while DTED (Digital Terrain Elevation Data) is used as a backup database [17-19]. Further details are given in Chapter 3.

10.2 MEASUREMENTS AND SIMULATION RESULTS

The first step in this study was to validate some simulated results with measurements. In tables 10-1, 10-2 and 10-3 below the simulation results for three different locations, in Thessaloniki are presented. The three different locations have the following characteristics.

- "Location 1": Hortiatis crossroads, altitude=514 m, latitude 40.6246N, longitude 23.0708E, d=4.3 km, azimuth = 320^0 and tilt = -6.1^0.
- "Location 2": Profitis Elias, altitude=551 m, latitude 40.6404N, longitude 23.0399E, d=7.4 km, azimuth = 315^0 and tilt = -3.3^0.
- "Location 3": Rooftop-building in the center of Thessaloniki, altitude=18 m, latitude 40.61582N, longitude 22.95577E, d=12.8 km, azimuth = 280^o and tilt = -4.3^o.

Table 10-1. Measured and calculated field-strength values at "Location 1".

No.	TV station	E (dBμV/m) measured	E (dBμV/m) calculated	Differences (dB)
1	SKAI	119.7	115.1	+4.6
2	m.TV	114.0	114.2	-0.2
3	MEGA	113.7	115.2	-1.5
4	ALTER	111.3	114.2	-2.9
5	STAR	110.8	113.0	-2.2
6	ALPHA	110.0	115.0	-5.0
7	ET-3	108.8	116.6	-7.8
8	NET	108.8	115.5	-6.7
9	TV 100	102.4	104.7	-2.3
Average				2.7
Standard Deviation				3.7

In Figures 10-1, 10-2 and 10-3 differences between measurements and simulations are shown in bar-graph diagrams. In all three cases, the transmission center was located at the Hortiatis mountain antenna park around 13 km southeast of Thessaloniki city center (N 40.5962–E 23.1029, altitude 950 m, in the middle of the antenna park).

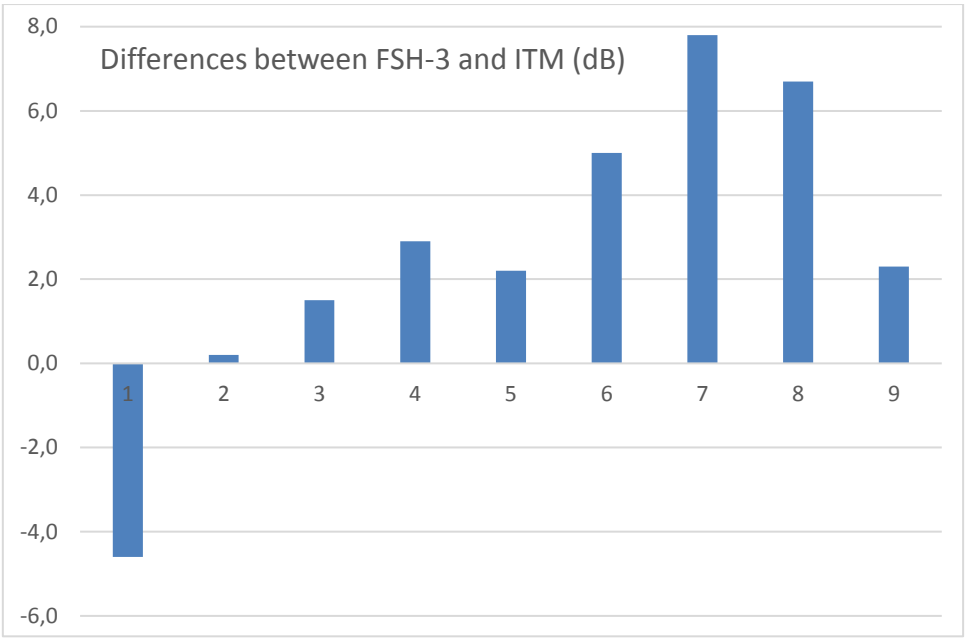

Figure 10-1: Differences (dB) between measurements and simulations (ITM Model) at "Location 1" for Greek TV stations.

Table 10-2. Measured and calculated field-strength values at "Location 2".

No	TV station	E (dBμV/m) measured	E (dBμV/m) Calculated	Differences (dB)
1	NET	114.7	113.4	-1.3
2	ET-3	114.0	113.3	-0.7
3	SKAI	112.2	111.4	-0.8
4	MEGA	111.8	111.5	-0.3
5	m.TV	109.8	110.2	+0.4
6	ALTER	109.4	110.3	+0.9
7	STAR	109.3	109.2	-0.1
8	TV 100	100.0	101.3	+1.3
9	ALPHA	108.6	111.1	+2.5
10	ERT DVB-T	101.9	101.6	-0.3
11	DIGEA DVB-T	104.9	105.6	+0.7
Average				0.2
Standard Deviation				1.1

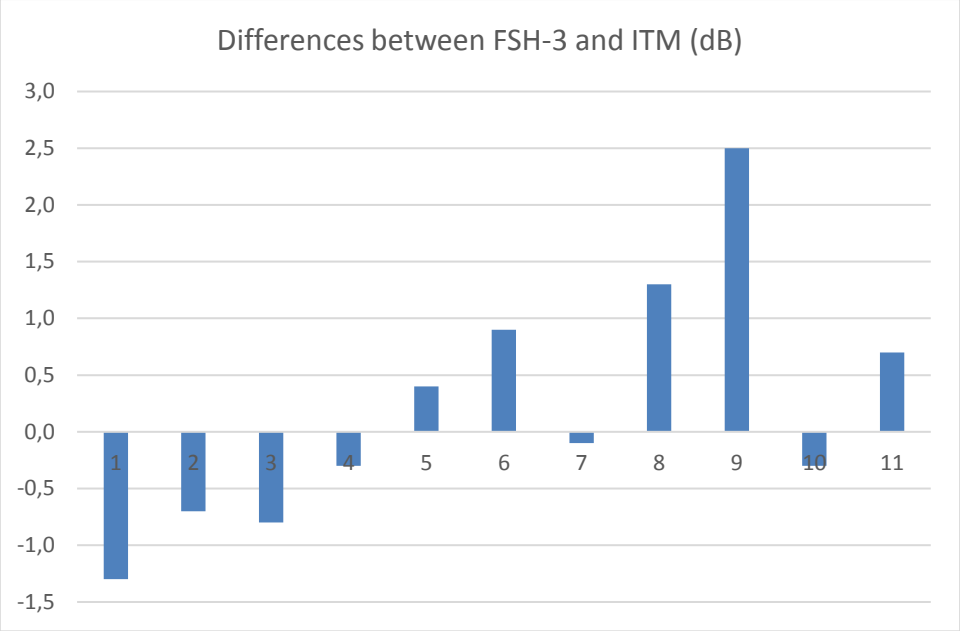

Figure 10-2: Differences (dB) between measurements and simulations (ITM Model) at "Location 2" for Greek TV stations.

These results are compared with highly accurate field measurements that were made with an FSH3 Rohde & Schwarz portable spectrum analyser using a Schwarzbeck SBA 9113 biconical antenna, and low-loss Suhner coaxial cable. More validation measurements have been conducted but due to space limitations, they cannot be presented. In Figure 10-4 an average Fresnel diagram for the TV stations at measurement location 3 is presented. It can be seen from that figure that there is a clear line of sight and no obstacles are located within the first Fresnel zone, therefore there are no additional losses due to diffraction. This figure is presented indicatively, as for most presented cases the measurement conditions are with a clear line of sight and a minimum of diffraction losses. In all presented simulations the antenna height was varied from 0.5m to 2.5 m and the value where the signal is maximum was held. The measurements with the spectrum analyser were made with the MAX-HOLD option on and a corresponding change in the height of the receiving antenna, between 0.5 and 2.5 m from the ground.

Table 10-3. Measured and calculated field-strength values at "Location 3".

No.	TV station	E (dBμV/m) measured	E (dBμV/m) calculated	Differences (dB)
1	SKAI	109.2	106.8	+2.4
2	m.TV	107.9	105.6	+2.3

3	ALPHA	106.5	106.2	+0.3
4	TV-100	98.7	96.8	+1.9
5	STAR	104.6	103.5	+1.1
6	ALTER	104.5	103.4	+1.1
7	ET-3	103.6	109.0	-5.4
8	MEGA	102.1	106.9	-4.8
9	NET	101.8	108.9	-7.1
Average				-0.9
Standard Deviation				3.7

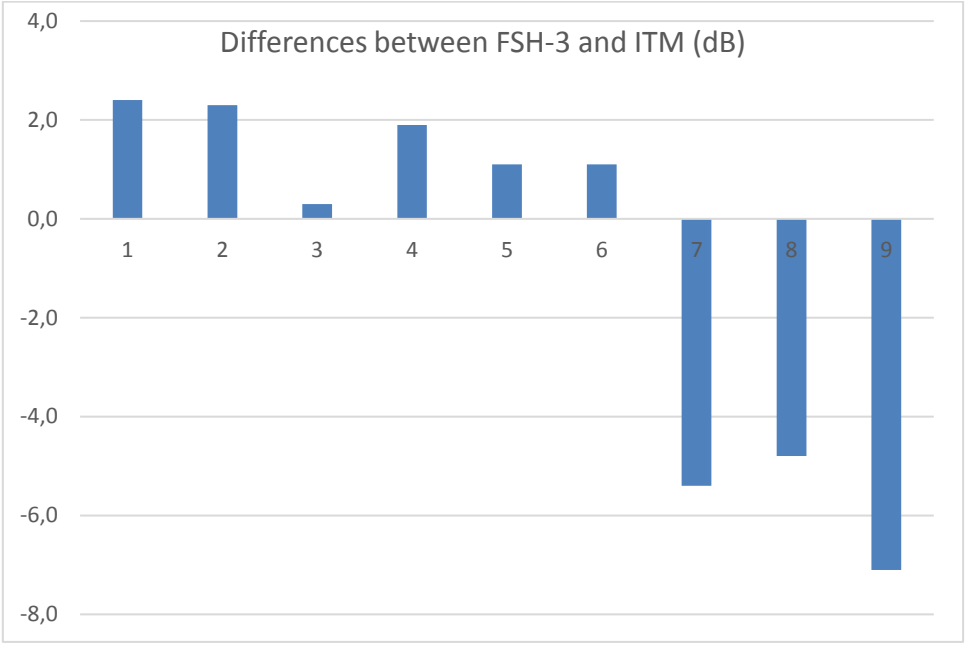

Figure 10-3: Differences (dB) between measurements and simulations (ITM Model) at "Location 3" for Greek TV stations.

For the above results, the operating frequencies, the transmission power P (kW), the Effective Radiated Power (ERP), the height of the antenna mast (m) and the type and gain of the transmitting antenna system (dBd or dBi), were involved. In Figure 10-4, Elevation profile from Hortiatis to Thessaloniki, first (1^{st}) Fresnel zone, 0.6 times of Fresnel zone (0.6F) and Line-Of-Sight (LOS) line, for the TV stations at measurements location 3, is depicted.

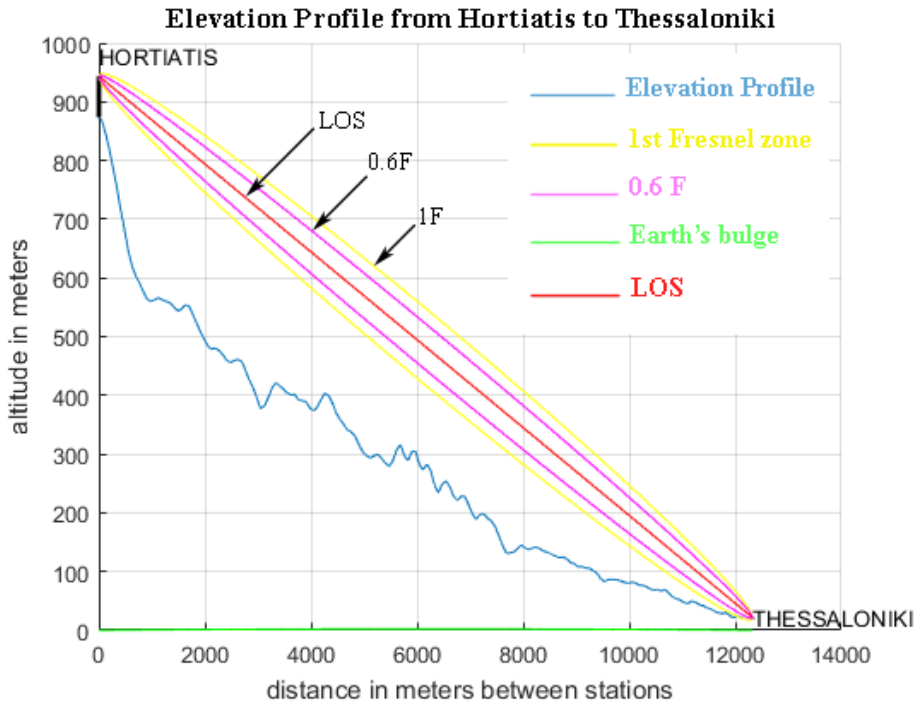

Figure 10-4: Elevation Profile, LOS, and Fresnel zones (1F & 0.6F) for the TV stations at "Location 3".

Comparing the point measurements made with the spectrum analyser and the simulation results, it is seen that the simulation is very near to the measured results in the vast majority of cases (to within 2 dB) except some cases of stations that are known to use smaller down-tilt angles than the ones needed for orientation of the antenna beam to the city center. It is concluded that the exact antenna pattern, including the tilt effects, should be taken into account with more detail in the future versions of the software.

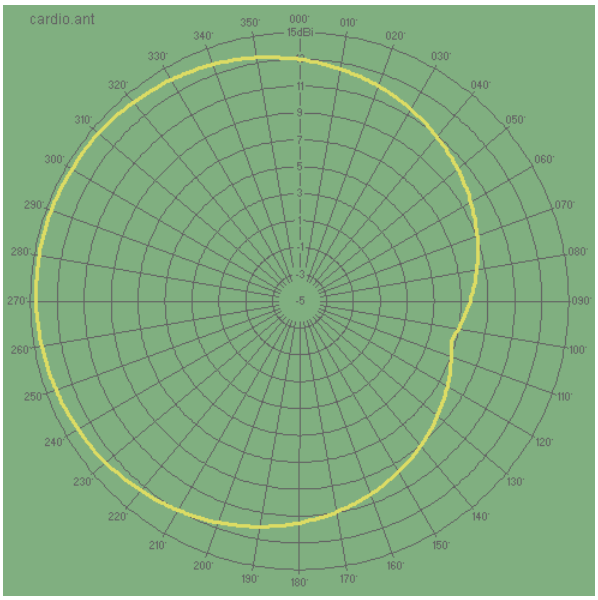

Figure 10-5: The radiation pattern of "cardio" type antenna with a 285 ^{o} peak radiation azimuth.

10.3 COVERAGE MAPS

Coverage maps were created using the "Single Polar Coverage" option of the software with 0.01º step size and considering as a main antenna the transmitting antenna in the area of Hortiatis mountain. For most coverage maps the “cardio” antenna radiation pattern was used with an azimuth of 285º, thus directed to the city center. This radiation pattern is shown in Figure 10-5 and is the one nearest to the actual one used by the station operators that are most commonly using bays of 4 UHF TV panels in 3 directions from this broadcasting site.

In creating the coverage maps slightly lower levels than the indicated values (see Table 9-3) were used to cover also the cases of marginal reception. The coverage map of the public broadcaster ERT on channel 23 UHF is presented in Figure 10-6.

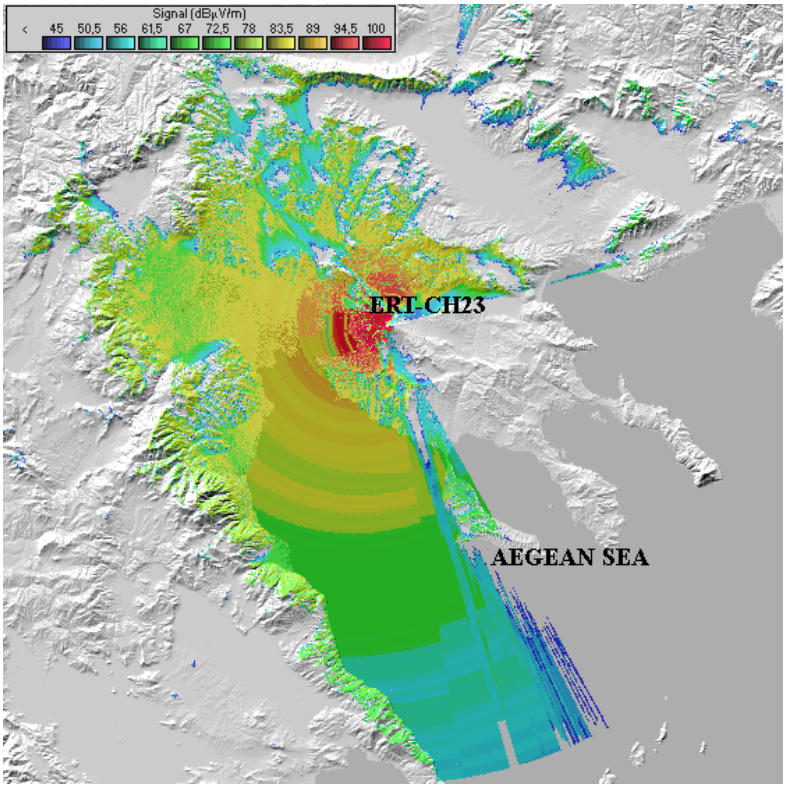

Figure 10-6: Coverage map for ERT DVB-T, UHF-CH23 (N40.5976-E23.0998, 871 m altitude, 70 m antenna tower, cardio antenna, azimuth 285º, P:1.6 kW, ERP:40.5 dBW).

To compare the DVB-T coverage with analog UHF-TV a coverage map for ET3 channel transmitting from the same antenna tower on channel UHF-27 was created. The coverage map for ET3 analog transmission is shown in Figure 10-7. For the DVB-T coverage map, the acceptable lower limit was set to 45 dBµV/m (areas with deep blue color) which is 2 dB less than the suggested limit. For the analog TV coverage map, the limit was set to 60 dBµV/m which is 10dB less than the suggested limit.

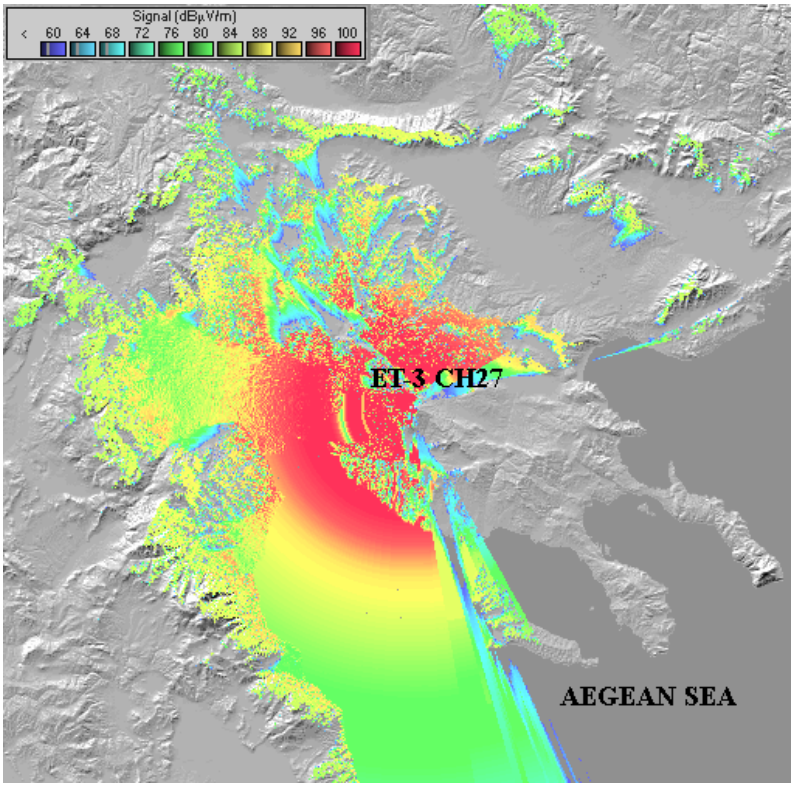

Figure 10-7: Coverage map for ET-3 UHF-27 PAL (N40.5976-E23.0998, altitude 871 m, 70 m antenna tower, cardio antenna, azimuth 285^{o}, P: 10 kW, ERP: 54 dBW).

In digital modulation, the margin under the suggested threshold in which an image is acceptable, is very small. On the other hand, for the analog case, even with the low signal the TV image is snowy but still watchable. For both cases, the maximum signal level was set to 100 dBμV/m (a dark red area close to the transmitting antennas).

Comparing these two coverage maps it is observed that both analog and digital channels cover almost the same area. For the analog channel, the signal is expected to be much stronger closer to the transmitting antenna. Special care needs to be taken in the areas where the coverage is expected to be marginal.

Next map created was for the DIGEA private TV station transmitting consortium on channel UHF-25 and it is depicted in Figure 10-8. Again, it is observed that the coverage is very good in the area of Thessaloniki. However, a very high-power harmful analog TV interference comes from neighboring Bulgaria to create serious problems to the DIGEA transmissions in the region of Veria southwest of Thessaloniki, cf. Figure 10-9. This is a classical case of an analog TV transmission interfering with a DVB-T transmission. In this case, the advantage goes to the analog transmission that can block completely the digital one, although it is coming from 165 km far from the reception area.

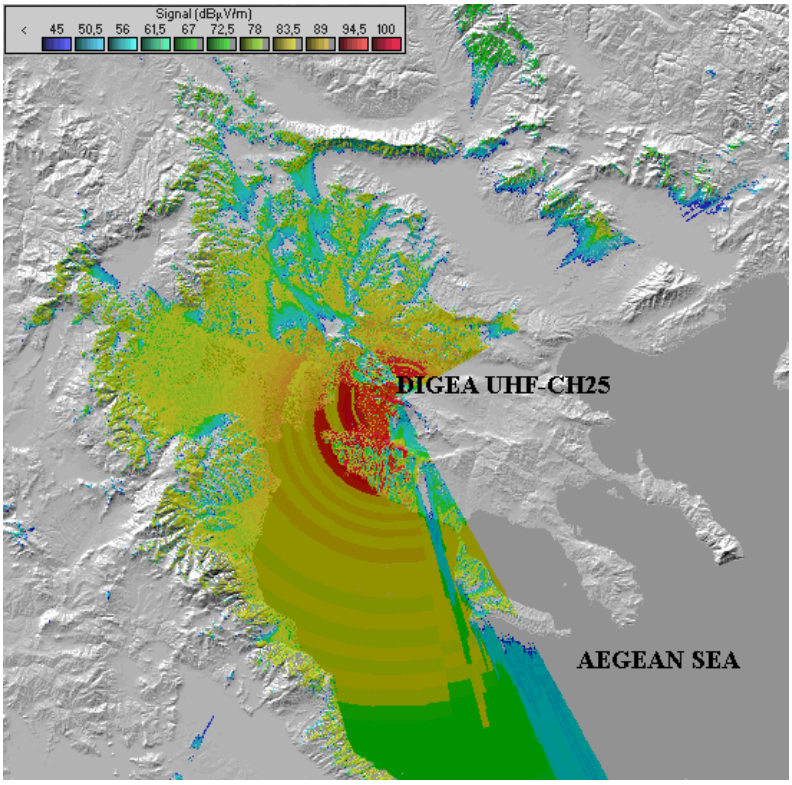

Figure 10-8: Coverage map for DIGEA DVB-T, UHF-CH25 (N 40.5972 -E 23.1008, 962 m altitude, 20 m antenna mast, cardio antenna, azimuth 285º, P: 2.5 kW, ERP: 45 dBW).

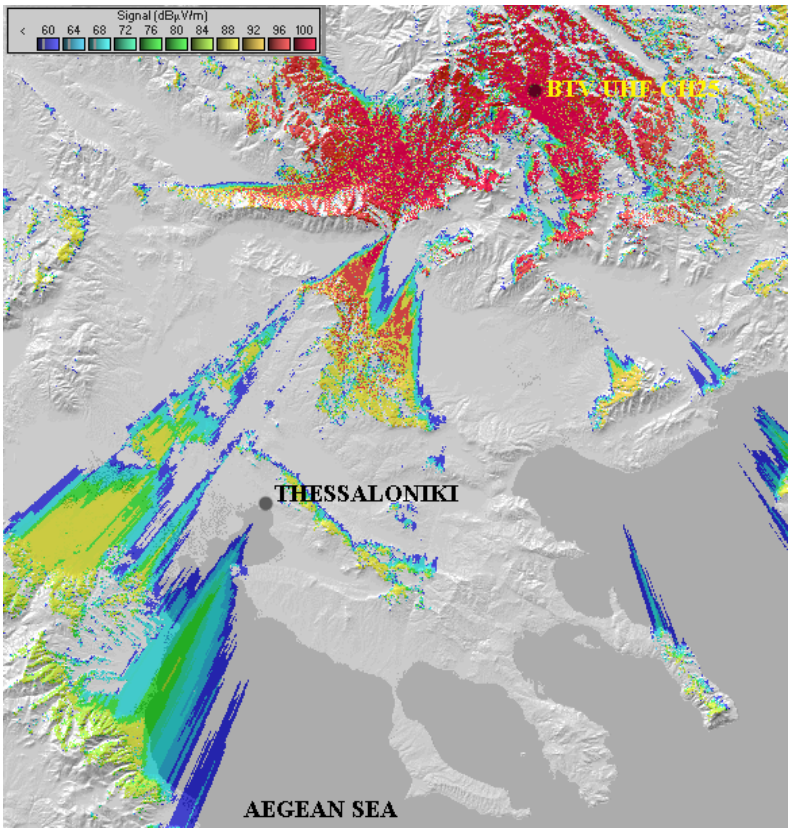

Figure 10-9: Coverage map for BTV UHF-CH25, PAL, mount Oreljak, Goce Delchev, (N 41.5702 - E 23.6125, altitude 2073 m, 90 m antenna tower, omni antenna, P: 20 kW, ERP: 55dBW).

The last coverage map was created for our experimentally transmitting station located on the campus of ATEI Thessaloniki in the region of Sindos. This coverage map is shown in Figure 10-10.

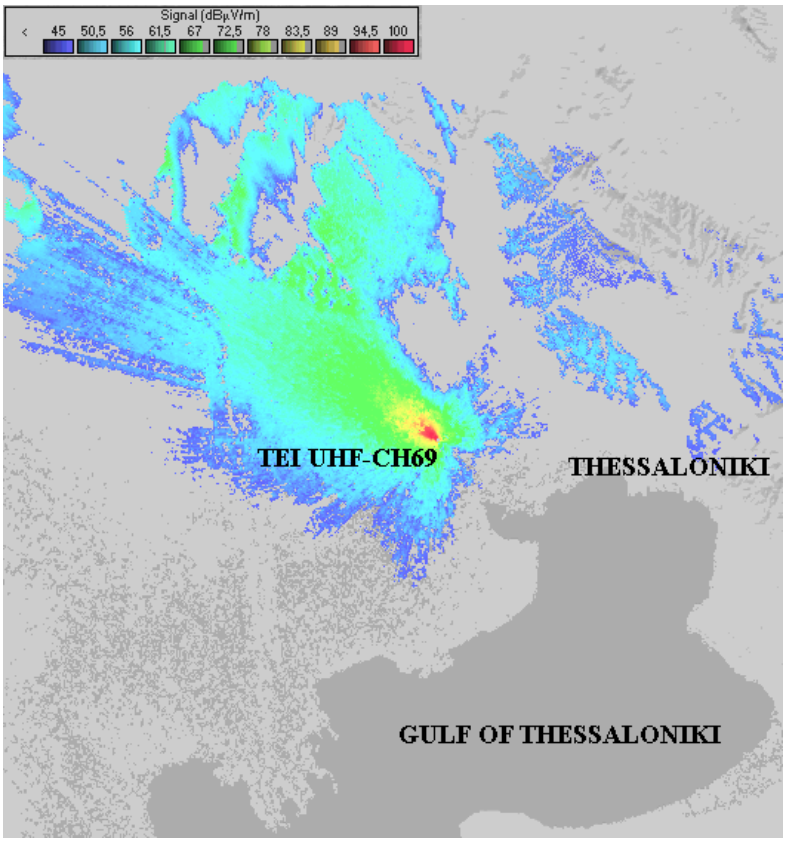

Figure 10-10: Coverage map for TEI DVB-T, 1 UHF panel, UHF-69 (N 40.6556–E 22.8067, altitude 2 m), 18 m antenna tower, "corner" antenna pattern, azimuth 310^{o}, HPBW: 60^{o}, P: 2W, ERP: 13 dBW).

This is a low power transmitting station that is used by the students and researchers in the university in order to make experiments and measurements and thus acquire technical expertise on the DVB-T equipment and propagation characteristics. The original target of the project was to cover the area of the university campus and the city of Sindos. As is seen from the coverage map in Figure 10-10 this target is easily achieved.

10.4 SUMMARY

Comparing the simulation and measurements results it is concluded that the accuracy of the Radio Mobile software using the Longley-Rice propagation model is satisfactory and it can be used as a very helpful tool to predict the coverage of DVB-T stations. According to the produced coverage maps, it is seen that the digital TV channels can

cover almost the same area as the analog ones but with much less transmitting power due to the lower reception signal levels. Our future research will focus on more measurements without a clear line of sight, including obstructions, and to greater distances from the transmitting antennas and their comparison to simulation results calculated with various propagation models.

10.5 REFERENCES

[1] Tomáš Kratochvíl, From Analog to Digital Television — the common way how to digitize European broadcasting, *History of Telecommunications Conference*, 2008, pp. 164 – 169.

[2] U. Ladebusch, C.A. Liss, Terrestrial DVB (DVB-T): A Broadcast Technology for Stationary Portable and Mobile Use, *Proc. of the IEEE*, Vol. 94. No.1, January 2006.

[3] Implementation guidelines for a second-generation digital terrestrial television broadcasting system (DVB-T2), *BlueBook A133, Digital Video Broadcasting (DVB) Std*. DVB Document A133, Dec. 2009.

[4] Digital Video Broadcasting (DVB). DVB-NGH Commercial Requirements. *Technical Report CM-NGH015*, May 2009.

[5] A. Ligeti, J. Zander, Minimal cost coverage planning for single frequency networks, *IEEE Trans. Broadcasting*, Vol. 45, No. 1, 1999, pp. 78-87.

[6] Digital Video Broadcasting (DVB); Frame structure channel coding and modulation for a second-generation digital terrestrial television broadcasting system (DVB-T2), *ETSI Std. EN* 302 755 V1.1.1, Sep. 2009.

[7] Digital Video Broadcasting (DVB); Frame structure channel coding and modulation for digital terrestrial television broadcasting system (DVB-T), *ETSI Std. EN* 300 744 V1.6.1, Jan. 2009.

[8] Poikonen, J., Gomez-Barquero, D., Validation of a DVB-H dynamic system simulator using field measurements, *IEEE International Symposium on Broadband Multimedia Systems and Broadcasting*, 2008, pp. 1-6.

[9] Raffaele Di Bari, Maurice Bard, Amaia Arrinda, Paolo Ditto, Giuseppe Araniti, John Cosmas, Kok Keong Loo and Rajagopal Nilavalan, Measurement Campaign on Transmit Delay Diversity for Mobile DVB-T/H Systems, IEEE *Transactions on Broadcasting*, VOL. 56, No. 3, September 2010.

[10] Inaki Eizmendi, Gorka Prieto, Gorka Berjon-Eriz, Manuel Velez, Susana Correia, Amaia Arrinda, Pablo Angueira, HDTV field trials using DVB-T and DVB-T2 broadcasting systems, *IEEE International Symposium on Broadband Multimedia Systems and Broadcasting*, Shanghai, China, March 2010.

[11] Radio Mobile software, available at URL, http://www.cplus.org/ rmw/rm.html.

[12] A. G. Longley and P. L. Rice, Prediction of Tropospheric radio transmission loss over irregular terrain., a computer method-1968, ESSA Tech. Rep. ERL 79-ITS 67, U.S. Government Printing Office, Washington, DC, July 1968.

[13] Kenneth Bullington, Radio Propagation for Vehicular Communications, *IEEE Transactions on Vehicular Technology*, Vol. VT-26, No.4, November 1977.

[14] Y. Okumura, E. Ohmori, T. Kawano, and K. Fukuda, Field Strength and its Variability in VHF and UHF Land-Mobile Service, Rev. Elec. Comm. Lab., Vol. 16, No. 9-10, pp. 825-873, 1968.

[15] Radio Mobile software available on line at URL, http://www.cplus.org/rmw

[16] NASA, "Shuttle Radar Topography Mission data". Available on line at URL, http://www2.jpl.nasa.gov/srtm/.

[17] The SRTM (3 arc-seconds) version V2 data can be obtained through this URL, https://dds.cr.usgs.gov/srtm/version2_1.

[18] The SRTM (1 arc-second) data can be downloaded from USGS EROS Data Center and can be obtained, under some restrictions, through this URL, https://e4ftl01.cr.usgs.gov/SRTM/SRTMGL1.003/2000.02.11/

11 CONCLUSIONS - FUTURE WORK

11.1 CONCLUSIONS

Classical propagation prediction models have been compared in this research for the VHF and UHF TV broadcasting frequencies, and FM frequencies. The research was mostly focused on propagation in mountainous terrain, and in long propagation paths. Studying and comparing the measurements and simulations results emphasis must be given to the following:

1. The Longley-Rice propagation model accurately predicts the field-strength values at least at relatively short distances when there is significant obstruction of the Fresnel ellipsoid in the propagation path. As the distance increases, the accuracy gradually gets worse, giving in some cases overestimation of the order of 10 dB especially in the FM band and this shows the shortcomings of the free-space model for long distances at lower VHF frequencies. The Longley-Rice model clearly overestimates field-strength in the FM case, and this cannot be due to the calculation of diffraction losses. Most probably, this is due to the much stronger reflection of lower frequency FM radio signals leading to destructive vector addition at the measurement points, after a certain distance. A 2-ray model with a break-point distance depending upon the antenna heights would be preferable in this case. On the other hand, for propagation paths with large obstructions of the Fresnel ellipsoid leading to substantial attenuations of the order of 10 – 20 dB the Longley-Rice model seems again to underestimate the obstruction loss in the vast majority of cases (and mainly in the FM long distance cases). Consequently, there is a need for correcting the model, especially in the large-distance (DX) mode, and in the coverage limit zone, because as it is, its behaviour is overly optimistic and particularly in the FM band where, even in the absence of obstructions and in longer distances, the calculated values can be 10 dB higher than the measured field-strength values. It seems clear from our research that the ITM model applied by Radio Mobile program generally gives, in most cases, much better results than the ITM model applied by the SPLAT! software which means that Radio Mobile makes a more accurate application of the ITM model (or the author of the Radio Mobile made some successful modifications or additions to the ITM program) than SPLAT! Although the Longley-Rice model presents some inaccuracies in estimating the field strength, it remains a valuable tool for path loss calculations in electromagnetic propagation. Even though it was presented for the first time in the 1960's and originally used for the planning of analog TV broadcasting and

channel allocation in the US, it is still being used to date. In fact, it is the method of choice in the United States, and almost exclusively used by the FCC (Federal Communications Commission). The FCC's Office of Engineering and Technology (OET) has recently released an updated version of the model to calculate TV station coverage and potential interference to repack the TV stations coverage areas.

2. The ITWOM (SPLAT! v1.4.0) propagation model was recently proposed, claiming an improved accuracy over the ITM. However, early simulations results and measurements in point-to-point path analysis with ITWOM do not verify these claims. The ITWOM has a somewhat better accuracy for distances less than 20km, but very big differences for distances larger than 40km.

3. The use of propagation curves in Recommendation ITU-R P.1546 gives significant errors, mainly at distances longer than 50 km. The predictions produced by Recommendation ITU-R, P.1546 propagation model strongly show that this model requires corrections for mixed paths, but also for paths over flat terrain. I think that the model has more than one flaw, making error tracking difficult and so, it is difficult to give a complete solution but only some indications for possible improvements could be given. Maybe a correction on the implementation of the TCA (Terrain Clearance Angle) at the receive side gives better prediction results. I believe that the 100% cold sea curves should be corrected, and similar conclusions arise from simulations and measurements.

4. The Hata-Davidson model with HAAT, despite being a very simple empirical model, gives in some cases reasonable results and certainly better than the ITU-R P.1546 propagation model. This model underestimates path loss in distances greater than 50km and should be used very carefully in cases with a great number of obstacles.

5. The Single Knife-Edge propagation model, although it is a very simple deterministic model, in many cases, where the main obstacle is the critical one producing the main part of attenuation, delivers reasonable results very close to the measured ones.

6. Deygout, Epstein-Peterson and Giovaneli approaches are approximating multiple knife-edge diffractions using geometrical constructions. All the three of them give satisfactory results, and they are classical well-established models. Their relative accuracy was found to be comparable in the case studies of this paper. They proved to be more accurate than the Longley-Rice model over long paths including diffracting obstacles in the VHF-TV Band. The use of SRTM1 maps in conjunction with these models though it produced more detailed elevation profiles comparing with that of the SRTM3 maps it did not give significantly different simulation results, so the smaller

SRTM3 maps were used in this survey. Deygout's model for three and four obstacles, in our research, proved to give the same results as Deygout's double knife-edge model. Deygout's model with a correction factor gives rather worse simulation results and it is not suggested for use. Epstein-Peterson's model proved to be as accurate as Deygout's model and in some cases better than it. Giovaneli's model, an improvement of Deygout's model, proved to have some issues in some cases and I would not suggest using it in usual studies. A further improvement in diffraction loss calculation accuracy is expected from Vogler's rigorous method which has not been used in our research.

Comparing the simulation and measurements results in our research, it is concluded that the accuracy of the Radio Mobile software using the Longley-Rice propagation model is satisfactory and it can be used as a very helpful tool to predict the coverage of DVB-T stations. Also, the MATLAB programs for Deygout, Epstein-Peterson and Giovaneli models give accurate simulation results and can be used as a very useful tool to predict path loss and field strength in point-to-point prediction mode.

According to the produced coverage maps, it is seen that the digital TV channels can cover almost the same area as the analog ones but with much less transmitting power due to the lower reception signal levels. The measured UHF-TV band spectra in the cities of Thessaloniki and Skopje pre- and post-ASO clearly demonstrate the economies made on spectrum occupation by the passage to digital television. Additionally, for the same coverage area, lower field-strength values are required, thus leading to lower transmitted powers. Furthermore, a study for the city of Skopje reveals that TV white space availability is much higher in the post-ASO era leading to an increased potential throughput of the secondary system in Mbits/s.

11.2 FUTURE WORK

Our future research will focus on more measurements without a clear line of sight, including obstructions, and to greater distances from the transmitting antennas and their comparison to simulation results calculated with various propagation models. Some modifications in the Deygout and Epstein-Peterson models need to be further studied. A modification of the Giovaneli's model will also be done to produce more accurate simulation results in cases where the secondary obstacle lies on the right side of the primary one.

Other areas of further research are:

- Propose an improved Longley-Rice model with more accurate diffraction calculation. During this survey, it has been noticed, that the Longley-Rice model in some cases gives large negative errors using, in my opinion, Double Knife-Edge model diffraction plus the spherical Earth diffraction instead of using the Single Knife-Edge diffraction. That is why an improved diffraction calculation must be proposed.
- Propose an extended Hata model to replace Hata-Davidson model.
- Antenna pattern of the transmitter antenna.
- The shape of the obstacles (rounded, cylindrical, etc.).
- Time percentage (i.e. 10% - 50% - 90%).
- Location variability (based on terrain roughness, frequency and nearby trees and buildings).
- Attenuation factor for vegetation, soil moisture, trees heights (a value of additional height will be added for vegetation and trees). Perhaps for each vegetation category an approximate canopy height could be given to calculate path loss. Also, path loss which is caused by old and young forests should be considered.
- Reflection coefficient for bare ground, forest, fresh water, sea water, marsh, urban, and suburban.
- Path loss due to tropospheric scatter.
- Implementation of this work to Automobile Radar. This survey considers the obstacles to calculate signal path loss, so it can be used in Automobile radars in conjunction with sophisticated software (like Artificial Intelligence) to avoid stable or moving obstacles and to prevent accidents.

12 APPENDIX

12.1 MATLAB CODE FOR DEYGOUT'S MODEL

The code for Deygout's model is given.

- First, the required data for the program´s operation are imported. These are the following :
  a) Frequency f of the transmitted signal in MHz
  b) Transmitted Power (EIRP) in dBm.
  c) Transmitter Antenna height, Ht in meters
  d) Receiver antenna height, Hr in meters
  e) Transmitter Name
  f) Transmitter Longitude
  g) Transmitter Latitude
  h) Receiver name
  i) Transmitter Longitude
  j) Transmitter Latitude

  Lines 41 to 58 doing this in MATLAB code as you can see below.

```
41 %====================================================================
42 %                          INPUT PARAMETERS
43 %====================================================================
44 disp('INPUT PARAMETERS');
45 disp('k-factor =1.33 (effect of the atmosphere) for all calculations.');
46 % the above disp command works only for underlined blue text
47 f=input('Operating Frequency f in MHz, f= ');
48 Pt=input('EIRP in dBm, Pt= ');
49 Ht=input('Antenna Transmitter height  Ht in m, Ht= ');
50 Hr=input('Antenna Receiver height  Hr in m, Hr= ');
51 Tname = input('Transmitter name? :','s');%'s' indicates that Tname is a string.
52 % Transmitter coordinates
53 x(1)=input('Transmitter LONG, LONG= ');
54 y(1)=input('Transmitter LAT, LAT= ');
55 Rname = input('Receiver name? :','s');%'s' indicates that Rname is a string.
56 % Receiver coordinates
57 x(2)=input('Receiver LONG, LONG= ');
58 y(2)=input('Receiver LAT, LAT= ');
```

- Elevation profiles are created with the use of the excellent MATLAB program "readhgt.m", that was created by François Beauducel [18] on 25 August 2012 and

updated on 27 December 2016. The function “readhgt.m” imports “.hgt files” (binary data) from NASA SRTM global digital elevation model of Earth land, and returns coordinates vectors latitude and longitude, and a matrix of elevation values. The function includes also an automatic download of data from the USGS SRTM web server. So, importing latitude and longitude of a place, we can get the proper data from the web server and plot an elevation profile and a geophysical map of this place anywhere in the world. To get the right colors on the plotted maps, use of the “seacolor.m”, “landcolor.m” and “dem.m” functions, also created by the same author, in conjunction with the “readhgt.m” must be done.

Lines 59 to 152 doing this in MATLAB, involving equirectangular approximation and Earth’s bulge. These lines are listed below.

```
59 %==================================================================
60 %    READ OF readhgt AND CREATING GEOPHYSICAL MAP AND ELEVATION PROFILE
61 %==================================================================
62 % READHGT Import/download NASA SRTM data files (.HGT).
63 % READHGT(LAT,LON) downloads the tiles and plots SRTM data corresponding
64 % to LAT and LON (in decimal degrees) coordinates (lower-left corner)
65 % from the USGS data server. 'https://dds.cr.usgs.gov/srtm/version2_1';
66 % (needs an Internet connection and a companion file "readhgt_srtm_index.txt")
67 % in which it finds the subpath for SRTM3 aND SRTM1 (USA)files.
68 % For better plot results, it is recommended to install DEM personal
69 % function available at author's  MATLAB page(Francois Beauducel).
70 % DEM(X,Y,Z) plots the Digital Elevation Model defined by X and Y
71 % coordinate vectors and elevation matrix Z, as a lighted image using
72 % specific "landcolor" and "seacolor" colormaps. DEM uses IMAGESC
73 % function which is much faster than SURFL when dealing with large
74 % high-resolution DEM. It produces also high-quality and moderate-size
75 % Postscript image adapted for publication.DEM uses  landcolor.m
76 % seacolor.m
77 X=readhgt(39:41,21:24,'merge','crop','plot');
78 xi=linspace(x(1),x(2),4000);
79 yi=linspace(y(1),y(2),4000);
80 zi=interp2(X.lon,X.lat,double(X.z),xi,yi,'linear');
81 % Plot the red line in geophysical map
82 hold on,plot(xi,yi,'r'),hold off
83 % Display the names of transmitter and receiver on map in red line
84 txt1 = Tname;
85 text(x(1),y(1),txt1)
```

```
txt2 = Rname;
text(x(2),y(2),txt2)
%=====================================================================
%         EQUIRECTANGULAR APPROXIMATION (Haversine Formula)
%          (RHUMB LINE OR LOXODROME) OF THE GREAT CIRCLE
%=====================================================================
% Distance along this path, see equirectangular approximation.doc.
% I changed 6370 km erath radius in 6370000 in meters so the result is in
% meters,because MATLAB's default is in meters.
di=sqrt(((xi-x(1)).*cosd((y(1)+yi)/2)).^2+(yi-y(1)).^2)*6370000*pi/180;
% Beauducel gives the approximate formula below which gives similar results
% di=sqrt(((xi-x(1)).*cosd(yi)).^2+(yi-y(1)).^2)*6370000*pi/180;
% if you give here plot(di,zi)plots elevation profile without earth's bulge
dmin=di(1);
 dmax=di(4000);
 zmin=zi(1)+Ht;% Ht is trasmitter antenna height
 Htransmitter=['Total Transmitter Antenna Height ',num2str(zmin),'m'];
 disp(Htransmitter)
 zmax=zi(4000)+Hr;% Hr is receiver antenna height.
 Hreceiver=['Total Receiver Antenna Height ',num2str(zmax),'m'];
 disp(Hreceiver)
 %=====================================================================
 %                                CORRECTION
 %     FOR EARTH'S CURVATURE (earth bulge)AND ATMOSPHERIC DIFFRACTION
 %=====================================================================
 % In fact the effective curvature of the Earth can be calculated by adding
 % a parabolic approximation of the effective Earth curvature to the path
 % profile terrain data before finding horizons. One such parabolic function
 % that can be used is r=dt*dr/2r=dt*(d-dt)/2r=dr*(d-dr)/2r. Where r=k*ro
 % and ro=earth radius=6370km=6370000m, and usually k=4/3=1.333.
 % In MATLAB all parameters must be in meters(m),(default in MATLAB):
 % so r=(di-dmin)*(dmax-di)/2*1.333*6.370.000=0.000000059*(di-dmin)*(dmax-di)
 % See for further details, folder "Earth bulge" in PhD folder.
 % Here : (di-dmin) is the distance between correction point and transmitter in meters
 % and (dmax-di) is the distance between correction point and receiver in
 % meters. The elevation changes if you change the constant k.
 % So finally my correction formula is : 0.000000059*(di-dmin)*(dmax-di)
 r=0.000000059*(di-dmin).*(dmax-di);
 zk=zi+r;% adding Earth's bulge
 %=============================================================
```

```
126 %                          PLOTS THE ELEVATION PROFILE
127 %============================================================
128 figure
129 hold on,plot(di,zk)
130 % Display the names of transmitter and receiver on elevation profile
131 % we multilpy Ht and Hr by 2, 2*Ht and 2*Hr to move text up, othewise it
132 % conflicts with the lines.
133 txt1 = Tname;
134 text(di(1),zi(1)+2*Ht,txt1)
135 txt2 = Rname;
136 text(di(4000),zi(4000)+2*Hr,txt2)
137 %-------------------------------------------------------------------------------------------------
138 title(['Elevation Profile from ' sprintf('%s',char(Tname)) ' to ' sprintf('%s',char(Rname))]);
139 xlabel('distance in meters between stations');
140 ylabel('altitude in meters');
141 % plot the Earth curvature curve
142 hold on,plot(di,r,'g')
143 % plot the LOS red line in elevation profile
144 hold on,plot([dmin dmax],[zmin zmax],'r')
145 % plot the antennas in figure
146 % Transmitter Antenna Height, the formula is: line([X X], [LowY HighY])
147 % We plot again Ht to show Transmitter Antenna, although it was plotted in zmin=zi(1)+Ht
148 line([di(1) di(1)],[zi(1) zi(1)+Ht],'color','k','LineWidth',2)
149 % Receiver Antenna Height, the formula is: line([X X], [LowY HighY])
150 % We plot again Hr to show Receiverer Antenna, thow it was plotted in
151 % zmax=zi(4000)+Hr
152 line([di(4000) di(4000)],[zi(4000) zi(4000)+Hr],'color','k','LineWidth',2)
```

- In lines 153 to 200, the program plots the 1st Fresnel zone and the 0.6 times the 1st Fresnel zone and intersects the elevation profile with the 0.6 times the 1st Fresnel zone.

```
153 %=====================================================================
154 %        PLOT THE ELLIPSES - 1st FRESNEL ZONE (1F)- 0.6 OF FRESNEL ZONE (0.6)
155 %=====================================================================
156 x1=dmin;
157 y1=zmin;
158 x2=dmax;
159 y2=zmax;
160 % Plot of the 1st Fresnel zone
161 fr=f*1000000;% f in Hz
```

```
c=300000000;% c light speed 300000000m/s
l=c/fr; % l=wave length in meters
a = 1/2*sqrt((x2-x1)^2+(y2-y1)^2);
r = sqrt(l*a/2);% b=r
t = linspace(0,2*pi);
X = a*cos(t);
Y = r*sin(t);
w = atan2(y2-y1,x2-x1);
x = (x1+x2)/2 + X*cos(w) - Y*sin(w);
y = (y1+y2)/2 + X*sin(w) + Y*cos(w);
hold on, plot(x,y,'y')
grid on
% Plot the 0.6 times Fresnel zone, the upper half which does not intersects
% with the obstacle
r = 0.6*sqrt(l*a/2);% b=r
t = linspace(0,2*(pi/2));
X = a*cos(t);
Y = r*sin(t);
w = atan2(y2-y1,x2-x1);
x = (x1+x2)/2 + X*cos(w) - Y*sin(w);
y = (y1+y2)/2 + X*sin(w) + Y*cos(w);
hold on, plot(x,y,'m')
% Plot the 0.6 times Fresnel zone, the bottom half which intersects
% with the obstacles
r = 0.6*sqrt(l*a/2);% b=r
t = linspace(0,2*(-pi/2));
X = a*cos(t);
Y = r*sin(t);
w = atan2(y2-y1,x2-x1);
x = (x1+x2)/2 + X*cos(w) - Y*sin(w);
y = (y1+y2)/2 + X*sin(w) + Y*cos(w);
hold on, plot(x,y,'m')
%=====================================================================
%         INTERSECT THE 0.6F AND THE ELEVATION PROFILE.
%=====================================================================
[ki,li]=polyxpoly(x, y, di, zk, 'unique');% polyxpoly from mapping Toolbox.
% 'unique' filters out duplicate intersections, which may result
% if the input polylines are self-intersecting.
mapshow(ki, li, 'DisplayType','point','Marker','o');
```

- In lines 200 to 319 the program checks if there are intersection points and if there are no intersection points calculates free space path loss and field strength, if there are two intersection points which means one obstacle the program calculates Single Knife-Edge path loss and field strength at the point located receiver.

```
%=====================================================================
%      CHECK IF MATRIX [ki,li] IS EMPTY (FREE SPACE PATH LOSS) OR NOT.
%=====================================================================
if isempty([ki,li]) % FREE SPACE PATH LOSS CALCULATION
disp('No obstructions detected')
% COMPUTE FREE SPACE PATH LOSS IN DBI WHERE f in MHZ and d in km
FSPL=32.45+20*log10(f)+20*log10(di(4000)/1000);
V=['Free Space Path Loss=',num2str(FSPL),'dB'];
disp(V)
% CALCULATION: E(dBμV/m)=P(dBm)-PL+20logf(MHz)-Gr(dBi)+77.2
% IN OUR COMPUTE WE CONSIDER Gr(dBi)=0
E=Pt-FSPL+20*log10(f)+77.2;
U=['Field Strength E =',num2str(E),' dBuV/m'];
disp(U)
%=====================================================================
else
% Calculation of rows and columns of matrix [ki,li]
% sizeOfMatrix = size([ki,li])
% Calculation of rows of matrix [ki,li], ki-->Distance, li-->Height
nRows = size([ki,li], 1); % 1 stands for the first dimension
Row=nRows/2;% because each obstructions is counted twice, we devide by 2
disp(' Distance(ki) Height(li) (in meters) ')
disp([ki,li])
M=['There are ',num2str(Row),' obstructions at ki and li positions.'];
disp(M)
DASH'==========================================================';
disp(DASH)
DASH'==========================================================';
disp(DASH)
%=====================================================================
if Row==1
%=====================================================================
% If Row=1 MEANS THAT WE HAVE 1 OBSTACLE SO SINGLE KNIFE-EDGE MODEL
%=====================================================================
disp('Single Knife-Edge calculation begins');
```

```
% I consider that I have only 2 intersection points li(1)and li(2)
% because in Knife-Edge model we take into account the first obstacle
% otherwise the model becomes too complicated.li-->Heihgt, ki-->distance
% Find the indices of c1 and e1 in matrix di.
index=find(di<ki(2) & di>ki(1));
% Find the first and last element of indices matrix index,
% index(1) and index(end).
f1=index(1);
f2=index(end);
% Using indices from above find the elements in zk creating a submatrix mi
mi=zk(f1:f2);
% find the max of matrix mi, maxheight.
maxheight=max(mi);
Mh=['Height of Single Knife-Edge=',num2str(maxheight),' m'];
disp(Mh)
% find the index of maxheight in matrix mi which will
% be the same in matrix d1,sometimes we have two (2) same index
% so we take the first one, index(1).
% In general, when we are dealing with floats,
% always try to avoid exact comparisons and look for proximity,
% that's why we use the formula below instead of index=find(mi==maxheight).
index = find( abs(mi-maxheight) < 0.0001 );
f3=index(1);
% Create a submatrix d1 of di with indices f1,f2.
d1=di(f1:f2);
D1=d1(f3);
Md=['Horizontal distance between Transmitter and Single Knife-Edge =',num2str(D1),' m'];
disp(Md)
% Now I find Earth radius r1 in this point because I need the coordinates of
% the line "maxheight" which are : start point(D1,r1)and
% end point(D1,maxheight) to plot Knife-Edge1 with the use of
% the command  "line"
r1=0.000000059*(D1-dmin).*(dmax-D1);
% Plot the vertical line of Single Knife-Edge
line([D1 D1],[r1 maxheight],'color','k','LineWidth',1)
% Intersect the 1st Knife-Edge line and the LOS Line
% The command "polyxpoly" does not work here because these two lines
% don't intersect but the their extensions intersect, so if I use
% the command "polyxpoly" i get the message 'empty matrix',that's why we
% use algebra in finding intersection points between two lines,
```

```
% see explanation doc.
% In MATLAB backslash operator (\)is used to solve systems of linear
% equations Ax=B ==>x=A\B.
A=[(zmax-zmin),-(dmax-dmin);(maxheight-r1),-(D1-D1)];
b=[(zmax-zmin)*dmin-(dmax-dmin)*zmin;(maxheight-r1)*D1-(D1-D1)*r1];
Intersectionpoint=A\b;
% Parameter h in formula v, i.e. height between Knife-Edge and LOS line
h=maxheight-Intersectionpoint(2);
Ph=['Height between Single Knife-Edge line and LOS, h =',num2str(h),' m'];
disp(Ph)
%-------------------------------------------------------------------------------
% Find the length of the LOS red line.
length = sqrt((dmax-dmin).^2+(zmin-zmax).^2);
LOS=['LOS length =',num2str(length),' m'];
disp(LOS)
%-------------------------------------------------------------------------------
% Find the distance between Knife-Edge and Receiver
% which is D2=dmax-D1.
D2=dmax-D1;
DHrKE=['Horizontal distance between Single Knife-Edge and Receiver =',num2str(D2),' m'];
disp(DHrKE)
% Calculating v parameter of fresnel Integral
v=h*sqrt((2*dmax)/(l*D1*D2));
Fv=['Fresnel Parameter v=',num2str(v)];
disp(Fv)
% Approximate solution for equation Gd(dB)=20log[F(v)]provided by Lee.
Gd=KnifelossLee(v);
KED1=['Single Knife-Edge Path Loss Gd =',num2str(Gd),' dB'];
disp(KED1)
%-------------------------------------------------------------------------------
% Computing the Total Path Loss after Single Knife-Edge Model
FSPL=32.45+20*log10(f)+20*log10(di(4000)/1000);
V=['Free Space Path Loss =',num2str(FSPL),' dB'];
disp(V)
% The Total Path Loss in dB is the sum of Free Space Path Loss
% and Knife-Edge Path Loss.
Gtotal=FSPL+abs(Gd);
Gt=['Single Knife-Edge Path Loss =',num2str(Gtotal),' dB'];
disp(Gt)
% And in dBuV/m is :
```

```
316 Etotal=Pt-Gtotal+20*log10(f)+77.2;
317 Et=['Field Strength =',num2str(Etotal),' dBuV/m'];
318 disp(Et)
319 % END OF SINGLE KNIFE EDGE CALCULATION
```

- Now if there are two or more obstacles the program finds these two obstructions, the primary and the secondary one calculating all Fresnel parameters of all obstacles as if they were alone and select the maximum v_1 and the second maximum v_2, defining so the dominant and the predominant obstacle. The program displies v_1 and v_2. Then implements the proper model, here Deygout's model. Lines 320 to 404 do this.

```
320 %==========================================================================
321 %==========================================================================
322 else
323 % AUTOMATION PROGRAM FINDS ALL THE HEIGHTS AND MAX1 AND MAX2 FOR
324 % FRESNEL PARAMETERS V1 & V2
325 % Preallocation of matrix V
326 V=zeros(1,nRows);
327 %--------------------------------------------------------------------------------------------------
328 for a=1:2:nRows
329 indexA=find(di<ki(a+1) & di>ki(a));
330 % Find the first and last element of indices matrix index,
331 % index(1) and index(end).
332 f1=indexA(1);
333 f2=indexA(end);
334 % Using indices from above find the elements in zk creating a submatrix mi
335 mi=zk(f1:f2);
336 % find the max of matrix mi, maxheight.
337 maxheight=max(mi);
338 Mh=['Height of Knife-Edge=',num2str(maxheight),' m'];
339 disp(Mh)
340 % find the index of maxheight in matrix mi which will
341 % be the same in matrix d1,sometimes we have two (2) same index
342 % so we take the first one,index(1).
343 % In general, when we are dealing with floats,
344 % always try to avoid exact comparisons and look for proximity,
345 % that's why we use the formula below instead of index=find(mi==maxheight).
346 indexB = find( abs(mi-maxheight) < 0.0001 );
347 f3=indexB(1);
348 % Create a submatrix d1 of di with indices f1,f2.
```

```
d1=di(f1:f2);
distance=d1(f3);% distance is D1
Md=['Horizontal distance of Knife-Edge from transmitter =',num2str(distance),' m'];
disp(Md)
% Earth radius r1 in this point.
r1=0.000000059*(distance-dmin).*(dmax-distance);
line([distance distance],[r1 maxheight],'color','k','LineWidth',1)
% Intersect the Knife-Edge line and the LOS Line
A=[(zmax-zmin),-(dmax-dmin);(maxheight-r1),-(distance-distance)];
b=[(zmax-zmin)*dmin-(dmax-dmin)*zmin;(maxheight-r1)*distance-(distance-distance)*r1];
Intersectionpoint=A\b;
% Parameter h in formula v, i.e. height between Knife-Edge line and LOS
h=maxheight-Intersectionpoint(2);
Ph=['Height between Knife-Edge line and LOS, h =',num2str(h),' m'];
disp(Ph)
% Find the length of the LOS red line.
length = sqrt((dmax-dmin).^2+(zmin-zmax).^2);
LOS=['LOS length =',num2str(length),' m'];
disp(LOS)
% Find distance D1 between Transmitter and Knife-Edge.
D1=distance;
DHtKE=['Horizontal distance between Transmitter and Knife-Edge =',num2str(D1),' m'];
disp(DHtKE)
% Find distance D2 between Knife-Edge and Receiver.
D2=dmax-D1;
DHrKE=['Horizontal Distance between Knife-Edge and Receiver =',num2str(D2),' m'];
disp(DHrKE)
% Calculating v parameter of fresnel Integral
v=h*sqrt((2*(D1+D2))/(l*D1*D2));
Fv=['Fresnel Parameter v=',num2str(v)];
disp(Fv)
% Here we create a matrix V(a), that contains all the parameters v from the
% for...next loop
V(a)=h*sqrt((2*(D1+D2))/(l*D1*D2));
DASH'============================================================';
disp(DASH)
% Because the matrix V(a) contains zeros and so it gives wrong indexes of
% the maximum value 1 (max1) and the maximum value 2 (max2), we delete all
% zeros from matrix V(a) creating a matrix L that has all the data of
% matrix V(a) but without zeros.
```

```
L = V(V~=0);
[max1,idx1]= max(L);% we find the max value.
L(idx1)=NaN;
[max2,idx2]= max(L);% we find the second max value.
L(idx1)=max1;
DASH'============================================================';
disp(DASH)
end
DASH'============================================================';
disp(DASH)
MAXV=['The maximum V1 =',num2str(max1),' and it is caused by obstacle ' ,num2str(idx1)];
disp(MAXV)
MAXV=['The maximum V2 =',num2str(max2),' and it is caused by obstacle ' ,num2str(idx2)];
disp(MAXV)
DASH'============================================================';
disp(DASH)
```

- Lines 405 to 619 implement the Deygout's model. Using the same methodology, we created the programs for Epstein-Peterson's model and Giovaneli's model.

```
%====================================================================
%                              DEYGOUT MODEL
%====================================================================
%                               1st KNIFE-EDGE
%====================================================================
% li-->Heihgt, ki-->distance
% Find the indices of c1 and e1 in matrix di.
% The program gives the number of the obstacle, i.e 9 obstacle but we want
% the intersection points. For the 9th(idx1=9) obstacle the intersection
% points are 17 and 18.How do we find these? We say a2=2*idx1=2*9=18 and
% a1=a2-1=18-1=17. That is the logic for lines 345 ,346 (below),422 and 423.
a2=2*idx1;
a1=a2-1;
index=find(di<ki(a2) & di>ki(a1));
% Find the first and last element of indices matrix index,
% index(1) and index(end).
f1=index(1);
f2=index(end);
% Using indices from above find the elements in zk creating a submatrix mi
mi=zk(f1:f2);
% Find the max of matrix mi.
maxheight1=max(mi);
```

```
Mh=['Height of 1st Knife-Edge=',num2str(maxheight1),' m'];
disp(Mh)
% find the index of maxheight1 in matrix mi which will
% be the same in matrix d1,sometimes we have two (2) same index
% so we take the first one,index(1).
% In general, when we are dealing with floats,
% always try to avoid exact comparisons and look for proximity,
% that's why we use the formula below instead of index=find(mi==maxheight1).
index = find( abs(mi-maxheight1) < 0.0001 );
f3=index(1);
% Create a submatrix d1 of di with indices f1,f2.
d1=di(f1:f2);
D1=d1(f3);
%--------------------------------------------------------------------------
% Earth radius r1 in this point.
r1=0.000000059*(D1-dmin).*(dmax-D1);
%--------------------------------------------------------------------------
% Plot the vertical line of the 1st Knife-Edge.
line([D1 D1],[r1 maxheight1],'color','k','LineWidth',1)
% Intersect the Knife-Edge line and the LOS Line
A=[(zmax-zmin),-(dmax-dmin);(maxheight1-r1),-(D1-D1)];
b=[(zmax-zmin)*dmin-(dmax-dmin)*zmin;(maxheight1-r1)*D1-(D1-D1)*r1];
Intersectionpoint=A\b;
% Parameter h1 in formula v, i.e. height between 1st Knife-Edge and LOS
h1eff=maxheight1-Intersectionpoint(2);
Ph=['Height between 1st Knife-Edge and LOS, h1eff =',num2str(h1eff),' m'];
disp(Ph)
% Find the length of the LOS red line.
length = sqrt((dmax-dmin).^2+(zmin-zmax).^2);
LOS=['LOS length =',num2str(length),' m'];
disp(LOS)
% Distance between  Transmitter and 1st Knife-Edge,
DHtKE=['Horizontal distance between Transmitter and 1st Knife-Edge D1 =',num2str(D1),' m'];
disp(DHtKE)
% Distance between 1st Knife-Edge and Receiver.
D2=dmax-D1;
DHrKE=['Horizontal distance between 1st Knife-Edge and Receiver D2=',num2str(D2),' m'];
disp(DHrKE)
% Calculating v1 parameter of fresnel Integral
v=h1eff*sqrt((2*dmax)/(l*D1*D2));
```

```
Fv=['Fresnel Parameter v1=',num2str(v)];
disp(Fv)
% Approximate solution for equation Gd(dB)=20log[F(v)]provided by Lee.
Gd1=KnifelossLee(v);
SKE=['1st Knife-Edge Path Loss Gd1 =',num2str(Gd1),' dB'];
disp(SKE)
DASH='---------------------------------------------------------------------';
disp(DASH)
%=====================================================================
%                    2nd KNIFE-EDGE
%=====================================================================
% 2nd Knife Edge calculation begins
% li-->Heihgt, ki-->distance
% Find the indices of c1 and e1 in matrix di.
a4=2*idx2;
a3=a4-1;
index=find(di<ki(a4) & di>ki(a3));
% Find the first and last element of indices matrix index,
% index(1) and index(end).
f1=index(1);
f2=index(end);
% Using indices from above find the elements in zk creating a submatrix mi
mi=zk(f1:f2);
% find the max of matrix mi, maxheight2.
maxheight2=max(mi);
Mh=['Height of 2nd Knife-Edge=',num2str(maxheight2),' m'];
disp(Mh)
% find the index of maxheight2 in matrix mi which will
% be the same in matrix d1,sometimes we have two (2) same index
% so we take the first one,index(1).
% In general, when we are dealing with floats,
% always try to avoid exact comparisons and look for proximity,
% that's why we use the formula below instead of index=find(mi==maxheight2).
index = find( abs(mi-maxheight2) < 0.0001 );
f3=index(1);
% Create a submatrix d1 of di with indices f1,f2.
d1=di(f1:f2);
D3=d1(f3);
Md=['Distance between Transmitter and 2nd Knife-Edge D3=',num2str(D3),' m'];
disp(Md)
```

```
% Find distance between 2nd Knife-Edge and Receiver.
D4=abs(dmax-D3);
DHrKE2=['Distance between Receiver and 2nd Knife-Edge D4=',num2str(D4),' m'];
disp(DHrKE2)
% Distance between the two Knife-Edge is D5.
D5=abs(D3-D1);
DM1M2=['Distance between the Two Knife-Edges D5=',num2str(D5),' m'];
disp(DM1M2)
%-------------------------------------------------------------------------
% Earth radius r2 in this point.
r2=0.000000059*(D3-dmin).*(dmax-D3);
%-------------------------------------------------------------------------
% Plot the vertical line of the second Knife-Edge.
line([D3 D3],[r2 maxheight2],'color','k','LineWidth',1)
% Intersect the Knife-Edge 2 line and the LOS Line.
A=[(zmax-zmin),-(dmax-dmin);(maxheight2-r2),-(D3-D3)];
b=[(zmax-zmin)*dmin-(dmax-dmin)*zmin;(maxheight2-r2)*D3-(D3-D3)*r2];
Intersectionpoint=A\b;
% Parameter h in formula v, i.e. height between Knife-Edge line and LOS
h2=maxheight2-Intersectionpoint(2);
Ph2=['Height between 2nd Knife-Edge  and LOS, h2 =',num2str(h2),' m'];
disp(Ph2)
%-------------------------------------------------------------------------
% Plot the line from maxheight1 to Transmitter, i.e. line TM1
% Coordinates are (D1,maxheight1) and (dmin,zmin).
line([dmin D1],[zmin maxheight1],'color','k')
%-------------------------------------------------------------------------
% Plot the line from maxheight1 to Receiver, i.e. line M1R.
% Coordinates are (D1,maxheight1) and (dmax,zmax).
line([dmax D1],[zmax maxheight1],'color','k')
%-------------------------------------------------------------------------
% HERE WE CALCULATE INTERSECTION POINT BETWEEN MAXHEIGHT2 AND M1R
% IF SECONDARY OBSTACLE LIES ON THE RIGHT OF PRIMARY OR M1T IF
% SECONDARY OBSTACLE LIES ON THE LEFT OF PRIMARY
% Observe that h2eff is the same with Epstein-Peterson h2 and Giovaneli h2.
%=========================================================================
% IF D1<D3 MEANS THAT THE SECONDARY OBSTACLE LIES ON THE RIGHT OF   THE
MAIN
%=========================================================================
if D1<D3
```

```
546  % D1<D3 means that secondary obstacle M2 lies on the right of the main
547  % obstacle M1, so its maxheight2 intersects with line M1R.
548  % So we intersect the line maxheight1-R(M1R) and maxheight2
549  % Coordinates are (distance1,maxheight1) and (distance2,maxheight2).
550  % we use distances D5,D4 for the secondary obstacle.
551  A=[(maxheight1-zmax),-(D1-dmax);(maxheight2-r2),-(D3-D3)];
552  b=[(maxheight1-zmax)*dmax-(D1-dmax)*zmax;(maxheight2-r2)*D3-(D3-D3)*r2];
553  Intersectionpoint=A\b;
554  h2eff=maxheight2-Intersectionpoint(2);
555  DH2=['Height between maxheight2 and line M1R h2eff=',num2str(h2eff),' m'];
556  disp(DH2)
557  D5=abs(D3-D1);
558  D4=abs(dmax-D3);
559  % calculating v2
560  v=h2eff*sqrt((2*(D4+D5))/(l*D4*D5));
561  Fv=['Fresnel Parameter v2=',num2str(v)];
562  disp(Fv)
563  % Approximate solution for equation Gd(dB)=20log[F(v)]provided by Lee.
564  Gd2=KnifelossLee(v);
565  DKE=['2nd Knife-Edge Path Loss Gd2 =',num2str(Gd2),' dB'];
566  disp(DKE)
567  DASH='---------------------------------------------------------------------';
568  disp(DASH)
569  %=====================================================================
570  % ELSE D1>D3 MEANS THAT THE SECONDARY OBSTACLE LIES ON THE LEFT OF THE
MAIN
571  %=====================================================================
572  else
573  % else means that D1>D3 and the secondary obstacle M2 lies on the left of the main
574  % obstacle, so its maxheight2 intersects with line M1T.
575  % So we intersect the line maxheight1-T(M1T) and maxheight2.
576  % Coordinates are (distance1,maxheight1) and (distance2,maxheight2).
577  % Now we use distances D3,D5.
578  A=[(maxheight1-zmin),-(D1-dmin);(maxheight2-r2),-(D3-D3)];
579  b=[(maxheight1-zmin)*dmin-(D1-dmin)*zmin;(maxheight2-r2)*D3-(D3-D3)*r2];
580  Intersectionpoint=A\b;
581  h2eff=maxheight2-Intersectionpoint(2);
582  DH2=['Height between maxheight2 and line M1T h2eff=',num2str(h2eff),' m'];
583  disp(DH2)
584  % calculating v2
```

```
585  v=h2eff*sqrt((2*(D3+D5))/(l*D3*D5));
586  Fv=['Fresnel Parameter v2=',num2str(v)];
587  disp(Fv)
588  % Approximate solution for equation Gd(dB)=20log[F(v)]provided by Lee.
589  Gd2=KnifelossLee(v);
590  DKE=['2nd Knife-Edge Path Loss Gd2 =',num2str(Gd2),' dB'];
591  disp(DKE)
592  DASH='---------------------------------------------------------------------';
593  disp(DASH)
594  end
595  %=====================================================================
596  %              TOTAL PATH LOSS AFTER TWO KINFE-EDGES
597  %=====================================================================
598  FSPL=32.45+20*log10(f)+20*log10(di(4000)/1000);
599  V=['Free Space Path Loss =',num2str(FSPL),' dB'];
600  disp(V)
601  % The Total Path Loss in dB is the sum of Free Space Path Loss
602  % and the 2 Knife-Edge Path Loss, Gd1 and Gd2.
603  Gtotal=FSPL+abs(Gd1)+abs(Gd2);
604  Gt=['Double Knife-Edge Path Loss (DEYGOUT) =',num2str(Gtotal),' dB'];
605  disp(Gt)
606  % And in dBuV/m is :
607  Etotal=Pt-Gtotal+20*log10(f)+77.2;
608  Et=['Field Strength =',num2str(Etotal),' dBuV/m'];
609  disp(Et)
610  DASH='**************************************************************************';
611  disp(DASH)
612  MINFSA=['         The minimum Field Strength is ',num2str(round(Etotal,1)),' dBμV/m .'];
613  disp(MINFSA)
614 MINFSB=['and is caused between the Main Obstacle ',num2str(idx1),' and the Secondary obstacle '
,num2str(idx2), '.',];
615  disp(MINFSB)
616  DASH4='**************************************************************************';
617  disp(DASH4)
618  end
619  end
```